

Kinase-Anchoring Proteins and the Intracellular Targeting of cyclic Adenosine Monophosphate (cAMP)-Dependent Protein Kinase

Thesis submitted for the degree of
Doctor of Philosophy
at the University of Leicester

by

Alison Jane Davis BSc (Hons.), MPhil
Department of Cell Physiology & Pharmacology,
University of Leicester

August 2007

UMI Number: U495536

All rights reserved

INFORMATION TO ALL USERS

The quality of this reproduction is dependent upon the quality of the copy submitted.

In the unlikely event that the author did not send a complete manuscript and there are missing pages, these will be noted. Also, if material had to be removed, a note will indicate the deletion.



UMI U495536

Published by ProQuest LLC 2013. Copyright in the Dissertation held by the Author.
Microform Edition © ProQuest LLC.

All rights reserved. This work is protected against
unauthorized copying under Title 17, United States Code.



ProQuest LLC
789 East Eisenhower Parkway
P.O. Box 1346
Ann Arbor, MI 48106-1346

2.3.2.12 AKAP12.....	16
2.3.2.13 AKAP13.....	17
2.3.2.14 AKAP14.....	20
2.3.2.15 MAP2.....	20
2.3.2.16 Pericentrin.....	21
2.3.3 Direct Interaction between AKAPs and Ion Channels.....	21
2.3.3.1 Glutamate Receptors.....	21
2.3.3.2 L-Type Calcium & KCNQ-KCNE1 Channels.....	22
2.3.3.3 M-Type (KCNQ2/3) Potassium Channels.....	23
2.3.3.4 Calcium Activated Potassium Channels.....	23
2.3.3.5 Inwardly Rectifying Potassium Channels.....	23
3 Scope of Thesis.....	24
<u>Chapter 2 Methods & Materials</u>	26
1 Cell Culture.....	26
1.1 Routine Maintenance of Cell Lines.....	26
1.2 Cell Adhesion.....	26
2 Transient transfection.....	27
3 Immunocytochemistry.....	28
4 Subcellular Fractionation.....	29
5 Western Blotting.....	29
5.1 Polyacrylamide Gel Electrophoresis & Immunoblotting.....	29
6 AKAP79 Phosphorylation & Release Assay.....	30
7 Extraction & Separation of [³ H]-(poly) Phosphoinositides.....	31
8 Re-distribution of AKAP79 Upon PtdIns (4,5)P ₂ Depletion.....	32
9 Real-Time Study of AKAP79 Localisation.....	32
9.1 Construction of RII α -EGFP.....	32
9.2 Expression and Characterisation of RII α -EGFP.....	32
10 Co-immunoprecipitation.....	33
11 Live Confocal Imaging.....	34
12 Muscarinic Receptor Expression.....	34
13 Real-Time AKAP79 Re-distribution by PtdIns (4,5)P ₂ Depletion.....	34
14 Identification of the AKAP79 Binding Site on Kir2.1.....	35
14.1 Construction of GST Fusion Proteins.....	35

14.1.1 Method 1.....	35
14.1.2 Method 2.....	36
14.2 Expression of GST Fusion Proteins.....	38
14.2.1 Recovery Method: Standard.....	39
14.2.2 Recovery Method: Slowing Growth.....	39
14.2.3 Recovery Method: Recovery from Inclusion Bodies.....	39
14.2 GST-Pulldown Assays.....	40
15 Point directed mutagenesis.....	40
16 'Interfering' with the Kir2.1-AKAP79 Complex.....	41
17 GST Pulldown: In Rat Tissue.....	42
18 RII-His Overlay Assay.....	42
18.1 Expression & purification of RII-His protein.....	42
18.2 Assay.....	43
19 Electrophysiology.....	44
19.1 Electrophysiology: With Synthetic Peptides.....	44
20 Inhibition of Kir2.1-AKAP79 Complexes.....	45
20.1 Co-immunoprecipitation: pIRES2-(182-232)-EGFP Inhibition.....	45
20.2 Inhibition by Synthetic Peptides.....	45
20.2.1 Peptide Design.....	45
20.2.2 Co-Immunoprecipitation: With Synthetic Peptides.....	46

Chapter 3 Control of Intracellular Localisation of AKAP-PKA Complexes: The role of PKA and PKC

1 Introduction.....	47
2 AKAP79 is Targeted to the Plasma Membrane.....	48
2.1 AKAP79 Targets RII α to the Plasma Membrane.....	48
2.2 HEK293-AKAP79 Stably Expressing Cells.....	49
2.3 Regulation of AKAP79 Membrane Targeting by PKA &/or PKC.....	49
2.3.1 Subcellular Fractionation.....	50
2.3.1.1 Contents of Fractions.....	50
2.3.2 AKAP79 Phosphorylation and Release Assay.....	51
2.3.3 AKAP79 Phosphorylation and Immunocytochemistry.....	52
3 Conclusions.....	53

Chapter 4 Control of Intracellular Localisation of AKAP-PKA Complexes: The role of PtdIns(4,5)P₂

1 Introduction.....	55
2 Measurement of [³ H]-InsP _x and (poly) Phosphoinositides.....	55
3 Re-Distribution of AKAP79 Upon PtdIns(4,5)P ₂ Depletion.....	57
4 Real-Time Monitoring of AKAP79 Localisation.....	58
4.1 EGFP-tagging of RIIα.....	58
4.1.1 Expression and Characterisation of RIIα-EGFP.....	58
4.1.2 Does RIIα-EGFP Retain its Ability to Bind AKAPs?.....	58
4.1.3 Is RIIα-EGFP Functional in a Model System?.....	59
4.2 Muscarinic Receptor Expression.....	59
5 Conclusions.....	61

Chapter 5 Interactions between AKAP79 and Kir2.1: Identification of a Binding Site on Kir2.1

1 Introduction.....	65
1.1 Inwardly Rectifying Potassium Channels.....	66
1.1.1 The Kir2 Family.....	67
1.1.1.1 Regulation by PKA.....	67
2 AKAP79 Co-immunoprecipitates with Kir2.1, Kir2.2 and Kir2.3.....	68
3 Identification of an AKAP79 Binding Site on Kir2.1.....	69
3.1 GST Fusion Proteins and GST Pulldowns.....	69
3.2 Leucine Zipper Motifs.....	70
4 Modelling the AKAP79 Binding Site on Kir2.1.....	71
4.1 Tertiary Structure.....	71
5 Kir2.1-AKAP interactions <i>in vivo</i>	73
5.1 GST Pulldowns in Rat Tissue.....	73
5.2 RII Overlay Assay.....	73
6 Conclusions.....	74
6.1 Direct Association of AKAP79 with the C-terminal Domain of Kir2.1.....	75
6.2 A Novel Interaction Mediates AKAP79 Binding to Kir2.1 Channels.....	75
6.3 Kir2.1 Isolates AKAP150 from Rat Brain Homogenate.....	78
6.4 Kir2.1 Interaction with Potentially Novel AKAPs.....	79

<u>Chapter 6 Investigating the Functional Effects of AKAP79-Kir Channel Interaction.</u>	
1 Introduction.....	82
2 GST-C (182-232) Peptide Interferes with Kir2.1-AKAP79 Complex.....	83
3 Effect of Co-expression of AKAP79 and Kir2.1 on Channel Function.....	83
4 Endogenous Expression of an Interfering Peptide.....	84
4.1 Characterisation of pIRES2-(182-232)-EGFP.....	85
5 Synthetic Peptides.....	86
6 Conclusions.....	87
6.1 Interfering with the Kir2.1-AKAP79 Complex: Biochemically.....	87
6.2 Effect of AKAP79 on Kir2.1 Currents.....	88
6.3 Peptide 1 Inhibits cAMP Induced Kir2.1 Current.....	89
<u>Chapter 7 Final Discussion</u>	91
1 Control of intracellular localisation of AKAP-PKA complexes.....	92
2 Interactions between AKAP79 and Kir channels.....	93
3 Concluding Remarks.....	94
<u>References</u>	95
 <u>Appendices</u>	
Appendix One	
Composition of 4% Stacking Gel	
Composition of 10% Resolving Gel	
Appendix Two	
Synthetic Oligonucleotides Used to Construct RII α -EGFP	
Synthetic Oligonucleotides Used to Construct Kir2.1 Truncations	
Sequencing Primers Used Sequence pIRES2-(182-232)-EGFP	
Appendix Three	
EGFP-tagging RII α	
Appendix Four	
Construction of GST-Fusion Protein Encoding Plasmids	

Declaration

I declare that this thesis has been composed by myself and that the work described herein is my own except where stated.

A handwritten signature in black ink, appearing to read "H. Davis". The signature is written in a cursive style and is underlined with a single, sweeping horizontal stroke.

Acknowledgements

Well, it has been a long and bumpy road to this point, but with the support of a large number of people I'm finally here.

Special thanks to Dr. Caroline Dart for her supervision, support and apparent constant belief that this thesis would get written! I am very grateful and couldn't have asked for a better supervisor. I'd also like to extend special thanks to Dr. Laura Sampson for all her help and encouragement, and for keeping me amused with her singing whilst doing Western blotting!

Many thanks to Dr. Mark Hills for his help and advice in molecular biology, Prof. R.A. John Challis and Raj Mistry for their expertise in phosphoinositide assays and Jenny Kynaston for her help with the graphics. I'd also like to thank everyone in CPP past & present who are too numerous to mention.

And lastly, thank you to my family for their constant support, my friends for trying to be interested in what's kept me busy for so long (!) and to Lee Marsh for putting up with me being in a persistent state of stress and worry, for reminding me it will be worth it and for keeping me smiling.

ABBREVIATIONS

AC	Adenylyl cyclase
AEBSF	4-(2-aminoethyl)benzenesulfonyl fluoride
AFU	Arbitrary fluorescent units
AKAP	A kinase anchoring protein
AMPA	α -amino-3-hydroxy-5-methyl-4-isoxazole-propionic acid
ATP	Adenosine triphosphate
β AR	Beta adrenergic receptor
Ca^{2+}	Calcium
CaCl	Calcium chloride
CaM	Calmodulin
cAMP	Cyclic adenosine monophosphate
Ca_v	L-type calcium channels
CCh	Carbachol
cGMP	Cyclic guanosine monophosphate
CH_3OH	Methanol
CHCl_3	Chloroform
CHO	Chinese hamster ovary
COS-7	African Green Monkey kidney fibroblast cell line
D/D	Dimerisation and docking
DAG	1,2-diacylglycerol
dATP	Deoxyribonucleotide triphosphate A
dCTP	Deoxyribonucleotide triphosphate C
dGTP	Deoxyribonucleotide triphosphate G
DNA	Deoxyribonucleic acid
dNTP	Deoxyribonucleotide triphosphates
dTTP	Deoxyribonucleotide triphosphate T
EAG	Ether a-go-go
ECL	Enhanced chemiluminescence
EDTA	Ethylenediaminetetraacetic acid
EGFP	Enhanced green fluorescent protein
EGTA	Ethylene glycol tetraacetic acid
E_k	Equilibrium potential
EPAC	Exchange protein directly activated by cAMP
ERK	Extracellular signal-regulated kinase
FITC	Fluorescein
FRET	Fluorescence resonance energy transfer
GAP43	Growth associated protein 43
GFP	Green fluorescent protein
GK	Guanylate kinase-like
GluR1	Glutamate receptor 1 subunit
GPCR	G-protein coupled receptor
GRK	G protein-coupled receptor kinase
GSK	Glycogen synthase
GST	Glutathione S-transferase
HCl	Hydrochloric acid
HEK293	Human embryonic kidney cells
HEK293/M3	Human embryonic kidney cells expressing M_3 acetylcholine receptors
HEK293-AKAP79	Human embryonic kidney cells expressing AKAP79
HEPES	4-(2-hydroxyethyl)-1-piperazineethanesulfonic acid

His	Histidine
hrs	Hours
Ht31	Human thyroid peptide
Ht31-P	Human thyroid peptide containing proline substitutions
IBMX	3-Isobutyl-1-methylxanthine
IGF	Insulin-like growth factor
InsP ₃	Inositol 1,4,5-triphosphate
IPTG	Isopropyl-β-D-thiogalactopyranoside
IRES	Internal ribosomal entry site
K	Potassium
[K ⁺] _i	Internal concentration of potassium ions
[K ⁺] _o	External concentration of potassium ions
KCl	Potassium chloride
KCNQ-KCNE1	KvLQT1 channel
kDa	Kilodaltons
KH ₂ PO ₄	Potassium phosphate
Kir	Inwardly rectifying potassium channel
KirBac	Prokaryotic inwardly rectifying potassium channel
K _v LQT	Voltage gated potassium channel encoded by the gene KCNQ
LB	Luria Bertani
LTD	Long term depression
LTP	Long term potentiation
M	Molar
MΩ	Mega
MAGUK	membrane-associated guanylate kinase
MAP	Mitogen-activated protein kinase
MARCKS	Myristoylated alanine-rich C-kinase substrate
MEM	Minimal essential medium
MgSO ₄ ·7H ₂ O	Magnesium sulphate
mins	Minute
ml	Millilitre
mM	Millimolar
mm	Millimetre
ms	Milliseconds
mV	Millivolts
NaCl	Sodium chloride
NaHCO ₃	Sodium bicarbonate
NaOH	Sodium hydroxide
NEAA	Non-essential amino acids
nm	Nanometre
nM	Nanomolar
NMDA	<i>N</i> -methyl <i>D</i> -aspartate
NMR	Nuclear magnetic resonance
NMS	<i>N</i> -methylscopolamine
pA	Pico amperes
PBS	Phosphate buffered saline
PCR	Polymerase chain reaction
PDE	Phosphodiesterase
PDZ	Post synaptic density protein, <i>Drosophila</i> disc large tumor suppressor, and Zonula occuldens-1 protein
PH	Pleckstrin homology
PI3-K	Phosphoinositide 3-kinase
PI4-K	Phosphoinositide 4-kinase
PKA	cAMP-dependent protein kinase/ protein kinase A
PKC	Protein kinase C
PKD	Protein kinase D

PKN	Protein kinase N
PLC	Phospholipase C
PMA	Phorbol-12-Myristate-13-Acetate
PNACL	Protein and Nucleic Acid Chemistry Laboratory
PP1	Protein phosphatase 1
PP2A	Protein phosphatase 2A
PP2B	Protein phosphatase 2B/calcineurin
PSD	Postsynaptic density
PtdIns	<u>Phosphatidylinositol</u>
PtdIns(4,5)P	Phosphatidylinositol 4,5-phosphate
PtdIns(4,5)P ₂	Phosphatidylinositol 4,5-bisphosphate
RBD	Receptor-binding domain
RI	Regulatory subunit I
RII	Regulatory subunit II
ROMK	Renal outer medullar potassium channel/Kir1
rpm	Revolutions per minute
S.E.	Standard error
SAP97	Synapse-associated protein 97
SDS	Sodium dodecyl sulfate
SDS-PAGE	Sodium dodecyl sulfate polyacrylamide gel electrophoresis
SH3	Src homology 3
TAE	Tris-Acetate-EDTA
TALK	Potassium channel encoded by gene KCNK16 and 17
TASK	TWIK-related acid-sensitive potassium channels
TBST	Tris-buffered solution with Tween-20
TE	Tris-EDTA
THIK	Potassium channel encoded by gene KCNK12 and 13
TIRF	Total internal reflectance fluorescence
TREK	TWIK-related potassium channels
TRESK	Potassium channel encoded by gene KCNK18
TxR	Texas red
µg	Micro gram
µl	Micro litre
UV	Ultra violet
Wtm	Wortmannin

Amino acids

Alanine	A	Isoleucine	I
Arginine	R	Leucine	L
Asparagine	N	Lysine	K
Aspartic acid	D	Methionine	M
Cysteine	C	Phenylalanine	F
Glutamic acid	E	Proline	P
Glutamine	Q	Serine	S
Glycine	G	Threonine	T
Histidine	H	Tryptophan	W
Isoleucine	I	Tyrosine	Y
Leucine	L	Valine	V
Histidine	H		

ABSTRACT

KINASE-ANCHORING PROTEINS AND THE INTRACELLULAR TARGETING OF cAMP-DEPENDENT PROTEIN KINASE

Alison J. Davis August 2007

A kinase anchoring proteins (AKAPs) are a family of structurally diverse multidomain proteins classified solely by their ability to bind cAMP-dependent protein kinase/protein kinase A (PKA). AKAPs have been implicated in optimising the speed and specificity of signal transduction by targeting PKA and many other signalling proteins to the vicinity to their substrates. The aim of this thesis is to investigate the methods used by this diverse family of proteins in targeting their associated signalling proteins to appropriate intracellular locations.

In accordance to previous studies, we show that the prototypic AKAP, AKAP79 targets PKA to the plasma membrane. This subcellular localisation is mediated via interactions between basic regions on AKAP79 and acidic phospholipids in the plasma membrane. We use a combination of cell fractionation, immunocytochemistry and real time confocal imaging to investigate the regulation of AKAP79 membrane targeting. We show that while PKA and protein kinase C (PKC)-dependent phosphorylation of AKAP79 targeting residues has no effect on its subcellular localization, G_q -coupled receptor-driven depletion of the lipid anchor PtdIns(4,5)P₂ causes release of AKAP79 from the membrane. Receptor-mediated regulation of AKAP membrane binding may be an important feedback mechanism controlling the degree of access that AKAP-bound enzymes have to membrane-associated substrates. Real-time confocal imaging failed to show significant redistribution of AKAP79 following G_q -coupled receptor activation, which may reflect only limited short-range movements.

In addition to regulated association with membrane, we also show through co-immunoprecipitation studies a direct interaction between AKAP79 and all three members of the inwardly rectifying potassium channel Kir2 family. Using a combination of deletion analysis and structural modelling we show that AKAP79 binds the Kir2 family via a novel binding motif located on the C terminus of the ion channel and not via a leucine zipper as has been reported for other AKAP-channel interactions. Interestingly, we also show using a PKA regulatory subunit overlay assays that this region of Kir2.1 is capable of isolating other, potentially novel, AKAPs from rat brain and heart homogenates.

Finally, we use whole-cell patch clamp analysis to demonstrate that cAMP-dependent modulation of Kir2.1 channel activity is significantly enhanced in the presence of AKAP79, thus confirming an important role for AKAP79 in targeting PKA to key channel phosphorylation sites.

CHAPTER ONE

INTRODUCTION

Cells in higher organisms are not isolated entities; they have developed ways in which to communicate with each other and respond with the environment in which they live. This is achieved via the receiving and processing of signals through a large number of signalling pathways which are now recognised to exist in intricate networks. Given the complexity of these networks, several questions arise regarding how a cell ensures rapid and specific transduction of a given signal. One possible explanation lies in the theory of compartmentation. Here, the signalling molecules of each pathway appear to be physically organised into functionally separate units thereby optimising the speed and selectivity of signal transduction, whilst minimising unnecessary cross-talk between different pathways. Central to the theme of compartmentation are the anchoring or scaffolding proteins that orchestrate the structural assembly of these signalling units. The study of one particular scaffolding protein family: the A kinase anchoring proteins or AKAPs forms the basis of this thesis.

AKAPs are multi-domain, non-enzymatic proteins that are becoming increasingly accepted as a means of synchronising both the spatial and temporal features of cell signalling (Smith *et al*, 2006). They are a family of proteins that are structurally diverse yet functionally related; classified solely by their ability to compartmentalise cAMP-dependent protein kinase/ protein kinase A (PKA), thereby isolating different pools of PKA in the vicinity of relevant substrates and optimising signal transduction (Luo *et al*, 1990; Scott *et al*, 1990; Rubin, 1994; Colledge & Scott, 1999; Skalhegg & Tasken, 2000; Kapiloff, 2002; Smith & Scott, 2002). Here, as a means of introduction the individual components of the PKA signalling pathway will be discussed, before presenting evidence for the involvement of AKAPs in its structural and functional organisation.

1 The Protein Kinase A (PKA) Signalling Pathway

Cyclic adenosine monophosphate (cAMP) was the first so-called 'second messenger' to be identified (Rall & Sutherland, 1958) and consequently forms the basis of one of the best understood signal transduction pathways, figure 1. It is utilised by a large number of signalling pathways to regulate a variety of cellular processes including a huge array of metabolic and secretory processes, learning, muscle contraction, growth and ion channel conductance (Skalhegg & Tasken, 2000). cAMP is generated by the enzyme adenylyl cyclase following G-protein coupled receptor (GPCR) stimulation, and in turn activates the serine/ threonine kinase, PKA, which through phosphorylation of target proteins mediates the majority of the downstream signalling effects. The details of the pathway are discussed below.

1.1. Adenylyl Cyclase

Classically, activation of a GPCR by an extracellular ligand leads to activation of heterotrimeric G proteins which in turn stimulate the activity of the enzyme adenylyl cyclase. Activated adenylyl cyclase catalyses the formation of cAMP from adenosine triphosphate (ATP). To date nine isoforms of this large membrane-bound polypeptide have so far been identified in mammals (Hanoune & Defer, 2001) termed AC1-AC9, with the genes encoding AC5, AC6 and AC8 exhibiting splice variants (Cali *et al*, 1996). All isoforms are predicted to share a common secondary structure consisting of an intracellular N-terminus, 2 tandem cassettes (M1 and M2) each spanning the membrane 6 times, a 350 amino acid loop (C1) separating M1 and M2 and a large intracellular C-terminus (C2) (Iyengar, 1993; Cooper *et al*, 1995). The intracellular loop connecting M1 and M2 and the intracellular C terminus are both highly conserved across all isoforms and are predicted to be the sites of cAMP synthesis (Taussig & Gilman, 1995).

All adenylyl cyclase isoforms are constitutively active, but their activity can be up or down-regulated by the activation of G_s- or G_i-protein coupled receptors respectively (Tasken & Aandahl, 2004). Generally considered to be regulated by the α subunits, the adenylyl cyclases are also influenced by the G-protein $\beta\gamma$ dimer, calcium, protein kinase C (PKC), PKA, phosphatases and calmodulin (Tang *et al*, 1991; Iyengar, 1993; Xia *et al*, 1993; Cooper *et al*, 1995; Hanoune & Defer, 2001), with no two adenylyl cyclases regulated in exactly the same manner (Cooper *et al*, 1995).

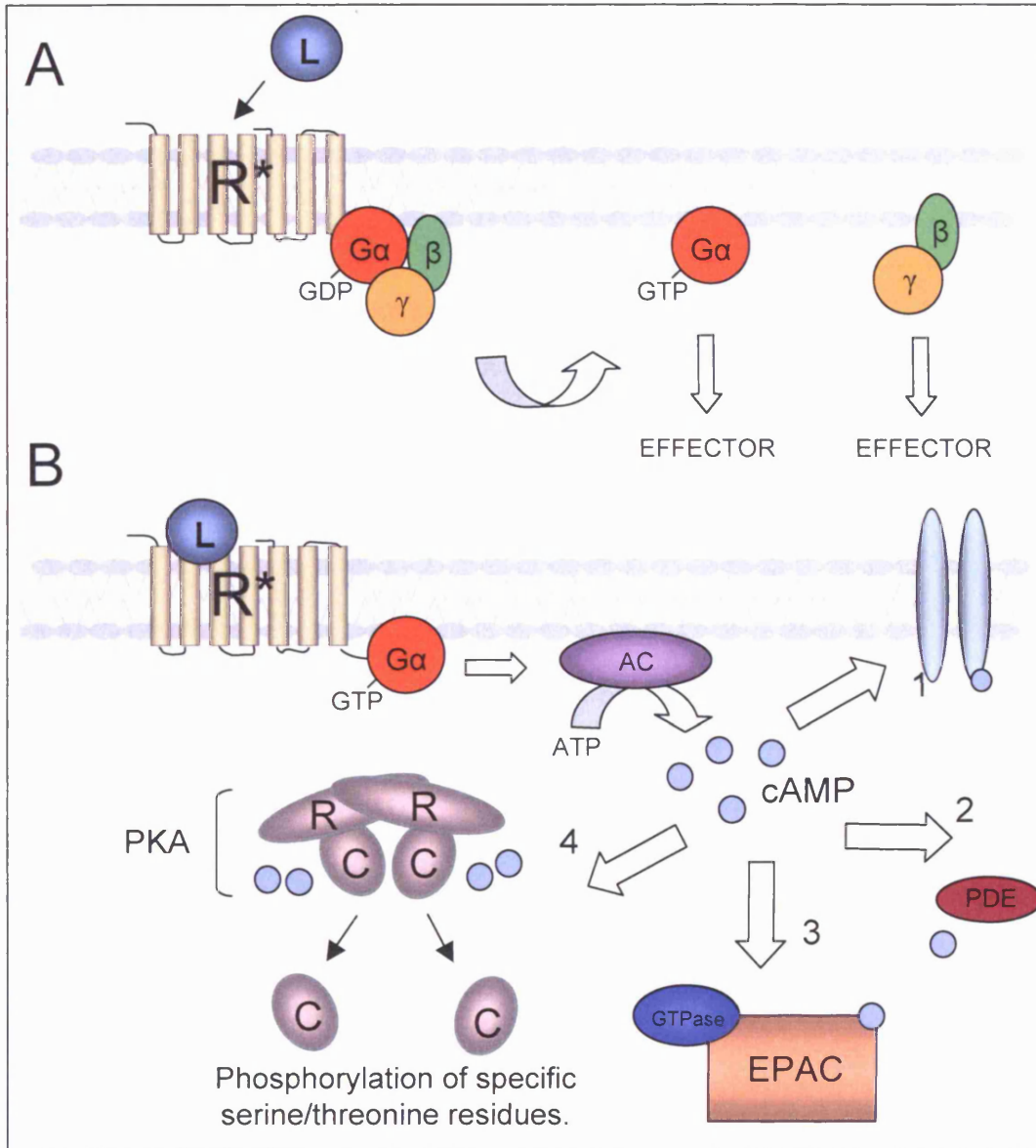


Figure 1. Schematic representing cAMP signalling pathway. **A. G protein activation;** an extracellular ligand (L) activates a G-protein coupled receptor (R^*) which in turn causes the affinity of the α subunit for GDP to decrease, allowing GTP to bind thus activating the α subunit and causing dissociation from the $\beta\gamma$ dimer. **B. Actions of cAMP;** $G\alpha_s$ stimulates the activity of adenylyl cyclase (AC) resulting in the formation of cAMP from ATP. Newly synthesised cAMP can be utilised by: 1 – cAMP gated ion channels; 2 – phosphodiesterases; 3 – EPACs; 4 – PKA where four cAMP molecules bind to each PKA regulatory (R) dimer, resulting in activation of the holoenzyme and release of the catalytic subunits (C). The freely diffusible catalytic subunits are then potentially able to modulate the activity of many downstream effectors such as ion channels and receptors by phosphorylating specific serine or threonine residues.

Tissue expression of each isoform of adenylyl cyclase appears to be quite precise. All adenylyl cyclases are expressed in the brain, although the specific localisation varies between each isoform (Hanoune & Defer, 2001).

1.2 cAMP

To date three main intracellular targets of cAMP has been elucidated: PKA, cyclic nucleotide-gated ion channels and the GTP-exchange protein EPAC (Exchange Protein directly Activated by cAMP; Fimia & Sassone-Corsi, 2001). Of these three targets, the majority of the intracellular actions of cAMP are mediated through the activation of PKA.

1.3 Protein Kinase A

The PKA holoenzyme exists as a complex of two catalytic subunits held in an inactive conformation through association with the regulatory subunit dimer (Beavo *et al*, 1975), figure 2A. Genes encoding three C subunits: C α , C β and C γ , and four R subunits: R1 α , R1 β , R2 α and R2 β have been identified and splice variants of C α , C β and R1 α have also been reported (Skalhegg & Tasken, 2000; Fimia & Sassone-Corsi, 2001). A combination of either two R1 or two R2 subunits with any two C subunits brings about the formation of the holoenzyme subtypes termed type I and type II respectively. Many PKA isoforms exist through the various possible regulatory and catalytic subunit combinations. The type I PKA holoenzyme is largely cytoplasmic, whereas the majority of the type II holoenzyme is associated with cellular structures (Scott, 1991).

Each PKA regulatory subunit possesses an amino terminus domain 45 residues in length essential for dimerisation, a catalytic subunit binding site and two carboxy terminal cAMP binding domains (Corbin *et al*, 1978; Colledge & Scott, 1999), see figure 2B. Four cAMP molecules must bind to the PKA regulatory dimer to bring about the dissociation of the holoenzyme. The newly free and active PKA catalytic subunits are then able to modulate many downstream effectors, altering the activity of target proteins by phosphorylating specific serine and threonine residues (Wang *et al*, 1991; Gibbs *et al*, 1992).

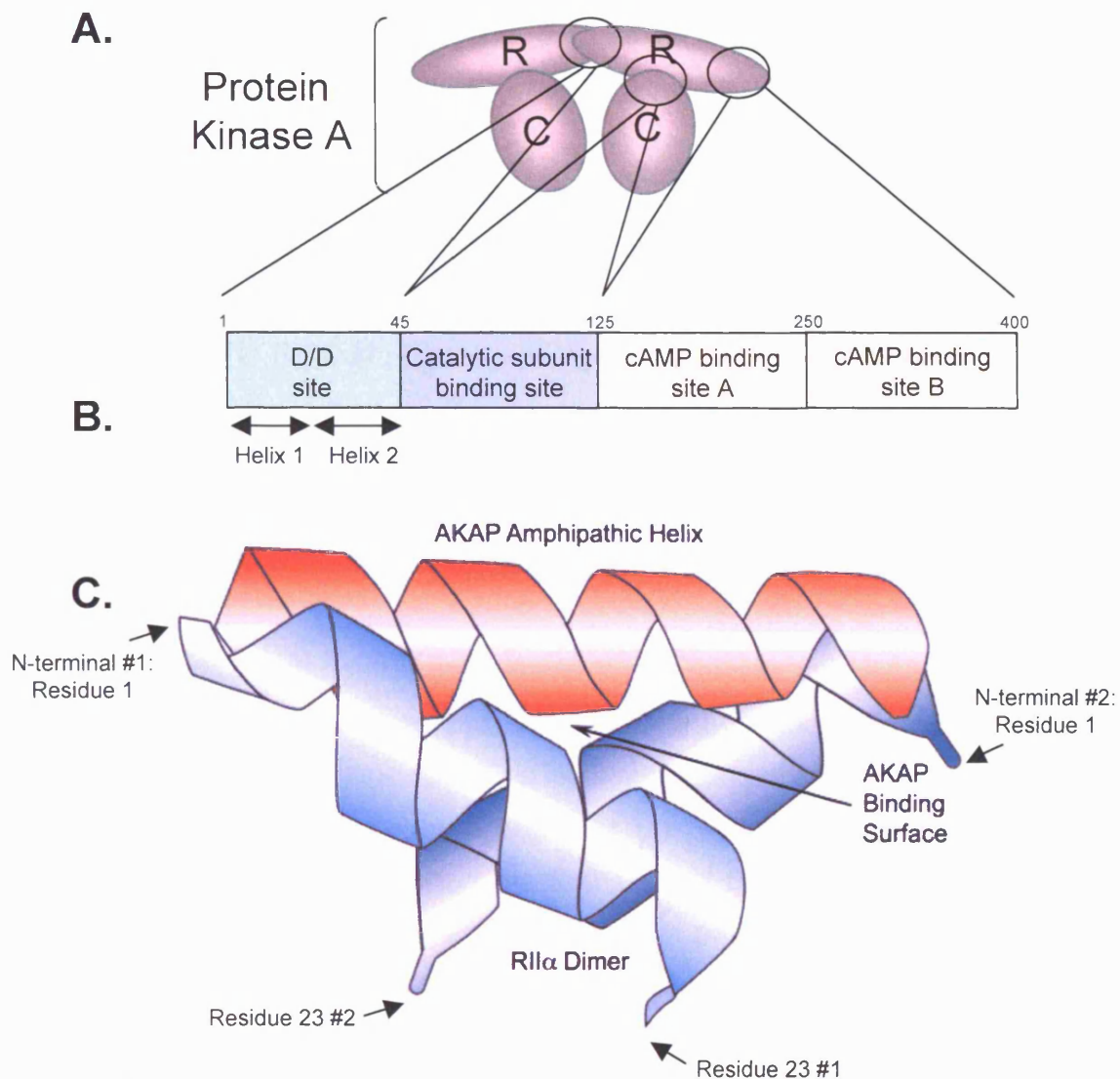


Figure 2. Schematic of the PKA regulatory subunit. **A.** The basic structure of the inactive PKA holoenzyme: consisting of two catalytic subunits (C) bound to each regulatory subunit (R) dimer. **B.** Domain structure of the RII subunit of PKA. D/D = dimerisation & docking site; the region at which the 2 regulatory subunits come together to form a dimer but also the site at which PKA interacts with the amphipathic helix of AKAPs. **C.** Ribbon schematic of the PKA-AKAP complex. Two RII helices, indicated in blue formed from two molecules coming together, form a dimer, where they are predicted to form a contact with an AKAP molecule, shown in red. Image taken and adapted from Colledge & Scott, 1999, kindly provided by Jenny Kynaston, Royal Holloway College, University of London.

The first 45 residues of each regulatory subunit also contain the AKAP docking interface, thus this region serves two functions; docking and dimerisation and is often referred to as the D/D domain (Scott *et al*, 1990; Luo *et al*, 1990; Carr *et al*, 1991). The D/D domain has two exposed faces: one highly hydrophobic, the site at which PKA interacts with the amphipathic helices of AKAPs, and the other highly charged (Morikis *et al*, 2002). Little is known about the charged face of the D/D domain. Through Nuclear Magnetic Resonance (NMR) structural analysis, the AKAP binding pocket of the PKA regulatory dimer is shown to be formed by an anti-parallel four-helix bundle in the RII D/D domain, see figure 2C (2 helices shown; Alto *et al*, 2003; Banky *et al*, 2003; Gold *et al*, 2006; Kinderman *et al*, 2006; Beene & Scott, 2007). The four-helix bundle is formed from each regulatory subunit having a hinge region within the D/D domain: the tertiary structure formed by the helical region essentially folding back on itself giving the appearance of 2 helices per regulatory subunit.

PKA regulatory subunit dimer formation is a prerequisite for AKAP binding (Scott *et al*, 1990), yet the dimerisation and AKAP-binding domains have been shown to be distinguishable from one another. This is shown by the deletion of the first 5 residues and/or replacement of residues 3 and 5 of RII with isoleucines, which eliminates AKAP binding but does not affect the formation of the PKA dimer (Hausken *et al*, 1994, 1996a). In addition to this, the residues at positions 6 and 7 in RII appear to confer stabilisation of the AKAP-PKA interaction (Hausken *et al*, 1996a). Furthermore, NMR data indicate that the AKAP-binding region on PKA RII α encompasses residue 1-23 with residues 24-44 serving as the dimer formation interface (Newlon *et al*, 1999).

Downstream from the dimerisation sites on the PKA regulatory subunits are the catalytic subunit binding domains, residues 45-125. Within this domain, amino acids R92 and R93 function to inhibit the catalytic subunits whilst in the holoenzyme conformation, but appear to be unnecessary in holoenzyme formation (Wang *et al*, 1991). These results contradict a previous study by Weldon & Taylor, 1985.

In its inactive tetrameric form, only one of the two cAMP binding sites of the PKA holoenzyme is exposed, cAMP binding site B (Skalhegg & Tasken, 2000). Upon binding of cAMP to this site, a conformational change results that allows binding of

the second cAMP molecule to binding site A.

The regulatory subunits of PKA show varied tissue expression over the various stages of cell development and differentiation (Skalhegg & Tasken, 2000). Mouse $R1\alpha$ is expressed in both heart and the central nervous system. $R1\beta$ expression shows a more restricted pattern being expressed in nervous tissue such as the spinal cord and brain. Both $R11\alpha$ and $R11\beta$ subunits are expressed in the brain, with $R11\alpha$ predominantly expressed in the heart and $R11\beta$ expressed in liver and fat tissue

2 Spatial Organisation of PKA Pathway

cAMP and other constituents of the PKA pathway were originally regarded as a freely diffusible molecules until it was found that different G_s -coupled receptors could selectively activate different PKA holoenzyme subtypes; in perfused rat hearts the adrenergic receptor agonist isoproterenol and prostaglandin receptor agonist prostaglandin E produced very different effects on PKA activity despite both increasing tissue cAMP (Hayes *et al*, 1979; Hayes & Brunton, 1982; Buxton & Brunton, 1983). There was also the question as to how the activation of PKA mediated such efficient phosphorylation of specific effectors given the potentially broad substrate specificity of this enzyme (Skalhegg & Tasken, 2000; Steinberg & Brunton, 2001). The millisecond timing of sympathetic neural regulation of cardiac contractile function, for example, requires a level of co-ordination that is unlikely to occur if the proteins involved float freely around the cell (Steinberg & Brunton, 2001). This problem at the core cellular signalling was realised early on. The codiscoverer of cAMP Ted Rall remarked in the mid-seventies that the simple freely diffusible model painted "the unsatisfying picture of the catalytic subunit of protein kinase swimming about, happily phosphorylating a variety of cellular constituents whether they need it or not" (Rall, 1975).

In answer to these questions, it would appear that specificity in signal transduction may be achieved, in part, through compartmentation of signalling machinery and an increasing number of reports show that this can occur at each step in the signalling pathway.

2.1 cAMP Compartmentation

Local cAMP gradients are formed and affected by: the ratio between degradation and accumulation; and/or the diffusion rate away from the plasma membrane (Dell'Acqua & Scott, 1997; Zaccolo *et al*, 2002). Degradation depends on the type and amount of phosphodiesterase (PDE) present at the site of generation (Rich *et al*, 2001a; Zaccolo & Pozzan, 2002). High concentrations of PDEs reduce cAMP levels and thus the ability of PKA to become active. The mechanisms that regulate cAMP diffusion rates are ambiguous, with theories including the existence of a barrier formed from the endoplasmic reticulum (Rich *et al*, 2000) and molecular 'channelling' from adenylyl cyclase to PKA (Hall & Hell, 2001), similar to that seen with the channelling of the products from metabolic enzymes (Hyde *et al*, 1988; Elcock *et al*, 1996; Srere, 2000).

2.2 Phosphodiesterases

Discovered in 1961 by Drummond and Perret-Yee, the only known route to degrade cAMP is through the actions of phosphodiesterases (PDEs; Drummond & Perret-Yee, 1961, 1962, 1963) and as such these enzymes limit the magnitude and duration of the cAMP-mediated GPCR signal (Houslay & Milligan, 1997; Houslay & Adams, 2003). Phosphodiesterases are characterised by their high affinity and specificity for cAMP (Bolger *et al*, 1997) and number approximately fifty different proteins (Venter *et al*, 2001). They are encoded by twenty-five genes which are classified into eleven families by their amino acid sequence, pharmacological properties, substrate specificity and allosteric regulatory properties (Beavo, 1988 & 1995; Conti *et al*, 1995; Soderling & Beavo, 2000; Mehats *et al*, 2002). Phosphodiesterases are regulated in a variety of ways e.g. by phosphorylation, G-proteins, cyclic nucleotides, calcium-calmodulin (Rich *et al*, 2001b).

The existence of multiple forms of PDEs and adenylyl cyclase, allows cells to dynamically tailor their cAMP signalling (Houslay & Milligan, 1997). Aside from cAMP degradation, phosphodiesterases have also been shown to regulate cGMP, insulin-like growth factor (IGF)-1, penile erectile function and through gene knock-out studies, roles for phosphodiesterases have been also been shown in fertility and mortality (Conti *et al*, 1995; Soderling & Beavo, 2000).

2.3 AKAPs

Signalling complexes are mediated by proteins that, depending on their specific role, are called adaptors, anchors or scaffolds. In general, although not mutually exclusive, adaptors possess multiple interaction domains and link two proteins that do not directly interact; scaffold proteins are defined as a protein with which at least two proteins associate; and an anchor is a protein which attaches other proteins to a specific site (Cho, 2006). A protein may be an anchor and a scaffold, the prototypic example of such a protein is an AKAP.

AKAPs were first recognised as contaminating proteins that tightly associated with highly purified preparations of bovine brain PKA (Sarkar *et al*, 1984). More detailed studies of these PKA-binding proteins were possible because they maintain their PKA binding capabilities after immobilisation onto nitrocellulose membranes (Lohmann *et al*, 1984). Consequently, the typical technique used to detect AKAPs is an overlay assay where the regulatory subunits of PKA are used as a probe. The use of such a technique has allowed the identification of the family of AKAPs that consists of more than 70 structurally distinct, yet functionally related proteins, defined by their ability to form a complex with PKA (Carlise Michel & Scott, 2002). It is however currently unknown what proportion of PKA is bound to AKAPs *in vivo*. Multiple AKAPs have been identified in a wide range of species from *Caenorhabditis elegans* and *Drosophila* to nematode worms, mice and humans (Wong & Scott, 2004).

AKAPs range in size from 15 to 450kDa with an average cell expressing between five to ten different AKAPs (Hausken & Scott, 1996b).

2.3.1 Structure of AKAPs

Due to their diversity, the structure of most AKAPs has not been readily documented, but is limited mainly to the analysis of the different domains within the full-length protein. All AKAPs possess an amphipathic helical region, characterised by hydrophobic residues on one face and charged residues on the other that is responsible for binding the regulatory subunit of PKA (Carr *et al*, 1991), and a domain responsible for targeting the AKAP-PKA complex to specific subcellular locations. In addition, some AKAPs also have further domains to bind other proteins

thus forming multi-protein complexes.

2.3.1.1 PKA Binding Domain

Secondary structure prediction analysis shows that the 14 - 18 residues that comprise the PKA binding domain on AKAPs form an amphipathic helix (Scott *et al*, 1990; Carr *et al*, 1991). Helical wheel alignments on over 20 AKAPs show hydrophobic residues aligned on one side of the helix while the opposite face is lined with polar side chains, figure 3 (Carr *et al*, 1992b; Miki & Eddy, 1999; Vijayaraghavan *et al*, 1999). The entire amphipathic helix is thought to 'slot' into a binding pocket formed by the N-terminal domains of each regulatory subunit of PKA (Carr *et al*, 1991; Newlon *et al*, 1997, 1999, 2001), also see figure 2.

While the hydrophobic face of the amphipathic helix on all AKAPs is conserved, the actual residue make-up varies, figure 3A. It is thought likely that it is this feature that accounts for different AKAPs possessing different affinities for RII (Herberg *et al*, 2000; Beene & Scott, 2007).

The vast majority of AKAPs specifically bind the RII subunits of PKA and not RI. However, some RI subunits are reported to interact with AKAPs, but often with much lower (micromolar) affinity than RII subunits (nanomolar affinity; Carr *et al*, 1992a; Burton *et al*, 1997; Huang *et al*, 1997a; Angelo & Rubin, 1998 & 2002; Banky *et al*, 2000; Herberg *et al*, 2000; Reinton *et al*, 2000). These AKAPs are known as dual AKAPs. It is thought the variation in AKAP binding specificity between RI and RII subunits may be due to the addition of aromatic side chains on the AKAP (Miki & Eddy, 1998, 1999; Angelo & Rubin, 1998, 2000).

2.3.1.2 Membrane targeting domain: Control of intracellular localization

The ability of signalling complexes to be targeted to different subcellular locations is a vital means of ensuring the specificity of intracellular signalling events. As such, AKAPs have employed a variety of specialised membrane targeting methods.

One of the first AKAPs to have their targeting sequence identified was the mammalian spermatid AKAP, S-AKAP84. S-AKAP84 contains an N-terminal hydrophobic region (residues 1-30) that exhibits similar properties to those described

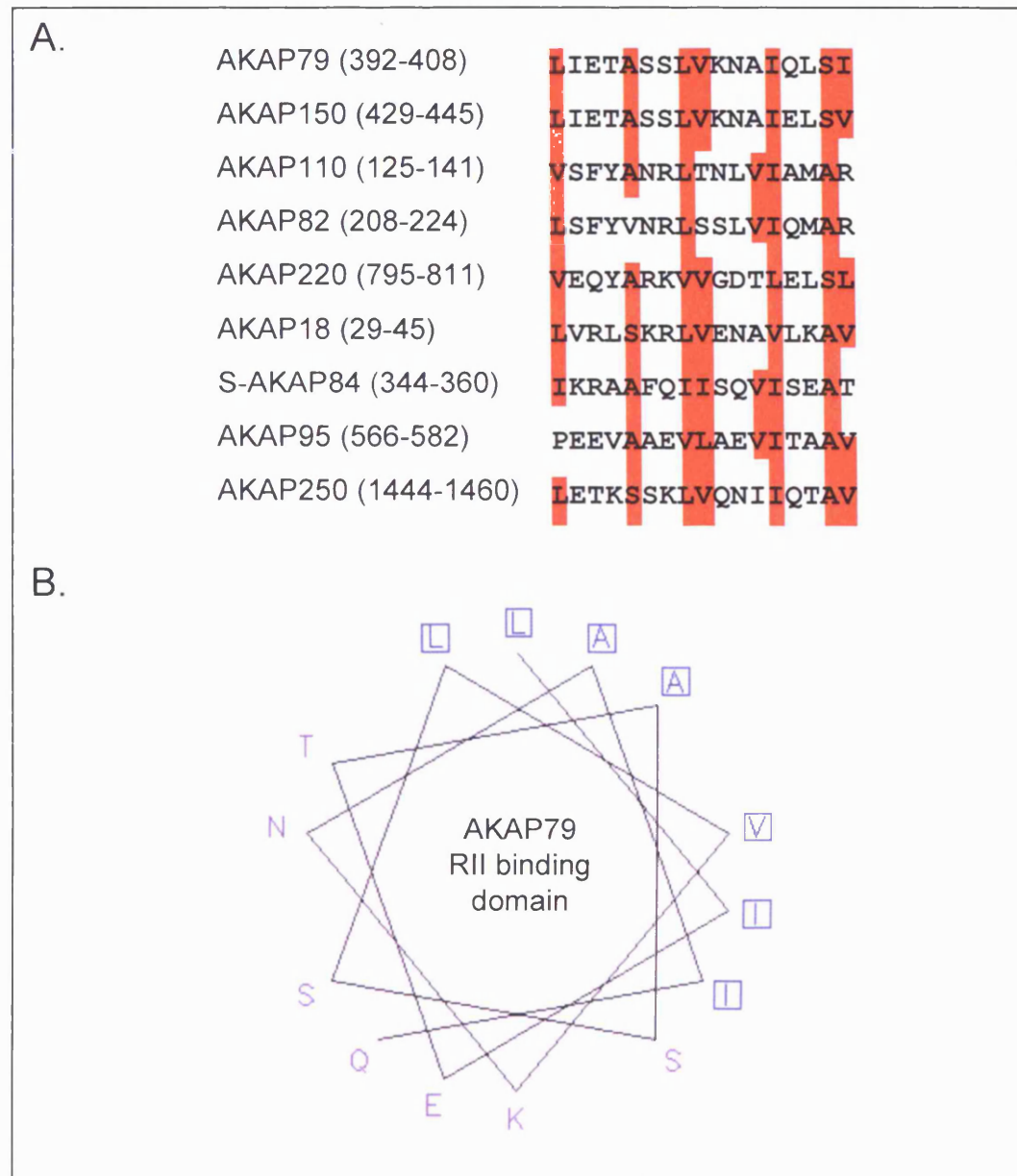


Figure 3. Alignment and helical wheel projection for RII binding domains on AKAPs. **A.** Taken and adapted from Vijayaraghavan *et al*, 1999; alignment of amino acids involved in RII binding to various AKAPs. Highlighted regions represent conserved functional properties. **B.** Helical wheel projection of RII binding domain on AKAP79, where charged or polar residues are shown in purple and hydrophobic residues are shown in blue.

for the N-terminal segment of NADH-cytochrome b_5 reductase, which targets the outer membrane of mitochondria by inserting its hydrophobic region directly into the outer membrane bilayer (Hahne *et al*, 1994; Lin *et al*, 1995; Chen *et al*, 1997). Therefore, it is suggested that S-AKAP84 is concentrated at the mitochondrial surface by similar means, ensuring PKA is localised close to the mitochondrial surface and components of the microtubule motor systems (Chen *et al*, 1997). It is thought that S-AKAP84 may be involved in cAMP stimulation of mitochondrial respiration during sperm activation (Lieberman *et al*, 1988).

D-AKAP1 belongs to the same family as S-AKAP84 and shares a homologous amino acid sequence, including the mitochondrial targeting sequence situated at the N-terminal region (Huang *et al*, 1997b).

Myristoylation (the protein modification where a myristoyl group is attached to an N-terminal glycine residue) and palmitoylation (the attachment of fatty acids to cysteines residues) play important roles in protein-membrane interactions. Unlike myristoylation, palmitoylation is a highly hydrophobic modification and as such often results in an irreversible binding to the membrane (Wang *et al*, 2006). These protein modifications are both required in the targeting of AKAP15 to the plasma membrane. This is shown with the triple mutagenesis of glycine 2 to alanine and cysteines 5 and 6 to serine in AKAP15 resulting in this AKAP becoming almost totally soluble (Gray *et al*, 1997, 1998a & b). Membrane targeting of AKAP18 appears to be mediated through myristoylation of glycine 1 and palmitoylation of cysteines 4 and 5 (Fraser *et al*, 1998).

Members of the AKAP12 family also use myristoylate modifications in order to target to membranes. In conjunction with this they also appear to target to membranes via electrostatic forces; where three distinct basic-rich regions on the N-terminus have been identified on AKAP250/gravin/SSeCKs (Streb & Miano, 2005). These three basic regions are highly homologous with the polybasic membrane-targeting domain of the MARCKs (Myrystoylated Alanine-Rich C-Kinase Substrate) proteins. In gravin/SSeCKS membrane targeting to this basic-rich domain may be regulated by the net charge (rather than any specific area) of the C-terminus, thus providing an interesting mechanism in dynamic regulation of AKAP localisation and hence signal

transduction.

Similarly, another AKAP that appears to interact with the plasma membrane in a similar manner to MARCKs is AKAP79. AKAP79 appears to target to the plasma membrane via three distinct basic and hydrophobic-rich regions at the N-terminus, where any two of these regions are necessary and sufficient for binding to the acidic negatively charged phosphatidylserine-based lipid bilayer (Dell'Acqua *et al*, 1998; Wang *et al*, 2006). These positively charged domains may also be involved in interactions with calcium and calmodulin (CaM; Dell'Acqua *et al*, 1998). It is currently unknown whether this interaction is due to a specific preference for the phospholipid PtdIns(4,5)P₂, simply due to an electrostatic mechanism or a combination of both.

Within the membrane-binding regions of AKAP79 are phosphorylation sites for both PKA and PKC. Consequently it has been suggested that targeting of this AKAP to the membrane may be regulated by phosphorylation. Here, serine residues become negatively charged by the addition of a phosphate group, neutralising the basic nature of the binding region and inhibiting interaction with acidic phospholipids (McLaughlin & Aderem, 1995; Swierczynski & Blackshear, 1996; Seykora *et al*, 1996; Dell'Acqua *et al*, 1998).

The bovine homologue AKAP75 is targeted to the actin-rich cortical cytoskeleton in non-neuronal cells. Just two membrane-targeting domains, T1 and T2 (corresponding to only two of the three binding regions in AKAP79, discussed above) are found in AKAP75 and AKAP150 and are required for inclusion into detergent-insoluble (membrane) fractions (Glantz *et al*, 1993; Li *et al*, 1996). Although it appears that AKAP75 co-localises with F-actin in the cytoskeleton, disruption of the actin filaments does not adversely affect the association of AKAP75 with the cytoskeleton, suggesting that AKAP75 targeting via T1 and T2 may be maintained through association with an additional unknown integral cytoskeletal protein. It should be noted that association with a multi-protein complex that resides close to the cytoskeleton is not currently ruled out (Li *et al*, 1996).

2.3.2 Multi-Protein Signalling Complexes

Aside from scaffolding PKA, AKAPs also function as scaffolds for a multitude of other

proteins including signal-transduction and signal-termination enzymes. This allows entire signalling complexes to be targeted to specific cellular locations and produces a situation whereby protein phosphorylation is only favoured when kinase activity is sufficiently powerful to overcome basal dephosphorylation.

Since the AKAP79 family were first discovered to be multivalent, figure 4, many other AKAPs have also been shown to colocalise PKA with other phosphorylation and dephosphorylation enzymes. Indeed, it is thought that most AKAPs, if not all, anchor not only PKA but other protein kinases as well as protein phosphatases, protein phosphodiesterases and other signal termination machinery (Smith *et al*, 2006).

The following sections outline the current knowledge of AKAP expression, function and known binding partners within cells, see also table 1. It should be noted that AKAPs were originally named according to their apparent molecular weight on SDS-polyacrylamide gels. Often the calculated molecular weight and apparent molecular weight on SDS-polyacrylamide gels differs. This discrepancy is thought to be because of the highly acidic nature of the central section of the molecule binding weakly to SDS and thus not migrating with the predicted mobility (Hirsch *et al*, 1992). This has become problematic where the same AKAP cloned from different species may have a different molecular weight, as with splice variants. Consequently a new nomenclature scheme for the AKAP family has been suggested (www.gene.ucl.ac.uk/nomenclature/genefamily/akap.html). It is however not readily used and so all known synonyms are listed in this section below. Where a specific AKAP is mentioned elsewhere in the text, the original designation is used, for example AKAP79 rather than AKAP5.

2.3.2.1 AKAP1/S-AKAP84/AKAP84/D-AKAP1/AKAP121/AKAP149/SAKAP84

Originally found in male germ cells, this AKAP accumulates predominantly by the outer mitochondrial membrane in the cytosol. It is thought to be involved in the targeting of PKA to the sperm midpiece (Lin *et al*, 1995). Reports also suggest it is localised to postsynaptic membranes of the vertebrate neuromuscular junction (Perkins *et al*, 2001). More recently however, splice variants at both the N and C termini were shown to be expressed in various other tissues, depending on the specific splice variant (Huang *et al*, 1999).

AKAP79: Accession number: P24588; 47kDa (migrates on SDS-polyacrylamide gels at 79kDa).

A. METTISEIHVENKDEKRSAEGSPGAERQKEKASMLCFKRRKKAALPKAGSEAADVARKCPQEAGASDQP
 EPTRGAWASLKRLVTRRRKRSESSKQKPLEGEMQPAINAEDADLSKKKAKSRLKIPCIKFPKRSNHSKI
 IEDSDCSIKVQEEAEILDITQTPLNDQATKAKSTQDLSEGISQKDGDEVCSNVSNISITSGEKVISVELGL
 DNGHSAIQGTLLILEEIEIETIKEKQDVQPQQASPLETSETDHQQPVLSDVPPPLPAIPDQQIVEEASNSTLESA
 PNGKDYESTEIVAEETKPKDTELSQESDFKENGITEEKSSEESKRMEPIAIIITDTEISEFDVTKSKNVPK
 QFLISAENEQVGVFANDNGFEDRTSEQYETLLIETASSLVKNAIQLSIEQLVNMASDDNKINLLQ

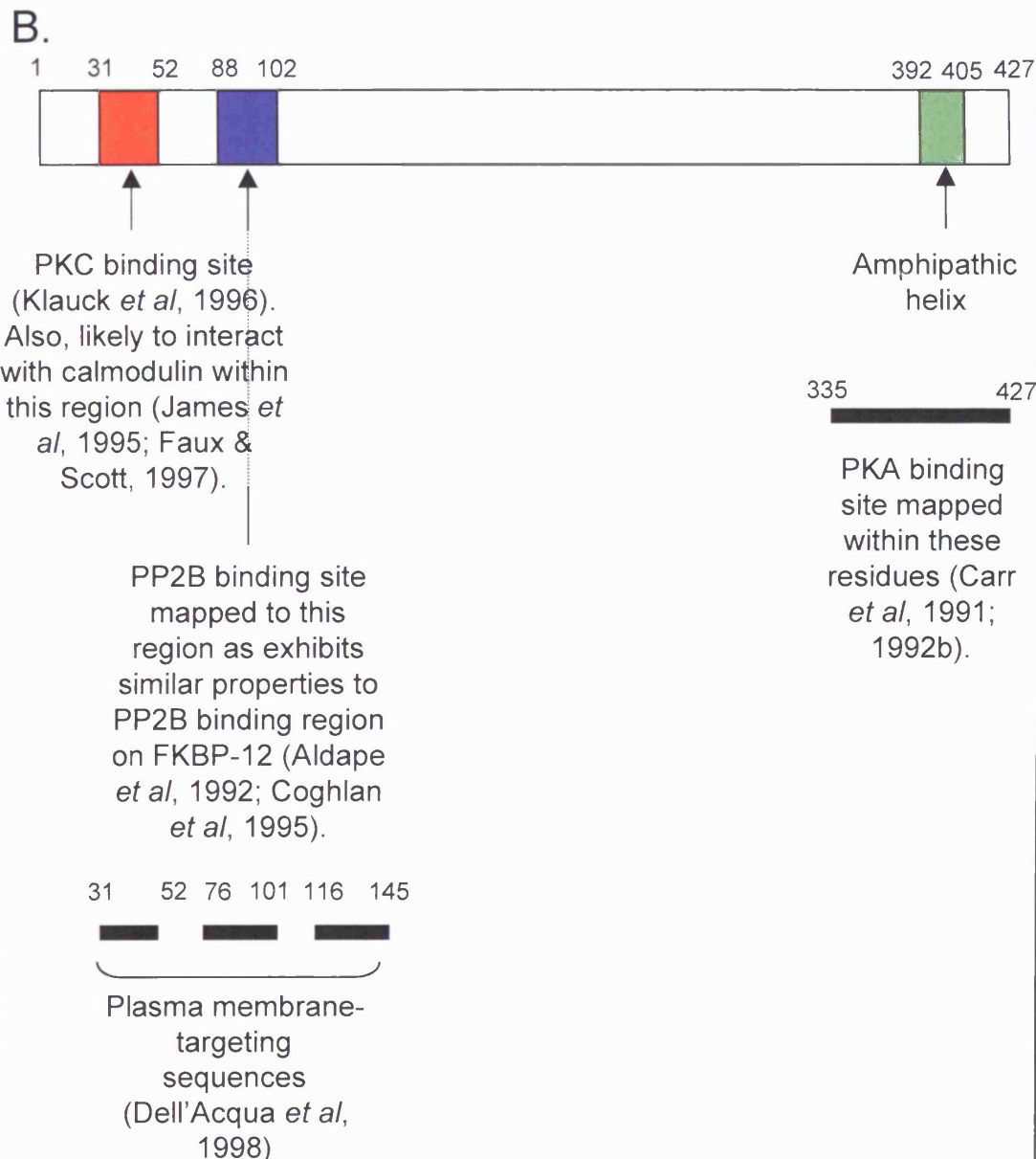


Figure 4. AKAP79. **A.** AKAP79 sequence. **B.** Schematic representation showing putative binding domains (for PKA and PKC phosphorylation sites on AKAP79 see figure 7). Whilst AKAP79 has been shown to directly interact with other proteins (the MAGUK proteins), to date, nothing is currently known about their specific binding sites.

2.3.2.2 AKAP2/AKAP-KL/KIAA0920/DKFZp564L0716

Found predominantly in the kidney and lungs where it associates with the actin cytoskeleton (Dong *et al*, 1998) and proximal to tubules in nephrons (www.expasy.org/uniprot/O54931).

2.3.2.3 AKAP3/AKAP110/SOB1

Localizes to the ribs of the fibrous sheath in the principal piece of the sperm tail (www.expasy.org/uniprot/O75969).

2.3.2.4 AKAP4/p82 Fsc1/hAKAP82/AKAP82

This AKAP only appears to be expressed in the testis where it is found on the fibrous sheath of the sperm tail (Johnson *et al*, 1997). It is likely to play a role in sperm capacitation, the process sperm undergo to enable penetration and fertilisation of an egg.

2.3.2.5 AKAP5/AKAP79/AKAP75/AKAP150

Human AKAP79 and murine AKAP150 are highly conserved. An extended repeat sequence in AKAP150 accounts for the higher molecular weight (Fraser *et al*, 2000).

These orthologues are expressed in relatively high abundance within neurones but may also be expressed in non-neuronal cells (Hirsch *et al*, 1992; Glantz *et al*, 1993). They are situated on the cytoplasmic surface of the plasma membrane (Sarkar *et al*, 1984; Bregman *et al*, 1989; Carr *et al*, 1991 & 1992b) where they may also interact with the cortical actin cytoskeleton (Li *et al*, 1996), as described above.

AKAP79 is predominantly expressed in the hippocampus and cerebral cortex where it localises to the post-synaptic density (PSD) and as such tethers PKA to the PSD so that it is in an ideal position to phosphorylate proteins such as α -amino-3-hydroxy-5-methyl-4-isoxazole-propionic acid (AMPA)-type glutamate receptors. The use of AKAP inhibitor peptides in electrophysiological recordings evoked run-down of AMPA receptor currents indicating the requirement of AKAPs for normal channel function (Rosenmund *et al*, 1994). It was later shown that AKAP-bound PKA enhances the phosphorylation of the AMPA receptor subunit, GluR1, and thus it is thought that this

stabilises the AMPA current (Tavalin *et al*, 2002; Esteban *et al*, 2003). Conversely, dephosphorylation of AMPA current appears to require AKAP-bound PP2B, as revealed using AKAP150 PP2B deletion mutants (Hoshi *et al*, 2005).

AKAP79/150 also couples to the M channel (KCNQ1-KCNE1 channel) in cervical ganglion neurones, more details of these interactions can be found below.

In addition to coupling to ion channels, AKAP79/150 can also bind to the prototypic GPCR, the β_2 -adrenergic receptor in a constitutive manner thus allowing tethered PKA to be situated close to phosphorylation sites on the third intracellular loop and C-terminal tail of the receptor (Fraser *et al*, 2000; Perry *et al*, 2002; Baillie & Houslay, 2005; Lynch *et al*, 2005). Also, AKAP79 affects phosphorylation of the β_2 -adrenergic receptor by G-protein coupled receptor kinase 2 (GRK2) through the anchoring of PKA. GRK2 is phosphorylated by PKA in response to agonist stimulation which in turn increases the ability of GRK2 to translocate to the membrane leading to receptor phosphorylation and its subsequent internalisation (Cong *et al*, 2001). GRK2 may then be phosphorylated by Erk1 or Erk2, returning GRK2 to its inactive state (Pitcher *et al*, 1999). This demonstrates the essential role of tethering PKA to the β_2 -adrenergic receptor through AKAP79 and represents a regulatory feedback loop where agonist activation of a G_s -coupled receptor and the production of cAMP are in turn attenuated by PKA phosphorylation of both the receptor and desensitizing kinase (Cong *et al*, 2001).

2.3.2.6 AKAP6/AKAP100/KIAA0311/mAKAP

Found in cardiac and skeletal muscle and in the brain, this family of AKAPs are localised to the nuclear membrane (Kapiloff *et al*, 1999) or sarcoplasmic reticulum of cardiomyocytes (McCartney *et al*, 1995; Marx *et al*, 2000) through a region that contains 3 spectrin-like repeat sequences (Kapiloff *et al*, 1999; Colledge & Scott, 1999). mAKAP complexes with PDE4D3 and PKA (Dodge *et al*, 2001) in such a way that upon PKA activation the catalytic subunits from mAKAP-anchored PKA phosphorylate mAKAP-anchored PDE4D3 at one of its PKA phosphorylation sites (S54; the other PKA phosphorylation site being at S13) thus up-regulating the activity of the mAKAP targeted phosphodiesterase. This causes cAMP catabolism leading to a decrease in active PKA levels with the re-formation of the holoenzyme into its

inactive state (Sette & Conti, 1996; Oki *et al*, 2000; Dodge *et al*, 2001). Through *in vitro* and cellular experiments, PKA phosphorylation of S13 on PDE4D3 has been shown to result in an increase in the affinity of PDE4D3 for mAKAP suggesting this PKA phosphorylation site acts to regulate and enhance termination of the mAKAP-anchored PKA signal (Carlise Michel *et al*, 2004).

mAKAP also complexes with ERK5 where this kinase serves to suppress PDE4D3 activity (Dodge-Kafta *et al*, 2005).

2.3.2.7 AKAP7/AKAP18/AKAP15

A low molecular weight anchoring protein that associates with L-type calcium channels (Gray *et al*, 1997). AKAP18 is the human homologue of rabbit AKAP15 (Fraser *et al*, 1998).

2.3.2.8 AKAP8/AKAP95/DKFZp586B1222

Localises to the nuclear matrix via a zinc-finger motif (Coghlan *et al*, 1994; Eide *et al*, 1998).

2.3.2.9 AKAP9/KIAA0803/AKAP350/AKAP450/CG-NAP/AKAP120/YOTIAO

This family of AKAPs are the result of alternative splicing of a single gene on chromosome 7q21 (Schmidt *et al*, 1999; Witczak *et al*, 1999). AKAP350 was the first identified (Keryer *et al*, 1993) followed by AKAP450 (Witczak *et al*, 1999) and CG-NAP (Takahashi *et al*, 1999). For simplicity, these 3 AKAPs are often but not exclusively grouped together as one and referred to as AKAP350/450 or just AKAP350 (Carlise Michel & Scott, 2002). All AKAP350 isoforms exhibit wide tissue distribution; northern blot analysis identified them in the liver, heart, brain, kidney and skeletal muscle (Schmidt *et al*, 1999), and are found localised to centrosomes and golgi (Takahashi *et al*, 1999; Witczak *et al*, 1999; Schmidt *et al*, 1999; Gillingham & Munro, 2000). Here they appear to scaffold PKA, PKC, the Rho-dependent protein kinase PKN, PP1, PP2A and PDE4DE, yet the functional relevance of PKA anchored at these locations is currently unknown (Takahashi *et al*, 2000; Diviani & Scott, 2001; Tasken *et al*, 2001).

Yotiao is the smallest splice variant in this AKAP family at 210kDa and targets PKA

and PP1 to the slow activating potassium channel (KCNQ1-KCNE1, also known as I_{Ks}) in the heart and the NR1A subunit of NMDA receptors in the brain. This signalling complex has been shown to regulate the phosphorylation state, and hence activity, of both the ion channel and receptor (Lin *et al*, 1998; Westphal *et al*, 1999, Marx *et al*, 2002).

2.3.2.10 AKAP10/D-AKAP2

Anchors PKA to co-transporters in the kidney (Burns-Hamuro *et al*, 2004) and to mitochondria (Huang *et al*, 1997b; Wang *et al*, 2001).

2.3.2.11 AKAP11/KIAA0629/AKAP220

Cloned from rat testicular tissue, this AKAP is thought to target PKA and PP1 to peroxisomes in testicular and sperm cells (Lester *et al*, 1996; Schillace and Scott, 1999; Reinton *et al*, 2000). The peroxisomal targeting domain is thought to consist of a cysteine, arginine, leucine motif located at the C-terminus of rat AKAP220 (Keller *et al*, 1991; Lester *et al*, 1996).

2.3.2.12 AKAP12/AKAP250/gravin/SSeCKS

This AKAP is shown to localise predominantly to the perinuclear membrane (Lin *et al*, 1996) as well as the cell periphery (Grove & Bruchey, 2001) and within the nucleus (Streb and Miano, 2005). The identification of such different subcellular locations is possibly due to the presence of different isoforms of AKAP12, namely AKAP250, gravin and SSeCKS.

Gravin interacts reversibly with the β_2 -adrenergic receptor via a region termed the receptor-binding domain (RBD; Shih *et al*, 1999; Fan *et al*, 2001; Tao *et al*, 2003; Wang *et al*, 2006). The RBD resides at the C-terminal tail of the GPCR and appears to be polytopic (i.e. involving multiple parts) in nature (Fan *et al*, 2001). The association between gravin and the β_2 -adrenergic receptor is essential for receptor resensitisation and recycling following agonist-induced activation, desensitisation and internalisation (Shih *et al*, 1999). Like the AKAP5 family, gravin functions to maintain the close proximity of PKA to the β_2 -adrenergic receptor yet unlike AKAP5, gravin's association with the β_2 -adrenergic receptor is increased upon agonist stimulation of the receptor (Tao *et al*, 2003). Indeed, the entire gravin-receptor-kinase complex

appears to be mobile with the AKAP following the internalised β_2 -adrenergic receptor away from the plasma membrane; this is the first example of a mobile AKAP complex (Fan *et al*, 2001).

The question of whether AKAP5 and AKAP12 are expressed in the same cells and hence operate together with the β_2 -adrenergic receptor remains to be answered. They have been shown to both be expressed in HEK293 cells (Lynch *et al*, 2005) and so one might speculate that it is likely to occur in other cells. However, at what levels of expression these two AKAPs may be found is not known and hence the subsequent co-effects on the β_2 -adrenergic receptor cannot be determined at present.

2.3.2.13 AKAP13/Ht31/BRX/AKAP-Lbc

Isolated from a thyroid cDNA library, Ht31 is a peptide analogous to the minimum region of an AKAP required for binding RII, residues 493-515 of the later discovered parent AKAP, AKAP-Lbc (1015-amino acid in length) (Carr *et al*, 1991; Rosenmund *et al*, 1994; Johnson *et al*, 1994; Lester *et al*, 1997). Subsequently this peptide has been frequently used to disrupt PKA-AKAP interactions and hence is a useful tool in AKAP identification. The creation of a cell soluble version of Ht31 by the addition of stearic acid to the N-terminus (Vijayaraghavan *et al*, 1997) has enabled this peptide to be used in an even wider range of experimental conditions.

AKAP-Lbc has been shown to complex PKA, PKC and protein kinase D (PKD; Carnegie *et al*, 2004) as well as acting as a guanine nucleotide exchange factor for the small GTPase Rho. Auto-phosphorylation of this AKAP by anchored PKA alongside simultaneous recruitment of PKC controls the activation and release of the anchored PKD and results in the inhibition of the activity of Rho (Diviani *et al*, 2001; Klussman *et al*, 2001; Carnegie *et al*, 2004).

Synonyms	Tissue	Subcellular Localisation	Proteins in Complex	References
AKAP1, S-AKAP84, AKAP84, D-AKAP1, AKAP121, AKAP149, sAKAP84	Testis, thyroid, lung, liver, kidney, skeletal muscle, heart.	Outer mitochondrial membrane in the cytosol, the postsynaptic membrane in the vertebrate neuromuscular junction, endoplasmic reticulum, sperm midpiece.	Protein kinase A (PKA), Protein Phosphatase-1 (PP1).	Lin <i>et al</i> , 1995; Trendelenburg <i>et al</i> , 1996; Huang <i>et al</i> , 1997a & 1999; Chen <i>et al</i> , 1997; Perkins <i>et al</i> , 2001.
AKAP2, AKAP-KL, KIAA0920, DKFZp564L0716	Kidneys, lungs, thymus, cerebellum.	Actin cytoskeleton, apical membrane of epithelial cells.	PKA.	Dong <i>et al</i> , 1998.
AKAP3, AKAP110, SOB1	Testis.	Localizes to the ribs of the fibrous sheath in the principal piece of the sperm tail.	G ₁₃ α.	Mandal <i>et al</i> , 1999; Vijayaraghavan <i>et al</i> , 1997 & 1999.
AKAP4, p82 Fsc1, hAKAP82, AKAP82	Testis.	Fibrous sheath of the sperm tail.	PKA.	Johnson <i>et al</i> , 1997; Miki <i>et al</i> , 1998; Brown <i>et al</i> , 2003.
AKAP5, AKAP79 (human), AKAP75 (bovine), AKAP150 (rat/mouse)	Brain.	Postsynaptic membrane, plasma membrane, actin cytoskeleton.	PKA, Protein kinase C (PKC), PP2B, N-methyl D-aspartate (NMDA) receptor, α-Amino-3-hydroxy-5-methyl-4-isoxazolepropionic (AMPA) receptor, Postsynaptic protein of 95kDa (PSD-95), Synapse-associated protein-97 (SAP-97), KCNQ2 channel, L-type voltage-gated Ca ²⁺ channel, Aquaporin water channels.	Sarkar <i>et al</i> , 1984; Bregman <i>et al</i> , 1989; Carr <i>et al</i> , 1991 & 1992b; Li <i>et al</i> , 1996; Perry <i>et al</i> , 2002; Baillie <i>et al</i> , 2005; Baillie and Houslay, 2005; Lynch <i>et al</i> , 2005; Coghlan <i>et al</i> , 1995; Klauck <i>et al</i> , 1996; Colledge <i>et al</i> , 2000.
AKAP6, AKAP100, KIAA0311, mAKAP	Heart, brain, skeletal muscle.	Nuclear membrane, sarcoplasmic reticulum.	PKA, Phosphodiesterase 4D3 (PDE4D3).	Kapiloff <i>et al</i> , 1999; McCartney <i>et al</i> , 1995; Marx <i>et al</i> , 2000; Dodge <i>et al</i> , 2001; Yang <i>et al</i> , 1998.

AKAP7, AKAP18, AKAP15	Heart, brain, skeletal muscle, pancreas.	Plasma membrane, cytoplasm, secretory vesicles.	PKA, Voltage- gated Ca ²⁺ channels, Voltage- gated Na ⁺ channels.	Fraser <i>et al</i> , 1998; Gray <i>et al</i> , 1997 & 1998a & b; Klussman <i>et al</i> , 2001.
AKAP8, AKAP95, DKFZp586B1222	Heart, brain, skeletal muscle, pancreas, kidney.	Nuclear matrix, chromosomes.	PKA.	Coghlan <i>et al</i> , 1994; Eide <i>et al</i> , 1998 & 2002; Collas <i>et al</i> , 1999; Steen <i>et al</i> , 2000.
AKAP9, KIAA0803, AKAP350, AKAP450, CG- NAP, AKAP120, Yotiao, Hyperion	Heart, brain, skeletal muscle, pancreas, kidney, skeletal muscle, thymus, spleen, lung, liver, placenta.	Neuromuscular junction, postsynaptic density, centrosomes, golgi.	PKA, PDE4D3, PP1, PP2A, Protein kinase N (PKN), PKC.	Dransfield <i>et al</i> , 1997b; Westphal <i>et al</i> , 1999; Takahashi <i>et al</i> , 1999 & 2000; Witczak <i>et al</i> , 1999; Schmidt <i>et al</i> , 1999; Gillingham & Munro, 2000; Diviani & Scott, 2001; Tasken <i>et al</i> , 2001; Lin <i>et al</i> , 1998; Marx <i>et al</i> , 2002; Carlson <i>et al</i> , 2001; Feliciello <i>et al</i> , 1999.
AKAP10, D-AKAP2	Brain, liver, lung, spleen, kidney.		PKA, mitochondria.	Huang <i>et al</i> , 1997b; Wang <i>et al</i> , 2001; Perkins <i>et al</i> , 2001; Burns- Hamuro <i>et al</i> , 2004.
AKAP11, KIAA0629, AKAP220, hAKAP220	Brain, testis.	Peroxisomes, vesicles, centrosomes.	PKA, PP1, Glycogen synthase-3 β (GSK3 β).	Lester <i>et al</i> , 1996; Schillace & Scott, 1999; Reinton <i>et al</i> , 2000; Schillace <i>et al</i> , 2001.
AKAP12, AKAP250, gravin, SSeCKS (mouse)	Endothelium.	Perinuclear membrane, nucleus, actin cytoskeleton, cytoplasm.	PKA, PKC, β_2 - adrenergic receptor (β_2 -AR).	Lin <i>et al</i> , 1996; Grove & Bruchey, 2001; Streb & Miano, 2005; Shih <i>et al</i> , 1999; Fan <i>et al</i> , 2001; Tao <i>et al</i> , 2003; Gordon <i>et al</i> , 1992 ; Nauert <i>et al</i> , 1997.

AKAP13, Ht31, BRX, AKAP-Lbc, Rt31	Ubiquitous.	Cytoplasm.	PKA, Rho, 14-3-3, PKC, Protein kinase D (PKD).	Carr <i>et al</i> , 1991 & 1992a; Rosenmund <i>et al</i> , 1994; Johnson <i>et al</i> , 1994; Lester <i>et al</i> , 1997; Carnegie <i>et al</i> , 2004; Diviani <i>et al</i> , 2001; Klussman <i>et al</i> , 2001a.
AKAP14, T-AKAP80, ezrin, AKAP78	Testis.	Actin cytoskeleton, cytoplasm, fibrous sheath of sperm tail.	PKA.	Carr <i>et al</i> , 1993; Mei <i>et al</i> , 1997; Sun <i>et al</i> , 2000a & b; Dransfield <i>et al</i> , 1997a.
Microtubule-associated protein-2 (MAP2)	Ubiquitous.	Microtubules.	PKA, Tubulin.	Theurkauf & Vallee, 1982; Lohmann <i>et al</i> , 1984; Herzog & Weber, 1978; Davare <i>et al</i> , 1999; Sarkar <i>et al</i> , 1984.
Pericentrin	Ubiquitous.	Centrosomes.	PKA, Dynein, γ -tubulin.	Nigg <i>et al</i> , 1985; De Camilli <i>et al</i> , 1986; Diviani <i>et al</i> , 2000.

Table 1. A Kinase Anchoring Proteins. Taken and adapted from Tasken & Aandahl, 2004; Wong & Scott, 2004.

2.3.2.14 AKAP14/TAKAP80

Found cytoplasmically in granulosa cells and in the fibrous sheath of the sperm tail (Carr *et al*, 1993; Mei *et al*, 1997).

2.3.2.15 MAP2

The microtubule-associated protein-2 (MAP2) family of proteins (MAP2A, MAP2B and MAP2C) are components of the neuronal cytoskeleton and are responsible for microtubule stabilisation, regulating organelle transport and anchoring signalling enzymes such as PKA (Theurkauf & Vallee, 1982; Sanchez *et al*, 2000). MAP2B has been shown to bind directly to class C L-type calcium channels *in vivo*, anchoring PKA close to channel phosphorylation sites (Davare *et al*, 1999).

2.3.2.16 *Pericentrin*

The centrosome is responsible for microtubule nucleation; pericentrin is a highly conserved centrosomal protein. Whilst the centrosome has long been recognised to bind PKA (Nigg *et al*, 1985; De Camilli *et al*, 1986), it is only relatively recently that the role of pericentrin in centrosomal PKA binding has been established (Diviani, *et al*, 2000). Interestingly, unlike conventional AKAPs, pericentrin binds PKA through a novel binding domain of 100 amino acids, rather than the 20 amino acids usually required, yet pericentrin is recognised by the standard AKAP binding site on regulatory subunit of PKA. The role played by pericentrin anchored PKA directed to centrosomal substrates is currently unknown.

2.3.3 *Direct Interaction between AKAPs and Ion Channels*

Although membrane tethering ensures close proximity of certain AKAP protein complexes to key integral membrane substrates, certain AKAPs also directly bind to these substrates thereby allowing more specific orientation of the signalling complex (Carnegie & Scott, 2003). As discussed above, receptors and ion channels represent an important group of kinase substrates and consequently AKAPs are involved in both rapid signal transduction via the regulation of ion channel currents and slower processes such as transcriptional regulation (Colledge & Scott, 1999). The mechanism/s by which AKAPs and ion channel proteins associate are still poorly understood, the current knowledge is detailed here.

2.3.3.1. *Glutamate Receptors*

NMDA and AMPA-type ionotropic glutamate receptors are found at the post-synaptic density in macromolecular signalling complexes with two classes of binding proteins, namely AKAPs and membrane-associated guanylate kinase (MAGUKs; Colledge *et al*, 2000). Through various protein-protein interactions AKAP79/150, PSD-95 and SAP97 play an important role in scaffolding PKA and PP2B/CaN close to these receptors thereby allowing efficient regulation of receptor activity, receptor trafficking and receptor endocytosis; phenomena linked to the induction and maintenance of long-term potentiation (LTP) and long-term depression (PTD; Colledge *et al*, 2000; Gomez *et al*, 2002). There is currently no data showing that AKAP79 directly binds to any of the glutamate receptors, instead all evidence points to the SH3 and GK

regions of the MAGUKs mediating AKAP binding to the PSD and glutamate receptors (Colledge *et al*, 2000).

2.3.3.2 L-type Ca channel & KCNQ1-KCNE1

In contrast to the polytopic gravin binding site on the β_2 -adrenergic receptor (Fan *et al*, 2001), the L-type Ca^{2+} channels, $\text{Ca}_v1.1/2$, and the delayed rectifier K^+ channel, KCNQ1-KCNE1, bind their respective AKAPs via leucine zipper motifs (Hulme *et al*, 2002 & 2003; Marx *et al*, 2002).

In the standard leucine zipper motif, leucine residues repeat every seventh amino acid, position d , and segments containing this motif exist in an α -helical conformation (Landschulz, 1988). However there are increasing numbers of reports where the leucine zipper motif contains residues other than leucine at position d , for example isoleucine or valine. Irrespective of type, residues at position d line up on one face of the α -helix (3.5 residues/turn) and allow oligomerisation with other coiled coil helices. Breaks in the heptad repeat are likely to disrupt the coiling and hence oligomerisation.

$\text{Ca}_v1.1$ (and possibly other Ca_v1 channels) utilizes a modified form of the motif at its C-terminus to bind the small membrane-associated AKAP15 (Hulme *et al*, 2002 & 2003). Mutagenic disruption of the modified leucine zipper motif suppresses AKAP15-ion channel binding and consequently reduces the PKA-dependent potentiation of skeletal muscle calcium channels.

The 210kDa AKAP, yotiao, binds to the C-terminus of KCNQ1-KCNE1 on the subunit hKCNQ1 via a leucine zipper motif and forms a complex with PKA and protein phosphatase 1 (PP1), thereby ensuring modulation of the channel upon activation of the β -adrenergic receptor (Marx, *et al*, 2002). Interestingly, a mutation within the yotiao binding site on hKCNQ1 (hKCNQ1-G589D) that occurs in long QT syndrome, disrupts the interaction between PKA, PP1 and effectively uncouples the ion channel from sympathetic modulation. It has been suggested that this may explain the high incidence of exercise-related fatal cardiac arrhythmias in long QT sufferers.

In addition to acting as an adapter protein by targeting PKA and PP1 to this slow

activating potassium channel, yotiao is thought to also serve a regulatory role in KCNQ1-KCNE1 activity (Chen & Kass, 2006). The results from studies mutating serine 27 (the PKA phosphorylation site in the amino terminus of KCNQ1) and the yotiao-binding site on KCNQ1 imply that yotiao is required not only for recruiting the appropriate kinase and phosphatase machinery to regulate channel phosphorylation, but also translates the phosphorylation-induced change into alteration of channel activity as it is itself subject to PKA phosphorylation following receptor stimulation (Chen *et al*, 2005; Chen & Kass, 2006).

2.3.3.3 M-type (KCNQ2/3) Potassium Channels

Originally known as M-type potassium channels, KCNQ channels are responsible for low-threshold, slow-activating potassium currents that are suppressed by activation of $G_{q/11}$ -coupled receptors (Brown *et al*, 1988; Marrion, 1997). Regulation of these channels is also dependent upon their phosphorylation state, with PKC and the calcium-dependent phosphatase calcineurin (PP2B) likely to be involved. In relation to this, AKAP150, which anchors PKC and PP2B along with PKA, has been shown to bind directly to KCNQ potassium channels at their C-terminus (Hoshi *et al*, 2003). To date nothing is known about the structural basis of this interaction.

2.3.3.4 Calcium-Activated Potassium Channels

Calcium-activated potassium channels are regulated through phosphorylation by several protein kinases, with results depending on cell type (Kume *et al*, 1989; Carl *et al*, 1991; Perez & Toro, 1994; Robertson *et al*, 1993). In airway smooth muscle cells Ht31 (the synthetic peptide of residues 493-515 of the human thyroid AKAP frequently used to disrupt the binding of PKA to the endogenous AKAP), but not Ht31-P (the inactive form of Ht31), prevented ATP-induced stimulation of the channel, thus suggesting the requirement of an AKAP to localise phosphorylation machinery close to the ion channel phosphorylation sites (Wang & Kotlikoff, 1996). It remains to be determined which AKAP is involved in the regulation of calcium-activated potassium channel activity, or indeed whether there is direct interaction between AKAP and channel.

2.3.3.5 Inwardly Rectifying Potassium Channels

Finally, and with particular relevance to this study, it has been shown that cAMP-

dependent modulation of whole-cell currents of the inwardly rectifying potassium channel, Kir2.1, requires the presence of the multivalent anchoring protein, AKAP79, and that Kir2.1 and AKAP79 exist together in a complex within intact cells (Dart & Leyland, 2001). Inwardly rectifying potassium (Kir) channels have been shown to serve a variety of physiological functions, ranging from maintaining the resting membrane potential and the pacing of both cardiac myocytes and neurones, to the pancreatic regulation of insulin secretion and renal K⁺ transport (Hille, 2001). As their name suggests, inwardly rectifying potassium channels favour the conduction of potassium ions into the cell, rather than out, a phenomenon has been ascribed to the reversible occlusion of the channel pore by intracellular magnesium (Vandenberg, 1987; Matsuda *et al*, 1987) and positively charged intracellular spermine and spermidine (Fakler *et al*, 1994 & 1995; Lopatin *et al*, 1994 & 1995; Ficker *et al*, 1994; Lu and MacKinnon, 1994, Wible *et al*, 1994). The activity of Kir channels can be regulated by: phosphorylation via serine/threonine and tyrosine kinases (Xu *et al*, 1996), phospholipids e.g. phosphatidylinositol 4,5 bisphosphate (Zhang *et al*, 1999) and G-proteins (Clapham, 1994; Dascal, 1997), although much of the data concerning the modulation of channel activity has been found to be conflicting and contradictory. It has been suggested, for example, that normal Kir2.1 channel function requires constant PKA phosphorylation (Fakler *et al*, 1994; Ruppertsberg & Fakler, 1996). PKA has also been reported to: enhance (Dart & Leyland, 2001; Monaghan *et al*, 1999), inhibit (Wischmeyer & Karschin, 1996; Koumi *et al*, 1995a/b) and even not be required at all (Jones, 1996; Kamouchi *et al*, 1997) for Kir2.1 channel function. The reasons for these variations are unknown, but may reflect the lack of appropriate signalling/phosphorylation machinery within the systems studied.

3 Scope of Thesis

In summary, AKAPs have been implicated in optimising the speed, selectivity and specificity of signal transduction by targeting PKA and many other signalling proteins in close vicinity to their substrates. What ultimately drives the preferential assembly of each AKAP with its specific signalling machinery is still currently unknown. One theory suggests is that it is the initial binding event between the AKAP and its target substrate, resulting in a series of conformational changes that signals the recruitment of the signalling enzymes (Smith *et al*, 2006).

The aim of this thesis is to investigate the different methods used by this structurally diverse family of proteins in targeting their associated signalling proteins to appropriate intracellular locations. Mechanisms involved in the regulation of subcellular targeting of AKAP79 to the plasma membrane are explored in Chapters 3 and 4; while a study of direct AKAP79 binding to the inwardly rectifying potassium channel, Kir2.1, forms the basis of Chapters 5 and 6.

CHAPTER TWO

METHODS & MATERIALS

1 Cell Culture

1.1 Routine Maintenance of Cell Lines

Human embryonic kidney (HEK) 293 cells were routinely cultured in Dulbecco's Eagle minimal essential medium (MEM) with Glutamax-1, supplemented with 10% foetal calf serum and 1% non-essential amino acids (NEAA) and kept at 37°C in 5% CO₂ humidified air. No antibiotics were used. Cells were routinely passaged twice a week; washing confluent cells with warm PBS and splitting them 1:10 with trypsin-EDTA (1ml/80cm² flask) to lift the cells. Cells were not used beyond passage 50.

Stable cell line HEK293-AKAP79, made in-house using the standard protocol, were routinely cultured as wildtype HEK293 cells with the addition of 1% geneticin (selection antibiotic) in the media.

HEK293/M₃ cells, a kind gift from Dr. G. Willars (University of Leicester, UK) (Tovey and Willars 2004), were cultured in MEM with Glutamax-1, supplemented with 10% foetal calf serum, 1% non-essential amino acids and gentamicin (50µg/ml) and kept at 37°C in 5% CO₂ humidified air. Cells were received at an unknown passage number, therefore in our hands cells were not used for more than 20 passages.

All media and reagents used in cell culture were purchased from Invitrogen, unless otherwise stated.

1.2 Cell Adhesion

HEK293 cells do not adhere strongly to plastic or glassware thus many cells can be lost during assays that require repeated washing. To prevent this poly-L-lysine (500µl/22mm coverslip) was added to the surface of the plastic or glass, left at room temperature for a minimum of 5 minutes, aspirated off and left to air-dry for 30 minutes prior to plating the cells as described above.

2 Transient Transfections

HEK293 and HEK293-AKAP79 cells were grown to ~80% confluency and HEK293/M₃ cells grown to ~50% confluency for transfection with Lipofectamine 2000 (Invitrogen), following manufacturer's instructions. In brief, 24 hours before transfection the cells were seeded into the appropriate flask or 6/12-well plate. On the day of transfection, Lipofectamine 2000 reagent¹ was diluted in OPTI-MEM I medium¹ and incubated at room temperature for 5 minutes. Meanwhile the DNA² was diluted in OPTI-MEM I medium¹. The diluted DNA and Lipofectamine 2000 reagent were then mixed together and incubated at room temperature for 20 minutes. The DNA-Lipofectamine 2000 reagent complexes were then added directly to the cells, gently mixed by rocking and returned to the incubator. The cells were used 24-48 hours post-transfection.

If the cells to be transfected were grown in media containing antibiotics, the media was changed and cells washed twice with media without antibiotics.

	6-WELL PLATE	12-WELL PLATE
Number of Cells	5 x 10 ⁵	2 x 10 ⁵
Volume of Media in Well	2ml	1ml
Lipofectamine 2000 Reagent: OPTI-MEM I medium	4μl:100μl	1.6μl:40μl
Plasmid DNA: OPTI-MEM I medium	Dependent on assay ² :100μl	Dependent on assay ² :40μl

Table 2. Conditions for transient transfection

¹ Details of the specific concentrations of plasmid DNA, Lipofectamine 2000 reagent and OPTI-MEM I medium can be found in table 2.

² Specific concentrations of DNA used in transfections shown in table 3.

cDNA	Concentration	Source
pIRES2-EGFP-F	6µg/coverslip	Kind gift from Dr. D. Lodwick
R11α-EGFP	2.2µg/well – for characterisation studies 0.22µg/well – for co-immunoprecipitation studies	Constructed in-house
pEGFP-N1	2.2µg/well	Clontech
pcDNA3-AKAP79	2.2µg/well	Kind gift from Prof. J. Scott
EGFP-PH _{PLCγ}	2µg/coverslip	Kind gift from Dr. J. Willets
EGFP-Kir2.1 ³	2.4µg/well – for co-immunoprecipitation studies 100ngµg/well – for electrophysiology	Kind gift from Dr. M. Leyland
EGFP-Kir2.2	2.4µg/well	Dr. Y. Kurachi, Osaka University, Japan
EGFP-Kir2.3 ⁴	2.4µg/well	Kind gift from Dr. M. Leyland
pIRES2-(182-232)-EGFP	2µg/well	Constructed in-house

Table 3. Concentration of cDNA used in transient transfections.

3 Immunocytochemistry

Cells (either HEK293 wildtype or HEK293-AKAP79) were seeded onto Poly-L-Lysine coated 19mm glass coverslips (prepared as described above) in normal growth media for 24 hours prior to transient transfection if required, with appropriate cDNA. 24 hours post-transfection cells were rinsed gently with PBS to remove any residual media before being permeabilised and fixed with 300µl ice-cold methanol then chilled to -20°C for 7 minutes. Coverslips were then washed 3 x 10 minutes before a brief incubation in PBS with 10% goat serum at room temperature followed by incubation overnight at 4°C with appropriate primary antibody diluted 200-fold in PBS with 10% goat serum. The following day the coverslips were washed 6 x 10 minutes with PBS, then incubated with goat secondary antibody conjugated with the fluorophore Texas Red (TxR) diluted in PBS + 10% goat serum for two hours at room temperature. Coverslips were washed 3 x 10 minutes and mounted onto microscope slides using anti-fluorescent mounting medium (Dako Ltd) before viewing. Confocal images were obtained using a PerkinElmer Ultraview™ imaging system with EGFP and TxR

³ Lavine *et al*, 2002 found that addition of an epitope tag to Kir channels did not affect functional channel assembly.

⁴ Kir2.3 is inserted between the *XhoI* and *BamHI* sites of pEGFP-C3.

excited using the 488nm and 600nm laser lines respectively. Emitted fluorescence was captured at 507nm for EGFP and 620nm for TxR.

4 Subcellular Fractionation

To assess the subcellular distribution of AKAP79 in HEK293-AKAP79 cells, methods were taken and adapted from Dell'Acqua *et al*, 1998. In brief, cells were grown to confluency in 175cm² tissue culture flasks, 1 flask/treatment, washed briefly with ice-cold PBS and incubated for 5 minutes in hypotonic lysis buffer (as described in Dell'Acqua *et al*, 1998; 200µl Triton X-100/100ml buffer, 20mM HEPES pH 7.4, 20mM NaCl, 5mM EDTA, 10µl protease inhibitor cocktail*/1ml buffer (*added fresh on day of experiment)). The lysed cells were then harvested and homogenised in a hand-held homogeniser (10 strokes) before being fractionated into soluble and insoluble fractions by centrifugation at 40,000g, 70,000g or 100,000g⁵ in a Beckman TL-100 tabletop ultracentrifuge using a TLA 100.3 rotor for 30 minutes. The supernatant (soluble) fraction was removed and stored on ice while the remaining pellet (insoluble) fraction was washed briefly with PBS and resuspended in 500µl hypotonic lysis buffer before protein content of both fractions was assessed using the Bradford Protein Assay. Equal levels of protein of both soluble and insoluble fractions were loaded and subsequently separated by SDS-polyacrylamide gel electrophoresis, transferred onto nitrocellulose and blotted with anti-AKAP79, anti-ERK1, anti-actin, anti-filamin or anti-calreticulin.

5 Western Blotting

All materials used in Western blotting were purchased from Sigma unless otherwise stated.

5.1 Polyacrylamide Gel Electrophoresis & Immunoblotting

Polyacrylamide gel electrophoresis was carried out as previously described (Dart & Leyland, 2001). Using the Mini-PROTEAN 3 electrophoresis system (Bio-Rad) protein extracts were resolved by SDS-polyacrylamide gel electrophoresis on 4%

⁵ The centrifuge speed was set in rpm therefore it was necessary to use the following equation:

$$\text{rpm} = 1000\sqrt{(g+11.17r)}$$

where g is the unit of acceleration and r is the radius of the rotor used.

SDS-polyacrylamide stacking⁶; 10% SDS-polyacrylamide resolving⁶ 0.75mm thick gels, run at 120mV for approximately 1 hour in running buffer (20mM Tris base, 186.5mM glycine, 17.1mM SDS per litre distilled water). Proteins were transferred electrophoretically onto nitrocellulose membranes (Hybond™ ECL™; Amersham) at 100mV for approximately 1 hour in transfer buffer (25mM Tris-base, 192mM Glycine, 20% v/v methanol) using wet transfer apparatus (Bio-Rad). Membranes were then blocked overnight at 4°C in a Tris-buffered solution (TBST) (20mM Tris-base, 137mM NaCl, 0.1% (v/v) Tween 20) containing 5% (w/v) Marvel skimmed milk powder. Membranes were incubated for 2 hours at room temperature with primary antibodies diluted in a TBST solution containing 1% (w/v) skimmed milk powder. Membranes were washed 3 x 10 minutes in TBST solution prior to 1 hour incubation at room temperature with horseradish peroxidase-conjugated secondary antibody diluted in a TBST containing 1% (w/v) skimmed milk powder. Labelled bands were visualised using enhanced chemiluminescence (ECL; Amersham Pharmacia Biotechnologies) followed by exposure to light-sensitive film (Hyperfilm™ ECL™; Amersham).

6 AKAP79 Phosphorylation & Release Assay

HEK293-AKAP79 cells in 175cm² tissue culture flasks were grown to ~90% confluency then serum starved in MEM with Glutamax-1, supplemented with NEAA and geneticin and without foetal calf serum, for 3 hours prior to agonist stimulation. To induce PKA phosphorylation, cells were stimulated by adding 40µM forskolin⁷ (rapid activator of adenylyl cyclase) to the media with 250µM 3-Isobutyl-1-methylxanthine⁷ (IBMX; a cAMP phosphodiesterase inhibitor) and 100nM okadaic acid⁷ (a specific inhibitor of phosphoserine/threonine protein phosphatase 1 and 2a). For PKC phosphorylation, the cells are treated with 100nM Phorbol-12-Myristate-13-Acetate⁷ (PMA; a PKC activator) plus 100nM okadaic acid. After 20 minutes incubation in 37°C, 5% CO₂ humidified air the media was removed and the cells washed in ice-cold PBS prior to lysis with 2ml/flask hypotonic lysis buffer (containing the phosphodiesterase and phosphatase inhibitors at the same concentrations as that used to treat the cells) for 5 minutes over ice. Cells were scraped off the flask bottom and homogenised as described above. The samples were then fractionated

⁶ See appendix 1 for composition of stacking and resolving buffers

⁷ All batches of drugs were purchased fresh from Calbiochem, diluted in DMSO, aliquoted and stored as a stock for a maximum of 4 weeks at -20°C according to manufacturer's data sheet. Drugs were freshly made up in PBS immediately prior to use.

at 100,000g for 30 minutes in a Beckman TL-100 tabletop ultracentrifuge with a TLA 100.3 rotor, equal amounts of protein loaded and resolved by SDS-PAGE and transferred electrophoretically onto nitrocellulose membrane and analysed by immunoblotting with anti-AKAP79 as previously described.

7 Extraction & Separation of [³H]-(poly) Phosphoinositides

Measurement of PtdIns, PtdIns(4,5)P and PtdIns(4,5)P₂ levels were prepared from cell monolayers following the removal of the acidified aqueous phase used to determine [³H]InsP_x (data not shown) as described previously (Jenkinson *et al*, 1994). In brief, any residual aqueous material was removed from HEK293-AKAP79 cells, previously incubated with 2.5µCi ml⁻¹ *myo*-[³H]-inositol for 48hrs, and lipids extracted by addition of 0.5ml/well acidified chloroform/methanol (CHCl₃:CH₃OH:conc HCl, 40:80:1 v/v/v). The cells were then scraped off the well and duplicates pooled into 4ml polypropylene/solvent resistant tubes. To induce phase partition, 0.31ml chloroform then 0.56ml 0.1M hydrochloric acid was added before vortexing to mix and subsequently centrifuging at 1,000g for 15 minutes. This gave 2 distinct phases; the top aqueous phase was removed and discarded and 400µl of the lower phase removed, dried in a stream of N₂ and stored at -20°C prior to further processing. Samples were then dissolved in 1ml chloroform and 200µl methanol before hydrolysis with 400µl of 0.5M NaOH in methanol/water (19/1 v/v) and a subsequent 20 minute incubation at room temperature with regular vortexing. An additional 1ml chloroform, 600µl methanol and 600µl water were added to samples, mixed and then centrifuged at 13,000rpm for 10 minutes. Again, two phases were produced where 1ml of the upper phase containing the phosphates as deacylation products, was neutralised by passage through a 1ml bed volume Dowex-50 column. The column was washed twice with 2ml water. The eluate was pooled and brought to pH7 using NaHCO₃ and subsequently added to Dowex (AG1-X8) formate anion exchange columns. The following fractions were collected as previously described (Downes & Wusteman, 1983) where PtdIns was collected by addition of 2x6ml 60mM ammonium formate/5mM disodium tetraborate, PtdIns(4,5)P was collected by addition of 2x6ml 400mM ammonium formate/ 100mM formic acid and PtdIns(4,5)P₂ was collected by addition of 4 x 3ml 1M ammonium formate/ 100mM formic acid. Radioactivity was determined and quantified by liquid scintillation spectrometry.

8 Re-distribution of AKAP79 Upon PtdIns (4,5)P₂ Depletion

HEK293-AKAP79 cells were seeded onto Poly-L-Lysine coated 19mm glass coverslips (prepared as described above) in normal growth media for 24 hours prior to transient transfection with 6µg/coverslip of pIRES2-EGFP-F. 24 hours post-transfection 10µM wortmannin and 300µM carbachol was added to the cells and returned to 37°C, 5% CO₂ humidified air for 30 minutes to induce PtdIns (4,5)P₂ depletion. Cells were then fixed and permeabilised with ice-cold methanol and imaged using confocal microscopy as described previously.

9 Real-Time Study of AKAP79 Localisation

9.1 Construction of RII α -EGFP

The N-terminal region of PKA RII α is responsible for binding anchoring proteins and subunit dimerisation (Hausken, Coghlan et al. 1994; Hausken and Scott 1996). Although the C-terminus region of PKA RII α contains the cAMP domains, it was deemed most appropriate to tag PKA RII α at the C-terminus. This is because we are using PKA RII α to investigate AKAP distribution and hence we wish to retain its ability to complex with AKAPs. The PKA RII α expression construct in pET-28b was a generous gift from J. Scott (Vollum Institute, Portland, Oregon). The RII α -EGFP fusion construct was produced as previously described (Leyland et al, 1999) where in brief, PKA RII α was PCR amplified from pET-28b using oligonucleotides that incorporated *Xho* and *Sac II* restriction sites into the product. The RII α product was subcloned into the pCR[®]-Blunt vector and sequenced. Upon confirmation of the correct sequence the RII α product was digested out of the subcloning vector, using *Xho* and *Sac II*, run on a 10% agarose gel and the band corresponding to RII α was cut out, purified and sub-cloned in-frame between the *Xho* and *Sac II* restriction sites of the pEGFP-N1 vector (BD Biosciences).

9.2 Expression and Characterisation of RII α -EGFP

HEK293-AKAP79 cells were seeded into 6-well plates and grown to ~80% confluency prior to transient transfection with RII α -EGFP cDNA or empty vector pEGFP-N1. 24 hours post-transfection cells were lysed in 500µl/well ice-cold lysis buffer (1M Tris-HCl, 250mM NaCl, 3mM EDTA, 3mM EGTA, 500µl Triton-X) with 10µl ml⁻¹ protease inhibitor cocktail (containing 4-(2-aminoethyl)benzenesulfonyl

fluoride (AEBSF), pepstatin, E-64, bestatin, leupeptin and aprotinin; Sigma) on ice for 5 minutes then centrifuged for 5 minutes at 4°C. Samples were mixed with 2x sample buffer (Sigma) in a 1:1 ratio and proteins separated by SDS-PAGE, transferred onto nitrocellulose membranes and membranes immunoblotted with either rabbit polyclonal anti-GFP (Santa Cruz) or mouse anti-PKA_{R11α}.

10 Co-immunoprecipitation

HEK293 cells were seeded into six-well plates, left for 24 hours to reach ~80% confluency then transiently transfected with the appropriate cDNA with 2 wells/construct transiently transfected hence ~ 10×10^5 cells/condition. Twenty four hours post-transfection, cells were briefly washed in PBS then lysed in ice-cold mammalian lysis buffer (containing 1M Tris-HCl, 250mM NaCl, 3mM EDTA, 3mM EGTA, 500μl Triton-X 100 and protease inhibitor cocktail (contains 4-(2-aminoethyl)benzenesulfonyl fluoride (AEBSF), pepstatin, E-64, bestatin, leupeptin and aprotinin) (1:100), and pelleted by centrifugation at 13,000rpm at 4°C, in a tabletop microcentrifuge. Approximately 50μl of dilute lysate was diluted ten-fold in lysis buffer and mixed with 50μl 2x sample buffer, heated at 95°C for five minutes and frozen until required. Immunoprecipitation was performed as previously described (Dart & Leyland, 2001). In brief, 5μg of primary antibody (either rabbit anti-GFP or mouse anti-AKAP79) or non-immune control serum (either rabbit or mouse respectively) was added to 360μl of cleared lysate and incubated with gentle inversion for approximately eighteen hours at 4°C. Protein A or A/G beads (Perbio) (approximately 60μl of bead mix) were washed 3 times in ice-cold PBS and added to the antibody/lysate mix and incubated for a further 2 hours at 4°C with gentle inversion. The protein-coupled agarose beads were pelleted by centrifugation and washed 5 times in ice-cold PBS. Immunoprecipitated beads were diluted in an equal volume of 2x sample buffer and heated at 95°C for 5 minutes. Immunoprecipitated proteins were then separated by SDS-polyacrylamide gel electrophoresis and subsequently analysed by immunoblotting as described above where membranes containing anti-GFP immunoprecipitated proteins were immunoblotted with anti-AKAP79 and membranes containing anti-AKAP79 immunoprecipitated proteins were immunoblotted with anti-GFP.

11 Live Confocal Imaging

HEK293 cells were seeded on Poly-L-Lysine coated, 19mm glass coverslips in normal growth media for 24 hours prior to transient transfection with appropriate cDNA. Twenty-four hours after transient transfection, the coverslips were examined on a confocal microscope with a constant perfusion of KREBS buffer (10mM HEPES, 4.2mM NaHCO₃, 10mM Glucose, 1.18mM MgSO₄·7H₂O, 1.18mM KH₂PO₄, 4.69mM KCl, 118mM NaCl, 2mM CaCl₂·2H₂O) at a temperature of 37°C. Confocal images were obtained using a PerkinElmer Ultraview™ imaging system with EGFP excited using the 488nm laser line.

12 Muscarinic Receptor Expression

Muscarinic receptor density in intact HEK293-AKAP79 cells was determined by 1-[N-methyl-³H]scopolamine methyl chloride (a muscarinic antagonist) binding as described in Willars *et al*, 1998. Where in brief, cells plated in a 24-well plate were grown to almost maximal confluency, media removed, cells washed and incubated at 37 °C for 1 hour in 1 ml of Krebs/Hepes buffer (10mM Hepes, 4.2mM NaHCO₃, 11.7mM glucose, 1.2mM MgSO₄, 1.2mM KH₂PO₄, 4.7mM KCl, 118mM NaCl 1.3mM CaCl₂, pH 7.4) containing a saturating concentration of 7nM [³H]NMS. Non-specific binding was determined by addition of 10 μM atropine. Cells were then quickly washed 2 x 1 ml of ice-cold Krebs/Hepes buffer and digested with 0.5 ml of 0.1 M NaOH before being neutralized with 0.5 ml of 0.1 M HCl and muscarinic density determined through detection of ³H by liquid-scintillation spectroscopy in 5 ml of Floscint IV.

13 Real-Time AKAP79 Re-distribution by PtdIns (4,5)P₂ Depletion

The PH domain of PLCδ1 binds to PtdIns(4,5)P₂ and as such may be used to monitor the location of this phosphoinositide in intact cells.

HEK293/M₃ cells were seeded on Poly-L-Lysine coated, 19mm glass coverslips in normal growth media for 24 hours prior to transient transfection with either 2μg EGFP-PH_{PLCδ1} or 2μg RIIα-EGFP encoding cDNA. Twenty-four hours after transient transfection, the coverslips were examined on a confocal microscope with a constant perfusion of KREBS buffer (10mM HEPES, 4.2mM NaHCO₃, 10mM Glucose,

1.18mM MgSO₄·7H₂O, 1.18mM KH₂PO₄, 4.69mM KCl, 118mM NaCl, 2mM CaCl₂·2H₂O) at a temperature of 37°C (5 ml min⁻¹) to identify positively transfected cells i.e. eGFP-PH_{PLCδ1} containing green cells. Once a field of view containing several cells had been identified, a perfusion cycle of KREBS buffer for 30 seconds, 10μM wortmannin/300μM carbachol-containing KREBS buffer for 1 minute and a 3 minute wash-out with KREBS buffer commenced.

Confocal images were obtained using a PerkinElmer Ultraview™ imaging system with EGFP excited using the 488nm laser line. Depletion in PtdIns(4,5)P₂ levels was detected by measuring the translocation of eGFP-PH_{PLCδ1} from the plasma membrane into the cytosol by creating a cytosolic region of interest just under the plasma membrane. Any movement of PtdIns(4,5)P₂ away from the membrane would enter this region of interest. Likewise, any translocation of RIIα-EGFP, and hence AKAP79, away from the membrane would also be detected in a similar fashion. Data was represented graphically as the average pixel intensity in that region versus time, expressed in arbitrary fluorescent units (AFU).

14 Identification of the AKAP79 Binding Site on Kir2.1

14.1 Construction of GST Fusion Proteins

14.1.1 Method 1

Specific oligonucleotide primers with unique restriction sites (*BamH1* and *Xho*) were designed (see appendix 2) (Invitrogen) to allow amplification by PCR of residues 182-282, 283-428, 182-232 and 233-282 from the cDNA encoding the full-length of Kir2.1.

DNA was amplified using 50ng wildtype Kir2.1 template DNA (pcDNA3-Kir2.1), 1μg of each primer, 1μl of 10mM dNTPs (a mix of all four dNTPs, each at a final concentration of 10mM; Invitrogen), 5μl 10x buffer (from Bio-X-Act Long DNA polymerase kit, Bionline), 1.5μl of 50mM MgCl₂, 38.5μl of sterile dH₂O and 1μl Bio-X-Act Long Polymerase (Bionline). A 40μl layer of mineral oil (Sigma) was overlaid on each sample to prevent any evaporation. The samples were put into a Biometra PCR machine and cycled 25 times at: 94°C for 1 minute; 55°C for 1 minute and 68°C for 0.05 seconds for each base to be amplified. The PCR machine was then held at 68°C for a further 10 minutes. PCR products were purified (StrataPrep Stratagene)

to remove residual mineral oil, dNTPs and excess primer, and analysed by agarose gel electrophoresis on 1.7% TAE (Tris-Acetate-EDTA) gel (50ml TAE, 0.85g agarose, 2 μ l ethidium bromide), run at 90mV for 45 minutes. Upon confirmation of amplification of the Kir2.1 C fragment, a thymine was added to the adenine-overhang produced by the Bio-X-Act non-proof reading enzyme (Bioline) and the PCR products ligated separately into the pCR[®]-Blunt vector (Invitrogen) and transformed into One Shot TOP10 (Invitrogen) bacterial cells using the standard 42°C heat shock technique. They were subsequently plated out onto Luria Bertani (LB) agar (Sigma) plates containing ampicillin (50 μ g/ml; Sigma), and incubated overnight at 37°C. Cultures of 12ml of LB broth (Sigma), containing ampicillin (50 μ g/ml), were inoculated with single colonies from these agar plates and placed in a 37°C, shaking (225rpm) incubator overnight. Glycerol stocks were subsequently produced by the addition of 900 μ l of bacterial broth to 600 μ l of 50% glycerol (Sigma) and stored -80°C until required. The bacteria were then pelleted at 5,000rpm for 5 minutes at 4°C in a benchtop centrifuge and DNA purified by Wizard[®] Plus SV miniprep (Promega) according to manufacturer's protocol. To identify which samples contain cDNA encoding vector plus insert, all samples were double digested with *Bam*H1 and *Xho* and analysed by agarose gel electrophoresis. All positive samples were verified by automated sequencing (PNAOL facility, University of Leicester) and analysed using Chromas, version 1.45. Positive samples, where the correct sequence had been incorporated into the pCR[®]-Blunt, were digested with *Bam*H1 and *Xho* and subcloned, in frame, into the pGEX-6P-1 bacterial expression vector before analysis by agarose gel electrophoresis.

14.1.2 Method 2

Further GST fusion protein constructs were needed to map the AKAP79 binding site on Kir2.1. However here, as the Kir2.1 fragments required were smaller than 50bp, the DNA was amplified under alternative conditions from those outlined above. In collaboration with Dr. M. Hills (then of Department of Genetics, University of Leicester) 50ng of full length Kir2.1 was PCR amplified with 1 μ g of each primer (see appendix 2), 0.05 U μ l⁻¹ *Taq* polymerase (ABgene), 1x PCR buffer (kept as an 11x stock; 45mM Tris-HCl pH 8.8, 11mM (NH₄)₂SO₄, 4.5mM MgCl₂, 6.7mM β -mercaptoethanol, 4.4mM EDTA, 1mM dATP, 1mM dCTP, 1mM dGTP, 1mM dTTP and 113 μ g/ml BSA) (Jeffreys *et al*, 1988), and an additional 0.085 μ l 2M Tris-HCl pH

9 and $0.05\mu\text{l}^{-1}$ of a 20:1 mix of Taq polymerase and cloned Pfu polymerase (Stratagene). For PCR under these conditions, initial denaturation was 94°C for 30 seconds followed by 35 cycles of: 94°C for 15 seconds; 57°C for 40 seconds; 70°C for 30 seconds. All these PCR reactions were carried out using a Biometra PCR machine.

Samples were then separated by agarose gel electrophoresis on a 4% Nuseive (SeaKem) gel and the band of interest identified using a hand held UV wand. A thin channel was cut out directly in front of and behind the appropriate band using a clean scalpel. Dialysis membranes, previously prepared by cutting to the approximate size of the channels and boiled in 1 x TE (10mM Tris, 1mM EDTA) for 10 minutes, were fed into the channels and tucked under the gel, such that the membrane in front of the band of interest would capture the DNA and the membrane behind would prevent larger contaminants also being electro-eluted. The gel was run at 3.33V cm^{-1} and progress was monitored by observing fluorescence of the ethidium bromide stained DNA with a UV wand until the entire sample had electro-eluted onto the membrane. With the continuous application of the current, the membrane was then smoothly removed from the gel and a corner trapped in the lid of a 1.5ml microcentrifuge tube. Separation of the DNA-containing solution from the membrane was achieved by centrifugation at 13,000rpm for 1 minute. The membrane was washed in $15\mu\text{l}$ of distilled water to remove any residual sample and centrifuged for a further 5 minutes in order to pellet any remaining agarose. The eluate was transferred to a fresh tube, ethanol precipitated and resuspended in $10\mu\text{l}$ of distilled water to recover the DNA.

Recovered DNA fragments were digested with *Bam*HI and *Xho* and the DNA quantified using agarose gel electrophoresis and compared to $5\mu\text{l}$ of Hyperladder I (Bioline), where the DNA concentration in each band is known. The insert and vector were ligated together using the Quick Ligation™ kit (New England Biolabs.) according to the manufacturer's protocol. The cDNA was then transformed into One Shot TOP10 competent bacterial cells using the standard 42°C heat shock technique and plated onto LB agar plates containing ampicillin ($50\mu\text{g/ml}$) and incubated at 37°C overnight. 12ml cultures of LB, containing ampicillin ($50\mu\text{g/ml}$), were inoculated with single colonies the following evening and placed in a 37°C , shaking (225rpm) incubator overnight. Glycerol stocks were subsequently produced by the addition of

900 μ l of bacterial broth to 600 μ l of 50% glycerol and stored -80°C until required. The bacteria were then pelleted at 5,000rpm for 5 minutes in a chilled (4°C) centrifuge and DNA purified by Wizard® Plus SV miniprep (Promega) according to manufacturer's protocol. To identify which samples contain DNA encoding vector plus insert, all samples were double digested with *Bam H1* and *Xho* and analysed by agarose gel electrophoresis.

14.2 Expression of GST Fusion Proteins

All GST gene fusion vectors possess a *tac* promoter thereby allowing expression of any protein fused to GST to be induced within the host bacteria upon addition of isopropyl- β -D-thiogalactopyranoside (IPTG; Stratagene). Yet obtaining the active protein from the bacteria can be problematic due to the creation of inclusion bodies; amorphous aggregates of denatured protein. The ability to predict if an expressed protein is easily accessible is generally not possible with studying hydrophobicity, charge and size acting as poor prognostic indicators. Consequently once the GST fusion protein cDNA had been constructed, all were subjected to a range of procedures⁸.

The cDNA was transformed into either BL21-SI or DH5 α competent cells (Gibco) and grown overnight in 12ml LB broth cultures containing 50 μ g/ml ampicillin, shaking at 37°C. The following morning the overnight culture was used to inoculate fresh LB broth, containing ampicillin (50 μ g/ml). Bacteria were grown by shaking (225rpm) at the appropriate temperature until the A₆₀₀ was between 0.5 and 0.8nm. Expression of the GST fusion proteins was subsequently induced with 1mM IPTG and incubation was continued for the appropriate time. The bacteria was pelleted by centrifugation at 5,000rpm for 5 minutes at 4°C in a benchtop centrifuge, supernatant discarded and pellets frozen at -20°C until required.

⁸ Details can be seen in Table 4.

RECOVERY METHOD	GROWTH TEMPERATURE	VOLUME OF OVERNIGHT CULTURE	TOTAL VOLUME	INITIAL GROWTH PERIOD	INDUCTION TIMING
Standard	37°C	200µl	12ml	~4hrs	~4hrs
Slow Growth	22°C	1.2ml	12ml	~8hrs	~15hrs
Solubilise Protein	37°C	200µl	12ml	~4hrs	~4hrs

Table 4. Details of dealing with insoluble proteins

14.2.1 Recovery Method: Standard

The cell pellet was allowed to thaw to room temperature, resuspended in 600µl of ice-cold phosphate-buffered saline (PBS) and subsequently lysed by mild sonication on ice. The post-sonicate suspension was then incubated with 60µl of 10% Triton X-100 before cell debris was pelleted at 13,000rpm for 10 minutes at 4°C and later discarded, saving the supernatant.

14.2.2 Recovery Method: Slowing Growth

As 14.2.1 except grown at 22°C.

14.2.3 Recovery Method: Recovery from Inclusion Bodies

The cell pellet was allowed to thaw to room temperature prior to resuspension in 1ml ice-cold TE and mild sonication on ice. Cell debris was pelleted at 13 000rpm in a microcentrifuge for 10 minutes at 4°C and discarded. The supernatant was resuspended in 1ml 8M urea and incubated at room temperature for 20 minutes before centrifuging for 10 minutes at 13,000rpm at 4°C. The supernatant was then dialysed against 1M urea for 2 hours at 4°C in dialysis tubing⁹ (Sigma) then PBS overnight and followed by a further 2 hours dialysis in PBS the following day. Any remaining cell debris was pelleted at 13,000rpm for 10 minutes at 4°C and later discarded, saving the supernatant.

To assess yield of recovered protein each supernatant was incubated for 30 minutes with 100µl of washed glutathione-agarose beads (Santa Cruz) at 4°C with gentle

⁹ Prepared according to manufacturer's instruction where in brief, membranes were placed under running water for 4 hours prior to treatment with 0.3% sodium sulphate at 80°C for 1 minute, wash in 60 °C water for 2 minutes, sulphuric acid wash and a final wash in 60°C water.

inversion. The beads were then washed 5 x 1ml ice cold PBS, diluted in equal volumes of 2x sample buffer, boiled at 95°C for 5 minutes before separation of protein by SDS polyacrylamide gel electrophoresis as described above. The gel was then stained with EZBlue™ Gel Staining Reagent (Sigma) according to manufacturer's instruction and dried using a gel drying kit (Promega). Here the stained gel was soaked in a solution of 40% methanol, 10% glycerol and 7.5% acetic acid for 5 minutes then placed in between 2 sheets of gel drying film moistened briefly with the same solution the gel was soaked in. The film and gel were then placed in the gel drying frame, air bubbles removed and air-dried for 24 hours. The gel was then safe to store and/or scan an image onto a computer.

14.2 GST-Pulldown Assays

Once the appropriate protein recovery method was determined, the experiment proper could take place. GST fusion protein-containing supernatant (see above) was added to 100µl of washed glutathione-sepharose beads (Amersham) and mixed by gentle inversion for 30 minutes at 4°C. Meanwhile, lysates of HEK293-AKAP79 cells were prepared by lysing the cells in 500µl/well lysis buffer and the plates incubated at on ice for 5 minutes. The cell debris was pelleted at 13,000rpm for 5 minutes at 4°C and later discarded. The supernatant was added to the glutathione-agarose-GST fusion protein beads and incubated for two hours at 4°C with gentle inversion. The protein complex coupled beads were pelleted by gentle centrifugation and washed 5 times with ice-cold PBS. The beads were resuspended in an equal volume of 2x loading buffer and heated at 95°C for 5 minutes to disassociate any protein complexes from the beads. Samples were separated by SDS-polyacrylamide gel electrophoresis and analysed by immunodetection with mouse anti-AKAP79.

15 Point directed mutagenesis

It has been shown that the L-type Ca²⁺ channel, Ca_v1.1, and the K⁺ channel, KCNQ1-KCNE1, bind their respective AKAPs via a hydrophobic α-helical region at their C-terminus (Hulme *et al*, 2002; Marx *et al*, 2002). By using the Pôle Bio-Informatique Lyonnais website's secondary structure consensus prediction, the predicted secondary structure of Kir2.1 was obtained. From this prediction, several α-helical regions were identified, figure 5. Two of these regions are clearly the membrane-spanning domains, M1 and M2, of Kir2.1. However, there were other regions within

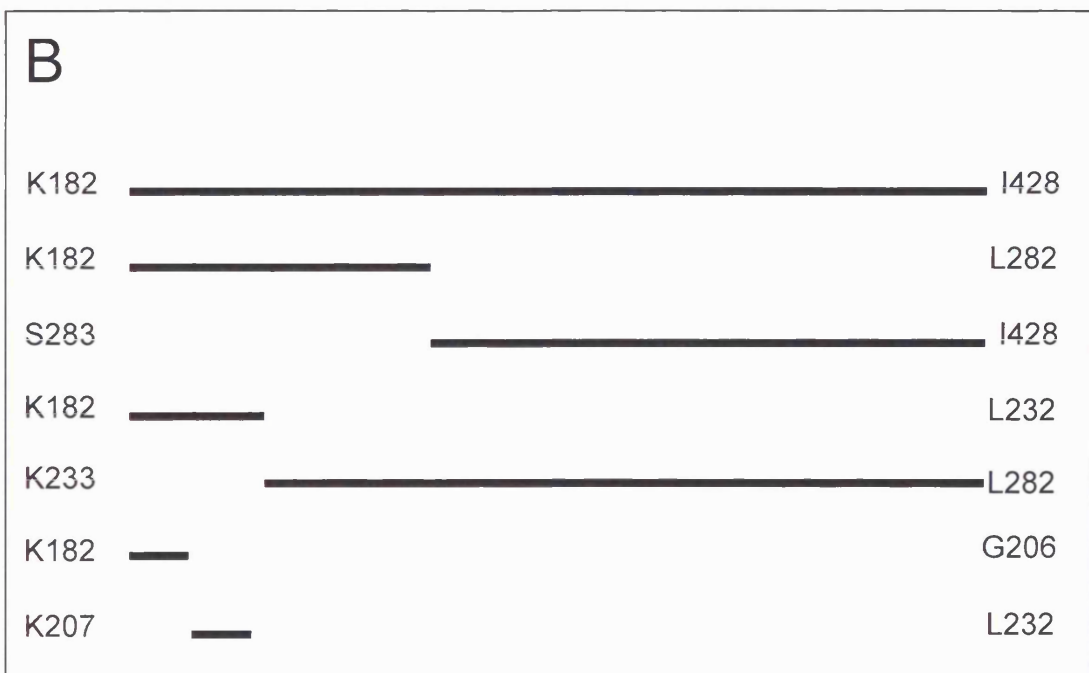
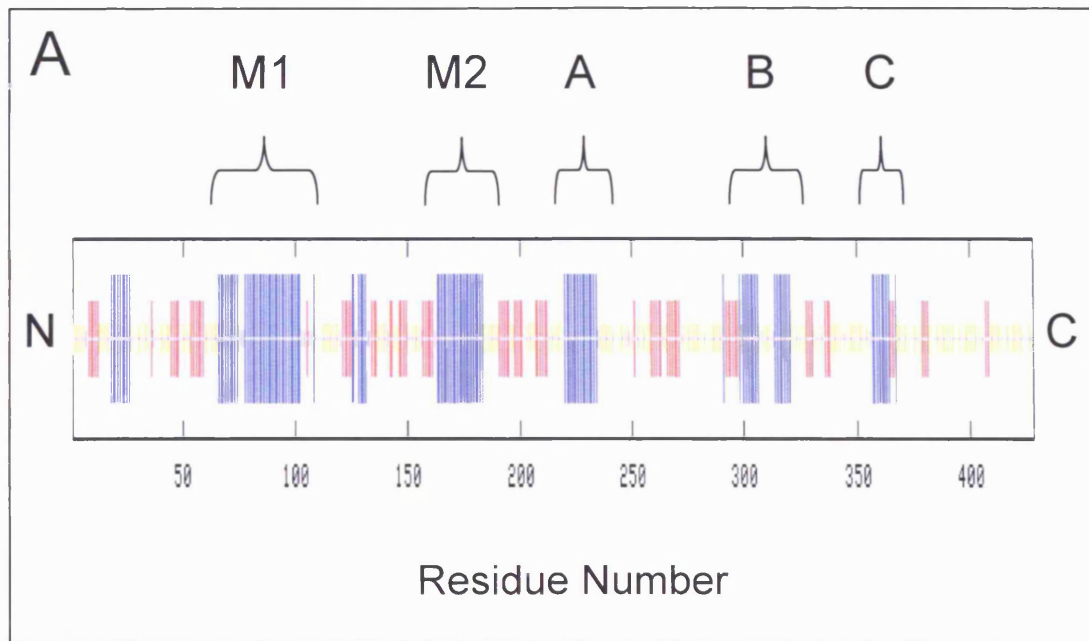


Figure 5. Secondary structure prediction of Kir2.1. A. Blue regions indicate α -helical structure, red regions indicate beta bridges and extended strands and the yellow regions indicate random coils within the structure of Kir2.1. B. GST fusion protein constructs corresponding to predicted hydrophobic α -helical regions within C-terminus of Kir2.1.

the C-terminal domain that were of interest, particularly the area spanning residues 220-235 as a heptad hydrophobic repeat was identified within this region of residues and so the possibility of AKAP79 binding Kir2.1 via a modified leucine zipper motif was also investigated.

Mutations of pGEX-6P-1-Kir2.1-C (182-232), corresponding to the identified heptad hydrophobic repeat: V194A, I201A, L208A, V194A/I201A, V194A/L208A, I201A/L208A, V194A/I201A/L208A, were generated by QuikChange mutagenesis (Stratagene) according to manufacturer's instructions. All constructs were verified by automated sequencing, carried out in-house by the Protein and Nucleic Acid Chemistry Laboratory (PNAACL), University of Leicester and analysed using Chromas, version 1.45.

16 'Interfering' with the Kir2.1-AKAP79 Complex

The following method for using GST proteins to disrupt protein-protein interactions were taken and adapted from Marx *et al*, 2002. Here, HEK293-AKAP79 cells were seeded into 6-well plates and grown until ~80% confluent at which time cells were transiently transfected with 2.4µg cDNA encoding EGFP-Kir2.1. GST-C (182-232) and GST-C (233-282) containing bacterial pellets (prepared as described in section 14.2) were resuspended in 600µl ice-cold PBS, briefly sonicated, 60µl of 10% Triton X100 added and centrifuged for 10 minutes at 13,000rpm on a benchtop microcentrifuge at 4°C. Meanwhile, 150µl of glutathione-sepharose bead slurry was taken and washed in 3x 1ml ice-cold PBS, added to the GST fusion protein supernatant and mixed with gentle inversion for 30 minutes at 4°C. The HEK293-AKAP79 cells transiently transfected with EGFP-Kir2.1 were lysed with 500µl of ice-cold lysis buffer containing 10µl ml⁻¹ of protease inhibitor cocktail for 5 minutes over ice. Cell debris was centrifuged at 13,000rpm for 5 minutes at 4°C. GST fusion protein attached glutathione-agarose beads were washed in 5x 1ml ice-cold PBS and added to HEK293-AKAP79 cell supernatant and mixed with gentle inversion overnight at 4°C. The following morning the glutathione bead slurry was spun briefly to sediment the beads and the supernatant added to 60µl of protein A/G conjugated beads pre-washed in 3x 1ml ice-cold PBS to 'pre-clear' the lysate of non-specific protein A/G binding constituents. This combination was mixed with gentle inversion for 1 hour at 4°C prior to removal of the protein A/G conjugated beads and

supernatant incubated with either 5µg rabbit anti-GFP or rabbit non-immune serum overnight at 4°C. The following day 60µl of protein A/G beads were washed in 3x 1ml ice-cold PBS and added to the antibody/lysate mix and incubated for 2 hours at 4°C with gentle inversion. The protein A/G beads were washed in 5x 1ml ice-cold PBS, diluted in 2x sample buffer and heated to 95°C for 5 minutes; this causes disassociation of any protein(s) and/or complexes conjugated to the beads. Samples were separated by SDS-polyacrylamide gel electrophoresis and analysed by immunodetection with mouse anti-AKAP79.

17 GST Pulldown: In Rat Tissue

GST-C (182-232) and GST-C (233-282) proteins were constructed, expressed, and recovered as previously described. GST fusion protein-containing supernatant was added to 100µl of washed glutathione-sepharose beads (Amersham) and mixed by gentle inversion for 30 minutes at 4°C. Rat brain or heart tissue samples¹⁰ were crushed with liquid nitrogen in a pestle and mortar and homogenised in 1ml mammalian lysis buffer. Cell debris was pelleted at 13,000rpm for 5 minutes at 4°C. The supernatant was divided into 2 separate samples and added to the glutathione sepharose beads fused to either GST-C (182-232) or GST-C (233-282) and incubated for 3 hours at 4°C with gentle inversion. The protein complex coupled beads were pelleted by gentle centrifugation and washed 5 times with ice-cold PBS. The beads were resuspended in an equal volume of 2x loading buffer and heated at 95°C for 5 minutes to disassociate any protein complexes from the beads. Samples were separated by SDS-polyacrylamide gel electrophoresis and analysed by either immunodetection with 1:1,000 goat anti-AKAP150 (Santa Cruz) or EZBlue™ Gel Staining.

18 RII-His Overlay Assay

18.1 Expression & purification of RII-His protein

The pET-28b plasmid containing mouse RIIα cDNA (a generous gift from Dr. J. D. Scott, Vollum Institute) was transformed into *Escherichia coli* BL21 (DE3) competent cells (Invitrogen) and cultured in LB containing 10µg/ml chlorphenicol

¹⁰ Organs were obtained from male Wistar rats weighing 250-300g killed by stunning and rapid cervical dislocation. Organs were then cut along the midline and rapidly frozen and stored at -80°C until required. The care and euthanasia of animals conformed to the requirements of The Animals (Scientific Procedures) Act 1986.

and 50µg/ml kanamycin overnight, shaking at 225rpm at 37°C. From the overnight culture, 0.2ml of bacteria was inoculated into 11.8ml of fresh LB-Chloro/Kan and cultured again by shaking at 225rpm at 37°C until the optical density measured 0.5-0.8 at 600nm, this was approximately 2 hours. RII α expression was induced by addition of final concentration of 1mM isopropyl- β -D-thiogalactopyranoside to the bacterial culture, with further incubation shaking at 225rpm for 4 hours at 37 °C. The bacteria were harvested by centrifugation, supernatant discarded and the pellet stored at -20°C until required for purification.

RII α proteins were purified using TALON® Metal Affinity Resin (Clontech) according to the manufacturer's protocol. In brief, pellets were resuspended in ice-cold extraction/wash buffer prior to incubation on ice for 30 minutes, followed by mild sonication on ice, centrifugation at 13,000rpm for 10 minutes at 4°C and allowed to bind to the resin for 30 minutes. The yield of recovered protein was analysed by SDS-PAGE and was sufficiently pure and at a high concentration to use in subsequent RII overlay assays. The resultant RII α protein was aliquoted and stored at -80°C until required.

18.2 Assay

Bacterial pellets of GST alone and GST-C (182-232) were solubilised as previously described and allowed to bind to glutathione-sepharose beads for 30 minutes at 4°C with gentle inversion. Meanwhile one and a half rat hearts dissected as described above were homogenised in 4.5ml mammalian lysis buffer prior to centrifugation at 13,000 for 5 minutes at 4°C. The GST protein bound glutathione-sepharose beads were washed 5x in ice-cold PBS and incubated with tissue lysate for 3 hours at 4°C with gentle inversion ahead of separation of proteins by SDS-polyacrylamide gel electrophoresis, transfer to nitrocellulose membrane and blocked overnight at 4°C in 5% milk-TBST as previously described. The following day two aliquots of RII α -His proteins were each resuspended in 50µl of TBST, one aliquot of RII α -His was then pre-incubated with 2µM of the blocking peptide Ht31 for 30 minutes at room temperature. After a brief wash in TBST the membranes were then incubated at room temperature with RII α -His or RII α -His+Ht31 for 90 minutes with gentle rocking. Membranes were then washed 3x, each for 10 minutes, in TBST and incubated with rabbit anti-His antibody (Santa Cruz), 1:500 in 1% milk-TBST for 90 minutes followed

by incubation with anti-rabbit HRP for 1 hour at room temperature and detection via ECL. TBST washes were included between each step as described above. Also see figure 6.

19 Electrophysiology

HEK293 and HEK293-AKAP79 cells were grown in 12-well plates to ~80% confluency prior to transient transfection with 100ng/well of cDNA encoding EGFP-Kir2.1. Whole cell currents were recorded from these cells 24-48 hours post-transfection as previously described (Dart and Leyland 2001) using an Axopatch 200A amplifier (Axon Instruments). Currents recorded in response to voltage steps were filtered at 5kHz (~3dB, 8-pole Bessel), digitised at 10kHz using a DigiData 1200 interface (Axon Instruments) and analysed using pClamp software. Electrodes were pulled from borosilicate glass (outer diameter 1.5mm, inner diameter 1.17mm; Clarke Electromedical) and polished to give a final resistance of approximately 4-5 M Ω when filled. The pipette filling solution contained 140mM KCl, 10mM EGTA, 1mM MgCl₂, 10mM HEPES, 1mM Na₂ATP and 0.5mM GTP; pH7.2. The external solution contained 70mM KCl, 70mM NaCl, 2mM CaCl₂, 2mM MgCl₂ and 10mM HEPES; pH7.2. In some experiments, 100 μ M cAMP (Calbiochem), 200nM okadaic acid and 200nM cypermethrin (a protein phosphatase 2B inhibitor; Tocris) was added to the pipette filling solution and the external solution. The junction potential between the pipette and external solutions was sufficiently small (<1.5mV) to be neglected. As far as possible, analogue means were used to correct capacity transients. Up to 90% compensation was routinely used to correct for series resistance. All experiments were performed at room temperature and the results are expressed as mean \pm S.E. Statistical significance was evaluated using the Student's unpaired t test.

19.1 Electrophysiology: With Synthetic Peptides

Electrophysiological studies were carried out as described above except here the peptides synthesised to various regions of Kir2.1 were added to the intracellular peptide filling solution at a final concentration of 10mM

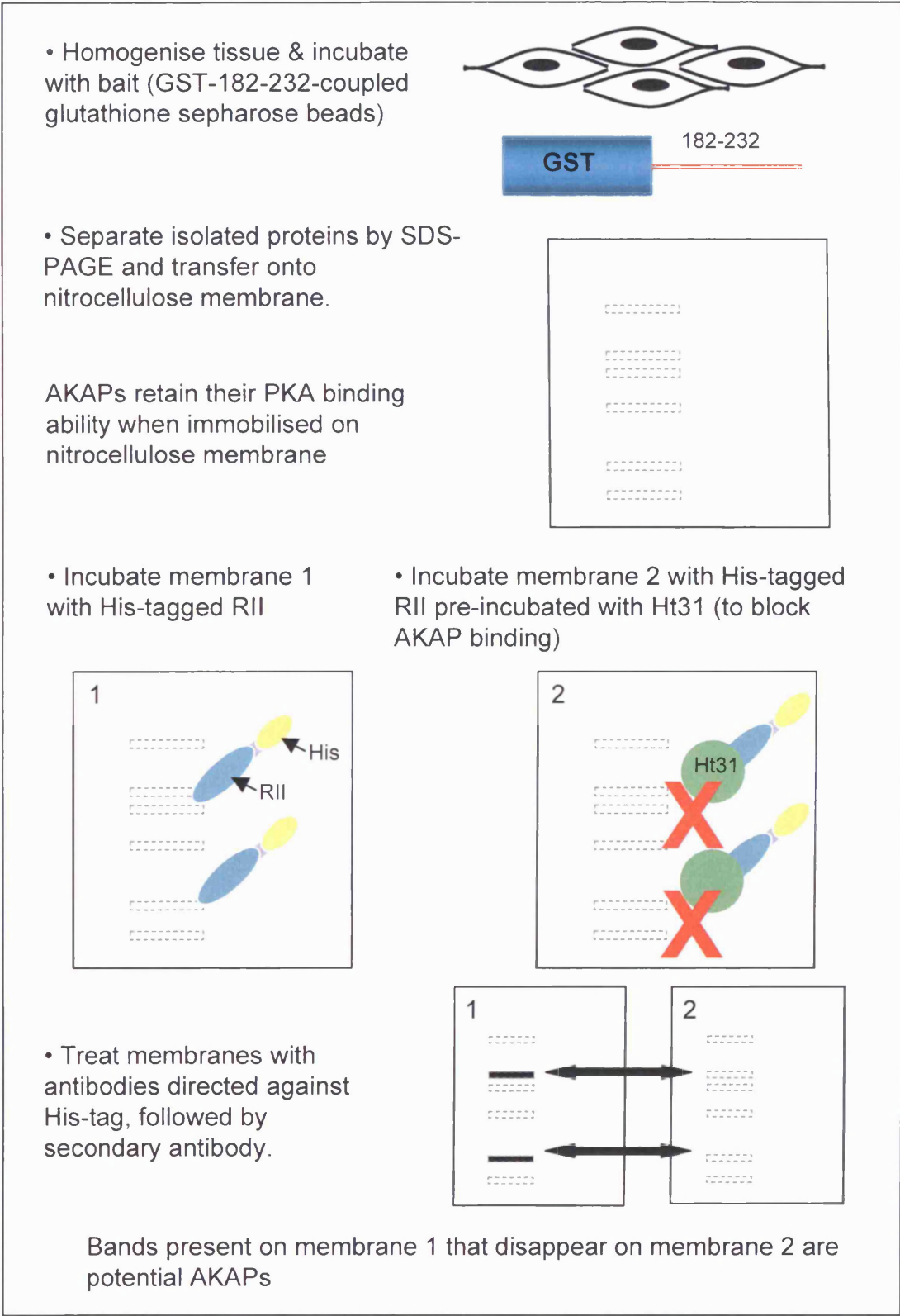


Figure 6. Cartoon depicting RII overlay assay protocol. See text for details.

20 Inhibition of Kir2.1-AKAP79 Complexes:

20.1 Co-immunoprecipitation: pIRES2-(182-232)-EGFP Inhibition

The following method for using pIRES2-(182-232)-EGFP in an attempt to inhibit Kir2.1-AKAP79 interactions was taken and adapted from Lavine *et al*, 2002. Here, HEK293-AKAP79 cells were seeded into 6-well plates and transiently transfected with 2µg/well EGFP-Kir2.1, as described above, whilst a separate set of HEK293-AKAP79 cells were transiently transfected with either 2µg 'empty' pIRES2-EGFP or 2µg pIRES2-(182-232)-EGFP. 24 hours post-transfection cells were briefly washed in PBS and lysed for 5 minutes with 800µl/well of lysis buffer plus protease inhibitor cocktail prior to centrifugation at 13,000rpm in a benchtop microcentrifuge for 5 minutes to sediment the cell debris. The supernatant from 1 well of EGFP-Kir2.1 was mixed with pIRES2-EGFP whilst another was mixed with pIRES2-(182-232)-EGFP by gentle inversion for 8 hours at 4°C. Each sample was divided into 2 and the lysate pre-cleared as described above followed by the addition of either 5µg rabbit anti-GFP or 5µg rabbit non-immune serum to each half sample and mixed with gentle inversion overnight at 4°C. The following day ~60µl of protein A/G slurry was washed 3x 1ml in ice-cold PBS then added to the lysate-antibody mix and incubated for 2 hours at 4°C with gentle inversion. The beads were washed in 5x 1ml ice-cold PBS, diluted in 2x sample buffer and heated to 95°C for 5 minutes. Samples were separated by SDS-PAGE, transferred onto nitrocellulose membranes and immunoblotted with mouse anti-AKAP79.

20.2 Inhibition by Synthetic Peptides

20.2.1 Peptide Design

Following EvoQuest™ Custom Peptide Synthesis recommendations, table 5, the subsequent peptides were designed: Peptide 1 = NETLVFSHNAVI, Peptide 2 = DGKLCL and Peptide 3 = VGNLRKSHLVEAHV.

The purity level of the synthesised peptides was >95%, with acetylation on the N-terminus and amidation on the C-terminus to protect against degradation.

RECOMMENDATIONS	
Ideally ≤ 15 residues	Purity of peptide decreases as length of peptide increases
Hydrophobic residues to total $< 50\%$	High concentration of hydrophobic residues results in solubility problems
Only 1 charged residue in every 5 residues	As above – reduced solubility
No valines in a row and/or no Val-Phe-Ile stretch	As above – extends synthesis time
Low concentration of Cys, Met and Trp	These residues are likely hydrogen bond forming and/or oxidising resulting in a reduction in purity

Table 5. EvoQuest™ Custom Peptide Synthesis Recommendations.

20.2.2 Co-Immunoprecipitation: With Synthetic Peptides

HEK293-AKAP79 cells were seeded into 6-well plates, transiently transfected with $2\mu\text{g/well}$ EGFP-Kir2.1 and co-immunoprecipitation carried out as described above. Here cell lysate was mixed with 10mM of each inhibitor peptide (1, 2 or 3) for 7 hours with gentle inversion at 4°C followed by addition of $\sim 60\mu\text{l}$ of protein A/G slurry, washed 3x 1ml in ice-cold PBS, and incubated for 1 hour at 4°C with gentle inversion. The beads were sedimented and discarded and the 'pre-cleared' supernatant was divided into 2 equal samples and incubated with either $5\mu\text{g}$ rabbit anti-GFP or $5\mu\text{g}$ rabbit non-immune serum and mixed with gentle inversion overnight at 4°C . The following day $\sim 60\mu\text{l}$ of protein A/G slurry, washed 3x 1ml in ice-cold PBS, was added to the lysate-antibody mix and incubated for 2 hours at 4°C with gentle inversion. The beads were washed in 5x 1ml ice-cold PBS, diluted in 2x sample buffer and heated to 95°C for 5 minutes. Samples were separated by SDS-polyacrylamide gel electrophoresis and analysed by immunodetection with mouse anti-AKAP79.

CHAPTER THREE

CONTROL OF INTRACELLULAR LOCALISATION OF AKAP-PKA COMPLEXES: The role of PKA and PKC

1 Introduction

Intracellular signalling is a highly regulated process that results in specific predictable transduction of signal despite a multitude of extracellular stimuli. Signalling often acts via reversible protein phosphorylation that is mediated through the opposing actions of protein kinases and phosphatases. AKAPs serve to pool these kinases and phosphatases by anchoring them to specific subcellular locations thereby dictating which phosphorylation machinery participates in the signal pathway and thus ensuring specificity in signal transduction.

The prototypic AKAP, AKAP79, is largely found within postsynaptic densities of cortical and hippocampal neurones (Carr *et al*, 1992b) where its subcellular target is the plasma membrane (Glantz *et al*, 1993; Ndubuka *et al*, 1993; Dell'Acqua *et al*, 1998). Targeting to the plasma membrane is achieved via three regions at the N-terminus of AKAP79. Each region is rich in basic amino acids that bind directly to acidic phospholipids in the cell membrane (Dell'Acqua *et al*, 1998).

Although AKAPs are defined by their ability to bind PKA, many are multivalent binding proteins coordinating the signalling of several different enzymes. AKAP79, for example, scaffolds the kinases PKA and PKC and the phosphatase PP2B/calcineurin (Coghlan *et al*, 1995; Klauck *et al*, 1996). Since the membrane-binding regions of AKAP79 contain distinct phosphorylation sites for both PKA and PKC, it has been suggested that targeting of this AKAP to the membrane may be regulated by phosphorylation (Dell'Acqua *et al*, 1998). AKAP79 would thus act as both a substrate and anchor for its associated kinases.

In the following chapter, the potential regulatory role of PKA and PKC in AKAP79 membrane targeting is investigated.

2 AKAP79 is Targeted to the Plasma Membrane

To confirm that AKAP79 localises to the plasma membrane within the model cell system used here, cDNA encoding AKAP79 was transiently transfected into HEK293 cells. The cells were subsequently fixed as described in Methods & Materials and the intracellular distribution of AKAP79 visualised by staining with anti-AKAP79 and FITC-conjugated secondary antibodies, figure 7. The image shows AKAP79 localized to the plasma membrane in accordance with previous studies (Glantz *et al*, 1993; Ndubuka *et al*, 1993; Klauck *et al* 1996; Dell'Acqua *et al*, 1998).

2.1 AKAP79 Targets RII α to the Plasma Membrane

In targeting the plasma membrane, AKAP79 should also localise its associated proteins, such as PKA, to the cell periphery (Glantz *et al*, 1993; Ndubuka *et al*, 1993; Klauck *et al*, 1996). To confirm this, the cellular distribution of the endogenous RII α regulatory subunit of PKA was compared in the presence and absence of over-expressed AKAP79. Endogenous RII α was found in abundance throughout untransfected HEK293 cells when visualised by immunochemical staining with anti-RII α , figure 8A. Figure 8B shows a pixel profile taken across a transverse section of one of the cells as indicated by the dotted line. The graph shows the relatively even distribution of RII α in a typical HEK293 cell. Upon over-expression of AKAP79 within these cells, a significant redistribution of the endogenous RII α from the cytoplasm to the cell periphery can be seen, figure 8C & D. Figure 8E shows an image of untransfected cells treated with anti-RII α preincubated with an RII α specific blocking peptide. The lack of staining indicates the RII α antibody is specific to RII α within these cells.

Organic solvents such as methanol are widely used as a fixative for immunocytochemistry; it works by dehydrating the cell and removing lipids. This is potentially an issue because if the plasma membrane is removed, cell components could in theory leak out of the cell. However, in hands it can be clearly seen that despite using this method of fixation, cytosolic RII remained distributed throughout

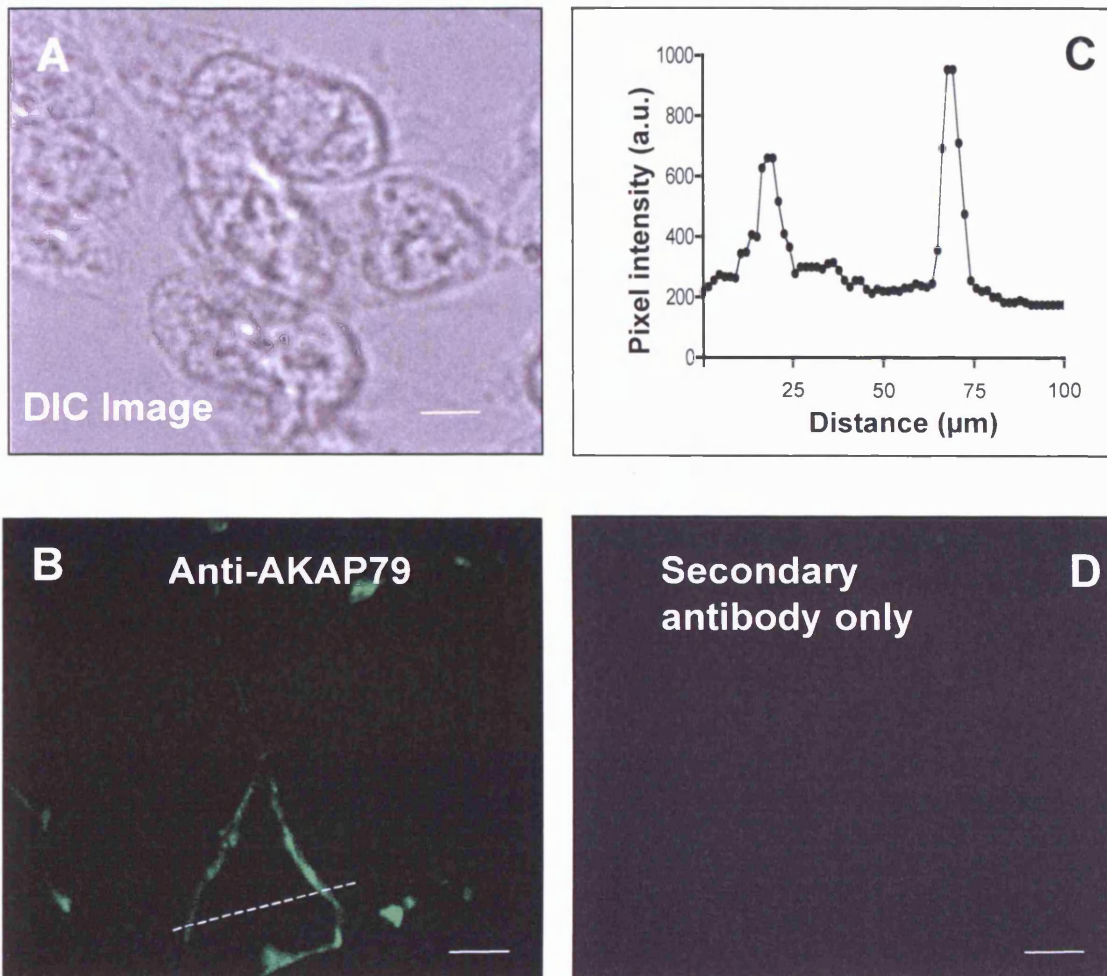


Figure 7. AKAP79 localises to the plasma membrane. **A.** HEK293 cells were transfected with cDNA encoding AKAP79 prior to methanol fixing and permeabilisation. **B.** Cells treated with antibodies directed against AKAP79, followed by FITC-conjugated secondaries show AKAP79 predominantly at cell periphery. **C.** Pixel profile along dotted line in **B.** **D.** Addition of FITC-conjugated secondaries alone confirms specificity of AKAP79 staining. Scale bars represent $20\mu\text{m}$.

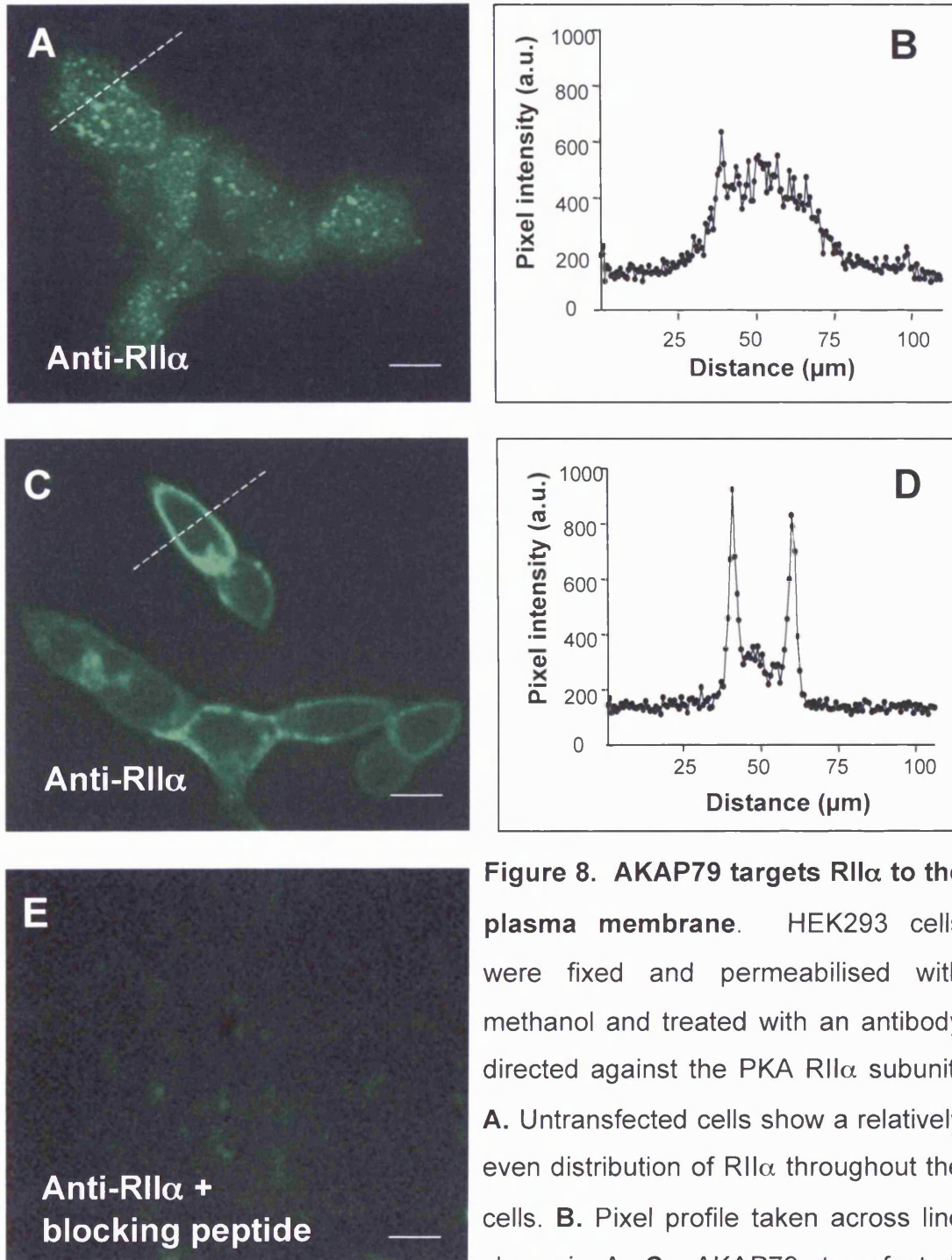


Figure 8. AKAP79 targets RII α to the plasma membrane. HEK293 cells were fixed and permeabilised with methanol and treated with an antibody directed against the PKA RII α subunit. **A.** Untransfected cells show a relatively even distribution of RII α throughout the cells. **B.** Pixel profile taken across line shown in **A.** **C.** AKAP79 transfected cells show a redistribution of RII α to the plasma membrane. **D.** Pixel profile taken across line shown in **C.** **E.** Untransfected cells were treated with anti-RII α preincubated with a specific blocking peptide. Lack of staining indicates the RII α antibody is specific to RII α within these cells. Scale bars represent 20 μm .

Untransfected cells show a relatively even distribution of RII α throughout the cells. Pixel profile taken across line shown in **A.** AKAP79 transfected cells show a redistribution of RII α to the plasma membrane. Pixel profile taken across line shown in **C.** Untransfected cells were treated with anti-RII α preincubated with a specific blocking peptide. Lack of staining indicates the RII α antibody is specific to RII α within these cells. Scale bars represent 20 μm .

the cell, figure 8A. Additionally, we show that expression of AKAP79, a plasma membrane targeting protein, in methanol fixed HEK293 cells produced clearly defined targeting of the protein to the cell periphery, figure 7B. As a consequence, in our hands we do not find methanol fixation to yield any problems regarding cell components being removed from the cell.

2.2 HEK293-AKAP79 Stably Expressing Cells

Having established AKAP79 acts as predicted (Glantz *et al*, 1993; Ndubuka *et al*, 1993; Dell'Acqua *et al*, 1998) by targeting both itself and PKA to the plasma membrane in our strain of wildtype HEK293 cells, a stable cell line of HEK293 cells over-expressing AKAP79 was prepared (data not shown) and used in all future experiments unless otherwise stated.

2.3 Regulation of AKAP79 Membrane Targeting by PKA &/or PKC

The membrane targeting sequences in AKAP79 (figure 9) contain PKA and PKC phosphorylation sites with a similar amino acid sequence to the membrane targeting domains found in Myrystoylated Alanine-Rich C-Kinase Substrate proteins (MARCKS), GAP43/neuromodulin and neurogranin (Dell'Acqua *et al*, 1998; Houbre *et al*, 1991; Aderem, 1992; Blackshear, 1993; Lu & Chen, 1997). As these proteins are modulated by PKC phosphorylation and by calmodulin, Dell'Acqua *et al* (1998) investigated the possibility that AKAP79 membrane/phospholipid binding might be regulated in a similar manner. Indeed they have shown that upon phosphorylation by PKC but not PKA, there is an increase in the level of AKAP79 found in soluble cytoplasmic fractions, implying that phosphorylation of key targeting residues may inhibit AKAP79-phospholipid interactions and lead to release of AKAP79 from the plasma membrane. This is potentially important because the uncoupling of AKAP79, and associated enzymes, from the membrane might represent a mechanism of down-regulating its ability to phosphorylate membrane-associated substrates. In an attempt to repeat and expand on these findings, the degree of AKAP79 membrane association was assessed in HEK293 cells following activation of PKA and/or PKC.

AKAP79

⁸⁰ASLKRLVTRRKRSESSKQOKPLEGEMQPAINAEDADLSK⁸¹KKAKSRLKIPCIKFPRGPKRSNHSKI¹⁴⁴

Figure 9. Potential PKA and PKC phosphorylation sites on AKAP79. AKAP79 contains several putative PKA (shown in blue text: S92, S94) and PKC (shown in red text: S81, S95, S117, S123, S142) phosphorylation sites; T87 (as shown in green text) highlights a potential joint PKA and PKC phosphorylation site.

2.3.1 Subcellular Fractionation

In initial experiments, Dell'Acqua *et al* (1998) performed cellular fractionation at a centrifugal force of 40,000g, while later experiments used 100,000g. To assess which protocol might give the most consistent separation of membrane and cytosolic fractions, preliminary fractionation experiments were carried out on HEK293-AKAP79 cells using a range of different centrifugal forces. All lysates were solubilised as described in Methods and Materials and used the mild detergent Triton X-100.

At each centrifugal speed tested, the majority of AKAP79 was found in the pellet/insoluble fraction, figure 10. Densitometric analysis of the Western blots treated with anti-AKAP79 shows a significant difference in AKAP79 distribution between soluble and insoluble fractions, (membrane bound AKAP79 as a % of total AKAP79: 40,000g = 87.4±2.0%; 70,000g = 93.5±1.9%; 100,000g = 94.7±0.7%) all with p value of < 0.0001.

When comparing the levels of AKAP79 in each soluble fraction, no significant difference was seen between 40,000g and 70,000g. However, a significant difference can be seen when comparing the results from fractionation at 40,000g and 100,000g, $p < 0.05$, with less AKAP79 in the soluble fraction of cells fractionated at 100,000g.

2.3.1.1 Content of Fractions

As a brief overview of other cellular components present in the soluble and insoluble material fractionated at each speed, we investigated the presence of 4 other proteins through fractionation as described above followed by immunoblotting. Extracellular signal-regulated kinase-1 (ERK-1), also known as a mitogen-activated protein kinase

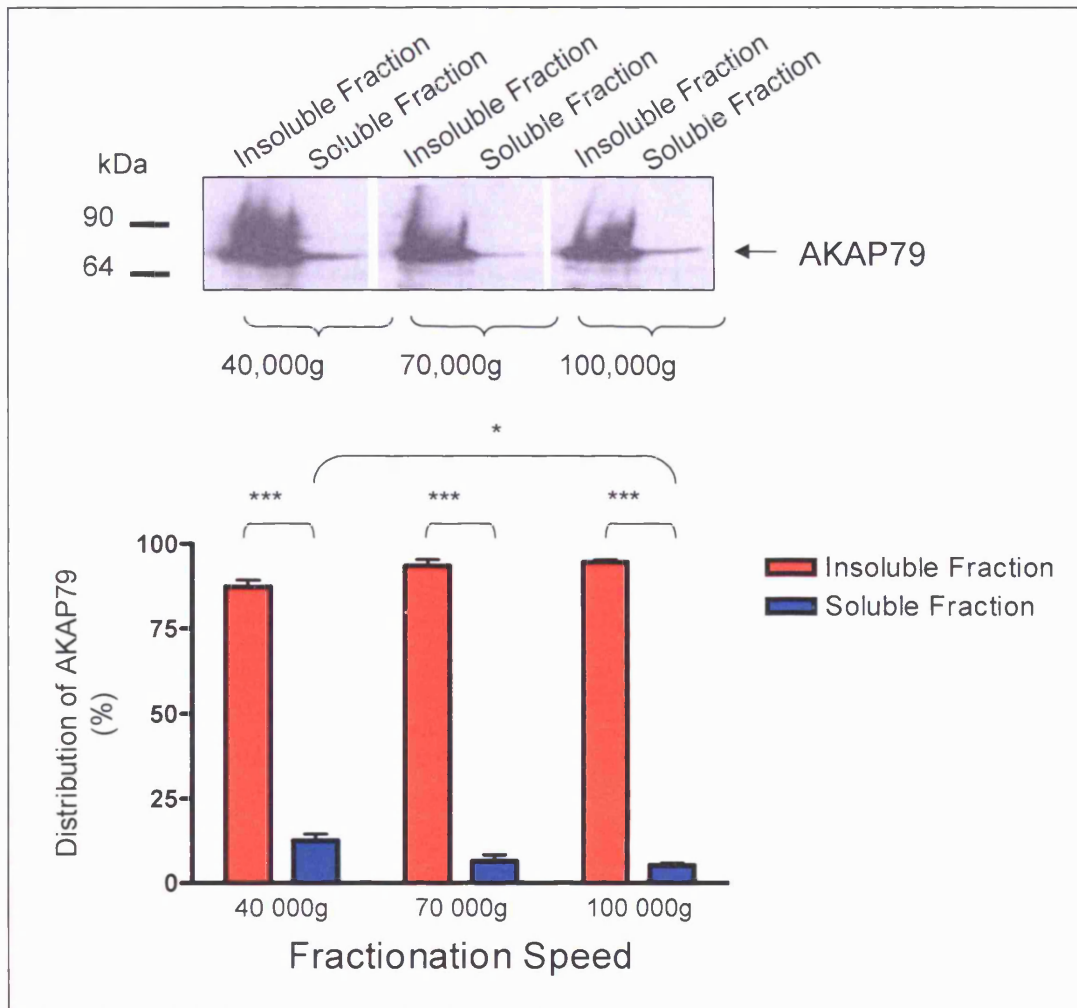


Figure 10. AKAP79 localises to the insoluble fraction of high speed fractionated HEK293-AKAP79 cells. HEK293 cells stably transfected with AKAP79 were solubilised with Triton X-100 crudely fractionated at 40,000g, 70,000g and 100,000g and the proteins within the soluble and insoluble fractions separated by SDS-PAGE. The proteins were transferred electrophoretically onto nitrocellulose membrane and immunoblotted with anti-AKAP79. AKAP79 is enriched in the insoluble membrane fraction in cell centrifuged at each speed (membrane bound AKAP79 as a % of total AKAP79: 40,000g = 87.4±2.0%; 70,000g = 93.5±1.9%; 100,000g = 94.7±0.7%) . All data shown are representative of 3 independent experiments, unpaired, two-tailed Student's t-test, $p < 0.0001$.

(MAPK) is a serine/threonine kinase expressed in the majority of mammalian tissues where it targets both cytosolic substrates and transcription factors. Figure 11A shows the majority of the fractionated material to be placed in the soluble fraction which corresponds to the cytosolic material of the HEK293-AKAP79 cells.

Actin is one of the three main types of protein filament constituents of the cytoskeleton; the others being microtubules and intermediate filaments. It participates in many cellular functions including maintaining cell shape and supporting the fragile plasma membrane to cell signalling. Figure 11B shows actin to be evenly distributed between the soluble and insoluble fractions.

The filamin family of actin-binding proteins function to cross-link actin filaments thereby stabilising the membrane, although recent data suggest a role in scaffolding and signalling transduction (Sampson *et al*, 2003). Figure 11C shows that like actin, filamin is evenly distributed between the soluble and insoluble fractions of lysed and fractionated HEK293-AKAP79 cells.

Calreticulin is a calcium binding protein that is located in storage compartments associated with the endoplasmic reticulum. It appears to function in a similar manner to the quality control chaperone calnexin, targeting proteins for degradation. Figure 11D shows significantly more calreticulin is present in the insoluble fraction of fractionated HEK293-AKAP79 cells than in the soluble fraction.

From data obtained for figures 10 and 11, all subsequent fractionation experiments were carried out at 100,000g since this produced the purer soluble fraction.

2.3.2 AKAP79 Phosphorylation and Release Assay

To investigate whether phosphorylation of AKAP79 targeting residues by PKA and/or PKC regulates the association of AKAP79 with the plasma membrane, PKA and/or PKC were artificially stimulated in intact cells by addition of forskolin (an adenylyl cyclase activator) and/or phorbol-12-myristate-13-acetate (PMA; an activator of PKC). Cells were then fractionated and the amount of AKAP79 in soluble and insoluble fractions compared by immunoblotting with anti-AKAP79 as described in Methods and Materials. A non-specific cAMP phosphodiesterase inhibitor and a

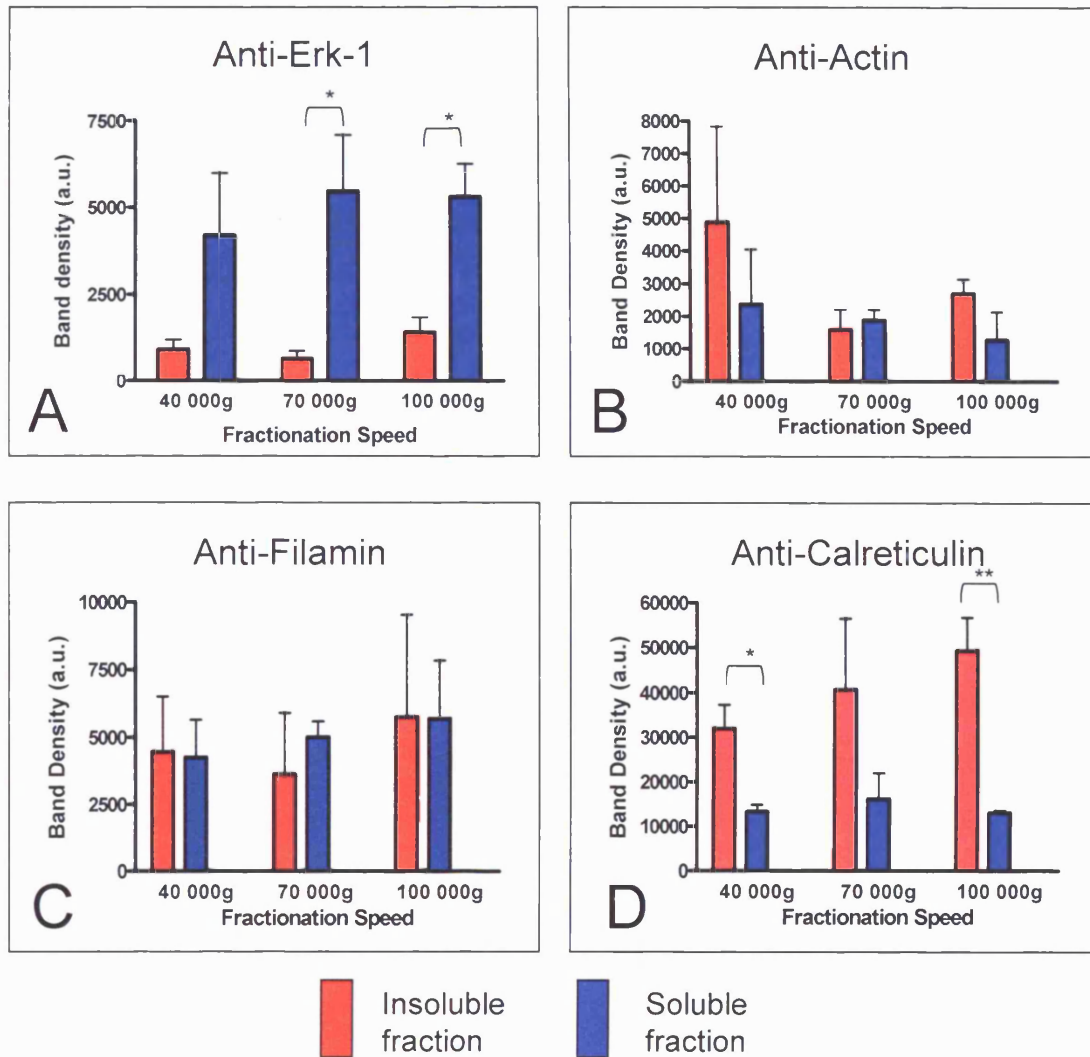


Figure 11. Distribution of various proteins in soluble and insoluble fractions isolated from HEK293-AKAP79 cells. HEK293 cells stably transfected with AKAP79 were solubilised with Triton X-100 and crudely fractionated at 40,000g, 70,000g and 100,000g and the soluble and insoluble fractions separated by SDS-PAGE. The proteins were transferred electrophoretically onto nitrocellulose membrane and immunoblotted with various antibodies. A. Erk-1 is enriched in the soluble cytoplasmic fraction, irrespective of fraction speed. B. Actin is found in equal amounts in the soluble and insoluble fractions, irrespective of fractionation speed. C. Filamin was found in equal amounts in the soluble and insoluble fractions at all fractionation speeds. D. Calreticulin appears enriched in the insoluble fraction at all fractionation speeds. All data shown are representative of 3 independent experiments. * $p < 0.05$, ** $p < 0.01$, *** $p < 0.001$, unpaired, two-tailed students t-test.

protein phosphatase inhibitor were included with all drug treatments to prevent the breakdown of cAMP and to ensure that the target phosphorylation sites on AKAP79 were not rapidly dephosphorylated, respectively.

In contrast to Dell'Acqua *et al* (1998), we found that activation of PKA and/or PKC did not significantly alter the level of plasma membrane binding of AKAP79. This is demonstrated by the lack of significant re-distribution of AKAP79 from the pellet to the soluble fraction, figure 12 (membrane bound AKAP79 as a % of total AKAP79: vehicle = $81.5 \pm 7.4\%$; PKA = $87.3 \pm 1.7\%$; PKC = $80.4 \pm 3.0\%$; PKA+PKC = $85.0 \pm 4.2\%$; mean \pm SEM, n=3).

2.3.3 AKAP79 Phosphorylation and Immunocytochemistry

It is possible that upon activation of PKA and/or PKC, AKAP79 uncouples from the plasma membrane but is essentially 'caught' by the underlying cortical cytoskeleton. It has been shown that there is often an association between AKAP79 and this cellular structure (Oliveria *et al*, 2003). Fractionating cells into insoluble and soluble fractions could therefore be too crude a technique to assess membrane association. As an alternative to fractionation and a potentially more sensitive means of assessing whether PKA and/or PKC phosphorylation modulates AKAP79 localisation immunocytochemistry in combination with confocal microscopy was used.

As a marker for the plasma membrane the plasmid pIRES2-EGFP-F was transiently transfected into HEK293-AKAP79 cells. Here, a farnesylation signal has been added to the carboxy terminal of EGFP which facilitates insertion of the fluorophore into the membrane. AKAP79 localisation was visualised using primary antibodies directed against AKAP79 and secondary antibodies conjugated with the fluorophore Texas Red. Since the excitation/emission spectra of EGFP and Texas Red do not overlap (EGFP excitation max 488nm; emission max 509nm; Texas Red excitation max 596nm; emission max 620nm), this allows us to visualise both the location of the membrane and of AKAP79 at the same time.

The results of these experiments confirmed our initial findings that PKA/PKC phosphorylation of AKAP79 does not regulate its targeting to the plasma membrane, figure 13. This was assessed quantitatively by comparing the position of AKAP79 to

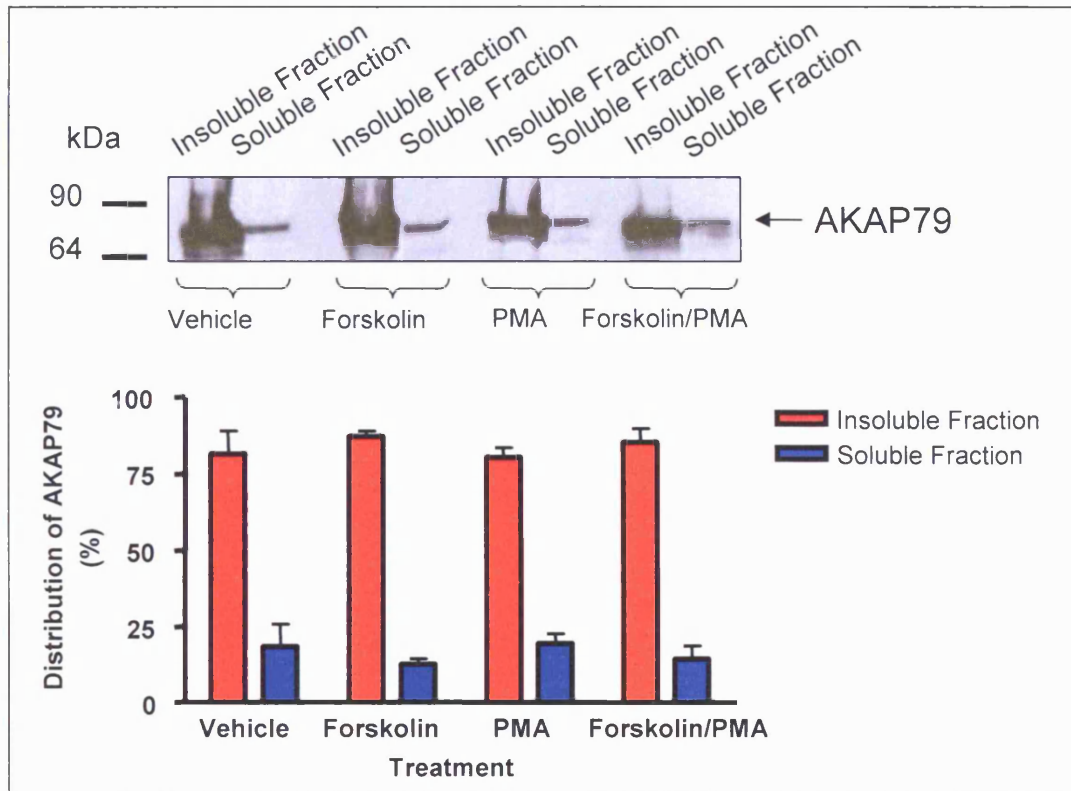


Figure 12. Activation of PKA and/or PKC in HEK293-AKAP79 cells does not cause redistribution of AKAP79. Whole HEK293 cells stably transfected with AKAP79 were treated with: forskolin, to activate PKA; PMA, to activate PKC and forskolin & PMA, to activate both PKA and PKC. Phosphatase and phosphodiesterase inhibitors were also included in cell treatments. Insoluble (pellet) and soluble fractions were prepared by centrifugation at 100,000g and subsequently run on SDS-PAGE gels. The proteins were transferred electrophoretically onto nitrocellulose membrane and immunoblotted with anti-AKAP79. No significant difference was seen between the insoluble fractions of vehicle-treated and drug treated cells (membrane bound AKAP79 as a % of total AKAP79: vehicle = $81.5 \pm 7.4\%$; forskolin = $87.3 \pm 1.7\%$; PMA = $80.4 \pm 3.0\%$; forskolin/PMA = $85.0 \pm 4.2\%$), suggesting that activation of PKA and/or PKC does not result in a significant re-distribution of AKAP79; unpaired, two-tailed, Student's t-test, $n=3$.

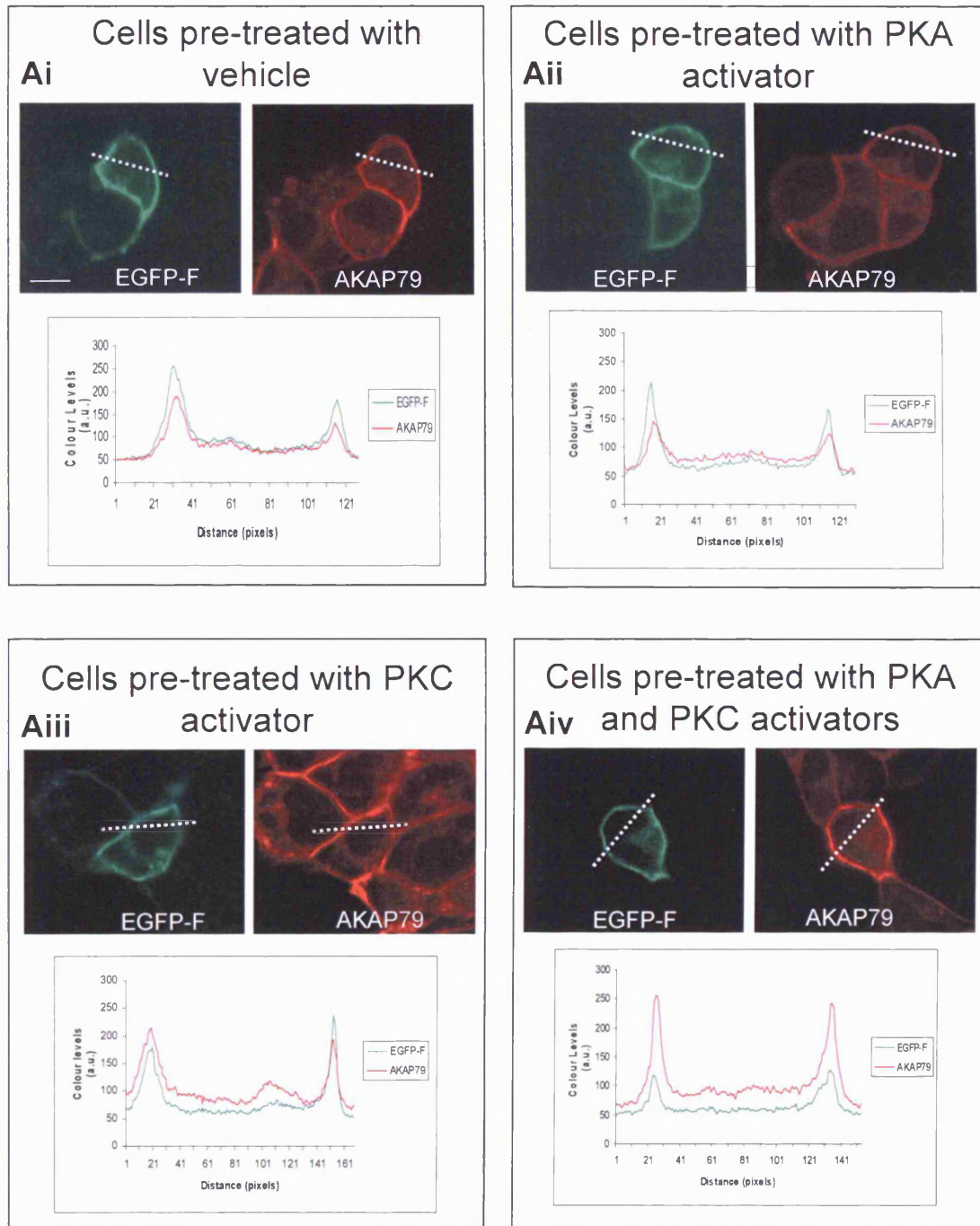


Figure 13. AKAP79 phosphorylation does not regulate membrane targeting. A. HEK293-AKAP79 cells transiently transfected with plasma membrane marker EGFP-F were treated with vehicle (i) or drugs to induce PKA (ii), PKC (iii) or PKA and PKC (iv) phosphorylation of AKAP79 prior to methanol fixing and imaging by confocal microscopy. Green staining depicts EGFP-F localisation, red staining (TxR) depicts AKAP79 localisation. Images correspond to a single representative confocal plane, scale bar representative of 20 μ m.

that of EGFP-F (i.e. the plasma membrane) following treatment activators of PKA and/or PKC. Figure 13A shows that following all treatments, the cellular distribution of EGFP-F and AKAP76 essentially overlap. The fitting of Gaussian curves to the peaks of the pixel profiles of AKAP79 and EGFP-F (see legend for details) allows the distance between the EGFP-F peak and the corresponding AKAP79 peak to be measured along with 'spread' of the fluorescence (the width of these peaks). Any changes in these measurements would suggest redistribution of that protein within the cell. Figure 13B shows that in each case, no significant difference was seen. These imaging studies confirm the findings of the AKAP79 release assays and show that activation of PKA and/or PKC does not result in significant AKAP79 redistribution away from the plasma membrane.

3 Conclusions

Previous work by Dell'Acqua *et al* (1998) suggest that as the membrane targeting domains of AKAP79 contain putative phosphorylation sites for PKA and PKC, targeting of this AKAP to the plasma membrane can be regulated directly via phosphorylation. They show that upon stimulation of PKA and PKC, AKAP79 becomes phosphorylated and is subsequently released from membrane particulate fractions, thereby implying that AKAP79 might function not only as an anchor but may also play a fundamental role in the regulation of kinase signalling pathways through the bulk movement of its associated enzymes away from the membrane. We set out to extend these studies.

Our work confirms a number of previous studies (Glantz *et al*, 1993; Ndubuka *et al*, 1993; Coghlan *et al*, 1995; Klauck *et al*, 1996; Dell'Acqua *et al*, 1998) showing that AKAP79 targets the plasma membrane, but fails to find evidence for regulation of this targeting by PKA or PKC phosphorylation. This is at odds to the findings of previous work by Dell'Acqua and colleagues and the reasons behind this discrepancy remain unclear.

One possible explanation for the difference could be that in our experimental set-up the targeting regions of AKAP79 remained unphosphorylated, despite treatment with PKA and PKC activators and exposure to phosphatase inhibitors. Since the protocol we followed in this study was essentially identical to that used by Dell'Acqua and

colleagues (1998), including the cell type used (HEK293), this seems unlikely. However since we did not measure AKAP79 phosphorylation levels this possibility cannot be entirely ruled out.

We also analysed the results of our study quantitatively. Although Dell'Acqua *et al* (1998) state that the data they showed was representative of similar results obtained in two or more additional experiments, they fail to show any statistical analysis. It is possible that more rigorous analysis of multiple blots may have revealed no significance difference between the level of AKAP79 in their control and stimulated fractions.

CHAPTER FOUR

CONTROL OF INTRACELLULAR LOCALISATION OF AKAP-PKA COMPLEXES: The role of PtdIns(4,5)P₂

1 Introduction

PtdIns(4,5)P₂ represents a minor percentage of the plasma membrane phospholipids, yet binds to and modulates a large number of signalling molecules (Rana & Hokin, 1990; Hilgemann *et al*, 2001). It is a substrate for the enzymes phospholipase C (PLC) and phosphoinositide 3-kinase (PI3-K), although only a small fraction of the total pool of PtdIns(4,5)P₂ appears to be accessible to the actions of PI3-K (Jackson *et al*, 1992; Batty & Downes, 1996). Hydrolysis of PtdIns(4,5)P₂ by PLC following G_q-coupled receptor stimulation results in the formation of 1,2-diacylglycerol (DAG) and inositol 1,4,5-triphosphate (Ins(1,4,5)P₃). Thus, activation of a subset of GPCRs results in the depletion of PtdIns(4,5)P₂ from the plasma membrane.

As previously mentioned, AKAP79 interacts with negatively charged acidic phospholipids of the plasma membrane (Dell'Acqua *et al*, 1998), thus targeting its associated signalling complex to the cell periphery and hence integral plasma membrane proteins, such as G-protein coupled receptors and ion channels. In the following chapter we investigate whether receptor-driven depletion of the lipid anchor PtdIns(4,5)P₂ has any effect upon the membrane association of AKAP79.

2 Measurement of (poly) Phosphoinositides

Before assessing the impact of PtdIns(4,5)P₂ depletion on AKAP79 localisation, we first investigated the experimental conditions required for significant agonist-induced depletion of this phospholipid. These experiments were carried out in collaboration with Prof. R. A. John Challiss and Mr Raj Mistry (Dept. of Cell Physiology & Pharmacology, University of Leicester).

HEK293 cells express an endogenous G_q-coupled M₃ muscarinic acetylcholine receptor population (Prof. R. A. John Challiss pers. comm.). This allows PtdIns(4,5)P₂ to be depleted physiologically in these cells by treatment with muscarinic acetylcholine receptor agonists such as carbachol.

HEK293-AKAP79 cells were incubated with [³H]-inositol for 48hr prior to stimulation with wortmannin (a potent PI3-K and PtdIns 4-kinase (PI4-K) inhibitor), see figure 14A for details of the PtdIns(4,5)P₂ signalling pathway, and/or carbachol (a commonly used cholinergic agonist).

The [³H]-inositol phosphate fraction was recovered (data not shown) and the relative amounts of each (poly)-phosphoinositide was assessed (see methods). Pre-treatment of HEK293-AKAP79 cells with wortmannin alone, carbachol alone or wortmannin and carbachol had little effect on the levels of PtdIns, figure 14B (percentage fall after 30 minutes: +Wtm = -3.89 ± 57.88%; +CCh = 5.09 ± 36.52%; +Wtm/CCh = -0.76 ± 13.42%). This is entirely as one would expect as wortmannin inhibits PI4-K, the kinase that hydrolyses PtdIns to PtdIns(4)P, and as such affects the signalling pathway downstream of PtdIns.

Levels of [³H]-PtdIns(4)P, figure 14C, remained constant throughout treatment with carbachol (percentage fall after 30 minutes: +CCh = 6.53 ± 82.49%), suggesting that demand and supply for this phospholipid are perfectly balanced during agonist stimulation. However, upon pre-treatment with wortmannin with or without subsequent addition of carbachol, there was a significant depletion of [³H]-PtdIns(4)P (percentage fall after 30 minutes: +Wtm = 108.82 ± 89.63%; +Wtm/CCh = 176.50 ± 80.91%). This implies that PI4-K needs to be constantly active to keep the levels of PtdIns(4)P stable within these cells.

Of particular significance to this study are the results regarding the levels of PtdIns(4,5)P₂, figure 14D. Again carbachol alone had little effect (percentage fall after 30 minutes: +CCh = 0.46 ± 46.22%), suggesting that during agonist stimulation there is a constant and rapid recycling of phosphoinositides. However, pre-treatment with 10µm wortmannin for 30 minutes, which inhibits the phosphorylation of PtdIns to PtdIns(4)P (the precursor of PtdIns(4,5)P₂) caused a 50.61 ± 28.54% decline in

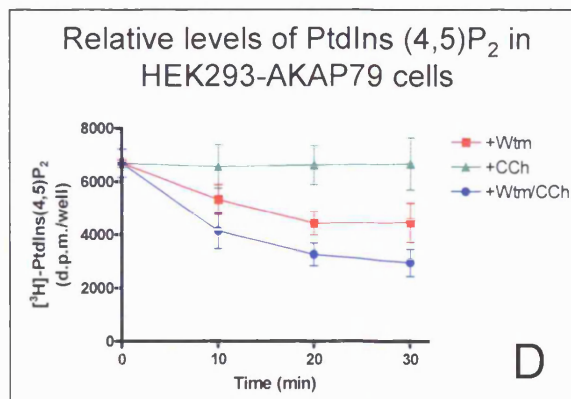
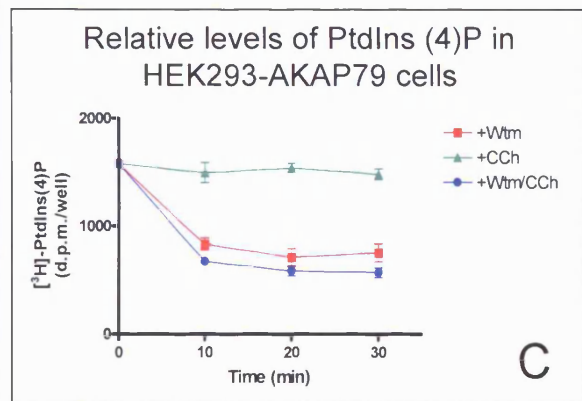
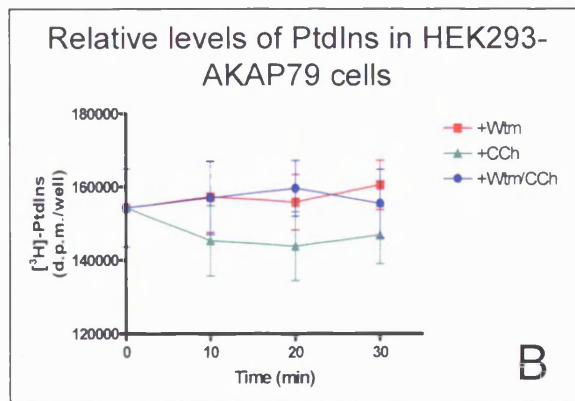
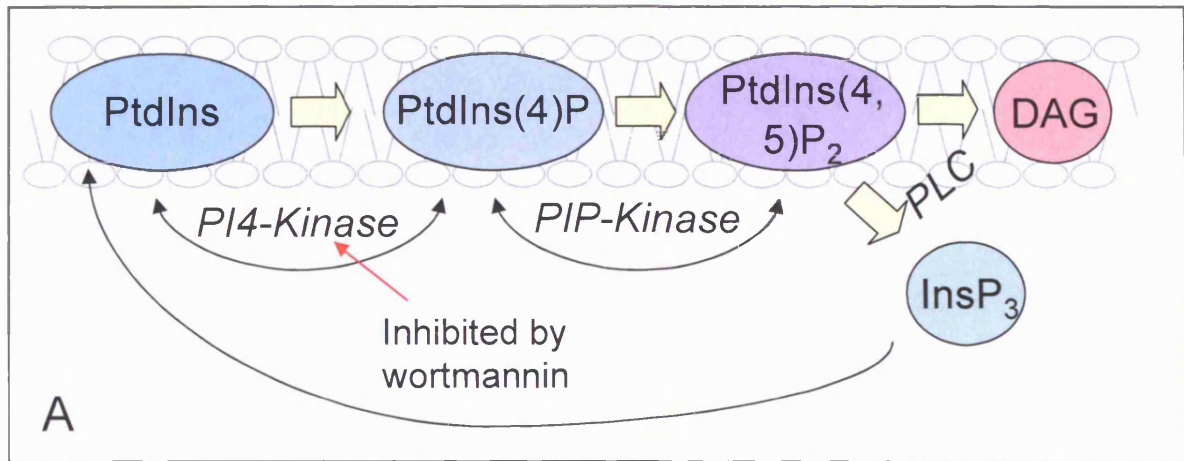


Figure 14. Extraction and separation of $[^3\text{H}]$ -(poly)phosphoinositides in HEK293-AKAP79 cells. **A.** PtdIns(4,5) P_2 synthesis pathway. Time course of 10 μM wortmannin-mediated (■), 300 μM carbachol-mediated (▲) or 10 μM wortmannin/300 μM carbachol-mediated (●) changes in **B.** $[^3\text{H}]$ -PtdIns, **C.** $[^3\text{H}]$ -PtdIns(4)P and **D.** $[^3\text{H}]$ -PtdIns(4,5) P_2 in HEK293-AKAP79 cells. Cells were pre-labelled with $[^3\text{H}]$ inositol and challenged with agonist at zero time. Results are means \pm S.E.M., $n=3$.

PtdIns(4,5)P₂ levels, while 10µm wortmannin + 300µm carbachol for 30 minutes caused a 128.07 ± 4.47% depletion.

3 Re-Distribution of AKAP79 Upon PtdIns (4,5)P₂ Depletion

Having established that pre-treatment with 10µm wortmannin + 300µm carbachol for 30 minutes causes a significant depletion of PtdIns(4,5)P₂ in HEK293-AKAP79 cells, we investigated what effect this has on the levels of AKAP79 anchored to the membrane using the fractionation assay previously described.

Figure 15 shows that incubation of HEK293-AKAP79 cells with wortmannin and carbachol resulted in 6-fold increase in the amount of AKAP79 present in the soluble cellular fraction compared to cells treated with vehicle alone. Treatment with wortmannin alone however did not produce a significant re-distribution of AKAP79 away from the insoluble pellet fraction (cytoplasmic AKAP79 as a % of total AKAP79: vehicle, 2.9 ± 0.2%; Wtm, 9.0 ± 3.0%; Wtm/CCh, 18.3 ± 1.7%; n=3). These data would be consistent with the depletion of PtdIns(4,5)P₂ causing a release of AKAP79 from the membrane into the cytosolic fraction.

To further investigate the effect of membrane PtdIns(4,5)P₂ depletion on AKAP79 localisation, immunocytochemical studies were performed on HEK293-AKAP79 cells transfected with cDNA encoding EGFP-F, to mark the plasma membrane, and pre-incubated with wortmannin and/or carbachol, figure 16A. Analysis revealed that pre-treatment with carbachol and/or wortmannin induced a significant narrowing in width of AKAP79 distribution at the membrane as compared to vehicle treated cells, figure 16B (measured as half height of Gaussian curve fitted to pixel profile across membrane: vehicle = 8.6 ± 0.5 pixel units; Wtm = 7.1 ± 0.4 pixel units Wtm/CCh = 5.6 ± 0.2% pixel units; n≥9). However, additional analysis revealed that pre-treatment with wortmannin and carbachol, but not wortmannin alone, also affected the width of the peak of the EGFP-F curves, figure 16C. This suggests that drug treatment has an effect on the membrane distribution of the control EGFP-F and indicates that caution is necessary in interpreting these results. It is also difficult to explain an apparent 'narrowing' of AKAP79 intensity near the membrane when one might have expected AKAP79 distribution to have become more diffuse following release from the membrane.

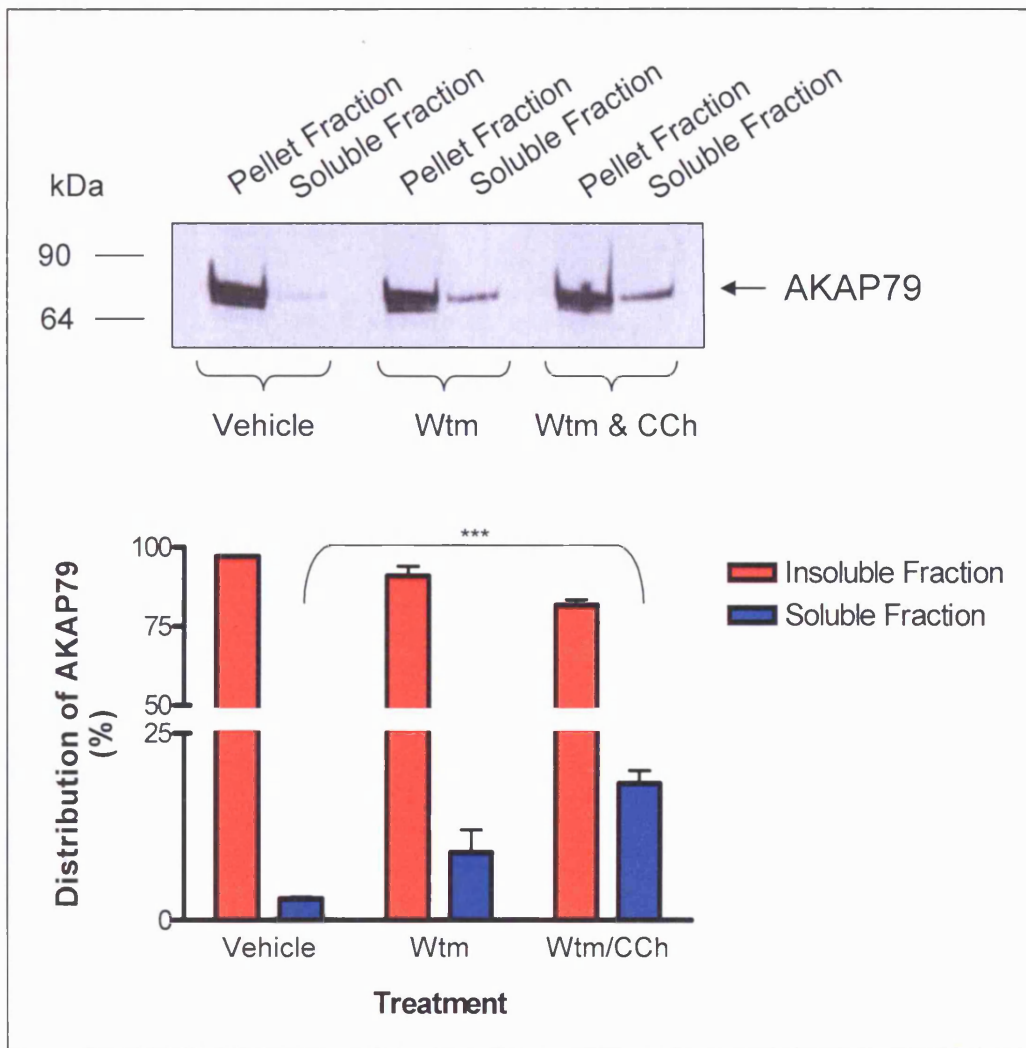


Figure 15. Depletion of $\text{PtdIns}(4,5)\text{P}_2$ causes redistribution of AKAP79. Whole HEK293 cells stably transfected with AKAP79 were treated with wortmannin (Wtm) and carbachol (CCh) to deplete phosphatidylinositol 4,5-bisphosphate ($\text{PtdIns}(4,5)\text{P}_2$). High-speed fractionation and Western blot analysis reveals a significant difference in the level of AKAP79 seen in the soluble fraction from cells treated with wortmannin and carbachol, compared to the soluble fraction from cells treated with vehicle alone ($p < 0.001$). No significant difference could be determined in AKAP79 localisation between vehicle and wortmannin only soluble fractions.

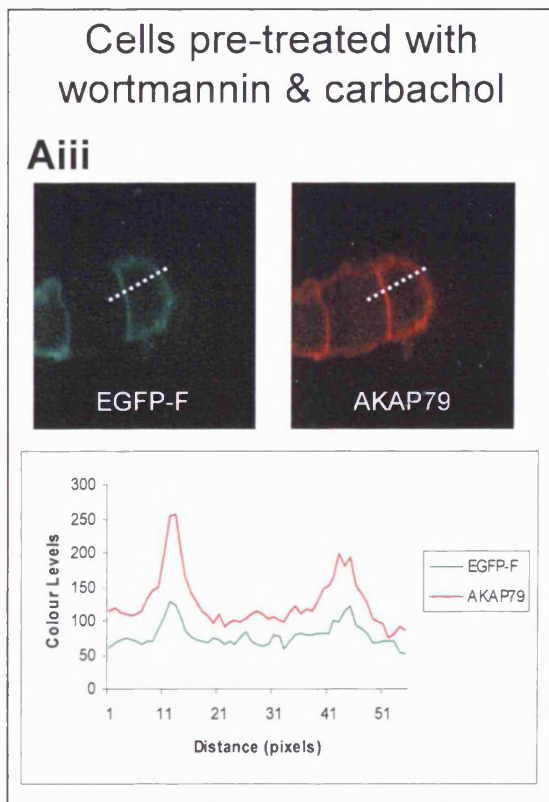
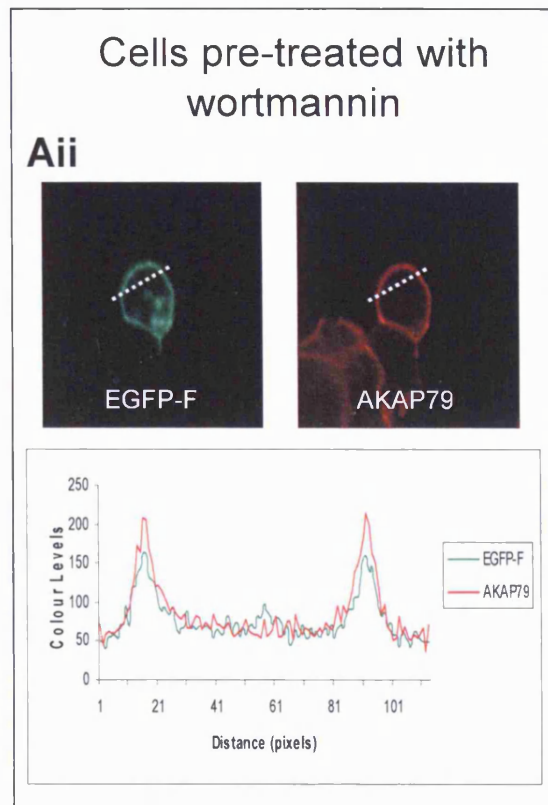
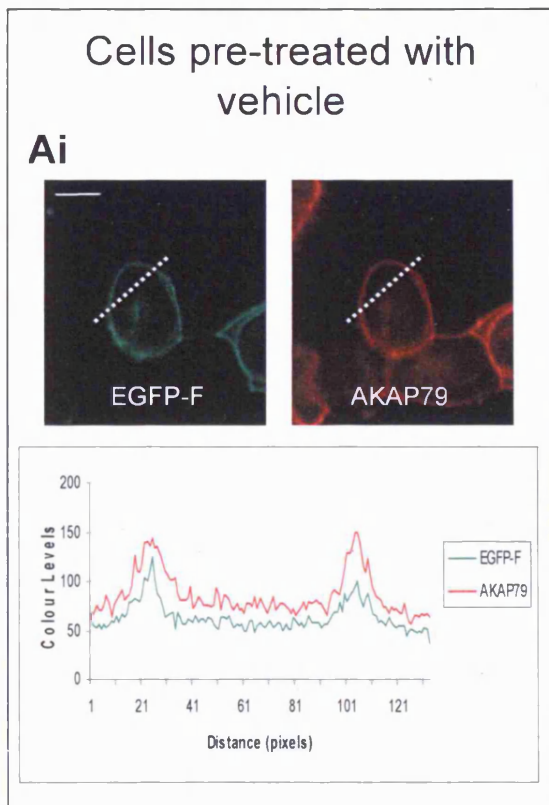


Figure 16. Muscarinic acetylcholine receptor agonists may regulate AKAP79 membrane targeting. HEK293-AKAP79 cells transiently transfected with cDNA encoding EGFP-F were pre-treated with CCh and/or Wtm for 30 minutes prior to fixation and permeabilisation with methanol and subsequently visualised with immunocytochemical techniques as described in Methods & Materials. Pixel profiles were taken (white dashed line) and plotted as shown to enable changes in AKAP79 distribution to be assessed when cells

were i. pre-treated with vehicle; ii. pre-treated with Wtm or iii. pre-treated with Wtm & CCh. Scale bar representative of 20 μ m.

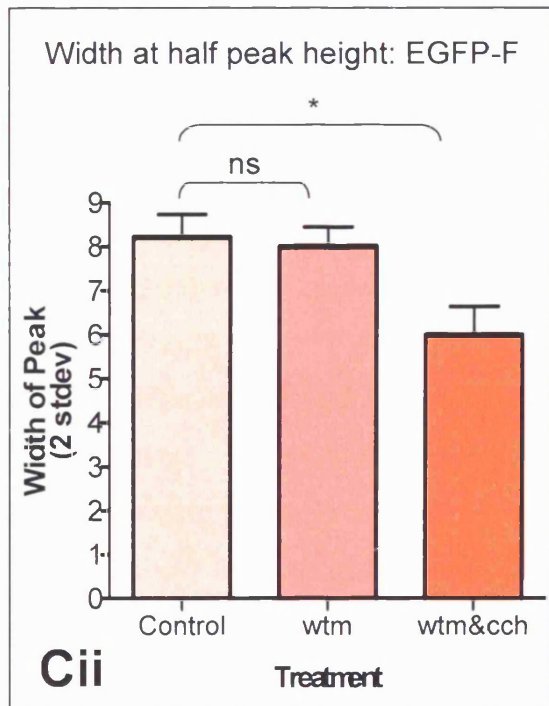
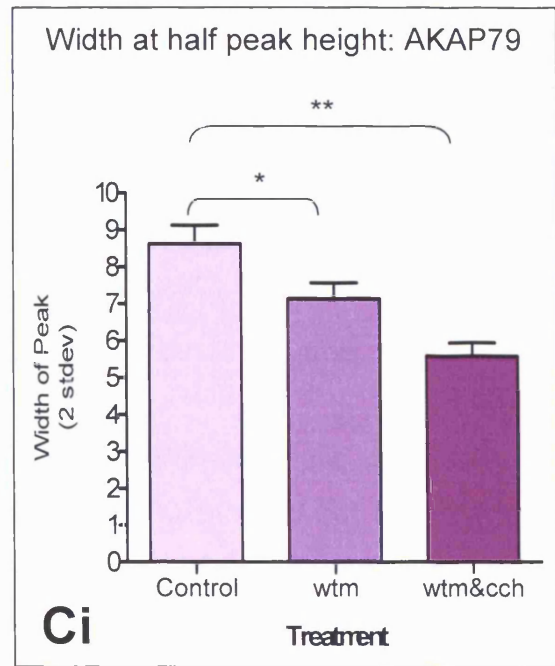
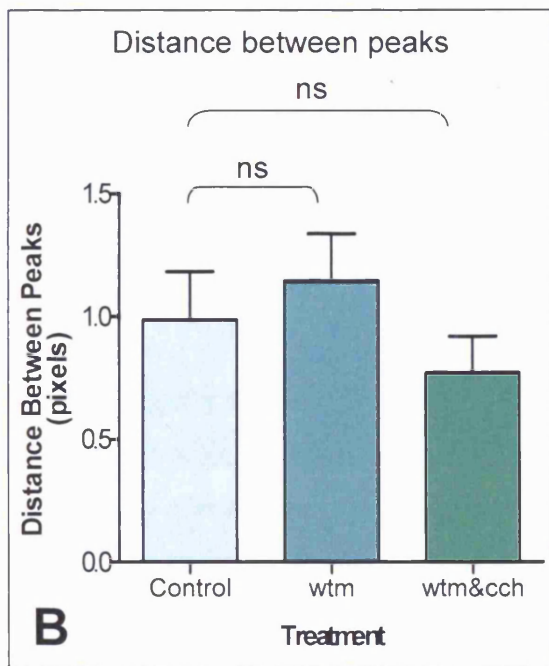


Figure 16. Muscarinic acetylcholine receptor agonists may regulate AKAP79 membrane targeting. Gaussian curves were fitted to the peaks from the pixel profile (using Origin® 6 data analysis program) and the distance between the peaks, at the same point at the membrane, was analysed as shown in histogram B.

C. From the Gaussian curves, the width at half peak height i.e. 2 times standard deviation, was taken and analysed in order to ascertain whether the spread of AKAP79 (i) or EGFP-F (ii) changes upon drug treatment. All data shown are representative of 3 independent experiments, with ≥ 3 cells from each condition imaged in each experiment. * indicates $p < 0.05$; ** indicated $p < 0.001$

From the Gaussian curves, the width at half peak height i.e. 2 times standard deviation, was taken and analysed in order to ascertain whether the spread of AKAP79 (i) or EGFP-F (ii) changes upon drug treatment. All data shown are representative of 3 independent experiments, with ≥ 3 cells from each condition imaged in each experiment. * indicates $p < 0.05$; ** indicated $p < 0.001$

4 Real Time Monitoring of AKAP79 Localisation

Given the inconclusive nature of the immunological studies, we set out to further investigate the effects of PtdIns(4,5)P₂ depletion on AKAP localisation using real time confocal imaging.

4.1 EGFP-tagging of RII α

To monitor the localisation and distribution of AKAP79 within cells we produced EGFP-tagged constructs of the regulatory subunit of PKA, RII α . As RII binds AKAPs with high affinity this allows us to study the distribution of AKAPs within the cells without tagging and potentially altering the AKAPs themselves. For details of how RII α -EGFP was constructed, refer to appendix three.

4.1.1 Expression and Characterisation of RII α -EGFP

Figure 17A and B show Western blot analysis of HEK293 cells transiently transfected with the cDNA construct encoding RII α -EGFP and immunoblotted with antibodies directed against either the EGFP tag or RII α . Figure 17A shows RII α -EGFP running as a single band with a molecular weight of 72kDa (lane 2) and EGFP running as a band at 27kDa (lane 3). Figure 17B shows native RII α running as a single band at 45kDa with RII α -EGFP at 72kDa. All additional bands represent unidentified, non-specific binding. Tagging the PKA regulatory subunit RII α with EGFP does not hinder its ability to express in HEK293 cells.

4.1.2 Does RII α -EGFP Retain its Ability to Bind AKAPs?

To cause minimal disruption to its interaction with AKAPs, the EGFP tag was added to the C-terminus of RII α , well away from its N-terminal AKAP-binding domain. However to confirm that EGFP-tagged RII α retains its ability to interact with AKAPs we carried out co-immunoprecipitation as described in Methods & Materials. HEK293 cells were transiently transfected with cDNAs encoding RII α -EGFP and AKAP79. Antibodies directed against the EGFP tag of RII α -EGFP were able to immunoprecipitate AKAP79, figure 18A. Conversely, antibodies directed against AKAP79 were able to co-precipitate RII α -EGFP, figure 18B. These results indicate that the addition the EGFP tag to the C-terminus of RII α does not adversely affect its ability to interact with AKAPs within cells.

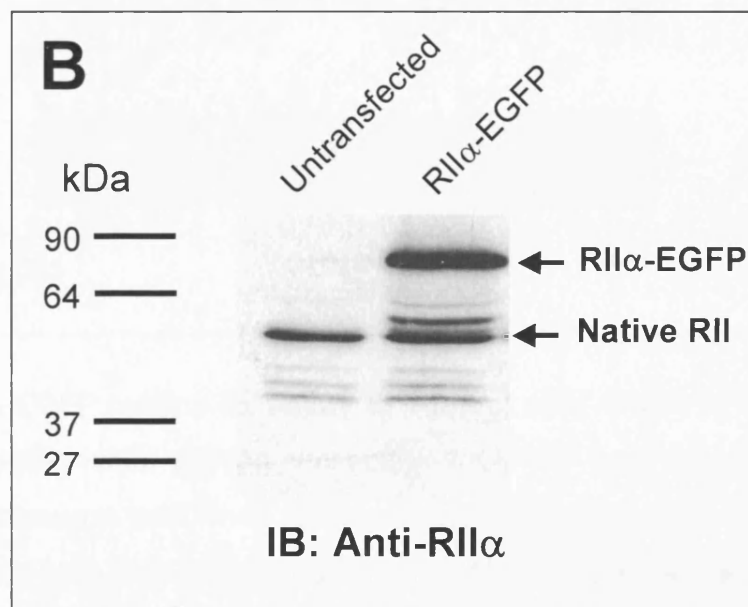
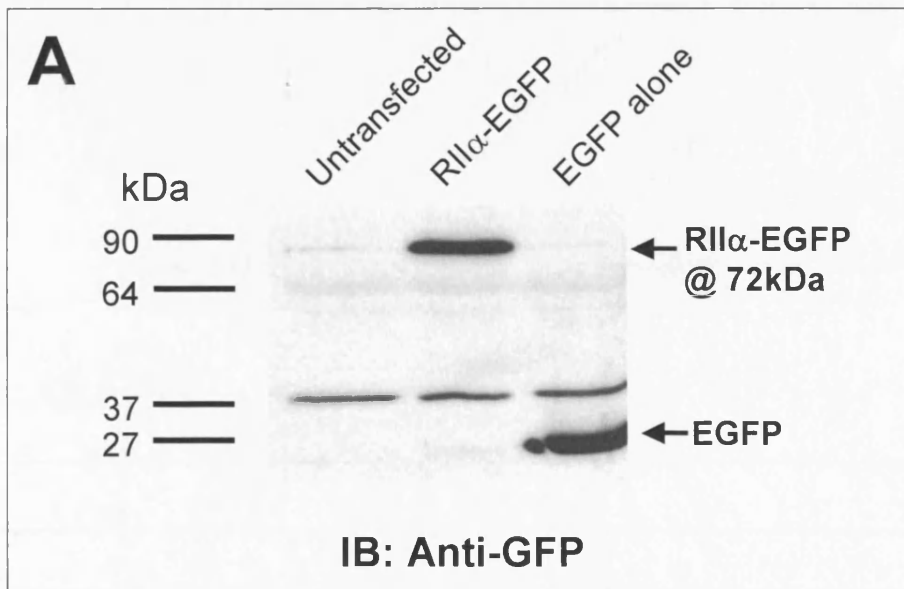


Figure 17. RII α -EGFP expression in a model system. HEK293 cells were transfected with the cDNA encoding RII α -EGFP. Proteins were separated by SDS-polyacrylamide gel electrophoresis and transferred onto nitrocellulose membrane. Western blots were performed using antibodies directed against either the EGFP tag (**A**) or RII α (**B**). **A**, RII α -EGFP runs as a single band with a molecular size of 72 kDa (lane 2). EGFP runs as a single band with a molecular size of 27 kDa (lane 3). An additional band visible in all three lanes represents non-specific binding to an endogenous HEK293 protein. **B**, Native RII α runs as a single band with a molecular size of 45 kDa. RII α -EGFP runs as a single band with a molecular weight of 72 kDa. Additional bands represent unidentified, non-specific binding.

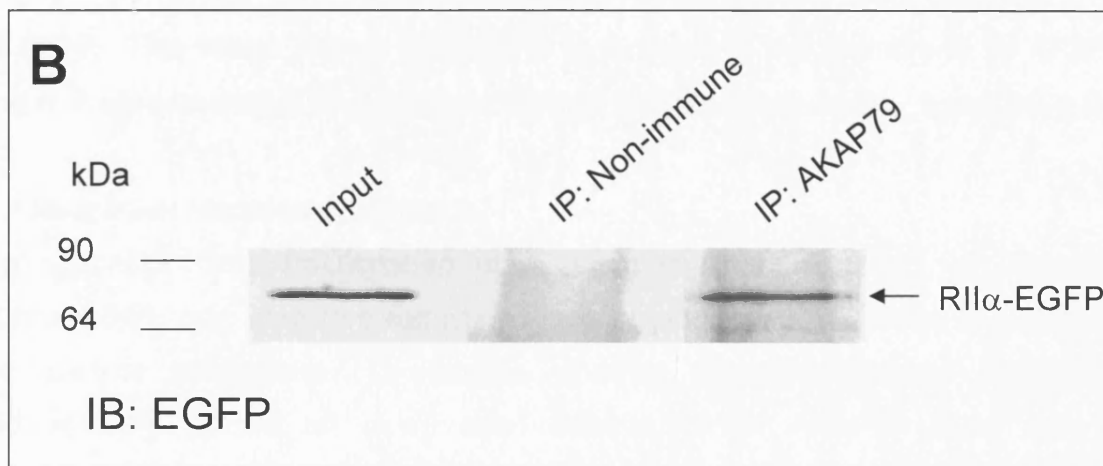
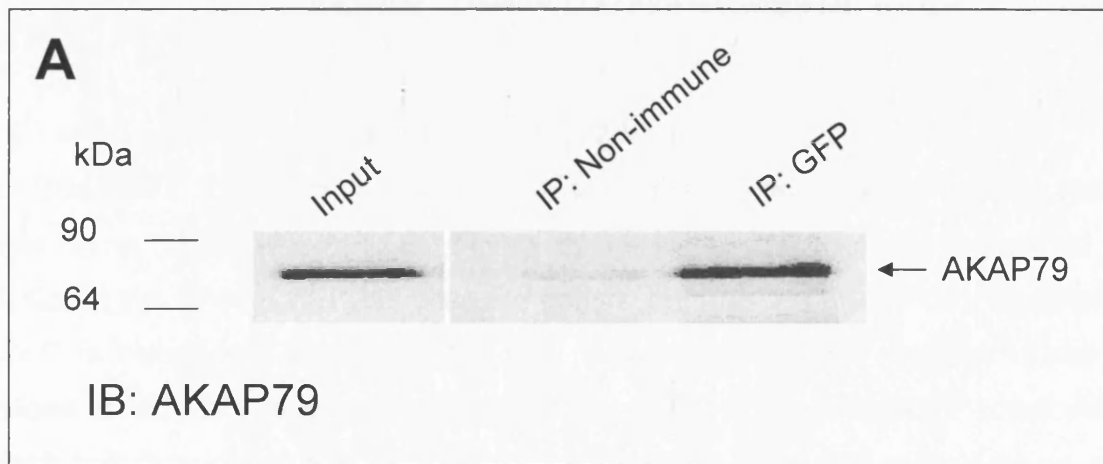


Figure 18. RII α -EGFP retains its ability to interact with AKAP79. HEK293 cells were co-transfected with cDNAs encoding AKAP79 and RII α -EGFP. Co-immunoprecipitation was performed using antibodies directed against the EGFP tag on RII α or rabbit non-immune control serum (**A**), or using antibodies directed against the AKAP79 or mouse non-immune control serum (**B**). Precipitated proteins were separated by SDS-polyacrylamide gel electrophoresis, transferred onto nitrocellulose membrane and immunoblotted with anti-AKAP79 (**A**) or anti-EGFP (**B**). 10% of the cell lysate was run in the extract lane.

4.1.3 Is RII α -EGFP Functional in a Model Cell System?

For RII α -EGFP to be useful as a probe to study the location of AKAPs within cells, it must mirror AKAP distribution. Figure 19 shows typical confocal images of live HEK293 cells. When HEK293 cells are transfected with the pEGFP-N1 vector alone EGFP is distributed throughout the cell, including within the nucleus. Confocal images of HEK293 cells transfected with RII α -EGFP show RII α -EGFP to be evenly distributed throughout the cytoplasm, but excluded from cell nuclei, figure 19B. Figure 19C shows a typical HEK293 cell co-transfected with RII α -EGFP and AKAP79. This image shows RII α -EGFP is targeted to the membrane by AKAP79, and is in agreement with the immunocytochemistry seen previously, figure 8C & D.

4.2 Muscarinic Receptor Expression

Our previous cell fractionation data suggest that depletion of membrane PtdIns(4,5)P₂ may lead to a reduction in the amount of AKAP79 that is anchored to the plasma membrane. To assess whether receptor-mediated depletion of PtdIns(4,5)P₂ causes an observable redistribution of AKAP79 away from the membrane, we transfected HEK293-AKAP79 cells with cDNA encoding RII α -EGFP and performed real-time confocal imaging on these cells following addition of 10 μ M wortmannin and 300 μ M carbachol. Our previous experiments had shown that these concentrations of wortmannin and carbachol cause a significant depletion in bulk cellular levels of PtdIns(4,5)P₂ within these cells (see this chapter Fig.11). As an additional control and to assess the level of PtdIns(4,5)P₂ depletion in individual cells we conducted parallel experiments in which HEK293-AKAP79 cells were transfected with EGFP-PH_{PLC δ 1}, a construct containing the pleckstrin homology domain of PLC δ ₁ which can be used to monitor membrane PtdIns(4,5)P₂ levels (Stauffer *et al*, 1998; Varnai & Balla, 1997).

Originally identified in pleckstrin, the major substrate for PKC in platelets (Ferguson *et al*, 1994; Harlan *et al*, 1994), pleckstrin homology (PH) domains have since been identified in many regulatory proteins and provide a site for interaction of signalling proteins with the membrane (Varnai & Balla, 1998). In many proteins, PH domains bind to phosphoinositides such as PtdIns(4)P, PtdIns(4,5)P₂ and Ins(1,4,5)P₃ (Ferguson *et al*, 1995; Lemmon *et al*, 1995; Salim *et al*, 1996; Harlan *et al*, 1994).

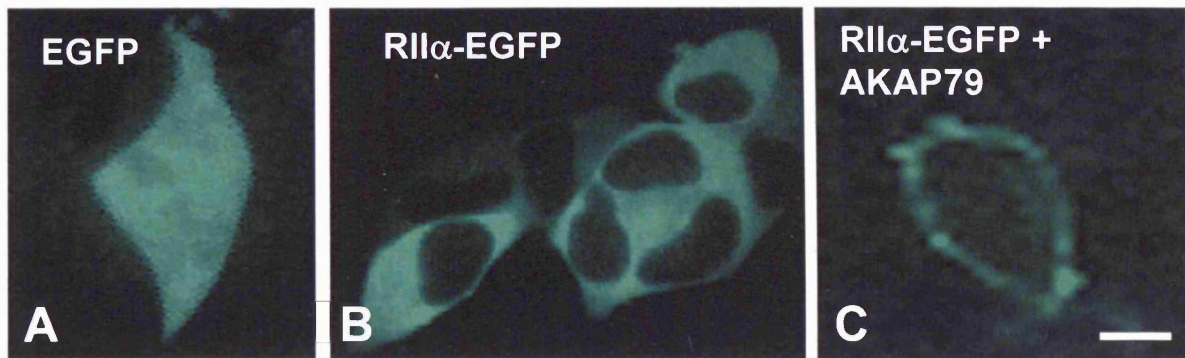


Figure 19. Functional expression of RII α -EGFP in HEK293 cells. Confocal image of live HEK293 cells transfected with **A.** the 'empty' pEGFP-N1 vector. EGFP can be seen distributed throughout cytoplasm and nucleus, **B.** RII α -EGFP. RII α -EGFP is distributed evenly throughout the cytoplasm, but is excluded from the nucleus, and **C.** RII α -EGFP and AKAP79. RII α -EGFP can be seen targeted to the plasma membrane through interaction with AKAP79. Scale bar representative of 20 μ m.

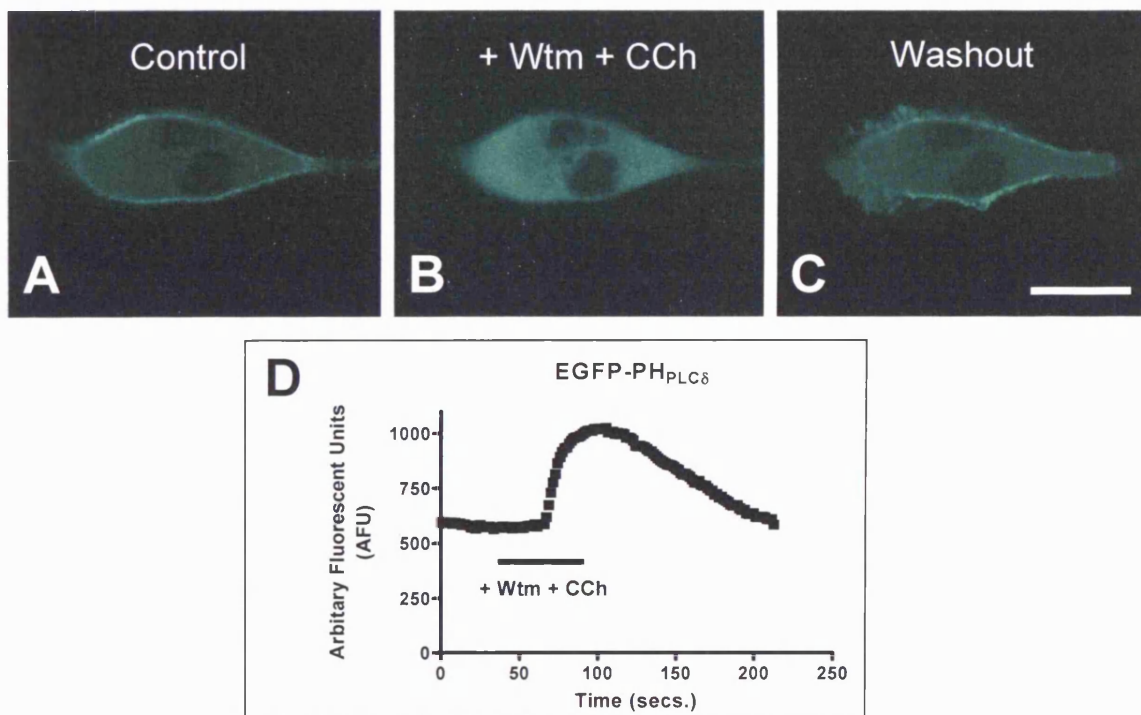


Figure 20. Using EGFP-PH_{PLC δ} to monitor membrane PtdIns(4,5)P₂. Real-time confocal imaging of HEK/M₃ cell transiently transfected with EGFP-PH_{PLC δ} . **A.** Under control conditions EGFP-PH_{PLC δ} is anchored to the membrane via interaction with PtdIns(4,5)P₂ and EGFP fluorescence is confined to the cell periphery. **B.** Addition of 10 μ M wortmannin & 300 μ M carbachol depletes PtdIns(4,5)P₂ and EGFP-PH_{PLC δ} loses association with the membrane and EGFP fluorescence moves into the cytoplasm. **C.** Upon drug washout PtdIns(4,5)P₂ levels recover and EGFP-PH_{PLC δ} reassociates with the membrane. Scale bar representative of 20 μ m. **D.** Time-course of change in fluorescence for a region of interest just below the membrane

The PH domain of PLC δ_1 has the highest affinity for PtdIns(4,5)P₂ compared to PH domains in other proteins (Ferguson *et al*, 1995) and as such is routinely used to specifically visualise cellular PtdIns(4,5)P₂ levels (Stauffer *et al*, 1997; Varnai & Balla, 1997). Under control conditions the PH domain of EGFP-PH_{PLC δ} is anchored to the membrane via interaction with PtdIns(4,5)P₂ and EGFP fluorescence is confined to the cell periphery. Upon PtdIns(4,5)P₂ depletion EGFP-PH_{PLC δ} loses association with the membrane and EGFP fluorescence moves into the cytoplasm.

In preliminary experiments, stimulation of HEK293-AKAP79 cells with wortmannin and carbachol for up to 10 minutes failed to generate significant or reproducible changes in the distribution of either RII-EGFP or, importantly, of EGFP-PH_{PLC δ} , data not shown. However, although HEK293 cells have an endogenous M₃ mACh receptor population, the specific levels vary between each strain. This is potentially important as a low receptor number will lead to lower levels of activated PLC and a low level of PtdIns(4,5)P₂ hydrolysis. As a consequence M₃ mACh receptor density was assessed by the binding of the muscarinic antagonist 1-[N-methyl-³H]scopolamine methyl chloride to intact HEK293-AKAP79 cells as described in Methods and Materials. In a strain of wild type HEK293 cells routinely used in the Cell Physiology & Pharmacology department, University of Leicester, the level of receptor was 33.4 fmol of receptor/mg of protein, HEK293-AKAP79 cells have 17.6 fmol of receptor/mg of protein (data not shown). It can be seen that for some reason the M₃ mACh receptor population in HEK293-AKAP79 is much lower than in wild-type HEK293. To allow maximum depletion of PtdIns(4,5)P₂ and thus assessment of whether a reduction in this plasma membrane phospholipid modulates AKAP79 localisation, HEK293/M₃ cells, a cell line that over-expresses M₃ mACh receptors were chosen for future experiments. These cells (a kind gift from Dr. G. Willars, University of Leicester) have an M₃ receptor level of approximately 1.7pmol/mg of protein (Tovey & Willars, 2004), 100x higher than the levels seen in HEK293-AKAP79 cells.

Figure 20 shows HEK293/M₃ cells transiently transfected with the PtdIns(4,5)P₂-monitoring construct EGFP-PH_{PLC δ} . Under control conditions (time point 0 seconds; left panel, A) EGFP-PH_{PLC δ} fluorescence is confined to the plasma membrane. This agrees with studies suggesting that the PH domain of this construct is anchored to

the membrane via interaction with PtdIns(4,5)P₂ (Garcia *et al*, 1995; Lemmon *et al*, 1995; Rebecchi & Pentylala, 2000; Nahorski *et al*, 2003). Following stimulation with wortmannin and carbachol and a depletion of PtdIns(4,5)P₂ in the membrane, EGFP-PH_{PLC δ} fluorescence moves from the plasma membrane to become uniformly distributed in the cytosol, figure 20 middle panel, B. Upon washout of agonists EGFP-PH_{PLC δ} translocates back to the plasma membrane signifying a return to basal PtdIns(4,5)P₂ levels, figure 20 right panel, C. Figure 20D shows fluorescence plotted against time for pooled region of interest data (n=9 cells) drawn just below the cell membrane and demonstrates the agonist-induced translocation of the EGFP-PH_{PLC δ} construct.

To investigate whether this agonist-induced depletion of PtdIns(4,5)P₂ leads to a similar redistribution of AKAP79, HEK293/M₃ cells were transiently transfected with RII α -EGFP and AKAP79 and the cellular distribution of the fluorescence monitored following treatment with wortmannin and carbachol. Figures 21A-C show that stimulation with wortmannin and carbachol produced no detectable redistribution of RII α -EGFP fluorescence, suggesting that membrane depletion of PtdIns(4,5)P₂ does not result in a substantial change in the location of AKAP79. Figure 21D shows fluorescence plotted against time for pooled region of interest data (n=10 cells) drawn just below membrane and reiterates that there is no significant translocation of AKAP79 within these cells following muscarinic receptor stimulation.

5 Conclusions

To investigate the possibility that receptor-driven depletion of the lipid anchor PtdIns(4,5)P₂ affects the association of AKAP79 with the plasma membrane, we first conducted control experiments to establish the conditions under which we could achieve a significant decrease in PtdIns(4,5)P₂. Measurement of cellular phosphoinositides showed that pre-treatment of HEK293-AKAP79 cells with 10 μ m wortmannin + 300 μ m carbachol for 30 minutes caused a 59.4 \pm 1.6% depletion of PtdIns(4,5)P₂. In membrane fractionation experiments, incubation of HEK293-AKAP79 cells with this concentration of wortmannin and carbachol resulted in 6-fold increase in the amount of AKAP79 present in the soluble cellular fraction compared to cells treated with vehicle alone, suggesting that depletion of membrane PtdIns(4,5)P₂ does indeed cause a release of AKAP79 from the membrane into the

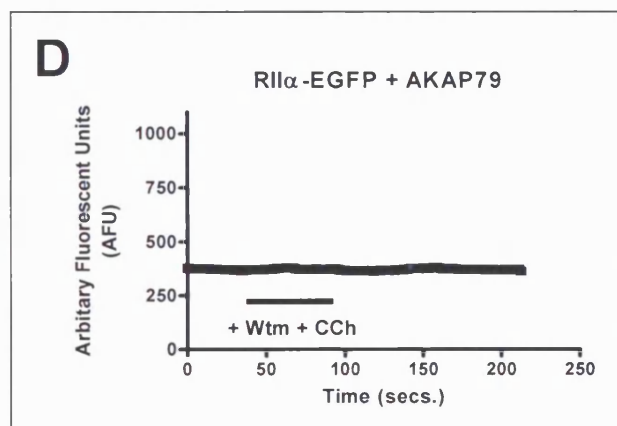
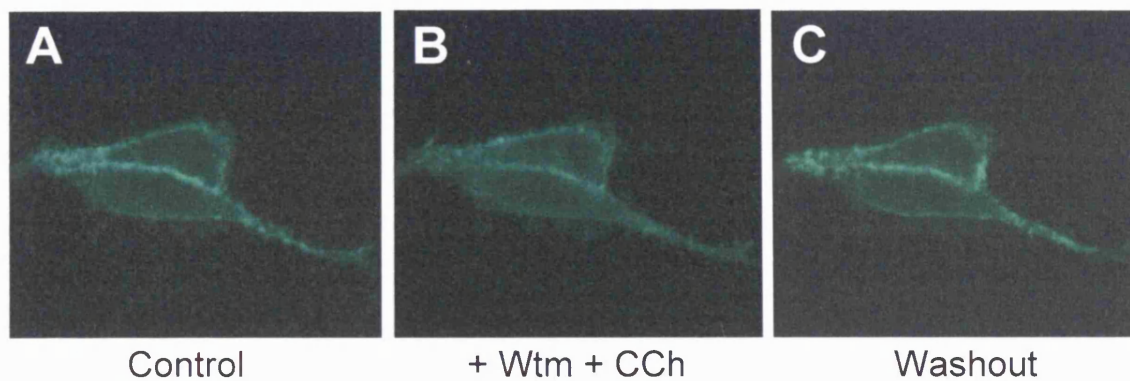


Figure 21. Receptor-driven depletion of membrane $\text{PtdIns}(4,5)\text{P}_2$ does not cause a significant redistribution of AKAP79. Real-time confocal imaging of HEK/ M_3 cells transiently transfected with AKAP79 and RII α -EGFP. **A.** Under control conditions RII α -EGFP is anchored to the membrane via interaction with AKAP79. **B.** Stimulation with wortmannin and carbachol produces no detectable redistribution of RII α -EGFP fluorescence. **C.** Drug washout. Scale bar representative of 20 μm . **D.** Time-course of change in fluorescence for a region of interest just below the membrane.

cytosolic fraction. Our attempts to visualize this apparent redistribution of AKAP79 unfortunately proved largely unsuccessful.

We initially attempted immunocytochemical studies on fixed HEK293-AKAP79 cells transfected with cDNA encoding the plasma membrane marker EGFP-F to assess whether pre-treatment with wortmannin and carbachol produced a significant shift in AKAP79 away from the membrane. The results of these experiments were inconclusive, largely because drug treatment was found to have a significant effect on the membrane distribution of the control membrane marker EGFP-F. We next undertook real-time confocal imaging of HEK293-AKAP79 transfected with cDNA encoding RII α -EGFP. RII α -EGFP binds to AKAP79 and acts as a marker protein for AKAP79 distribution. Use of RII α -EGFP as a marker means that AKAP79 itself does not have to be tagged with bulky EGFP proteins that might alter its function. Here as a control to ensure adequate depletion of membrane PtdIns(4,5)P₂ in individual cells during the course of our experiment, we conducted parallel experiments in which HEK293-AKAP79 cells were transfected the PtdIns(4,5)P₂-monitoring construct EGFP-PH_{PLC δ} . We found that treatment with wortmannin and carbachol for up to 15mins did not produce a significant or reproducible translocation of EGFP-PH_{PLC δ} from the membrane to the cytosol, suggesting that under these conditions, there is not significant depletion of membrane PtdIns(4,5)P₂. Prolonged exposure to wortmannin and carbachol, which we had previously showed produces a significant drop in this phospholipid, was deemed impractical in these particular experiments due to bleaching of the fluorophore and drift in confocal plane. We therefore switched to using a HEK293 cell line stably expressing high levels of M₃ receptors and in which significant falls in membrane PtdIns(4,5)P₂ could be observed using EGFP-PH_{PLC δ} within 30 seconds of wortmannin and carbachol application. Stimulation of these HEK293/M₃ cells transfected with AKAP79 and RII α -EGFP with wortmannin and carbachol produced no detectable redistribution of RII α -EGFP fluorescence, suggesting that membrane depletion of PtdIns(4,5)P₂ does not result in a substantial translocation of AKAP79 within these cells following muscarinic receptor stimulation.

This lack of any observable redistribution of AKAP79 does not conclusively rule out a role for receptor-driven depletion of PtdIns(4,5)P₂ in regulating AKAP79 membrane

association. AKAP79 has for example been shown to be extensively associated with the cytoskeleton (Oliveria *et al*, 2003), and may thus be prevented from moving freely into the cytosol. Interaction with the cytoskeleton and short-range redistribution may also ensure that AKAP79 can re-associate quickly with the correct signalling machinery when required.

Imaging techniques with a greater resolution (such as Fluorescence resonance energy transfer (FRET) or total internal reflection fluorescence (TIRF)) may ultimately be required to assess whether AKAPs are dynamically associated with the membrane. FRET exploits the difference in excitation and emission wavelengths of many fluorophores, where the emission of one fluorophore overlaps the absorbance of a second fluorophore. If the donor fluorophore is excited with the appropriate wavelength of light, the result is quenching of its emission and indirect excitation and emission from the acceptor fluorophore. However, the distance over which this energy transfer occurs is limited to approximately 10nm.

The use of FRET to investigate regulated AKAP79 anchoring would require a fluorophore-conjugated membrane-associated protein in close proximity to AKAP79 to act as either a donor or acceptor. Loss of the FRET signal between this protein and AKAP79 following receptor stimulation could be used to imply that these proteins had moved away from each other and out of energy transfer range.

An alternative to FRET might be to use TIRF imaging. Here, an evanescent wave is used to reduce the level of fluorescence from outside the focal plane, improving the signal-to-noise ratio and reducing the optical section to 5 times thinner than that of any current confocal microscope thereby improving spatial resolution; fluorophores outside 200nm will not be excited. TIRF could be used to investigate the regulation of AKAP79 targeting to the plasma membrane by simply GFP tagging AKAP79. With the focal plane set up such that it is situated just below the plasma membrane, if AKAP79 targeting is a dynamically regulated process, movement of this AKAP away from the membrane could result in movement out of the focal plane and hence loss of fluorescence.

Clearly, much additional work needs to be done to identify suitable membrane marker proteins and until this time the intriguing possibility of receptor-regulated AKAP membrane association cannot be entirely ruled out.

CHAPTER FIVE

INTERACTIONS BETWEEN AKAP79 AND KIR CHANNELS: Identification of binding site on Kir2.1

Aside from controlling localisation of PKA, AKAPs may also interact with membrane associated proteins, presumably to anchor pools of PKA close to substrate phosphorylation sites. Here we investigate this further, focussing on the integral membrane protein, the inwardly rectifying potassium channel Kir2.1.

1 Introduction

Potassium ion channels represent a diverse family of proteins that are expressed in both excitable and non-excitable cells (Reinmann & Ashcroft, 1999) and selectively conduct potassium ions across the cell membrane.

In most cells they play an essential role in maintaining and stabilising the resting membrane potential. In nerve and muscle cells, their ability to 'repolarise' the membrane helps them control action potential frequency and duration, while other functions include regulation of neurotransmitter release, hormone secretion, epithelial electrolyte transport, cell proliferation, apoptosis, tumour progression and potassium homeostasis (Jan & Jan, 1997a & b; Nichols & Lopatin, 1997; Coetzee *et al*, 1999; Lesage & Lazdunski, 2000; Yellen, 2002).

Potassium channels are made up of pore-forming α subunits that often co-assemble with accessory proteins. They are by far the largest and most diverse of the ion channel families, with over 70 different genes in the human genome coding for the principal subunits (Coetzee *et al*, 1999; Jenkinson, 2006; Alexander *et al*, 2006). Diversity is further increased by alternative splicing of α subunit genes, and by both homomeric and heteromeric assembly of the different α subunits.

Despite their variety, the number of transmembrane domains in each α subunit can be used to classify the K^+ channel superfamily into 3 distinct groups (Alexander *et al*,

2006). The first major group is made up of K⁺ channels that have six transmembrane (6TM) domains in each of their principal subunits. Four such subunits come together to form functional voltage- and/or Ca²⁺-activated K⁺ channels - these include the Kv family as well as members of the KCNQ, EAG, the Ca²⁺-activated Slo (which despite having 7TM domains are classified in this group) and the Ca²⁺-activated SK subfamilies (Bauer & Schwarz, 2001; Robbins, 2001; Yellen, 2002; Stocker, 2004; Alexander, 2006). The second group is made up of K⁺ channels that have four transmembrane (4TM) domains per subunit and comprises the 'leak' channels TWIK, TREK, TASK, TALK, THIK and TRESK. These contain two pore domains in each α subunit and the functional channel probably forms as a dimer (Lesage & Lazdunski, 2000; Patel & Honore, 2001). The final group, and the focus of this chapter, comprise the 2TM domain inward rectifier family which includes the strong inward rectifiers Kir2, the G protein-activated inward rectifiers Kir3 and the ATP-sensitive potassium channels Kir6 (Nichols & Lopatin, 1997; Ashcroft & Gribble, 1998; Stanfield *et al*, 2002).

1.1 Inwardly Rectifying Potassium Channels

Inwardly rectifying potassium (Kir) channels have been shown to serve a variety of physiological functions, ranging from maintaining the resting membrane potential and the pacing of both cardiac myocytes and neurones, to the pancreatic regulation of insulin secretion and renal K⁺ transport (Hille, 2001). Based on sequence and functional properties, the fourteen Kir channels are classified into seven subfamilies: Kir1.x – Kir7.x (Doupnik *et al*, 1995; Nichols & Lopatin, 1997; Schröder *et al*, 2002).

These ion channels, as their name suggests, allow potassium ions to move more easily into the cell than out. However, electrochemical conditions favouring potassium influx are rarely met in animal cells and thus, despite their name, inward rectifiers predominantly conduct outward potassium currents under physiological conditions (Minor *et al*, 1999).

The phenomenon of inward rectification results from reversible occlusion of the channel pore by intracellular magnesium (Vandenberg, 1987; Matsuda *et al*, 1987) and positively charged intracellular spermine and spermidine (Fakler *et al*, 1994 & 1995; Lopatin *et al*, 1994 & 1995; Ficker *et al*, 1994; Lu & MacKinnon, 1994; Wible *et*

al, 1994). Whilst this applies to all inwardly rectifying potassium channels, it has been shown that the sensitivity of these channels to intracellular spermine differs between different isoforms and directly relates to the degree of rectification (Fakler *et al*, 1994; Panama *et al*, 2004). Block by magnesium and polyamines does not conform to one-to-one binding and thus it has been suggested that the channel pore can hold more than one blocking molecule at a time (Yang *et al*, 1995).

1.1.1 The Kir2 family

Within the Kir2 family of ion channels, Kir2.1, Kir2.2 and Kir2.3 subunits have long been thought to be the only members (Kubo *et al*, 1993; Koyama *et al*, 1994; Makhina *et al*, 1994; Perier *et al*, 1994). However, in 1998 a fourth subunit, Kir2.4, was cloned from rat brain showing 53-63% similarity to the other Kir2 members (Topert *et al*, 1998).

Compared to voltage-gated potassium channels Kir channels have a relatively simple structure, and it is thought that Kir channels could be evolutionarily derived from the last two transmembrane spanning domains of the 6TM voltage-gated potassium channels (Jan & Jan, 1994).

Kir channels are tetrameric with each subunit comprised of only two membrane-spanning regions (M1 and M2) and with both N- and C-terminal regions residing inside the cell (Ho *et al*, 1993; Kubo *et al*, 1993). M1 and M2 are separated by a highly conserved re-entrant loop structure (H5, also known as the P region) that lines the channel pore and forms the selectively filter (Nichols & Lopatin, 1997).

1.1.1.1 Regulation by PKA

All four Kir2 channels are constitutively active and it has been suggested that for normal Kir2.1 function, constant channel phosphorylation by PKA is required (Fakler *et al*, 1994; Ruppertsberg & Fakler, 1996). Yet PKA has also been reported to: - enhance (Dart & Leyland, 2001; Monaghan *et al*, 1999), inhibit (Wischmeyer & Karschin, 1996; Koumi *et al*, 1995a/b) and even not be required at all (Jones, 1996; Kamouchi *et al*, 1997) for Kir2.1 channel function.

It is possible that the lack of consensus as to the role played by PKA phosphorylation stems from a difference in the signalling/phosphorylation machinery within the systems studied. It has been shown recently that cAMP-dependent modulation of whole-cell currents of the inwardly rectifying potassium channel, Kir2.1, requires the presence of the multivalent anchoring protein, AKAP79, and that Kir2.1 and AKAP79 exist together in a complex within intact cells (Dart & Leyland, 2001). Here, we extend this study by identifying a binding site of AKAP79 on the intracellular C-domain of Kir2.1.

2 AKAP79 Co-immunoprecipitates with Kir2.1, Kir2.2 and Kir2.3

It has previously been shown that Chinese Hamster Ovary (CHO) cells expressing both Kir2.1 and AKAP79 display significantly greater levels of whole cell current in response to elevated intracellular cAMP than cells expressing Kir2.1 alone (Dart and Leyland, 2001). Furthermore, AKAP79 was found to co-immunoprecipitate with Kir2.1 in COS-7 transfected cells indicating some association between these two proteins and suggesting that AKAP79 may function to anchor kinases close to vital phosphorylation sites on this inwardly rectifying potassium channel. Interactions between AKAPs and ion channels has been previously shown for the L-type calcium channel ($Ca_v1.1$), the KCNQ1-KCNE1 potassium channel and the ryanodine receptor/calcium release channel (Hulme *et al*, 2002; Marx *et al*, 2001 & 2002). The purpose of this study was to confirm and expand on the findings by Dart & Leyland, 2001, and map the residues serving as an AKAP79 binding site on Kir2.1.

HEK293-AKAP79 cells were transiently transfected with cDNAs encoding Kir2.1, Kir2.2 or Kir2.3. Due to a lack of reliable antibodies directed against the members of the Kir2 family, the cDNA encoding ion channels Kir2.1, 2.2 and 2.3 all included an N-terminal EGFP epitope tag thereby enabling the use of an anti-GFP antibody in subsequent co-immunoprecipitation experiments. Addition of an EGFP tag to these ion channels has been previously shown not to hinder their function (Leyland *et al*, 1999).

Figure 22 shows that antibodies directed against the EGFP epitope tag on Kir2.1, 2.2 and 2.3 were able to co-immunoprecipitate AKAP79 from HEK293-AKAP79 cell homogenates, while non-immune serum could not. This confirms and further

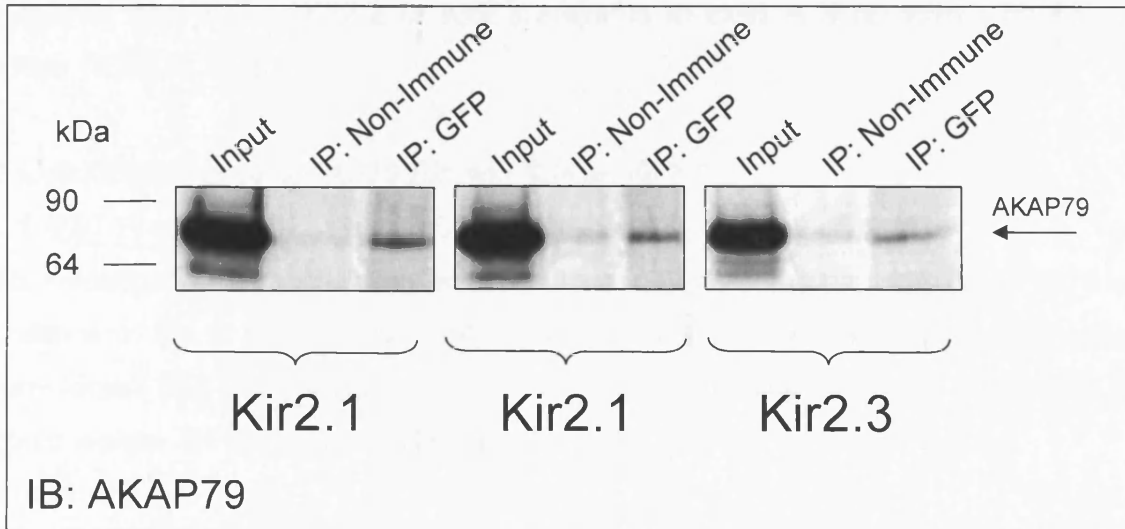


Figure 22. AKAP79 co-immunoprecipitates with Kir2.1, Kir2.2 & Kir2.3. HEK293-AKAP79 cells were transiently transfected with cDNAs encoding EGFP-Kir2.1, EGFP-Kir2.2 or EGFP-Kir2.3. Immunoprecipitations were performed using antibodies directed against the EGFP epitope tag on the ion channels or rabbit non-immune serum as described in Methods & Materials. Precipitated proteins were separated by SDS-polyacrylamide gel electrophoresis, transferred onto nitrocellulose membrane and immunoblotted with anti-AKAP79. 10% of cell lysate was run in the input lane. AKAP79 runs as a single band with a molecular size of 79kDa. Additional bands in input lanes represent unidentified, endogenous HEK293 proteins.

suggests that Kir2.1, Kir2.2 or Kir2.3 are able to exist in a complex with AKAP79 within HEK293 cells.

3 Identification of an AKAP79 Binding Site on Kir2.1

3.1 GST Fusion Proteins and GST Pulldowns

To investigate the site of interaction between Kir2 channels and AKAP79, fusion proteins of the C terminal intracellular region of the ion channel and glutathione S-transferase (GST) were constructed and used in pulldown assays to establish if they could isolate AKAP79 from cell lysates.

Many GST fusion proteins are not completely soluble and consequently sufficient levels of protein cannot be purified from crude lysates (Frangioni & Neel, 1993) as the majority of GST fusion protein may be lost in the post-sonicate pellet. Unfortunately this was the case with some of the GST fusion proteins we made and as such it was necessary to use a variety of methods to maximise the yield of the purified proteins. Here we show that varying the temperature in which the host *E. coli* is grown from 37°C to 22°C considerably increased the solubility and hence yield, figure 23.

Often the GST fusion protein yield is low because it is compartmentalised into inclusion bodies (Frangioni & Neel, 1993). A method often employed to release protein from these inclusion bodies is to use a denaturant. We demonstrate here that by using 8M urea to solubilise the *E. coli*, sufficient levels of protein can be obtained, figure 23. However, to ensure that the GST fusion proteins retained their functionality the urea was slowly removed via dialysis against PBS as described in Methods and Materials.

Initial GST pulldowns showed that the full length C-terminus of Kir2.1 is able to isolate AKAP79 from lysates of HEK293 cells transfected with cDNA encoding AKAP79. GST alone was unable to isolate AKAP79; AKAP79 binding above basal (GST alone) = GST-C (182-428) = 695.8 ± 139.4%, figure 24Bi and ii. This is in agreement with the findings of Dart & Leyland, 2001.

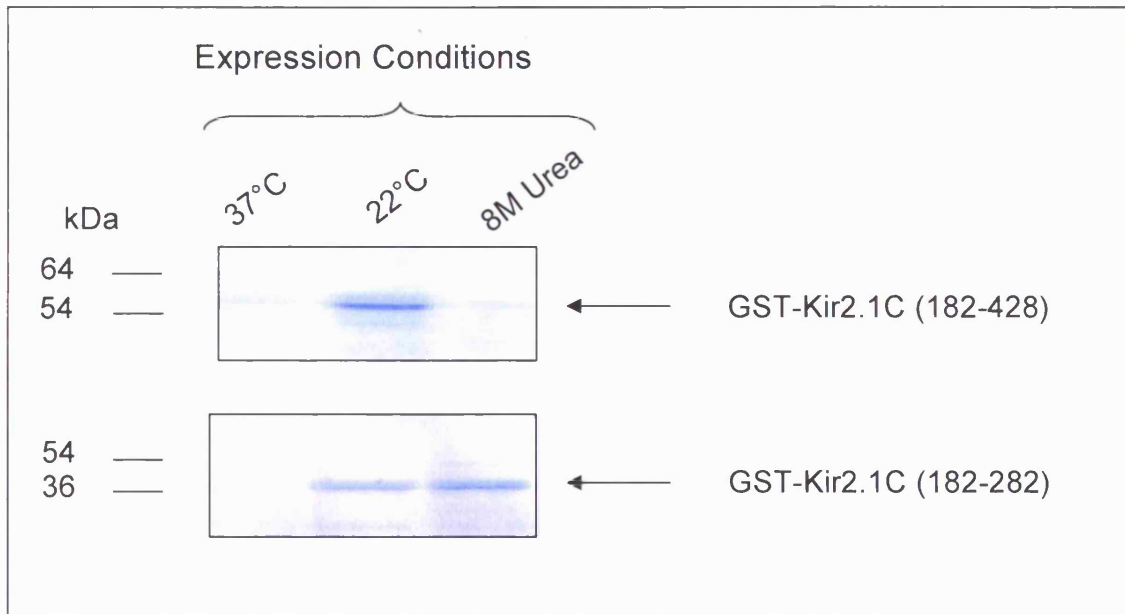


Figure 23. Expression and purification of GST-fusion proteins. Not all GST fusion proteins can be purified using the same procedures. Each GST fusion protein underwent three purification processes where the bacteria were grown at either 37°C or 22°C and solubilised with Triton X or grown at 37°C and solubilised with 8M urea. Subsequently the protein extracts were resolved by SDS-polyacrylamide gel electrophoresis and EZ™ stained to assess the relative protein levels, as described in Methods & Materials. Optimum levels of GST-Kir2.1 C (182-428) protein was achieved through growth of the host bacteria at 22°C whereas optimum levels of GST-C (182-282) could be achieved using either growth at 22°C and solubilisation with Triton X or growth at 37°C and solubilisation with 8M urea. Additional bands represent probable degradation products of GST proteins.

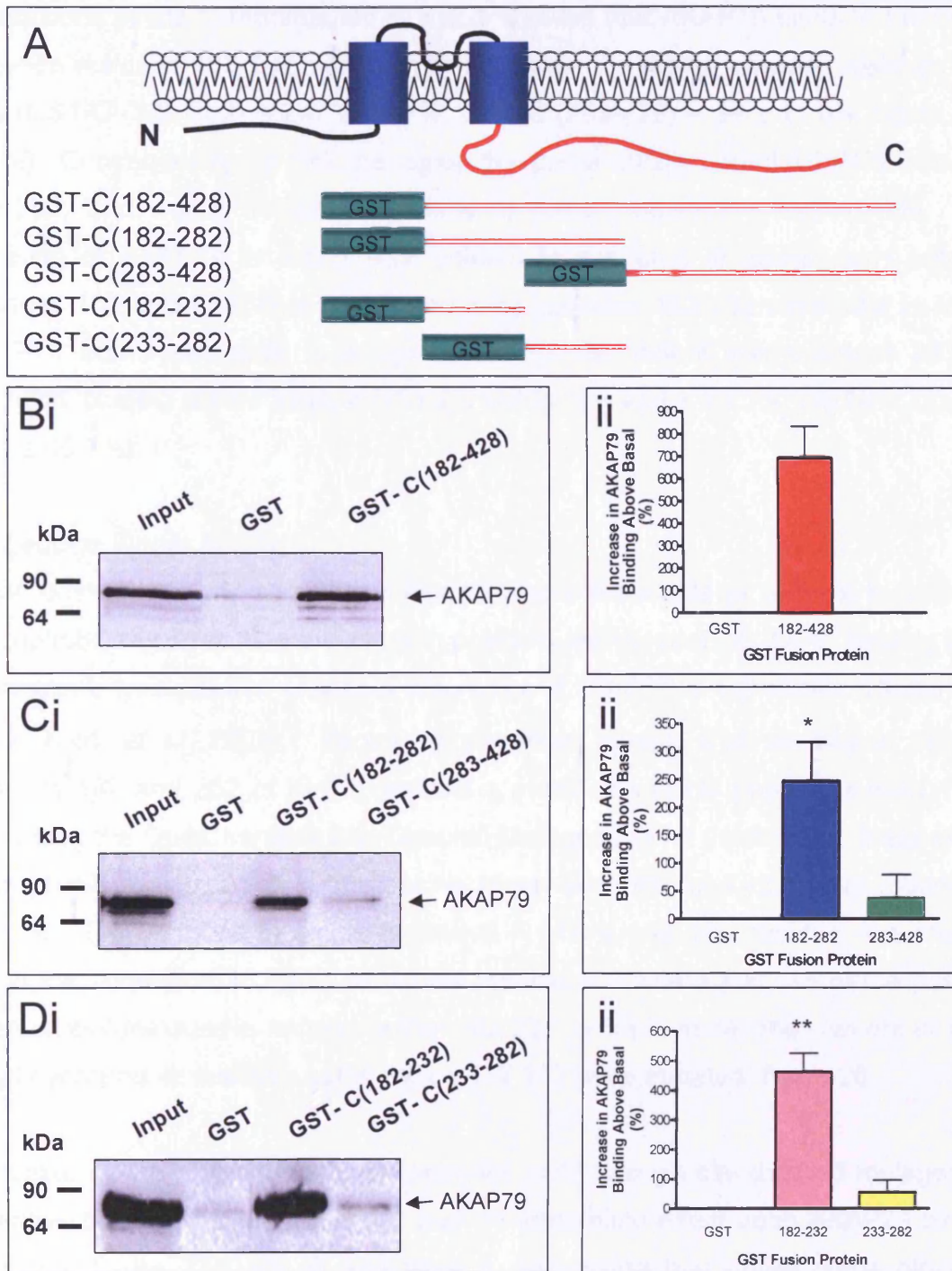


Figure 24. Identification of the AKAP79 binding site on Kir2.1. GST pulldowns show GST-C (182-232) is consistently able to isolate significantly more AKAP79 from AKAP79 transfected HEK293 cells compared to GST alone, GST-C (282-428) and GST-C (233-282). 10% of HEK293 cell lysate was run in the input lane. Histograms show an increase in AKAP79 binding above basal (GST alone) with GST-C (182-428) = $695.8 \pm 139.4\%$, GST-C (182-282) = $247 \pm 69.7\%$ GST-C (283-428) = $39 \pm 41.0\%$, GST-C (182-282) = $454 \pm 63.2\%$ & GST-C (233-282) = $61.5 \pm 40.7\%$. Mean \pm SEM; $n \geq 3$. * $p < 0.05$, ** $p < 0.01$, unpaired, one-tailed, Student's t-test. For each experiment, identical gels were stained with EZBlue™ to ensure that equal amounts of GST fusion protein were used for each pulldown.

Truncations of the C-terminal tail of Kir2.1 showed that AKAP79 binds to the region between residues 182-282 significantly more than the region between residues 283-428 (GST-C (182-282) = $247 \pm 69.7\%$; GST-C (283-428) = $39 \pm 41.0\%$, figure 24Ci and ii). Consequently we took the region that preferentially bound AKAP79 (residues 182-282) and made further truncations to narrow down the binding site. The tethering of AKAP79 to Kir2.1 was isolated to a stretch of amino acids between residues 182 and 232, figure 24Di and ii, as residues 182-232 were able to isolate AKAP79 from lysed cells to a significantly greater extent than residues 233-282 (AKAP79 binding above basal = GST-C (182-232) = $454 \pm 63.2\%$; GST-C (233-282) = $61 \pm 40.7\%$).

3.2 Leucine Zipper Motifs

It has been previously shown that leucine zipper-like motifs (a periodic repetition of hydrophobic residues at every seventh position) are required for AKAP binding to ion channels: L-type calcium channels (Ca_v1.1) and KvLQT1 ion channels (Hulme *et al*, 2002; Marx *et al*, 2002). Sequence alignment reveals that the region between residues 182 and 232 of Kir2.1 contains a modified leucine zipper-like motif, figure 25. Using the QuikChange® Site-Directed Mutagenesis kit (Invitrogen), these crucial hydrophobic residues within the leucine zipper-like motif of Kir2.1 were mutated to alanine. This resulted in single mutations – where only one residue was mutated within the sequence 182-232, or double mutations – where just two of the possible three crucial residues is mutated within 182-232, or triple mutations – where all three initial hydrophobic residues in the region 182-232 were mutated, figure 26.

Disruption of the modified leucine zipper-like motif through site-directed mutagenesis of single, double or triple mutations had no discernible effect upon AKAP79 binding to Kir2.1, figure 27A and B and table 6, suggesting that unlike some other ion channels, Kir2.1 does not target AKAPs through leucine zipper interactions and implies the existence of a novel AKAP binding motif.

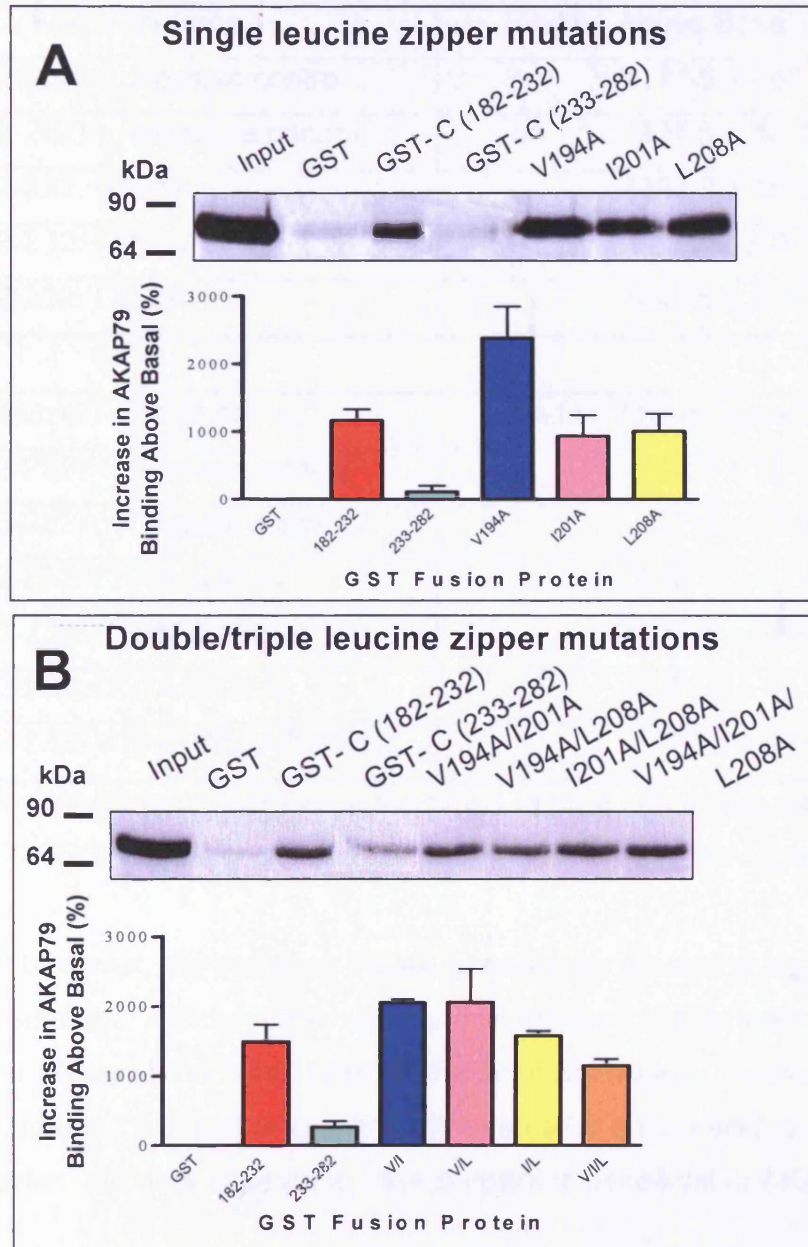


Figure 27. Mutations of residues in the Kir2.1 leucine zipper-like motif do not inhibit Kir2.1 binding to AKAP79. GST pulldowns showing comparable AKAP79 binding levels between GST-C (182-232) and single mutants (A): GST-C (V194A), GST-C(I201A) and GST-C(L208A), double mutants (B): GST-C (V194A/I201A), GST-C (I201A/L208A), GST-C (V194A/L208A), and triple mutant: GST-C (V194A/I201A/L208A). GST and GST-C (233-282) were unable to isolate AKAP79 from HEK293 transfected cells. 10% HEK293 cell lysate was run in the input lane. Histograms show a significant difference in AKAP79 binding between positive control (GST-C(182-232)) = $1492.22 \pm 431.11\%$ and negative control (GST-C(233-282)) = $266.44 \pm 148.6\%$ (mean \pm SEM $n \geq 3$). Mutation of residues potentially important in the leucine zipper-like motif did not significantly alter AKAP79 binding to Kir2.1 compared to positive control, $p > 0.05$, unpaired, two-tailed, Student's t-test. Interestingly, mutation V194A significantly increases AKAP79 binding. $p < 0.05$, unpaired, one-tailed, Student's t-test.

Single Mutants	Binding Above Basal (GST alone)
GST-C (182-232) Positive control	1177.5 ± 163.5%
GST-C (233-282) Negative control	127.5 ± 88.1%
GST-C (182-232: V194A)	2392.5 ± 463.1%
GST-C (182-232: I201A)	922.5 ± 308.7%
GST-C (182-232: L208A)	1042.5 ± 255.1%
Double/Triple Mutants	
GST-C (182-232) Positive control	1522.5 ± 284.9%
GST-C (233-282) Negative control	277.5 ± 85.8%
GST-C (182-232:V194A/I201A)	2047.5 ± 47.4%
GST-C (182-232: V194A/L208A)	2077.5 ± 480.9%
GST-C (182-232: I201A/L208A)	1582.5 ± 68.3%
GST-C (182-232: V194A/I201A/L208A)	1177.5 ± 94.4%

Table 6. Mutations of residues in the Kir2.1 leucine zipper-like motif do not inhibit Kir2.1 binding to AKAP79. Mean ±SEM, n≥3. No significant difference

Interestingly however, the mutation V194A consistently caused a significant increase in AKAP79 binding. Although this was not investigated further we suggest that this phenomenon is due to the substitution of the large amino acid, valine, for the smaller amino acid alanine. By replacing valine with a smaller amino acid, the region around V194 is exposed and this appears to have properties beneficial to AKAP79 binding.

4 Modelling the AKAP79 Binding Site on Kir2.1

4.1 Tertiary Structure

As a protein folds into its final tertiary structure, amino acids that might be separated by long lengths of primary sequence can often be brought into close proximity. This has important implications in studying protein-protein interactions as it is often difficult to predict which residues form 3-dimensional binding sites from studying linear primary sequence. To give us additional insight into the nature of the AKAP79 binding site on Kir2.1, we therefore set about modelling the tertiary structure of the cytoplasmic domains of Kir2.1.

Inward rectifying potassium channels possess a 'cytoplasmic pore' – an extension to the membrane spanning pore that effectively doubles the length of the ion conduction pathway (Nishida & MacKinnon, 2002; Kuo *et al*, 2003), figure 28. Analysis of the crystal structure and electrostatic nature of the pore suggests that this intracellular pore plays a unique role in inward rectification (Nishida & MacKinnon, 2002). The cytoplasmic pore appears to be lined with polar, negatively charged amino acid side-chains and hydrophobic amino acid side-chains that together provide ideal points at which polyamines can stick and occlude the ion conduction pathway.

The crystal structure for the cytoplasmic pore of the G protein-gated inward rectifier Kir3.1 and the prokaryotic KirBac1.1 has been resolved (Nishida & MacKinnon, 2002; Kuo *et al*, 2003). Upon sequence alignment of Kir2.1 to both of these channels, figure 29A and B, Kir3.1 shows the highest homology to Kir2.1, suggesting that these two ion channels share the most similar structure. By using the program RasMol, the Kir2.1 residues were mapped over the co-ordinates obtained for the X-ray crystal structure of the intracellular C-terminal domain of Kir3.1 and consequently provided a suggested tertiary structure of Kir2.1. Figure 30A, shows the four subunits that make up the cytoplasmic pore region of the functional channel. By focusing on a single subunit and highlighting residues 182-232 (that have been shown to bind AKAP79), figure 30B, one can see that there are two main regions, illustrated in red and blue, where these residues are exposed to the cytosol and thus could potentially bind intracellular proteins and hence possibly AKAP79. If we look at the amino acid sequence that makes up the exposed regions we see that they are formed by three distinct exposed sections of sequence, figure 30C, that fold together forming a hairpin loop.

To determine which of the exposed regions on the C domain of Kir2.1 bind AKAP79, 182-232 was truncated at residue 206, figure 31A. This essentially isolated each red region from the other and cuts the blue region in half. GST pulldown assays show that neither GST-C (182-206) nor GST-C (207-232) alone retain the ability to isolate AKAP79 from cell lysate, figure 31B, compared to the full length binding region 182-232; GST-C (182-232) = 289.8 ± 59.8%; negative control GST-C (233-282) = 64.7 ± 4.6%; GST-C (182-206) = 52.3 ± 69.6%; GST-C (207-232) = 8.4 ± 51.4%. This

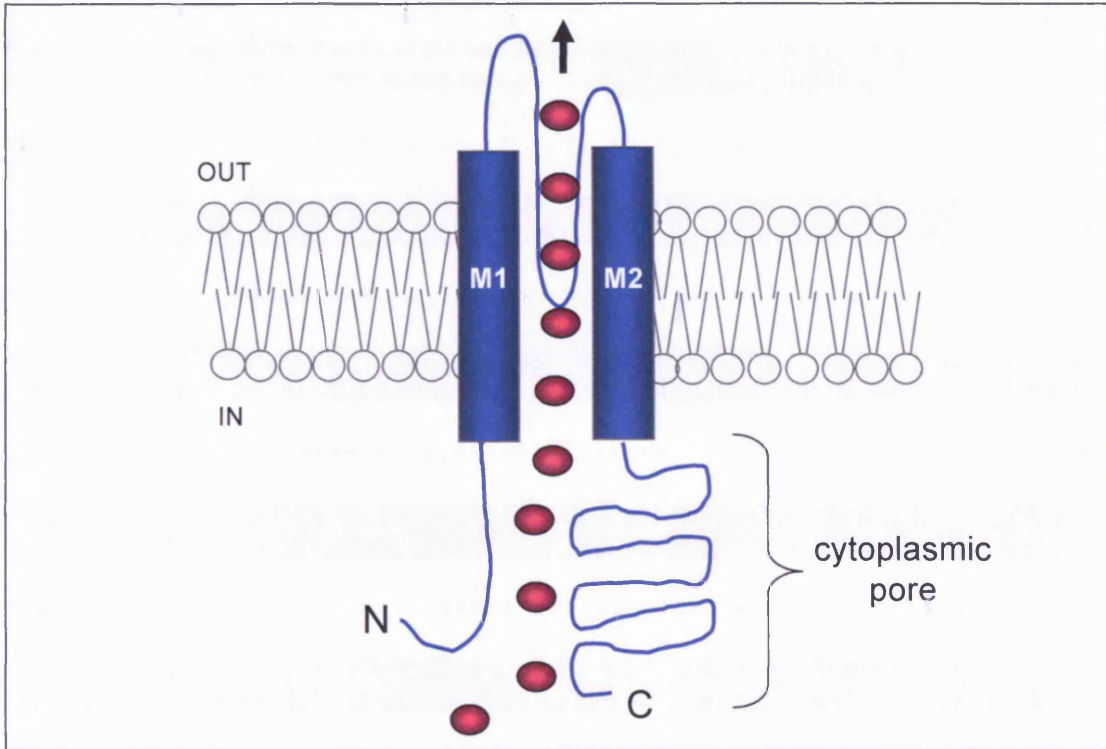


Figure 28. Cartoon depicting intracellular cytoplasmic pore. Ion pathway is extended to a length of 60 angstroms by the formation of a cytoplasmic pore, conserved amongst all inwardly rectifying potassium channels.

```

Kir2.1 ---MGSVRTNRYSIIVSSEEDGMKLATMAVANGPFGNGKSKVHTRQQCRSRFVKKDGHCVQFIN
Kir3.1 MSALRRKFGDDYQVVTSSSGSLQ----PQGPQGPPQQQLVPKKRQRFDKNGRCNVQHGK

Cons      :      : *.:*.:...* *      .:* ** : . :. : *..*.:*.:*.:*..*

Kir2.1 VGEKQRYLADIFTTCVDIRWRWMLVIFCLAFVLSWLFPGCVFWLIALHGDLDTSKVSK--A
Kir3.1 LGSETSERYLSDLFTTLVDLKWWRNLFIFILTYTVAWLFMASMWVVIAYTRGDLNKAHVQNYTP

Cons      :*.: .***:*:* **.:*** *..* *.:*.:*.:*.:*.:*.:*.:*.:*.:*.:*.:*

Kir2.1 CVSEVNSFTAFLFSIETQTTIGYGFRCVTDECPVAVFMVVFQSIIVGCIIDAFIIGAVMAKMA
Kir3.1 CVANVYNFSAFLFFIETATIGYGYRYITDKCPEGIILFLFQSIIVDAFLIGCMFIKMS

Cons      ***:* .*.:*** **.:*.:*.:* *.:** .:~::~*.:*.:*.:*.:*.:*.:*.:*.:*.:*.:*.:*

Kir2.1 KPKKRNETLVFSHNAVIAMRDGKLCIMWRVGNLRKSHLVEAHVRAQLLKSRTISEGEYIPLDQ
Kir3.1 QPKKRAETLMFSEHAVISMRDGKLTLMFRVGNLRNSHMVSAQIRCKLLKSROTPEGEFLPLDQ

Cons      :**** **:*.:***:*.:*.:*.:* **:*.:*.:*.:*.:*.:*.:*.:*.:*.:*.:*.:*

Kir2.1 IDINVGFDSGIDRIFLVSPITIVHEIDEDSPLYDLKQDIDNADFEIVVILEGMVEATAMTQ
Kir3.1 LELDVGFSTGADQLFLVSPLTICHVIDAKSPFYDLSQRSMOTEQFEVVVILEGIVETTGMTQ

Cons      :~::~*.:*.:*.:*.:* * * * .*.:*.:*.:*.:*.:*.:*.:*.:*.:*.:*.:*

Kir2.1 CRSSYLANEILWGHRYEPVLFEEKHYKVDYSRFHKTYEVPNTPLC-----
Kir3.1 ARTSYTEDEVLWGHRRFPVISLEEGFFKVDYSQFHATFEVPTPPYSVKEQEEMLLMSSPLIAP

Cons      .*:* :*.:*.:*.:* * : * : *.:*.:*.:* *.:*.:*..*

Kir2.1 -----SARDLAEKYIIL
Kir3.1 AITNSKERHNSVECLDGLDDISTKLPSKLQKITGREDFPKLLRMSSTTSEKAYSLGDLPMKIL

Cons      .* .*.: *

Kir2.1 SNANSFCYENEVALTSKEEEEDSENGVPESTSTDSPP-----GIDLHNQASVPLEPRPLRRE
Kir3.1 QRISVPGNSEKLVSKTTKMLSD--PMSQSVADLPKLOKMGAGPTRMEGNLPAKLRKMNSD

Cons      .. *. .:* *.** : * : .. : * ** * : :~::~* : * :. :

Kir2.1 SEI
Kir3.1 RFT

Cons

```

Figure 29A. Sequence alignment of Kir2.1 to Kir3.1. Using T-Coffee (Notredame, C *et al* 2000) the sequences of Kir2.1 and Kir3.1 were aligned to assess sequence similarity. This alignment reveals that these two inwardly rectifying potassium channels show a high degree of homology as indicated by the colour grading **BAD** **AVG** **GOOD**. Following standard amino acid consensus symbols “*” indicates the residues are identical; “.” indicates that conserved substitutions have been observed; “.” indicates a semi-conserved substitution has been observed.

```

Kir2.1      MGSVRTNRYSIVSSEEDGMKLATMAVANGFGNGKSKVHTRQQCRSRFVKKDGHCNVQFIN
KirBac1.1   ---MNVDPFSPHSSDSFA-QAASPARKPPRGRRISGTR-----EVIAT
Cons       ...: *  **:. . : * : *      * . :      **      :.*

Kir2.1      VGEKGQRYLADIFTTCVDIRWRWMLVIFCLAFVLSWLFVFCVFWLIALLHGDLDTSKVSK
KirBac1.1   YGMPASVW-RDLYYWALKVSWPVFFASLAALFVNNNTLFALLYQL-----GDAPIANQSP
Cons       *  .. :  *::  .::: *  :.. .  **:.  :.*  :: *      **  :: *

Kir2.1      ACVSEVNSPTAAFLFSIETQTTIGYGFRCVTDECPVAVFMVVFQSI VGCIIIDAFIIGAVM
KirBac1.1   P-----GTVGAPFFSVETLATVGYG--DMHPQTVYAHAIATLEIFVGMGSIALSTGLVF
Cons       .      .*..**:*:*:*  ::*:*  :  :  *  :...:  :**  *:  *  * :

Kir2.1      AKMAKPKKRNELVFSHNAVIAMRDGKLC LMWRVGNLRKSHLVEAHVRAQLLKSRIITSEG
KirBac1.1   ARFARPRAK---IMFARHAIVRPFNGRMTLMVRAANARQNVIAEARAKMRLMRREHSSEG
Cons       *:::*:*  :  :*::*::*::  :*::  **  *..*  *..  :.*::  :*::  .  :***

Kir2.1      EYIPLDQIDINVGFDSGIDRIFLVSPITIVHEIDEDSPLYDLSKQDIDNADFEIIVVILEG
KirBac1.1   -YELMKIHDLKLVRNE--HPIFLLG-WNMMHVIDESSPLEGETPESLAEGRAMLLVMIEG
Cons       *  ..  *:::  :.  .  **:.  .::*  **.*  **:.  :  :  :  :  :*::*::*

Kir2.1      MVEATAMTTQCRSSYLANEILWGHRYEPVLFEEKHYKVDYSRFHKTYEVPNTPLCSARD
KirBac1.1   SDETTAQVMQARHAWEHDDIRWHHRYVDLMSDVDGMTHIDYTRFNDTEPV-----
Cons       *::*  .  *.*  ::  ::*  *  ***  ::  :  .  :*::*::*  *  *

Kir2.1      LAEKKYILSNANSFCYENEVALTSKEEEDSENGVPESTSTDSPPGIDLHNQASVPLEPR
KirBac1.1   -----EPPGAAPDAQAFAAKPGEG-----DAR
Cons       ..  ...*::  :  :  *  *  .      :.*

Kir2.1      PLRRESEI
KirBac1.1   PV-----
Cons       * :

```

Figure 29B. Sequence alignment of Kir2.1 to KirBac1.1. Using T-Coffee (Notredame, C *et al* 2000) the sequences of Kir2.1 and KirBac1.1 were aligned as in figure 27A to assess sequence similarity. Although a high sequence homology is revealed, a higher degree of homology can be seen when aligning Kir2.1 to Kir3.1, figure 26A.

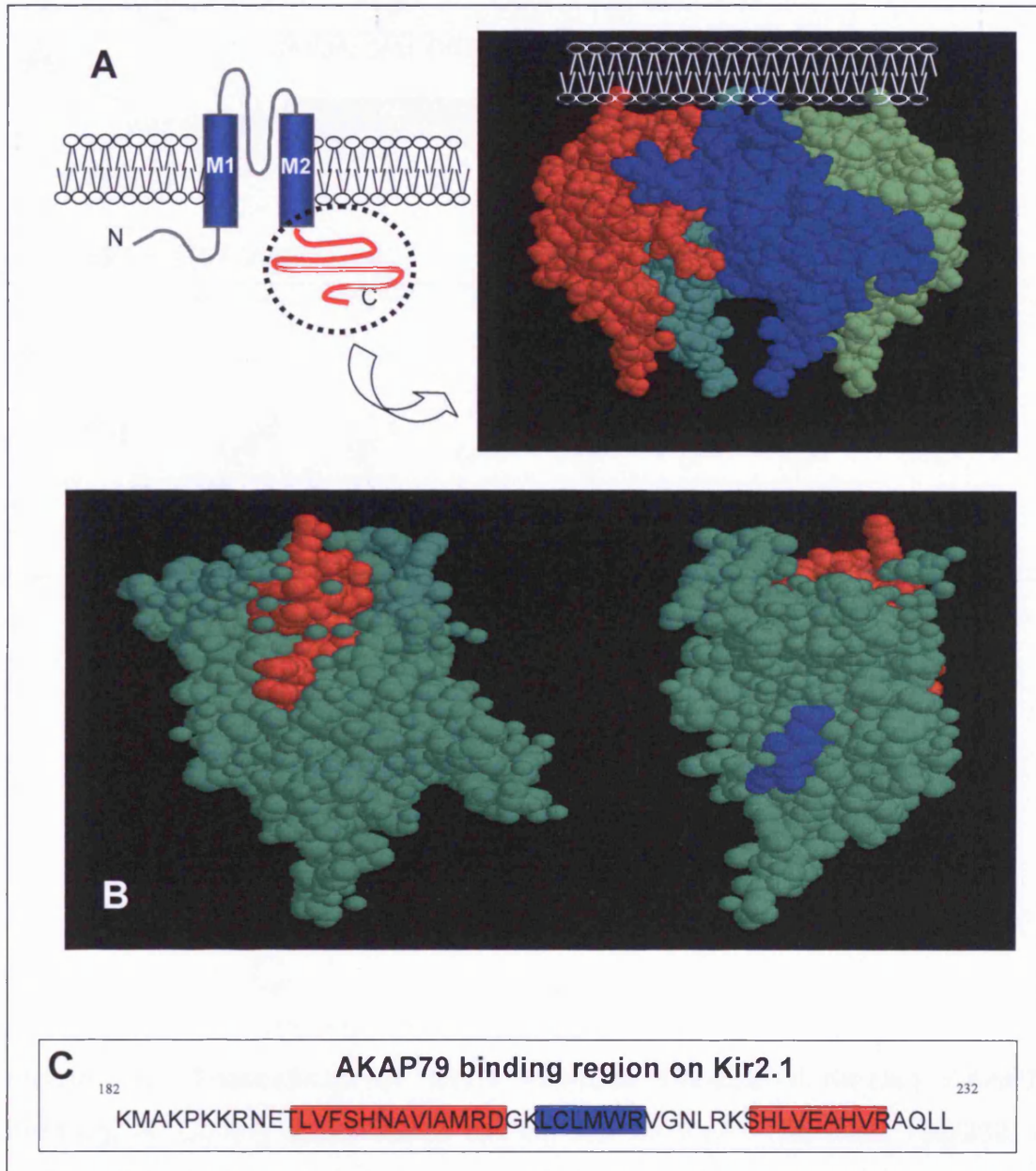


Figure 30. Predicted tertiary structure of the AKAP-binding region of Kir2.1. Using the computer program RasMol, the C terminal residues of Kir2.1 were mapped over the coordinates obtained from the crystal structure of the related channel, Kir3.1 (Nishida & MacKinnon, 2002), **A**. By focusing on a single subunit of the C terminal domain of Kir2.1, orientated at 2 different angles, the stretch of residues that binds AKAP79 (182-232) are seen to be exposed to the cytoplasm at 2 distinct regions (shown in red and blue) **B**. **C**. Primary sequence analysis of the red and blue areas in part B reveals the 2 exposed regions are composed of 3 separate sections of sequence that are brought together in the tertiary structure.

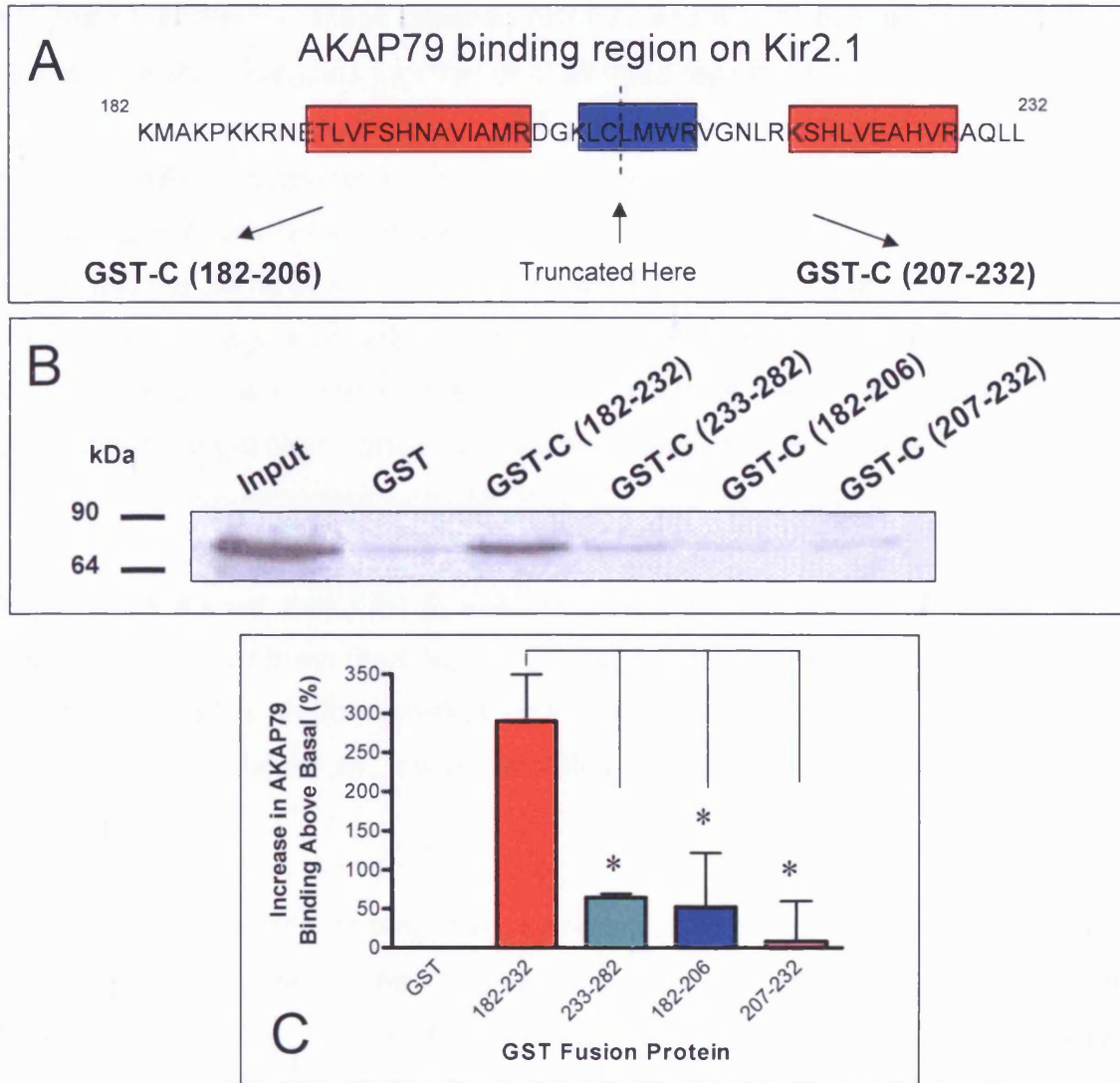


Figure 31. Truncations of Kir2.1 residues 182-232 eliminates AKAP79 binding. **A.** Cutting the AKAP79 binding site on Kir2.1, residues 182-232, at residue 206, separates the two upper regions of the binding site exposed to the cytoplasm and cuts the lower region in half (from figure 28). **B.** GST pulldown showing the positive control GST-C (182-232) is able to isolate significantly more AKAP79 from HEK293 than GST-C (233-282; negative control), GST-C (182-206) & GST-C (207-232). GST was unable to isolate AKAP79 transfected cells. 10% HEK293 cell lysate was run in the input lane. **C.** Histogram showing a significant difference in AKAP79 binding between positive control (GST-C(182-232)) = $289.8 \pm 59.8\%$ and negative control (GST-C(233-282)) = $64.7 \pm 4.6\%$ (mean \pm SEM $n \geq 3$). A significant difference in AKAP79 binding is also seen when GST-C(182-206) = $52.3 \pm 69.6\%$ and GST-C(207-232) = $8.4 \pm 51.4\%$ compared to the positive control. $p < 0.05$, unpaired, one-tailed, Student's t-test.

suggests that the interaction between AKAP79 and Kir2.1 requires either: a) the blue region, b) both red regions together or c) all three regions.

5 Kir2.1-AKAP interactions in vivo

5.1 GST Pulldowns in Rat Tissue

To assess the ability of Kir2.1 to interact with AKAPs from rat tissue, we used GST-C (182-232) (the region of Kir2.1 found to bind AKAP79) in pull-down assays with rat tissue homogenate. Here, the isolated proteins were separated by SDS-polyacrylamide gel electrophoresis, transferred onto nitrocellulose membrane and the membranes immunoblotted with anti-AKAP150 (the rat homologue of AKAP79).

Figure 32A shows that GST-C (182-232) was able to isolate substantially more AKAP150 from rat brain than GST-C (233-282), the negative control, or GST alone. Since AKAP150 is predominantly a neuronal protein, it is unsurprising that the GST fusion proteins failed to isolate significant amounts of AKAP150 from heart homogenates.

Unfortunately, despite testing five commercially available antibodies, plus one synthesised in-house, none of the antibodies against Kir2 channel proteins functioned reliably in immunoblotting or co-immunoprecipitation assays. Consequently, we are unable to conclusively say whether Kir2.1 and AKAP150 interact in rat brain tissue.

5.2 RII Overlay Assay

To determine whether Kir2.1 can potentially bind to, and form complexes with other AKAPs, aside from AKAP79/150, *in vivo*, we performed RII overlay assays, figure 33A and B. This technique relies on the fact that the amphipathic helical region on AKAPs that binds to the regulatory subunit of PKA is retained following SDS-polyacrylamide gel electrophoresis and transfer to nitrocellulose membrane. RII-binding proteins on the membrane can then be readily identified by incubating the membranes firstly with purified histidine-tagged RII protein and subsequently with antibodies directed against this histidine-tag. To control for non-specific RII binding a second membrane is incubated with RII-His which has been pre-incubated with the AKAP Ht31. This peptide binds to the AKAP binding site on RII and prevents RII-His

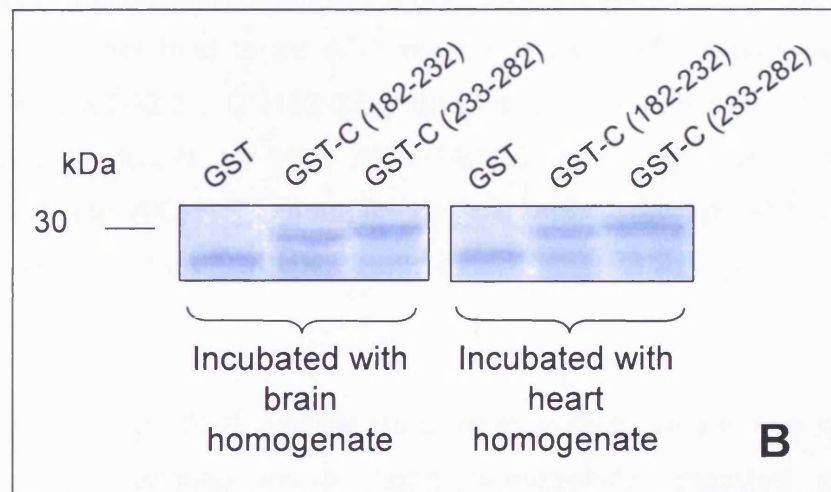
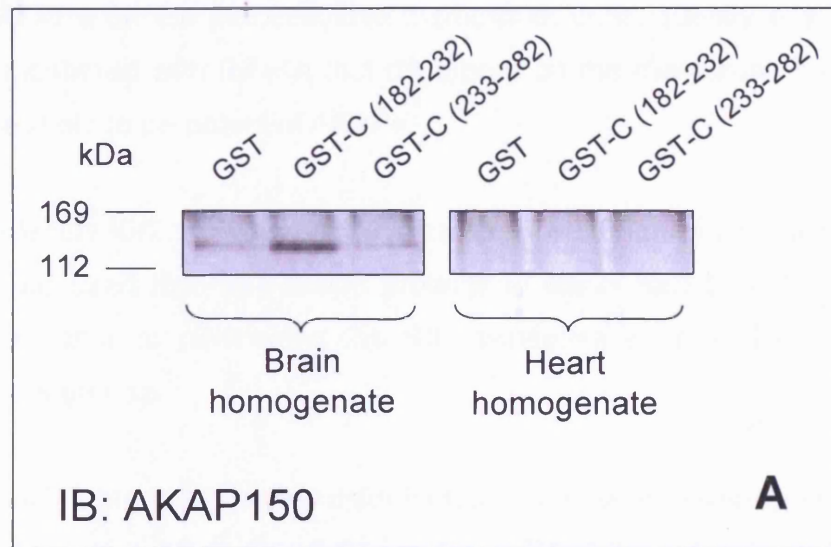


Figure 32. GST-C (182-232) isolates an anti-AKAP150 reactive protein from rat brain homogenate. **A.** GST pull-down showing GST-C (182-232) is able to isolate significantly more AKAP150 from rat brain, but not rat heart homogenate compared to GST alone and GST-C (233-282; negative control). **B.** GST fusion proteins were separated by SDS-polyacrylamide gel electrophoresis and the gel stained with EZStain™ to ensure equal amounts of each fusion protein were used in each pull-down. GST alone runs at ~26kDa, whilst GST-C (128-232) and GST-C (233-282) both run at 31kDa, all other bands represent probable GST degradation products.

binding to AKAPs on the nitrocellulose membrane, consequently any bands on the membrane incubated with RII-His that disappear on the membrane treated with RII-His-Ht31 are likely to be potential AKAPs.

In order to identify Kir2.1 binding AKAPs from rat heart, figure 33A, and brain tissue, figure 33C, we used the GST fusion proteins of either Kir2.1 C (182-232) or GST alone as bait prior to performing the RII overlay assay described above and in Methods and Materials.

Four potential RII-binding proteins were identified on the RII overlay assays following GST pulldowns; two were found in rat heart homogenate and two in rat brain homogenate. The proteins identified showed as bands that did not appear in the GST lane i.e. did not bind to the GST portion of the GST fusion protein; that were present in the GST-Kir2.1 C (182-232) lane i.e. that were isolated by the region of Kir2.1 previously found to bind AKAP79/150; but that disappeared following incubation with the AKAP-RII disrupter peptide Ht31. A duplicate SDS-PAGE gel was stained with EZStain™ to ensure that equal levels of GST proteins were loaded, figure 33B.

The GST-Kir2.1 C (182-232) isolated RII binding proteins, and hence potential Kir2.1 binding AKAPs, identified in rat heart homogenate migrated on the SDS-polyacrylamide gel with an apparent molecular weight of approximately 85kDa and 48kDa, whilst the proteins identified on the gel from rat brain migrated at approximately 90kDa and 70kDa. Of previously cloned and characterised AKAPs, the 85kDa and the 90kDa bands identified could correspond to AKAP84, AKAP-KL, AKAP95 or even AKAP100. Attempts to identify these potential AKAP by mass spectrometry were unfortunately unsuccessful due to the low amounts of protein present.

6 Conclusions

Our results make several advances towards understanding the mechanisms of interaction between AKAP79 and Kir2.1. Firstly, we show through co-immunoprecipitation studies that it is possible for a direct interaction to occur between AKAP79 and three members of the Kir2 family: Kir2.1, Kir2.2, Kir2.3.

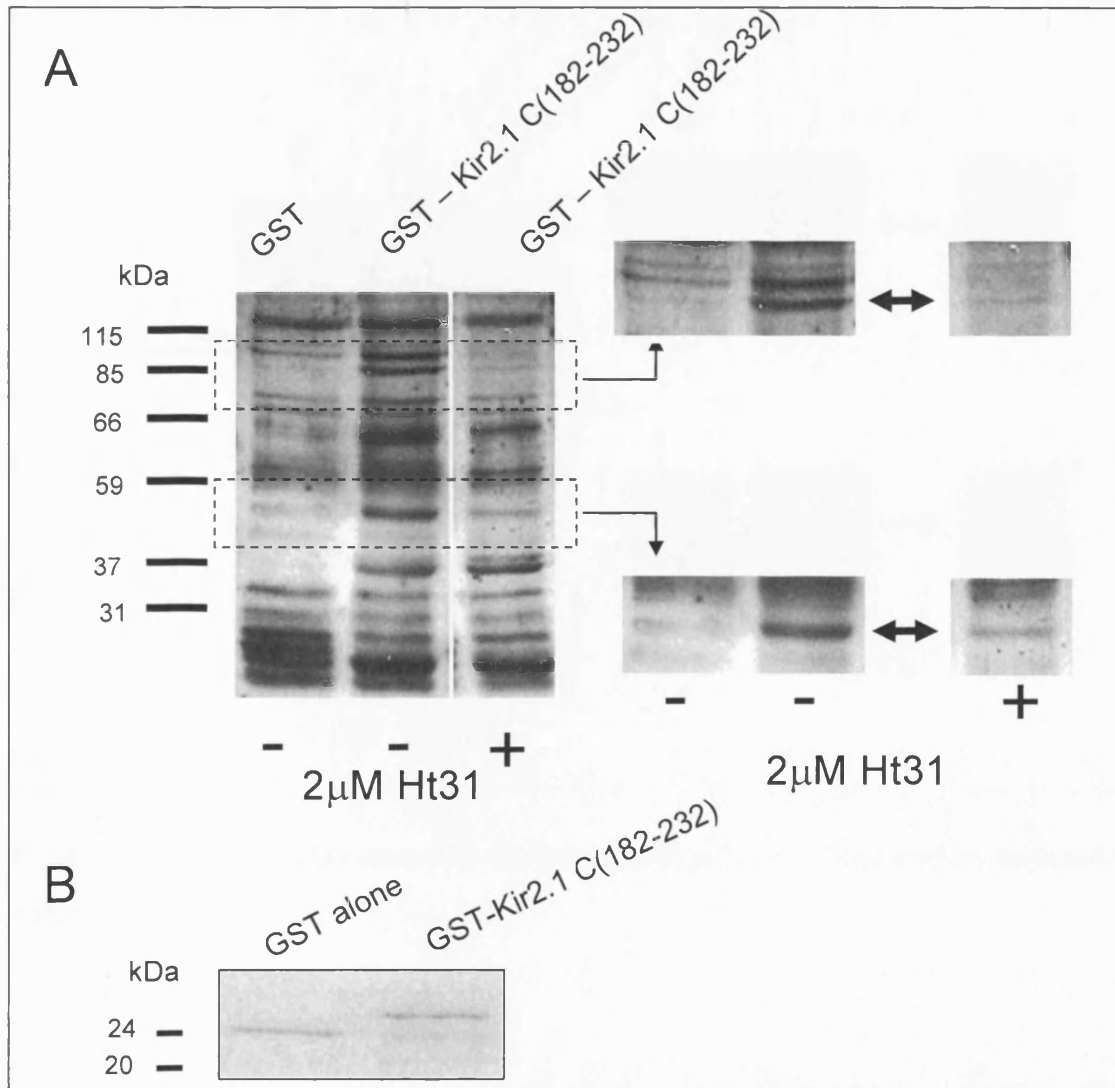


Figure 33. RII Overlay assay. **A.** Protein extracts from one and a half rat hearts were incubated with glutathione sepharose beads bound with GST or GST fused to the AKAP79 binding region on Kir2.1 (GST-182-232), prior to separation of proteins by SDS-PAGE on 10% polyacrylamide-Tris gels and transfer onto nitrocellulose membranes. Membranes were incubated for 2 hours at room temperature with the purified histidine-tagged regulatory subunit of PKA (RII-His), or with RII-His, preincubated with the disrupter peptide Ht-31. Membranes were subsequently washed and the presence of RII-binding proteins determined by immunoblotting with primary antibodies directed against the His-tag. Potential RII-binding proteins (AKAPs) are revealed as bands that disappear in the presence of Ht31 (indicated by arrows). **B.** A duplicate SDS-PAGE gel was run and subsequently stained with EZStain™ to ensure equal levels of GST proteins were incubated with tissue homogenate.

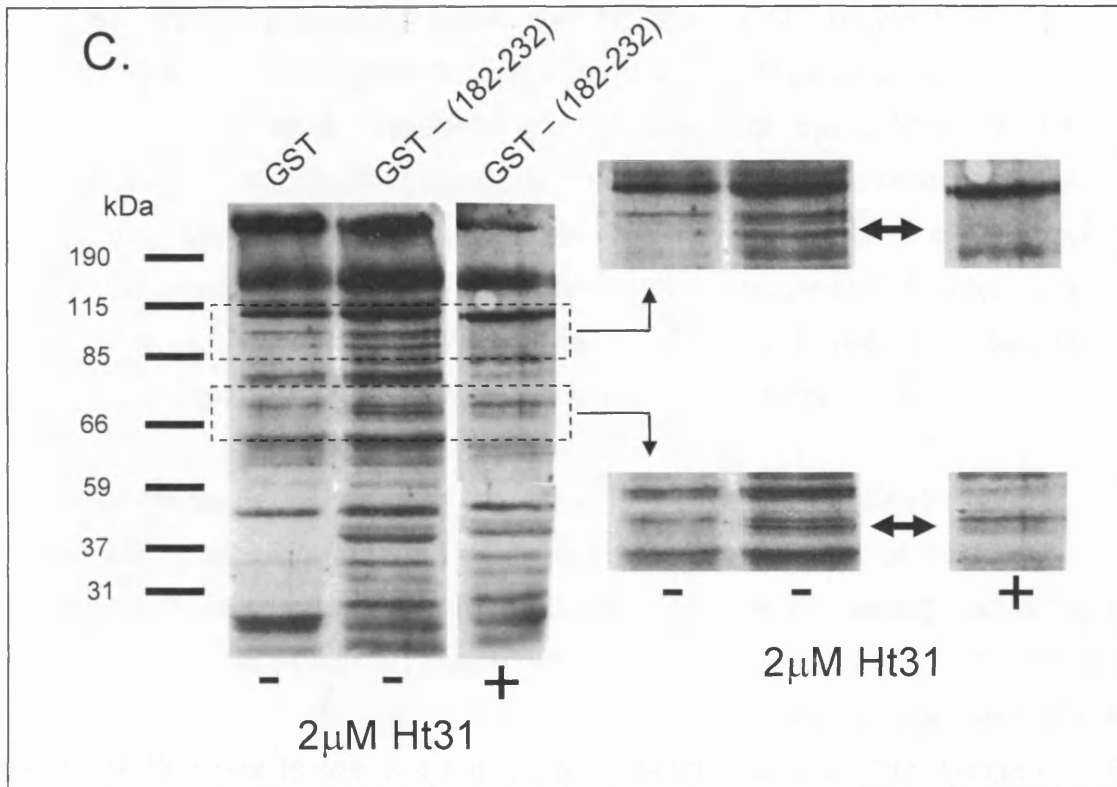


Figure 33C. RII overlay assay of rat brain homogenates conducted as detailed in Figure 33A.

Previously, only an association between AKAP79 and Kir2.1 had been demonstrated (Dart & Leyland, 2001). Secondly, we show that AKAP79 binds the Kir2 potassium ion channel family via a novel binding motif located on the C terminus of the ion channel and not via a leucine zipper as has been reported for other AKAP-channel interactions. Thirdly, a GST fusion protein containing the AKAP79 binding region of Kir2.1 was able to isolate AKAP150 from rat brain homogenate. Finally, we provide evidence to suggest the AKAP79 binding site on Kir2.1 (residues 182-232) may potentially interact with other AKAPs, as shown in RII overlay assays.

6.1 Direct Association of AKAP79 with the C-terminal Domain of Kir2.1

GST fusion proteins of the intracellular N and C domains of Kir2.1 had been previously screened for their ability to isolate AKAP79 from lysates (Dart & Leyland, 1998). They showed that GST fusion proteins of both domains of Kir2.1 were able to isolate AKAP79, whereas GST alone failed. They also showed that despite reports that AKAP79 binds to the Src homology 3 (SH3) and guanylate kinase-like (GK) domains of the PDZ protein PSD-95/SAP90, and that Kir2.1 possesses a conserved PDZ-domain recognition motif, a shortened GST fusion protein containing just the PDZ-domain recognition motif (residues 421-428) failed to isolate AKAP79. This was taken to suggest that AKAP79 binds directly to Kir2.1 and not via a C-terminal PDZ protein.

Here, we use deletion analysis of GST fusion proteins to identify a region of 50 amino acids (residues 182-232), situated just after the point at which the channel protein leaves the plasma membrane and enters the cytoplasm, that is sufficient for the interaction with AKAP79. These results are consistent with other reports on the interaction between ion channels and AKAPs, where AKAP targeting regions appear to reside on the C-terminus of other ion channels: L-type calcium channels and KCNQ1-KCNE1 channels (Hulme *et al*, 2002; Marx *et al*, 2002).

6.2 A Novel Interaction Mediates AKAP79 Binding to Kir2.1 Channels

Originally identified in transcription factors, leucine zippers were first thought to play a fundamental role in sequence-specific interactions with DNA (Landschulz *et al*, 1988). More recently however, leucine zippers, and indeed isoleucine zippers, have been shown to play a fundamental role in protein-protein interactions (Surks *et al*,

1999), specifically within AKAP-ion channel interactions (Marx *et al*, 2001; Hulme *et al*, 2002).

Recent reports showed that yotiao directly interacts with the KCNQ1 subunit of the KCNQ1-KCNE1 potassium channel and AKAP15 directly interacts with L-type Ca²⁺ channels via leucine zipper motifs (Marx *et al*, 2001; Hulme *et al*, 2002). Having narrowed down the AKAP79 binding site on Kir2.1 to a region of 50 amino acids we investigated the possibility that AKAP79 also targets PKA to Kir2.1 via a leucine zipper motif. Sequence analysis of Kir2.1 revealed a modified leucine motif, a periodic repetition of hydrophobic residues every seventh position, rather than the typical leucine residues every seventh position. In site-directed mutagenesis of GST fusion proteins, alanine substitution of critical hydrophobic residues in the leucine zipper-like motif did not eliminate interaction between AKAP79 and Kir2.1. If a leucine zipper-like motif were responsible for targeting AKAP79 to Kir2.1 it would be expected that this association would be abolished upon alanine substitution. Consequently, in contrast to L-type Ca²⁺ and KCNQ1-KCNE1 K⁺ channels, we suggest that Kir2.1 targets PKA to its phosphorylation site via AKAP79 through a mechanism independent of leucine zippers.

Through tertiary structure analysis we were then able to extend this work. The structures of two Kir channels have recently been reported; rat Kir3.1 (Nishida & MacKinnon, 2002) and bacterial KirBac1.1 (Kubo *et al*, 2003). Based upon sequence alignment between Kir2.1, Kir3.1 and KirBac1.1, Kir3.1 was chosen to be the most appropriate to use as a tertiary structure model of Kir2.1 due to their high homology and because both are eukaryotic.

By using the 3-D modelling program RasMol, Kir2.1 residues were mapped over the co-ordinates obtained for the X-ray crystal structure of the C-terminal domain of the closely related Kir3.1, providing us with a predicted structure for the AKAP-binding region of Kir2.1. This allowed us to identify residues within the binding region that were exposed to the cytosolic environment and were potentially free to interact with AKAP79.

Two distinct regions within the stretch of residues known to bind AKAP79 were found to be exposed. Primary sequence analysis revealed that these two distinct regions were made up of three separate sections of sequence between residues 182-232 (Fig. 28). The Kir2.1 protein folds back on itself between residues 182 and 232 forming a hairpin-line structure. The top and bottom of the hairpin are exposed to the cytoplasm and the middle section buried within the folded protein. The exposed top of the hairpin, which forms one potential AKAP binding site, is formed by two separate stretches of residues (190-203 and 218-225) and the bottom by residues 205-211. To assess how important these regions are to AKAP79 binding, we created GST-fusion proteins of regions 182-206 and 207-232 (Fig. 29A). This effectively separated the two regions that form the upper binding site and cut the lower binding site in half. These shortened fusion proteins failed to isolate AKAP79 in pulldown assays, suggesting one or both of these regions are important in the channel-AKAP interaction. It is clear from these findings that neither 190-203 nor 218-225 (the regions that make up the exposed top of the hairpin) alone are sufficient to bind AKAP79. If this upper region is involved in AKAP79 binding it seems these two stretches of amino acids must come together to form a cooperative binding site. Alternatively, the bottom of the hairpin (residues 205-211) may be the primary site of interaction.

Since completing this section of work, the crystal structure of the cytoplasmic domains of mouse Kir2.1, occluded by four cytoplasmic loops, has been published (Pegan *et al*, 2005). By using molecular replacement methods, this report shows the structure of mouse Kir2.1, with an additional 57 amino acids at the C-terminus, alongside that of the rat Kir3.1 i.e. the ion channel used here for mapping the AKAP79 binding site on Kir2.1. Pegan *et al* (2005) show that the core structures for Kir2.1 and Kir3.1 are “readily super-imposable”, strengthening the evidence we present here for the residues mapped to be responsible for binding AKAP79 on Kir2.1.

However, whilst the use of GST fusion system is a powerful and commonly used approach for the expression, purification and detection of fusion proteins in *E. coli*, caution should be exercised when the fusion protein being expressed is eukaryotic in origin. Prokaryotic protein synthesis is fundamentally different to that of eukaryotes

(Monne *et al*, 2005). This may result in misfolding and in-correct post-translational modifications of the expressed eukaryotic protein. Consequently, we cannot say definitively that the GST fusion proteins produced here folded in the native manner of the full-length Kir2.1 protein. An alternative bacterial expression system shown to possess qualities more suitable to eukaryotic protein overproduction is that of *Lactococcus lactis* (Monne *et al*, 2005). Here, the gram-positive lactic acid bacterium is able to grow to high densities without the need for aeration and contains a tightly regulated promoter system allowing reproducible expression even in the presence of toxic levels of protein (de Ruyer *et al*, 1996; Kunji *et al*, 2003). The resultant expressed protein appears to be highly reproducible, is not targeted into inclusion bodies and the system does not rely on the use of detergents in the purification process, as such could offer a substitute expression system for the GST fusion proteins used here.

6.3 Kir2.1 Isolates AKAP150 from Rat Brain Homogenate

Having established an interaction between AKAP79 and Kir2.1 in intact cells through co-immunoprecipitation and identified a potential binding site on the channel protein by GST-pulldown assays, we set about identifying the potential native AKAP partner of Kir channels *in vivo*. In the mammalian brain, all four Kir2 channels are widely expressed, but show differential distribution. Kir2.1 is most abundantly expressed in the olfactory system, cerebral cortex, midbrain and striatum (Karschin *et al*, 1996; Pruss *et al*, 2005). Interestingly, within the rodent brain AKAP150 is also widely distributed, the highest expression levels were found in similar areas to those expressing Kir2.1 i.e. the striatum, cerebral cortex and several forebrain regions including the olfactory tubercle (Glantz *et al*, 1992; Lilly *et al*, 2005; Ostroveanu *et al*, 2007).

Through GST pulldowns we were able to show that it is possible that AKAP79/150 or a closely related splice variant may interact *in vivo* with Kir2.1 within the brain. Unfortunately despite repeated attempts with a number of antibodies directed against the Kir family members we were unable to confirm this finding with co-immunoprecipitation and Western blot. The generation of more reliable Kir antibodies in future will hopefully confirm the existence of signalling complexes within the brain made up of Kir channels, AKAPs and their associated kinases.

6.4 Kir2.1 Interaction with Potentially Novel AKAPs

By using GST-Kir2.1 C (182-232) or GST alone (negative control) as bait prior to performing an RII overlay assay, we were able to detect the presence of several AKAPs that may associate with Kir2.1 via the AKAP79 binding site. In rat heart we identified two potential AKAPs that migrated with molecular weights of approximately 85kDa and 48kDa on 10% SDS-PAGE gels, while in rat brain we identified potential AKAPs at 90kDa and 70kDa.

Of previously cloned and characterised AKAPs, the 85kDa band in rat heart identified could correspond to the D-AKAP1/AKAP1 splice variant S-AKAP84. This AKAP has previously been shown to migrate on nitrocellulose membranes at approximately 90kDa from heart tissue (Kapiloff, 2002) and thus is a potential candidate for the AKAP identified on the RII overlay using rat heart homogenate. It seems unlikely that the 90kDa band identified in rat brain corresponds to S-AKAP84 as there are no known reports of this AKAP in brain tissue. Alternative splicing of members of the D-AKAP1 family at both the N and C- termini could dictate differential subcellular localisation of this AKAP to either the mitochondria or endoplasmic reticulum (Huang *et al*, 1999).

Another splice variant of the dual RII binding AKAP D-AKAP1, termed N1, is expressed at very low levels in the brain but higher levels in the heart (Huang *et al*, 1999). D-AKAP1 has a predicted molecular weight of 92kDa and thus could be a potential candidate for the bands identified at either 85kDa in heart homogenate or 90kDa in brain homogenate.

The 90kDa band identified in rat brain homogenate may be compatible with a splice variant of AKAP-KL. Whilst AKAP-KL is highly expressed in the kidney and lung, it is expressed at lower levels in the cerebellum, it also appears to be absent from many other tissues suggesting expression is differentially regulated *in vivo* (Dong *et al*, 1998). The principal isoforms in cerebellum are KL2A and KL2B with predicted molecular weights of 96kDa and 83kDa respectively, consequently either of these splice variants are a possible match. It is currently unknown what the significance of each splice variant of AKAP-KL is; however, it seems likely that the different isoforms

maybe differentially located, with the possibility of different PKA specificities. Subsequently this may provide a means of modulating the function and subcellular location of anchored PKA in response to environmental and developmental cues thereby assembling PKA with different signal transduction complexes as demand dictates (Dong *et al*, 1998).

AKAP100, belonging to the AKAP6 family, is highly expressed in the heart but lower levels are also found in the brain where it migrates with an apparent molecular weight of 100kDa, although its calculated molecular weight is 78kDa (McCartney *et al*, 1995). Although AKAP100 may correspond to the 85kDa band identified in rat heart, it seems more likely, based on the molecular weight at which it migrates on SDS-polyacrylamide gels, to be a candidate for the 90kDa band identified in rat brain. Of the brain regions tested, AKAP100 was identified in the cerebellum, basal ganglia, hippocampus and motor and frontal cortex's (McCartney *et al*, 1995). Regardless of tissue expression, AKAP100 specifically localises to the sarcoplasmic reticulum, yet the actual role played by AKAP100 anchored PKA is currently unknown at this subcellular location. However, AKAP100 anchored PKA could play a part in activating the ryanodine receptors found on the sarcoplasmic reticulum (Takasago *et al*, 1989) or indeed the sarcoplasmic reticulum-associated chloride channel (Kawano *et al*, 1992).

A final candidate for the RII binding protein migrating at 90kDa isolated from rat brain is AKAP95. It has a predicted molecular weight of 76kDa, yet has been shown to migrate at approximately 95kDa in Western blot analysis experiments (Coghlan *et al*, 1994). Antibodies directed against AKAP95 have detected 95kDa bands on Western blots of cellular extracts from rat liver, mouse kidney and mouse brain; while immunohistochemical analysis on mouse brain sections suggest a predominantly nuclear localization (Coghlan *et al*, 1994). It therefore seems unlikely that this particular AKAP forms a complex with the plasma membrane-associated Kir2 family.

Of particular interest are the RII binding protein isolated from rat heart and brain that migrated at approximately 48kDa and 70kDa respectively as there are no known AKAPs that migrate with these apparent molecular weights. Unfortunately, further analysis to confirm the identity of these AKAPs was not possible. The primary

sequence of proteins can be obtained using tandem mass spectrometry and although mass spectrometry technically only requires picomole quantities of protein for sequencing, we were unable to obtain sufficient amounts of protein from our samples. Indeed when we stained the SDS-polyacrylamide gel for total protein we were unable to distinguish any bands that related to the bands of interest seen on the immunoblots. An important further direction will be to purify and identify these potentially novel channel-interacting AKAP variants.

While AKAP150 is a predominantly neuronal protein and we were able to isolate significant amounts of this protein in GST-pulldowns (see Figure 32), curiously, we did not see a clear band corresponding to AKAP150 in RII overlay assays using rat brain homogenates. The area of the blot where we might expect to see AKAP150 on the RII overlay was however obscured by non-specific bands (Fig 30C), which may account for this.

As is often the case with RII overlays assays, the number of non-specific bands seen in both figure 33 A and 33C is somewhat high. This is possibly caused by non-specific binding of the His antibody. However, this was controlled for by using the PKA-AKAP disrupter peptide Ht31. As mentioned previously, this is a peptide analogous to the minimum region of an AKAP required for binding RII and as such is a useful tool in AKAP identification. In an RII overlay, any bands present on the membrane incubated with just RII-His antibody that subsequently disappear on the membrane incubated with RII-His pre-incubated with Ht31 are potential RII binding proteins and hence AKAPs. Thus, ultimately it should not be important the number of non-specific bands present on the Western blot. This is only an issue if the non-specific bands obscure specific RII binding as is likely with AKAP150 on the rat brain homogenate RII overlay. This could be overcome by using an alternative His antibody or tagging RII with a different epitope.

CHAPTER SIX

INVESTIGATING THE FUNCTIONAL EFFECTS OF AKAP79-KIR CHANNEL INTERACTION

1 Introduction

Previous studies have produced contradictory findings as to the role of PKA in Kir2.1 channel function. PKA has been shown to be required for normal channel functioning (Fakler *et al*, 1994; Ruppertsberg & Fakler, 1996), to enhance channel activity (Monaghan *et al*, 1999; Dart & Leyland, 2001) and to inhibit channel function (Wischmeyer & Karschin, 1996; Koumi *et al*, 1995a/b). There are also reports suggesting that PKA has no effect on Kir2.1 channel activity (Jones, 1996; Kamouchi *et al*, 1997). The reasons for these differences are unclear, but it is possible that it stems from a difference in the signalling/phosphorylation machinery within the wide range of systems studied.

It should not be forgotten that while a heterologous expression system has the advantage of offering a controlled environment, it may not entirely resemble the native conditions required for ion channel modulation. For example, when Kir1.1 (also known as ROMK1 channels) was expressed in *Xenopus* oocytes, elevated levels of cAMP had no apparent effect on channel current, yet when these channels were co-expressed with AKAP79, otherwise absent from *Xenopus* oocytes, a significant increase in whole cell current was recorded in response to an elevation of cAMP levels (Ali *et al*, 1998). Similarly, Kir2.1 currents have been shown to increase in response to increased intracellular cAMP, but only in the presence of AKAP79 (Dart & Leyland, 2001).

Here we investigate further the functional effects of the AKAP79-Kir2.1 interaction on channel sensitivity to cAMP/PKA modulation. We also discuss work in which we use our knowledge of the binding site of AKAP79 on Kir2.1 to construct interfering peptides to disrupt the interaction. The use of interfering peptides *in vivo* would give

important information as to the functional importance of kinase anchoring to channel and cellular physiology.

2 GST-C (182-232) Peptide Interferes with Kir2.1-AKAP79 Complex

In order to verify the findings showing that the AKAP79 binding region on Kir2.1 lies between residues 182-232, we used a method adapted from Marx *et al*, 2002. Here, GST-Kir2.1 C (182-232), the putative AKAP79 binding region of Kir2.1, or GST-Kir2.1 C (233-282), the negative control, was incubated with lysates of HEK293-AKAP79 cells transiently transfected with full-length Kir2.1 epitope tagged with EGFP and a co-immunoprecipitation performed. A decrease in the ability of anti-GFP to co-immunoprecipitate AKAP79 was taken to indicate a disruption of the Kir2.1-AKAP79 complex.

Figure 34A shows that antibodies directed against the GFP tag on Kir2.1 were unable to isolate AKAP79 from cellular lysates that had been incubated with GST-Kir2.1 C (182-232). In contrast, anti-GFP co-immunoprecipitated significant amounts of AKAP79 from cell lysates treated with the negative control, GST-Kir2.1 C (233-282). Densitometric analysis, figure 34B, revealed that levels of AKAP79 isolated from cell lysate in the presence of GST-Kir2.1 C (182-232) were only $98.4 \pm 45.9\%$ above basal (IP: non-immune), while cells treated with GST-C (233-282), the negative control, showed an increase in AKAP79 binding of $488.5 \pm 62.2\%$ above basal (n=3). This suggests that GST-Kir2.1 C (182-232) interferes with the AKAP79-Kir2.1 complex and further supports the notion that the AKAP79 binding site on Kir2.1 lies between residues 182-232.

3 Effect of Co-expression of AKAP79 and Kir2.1 on Channel Function

To investigate the effect of AKAP79 on Kir2.1 function, membrane currents were recorded from HEK293 and HEK293-AKAP79 cells 24-48 hours after transient transfection with cDNA encoding Kir2.1-EGFP using the conventional whole-cell patch clamp technique. Expression of the Kir2.1-EGFP construct allowed a positive visual selection of cells expressing the ion channel. Currents were recorded, figure 35A, in response to voltage steps from a holding potential of -17mV (the equilibrium potential for K^+ (E_K) under these recording conditions) to test potentials ranging from +60mV to -100mV in 10mV increments, figure 35B. Outward currents are shown as

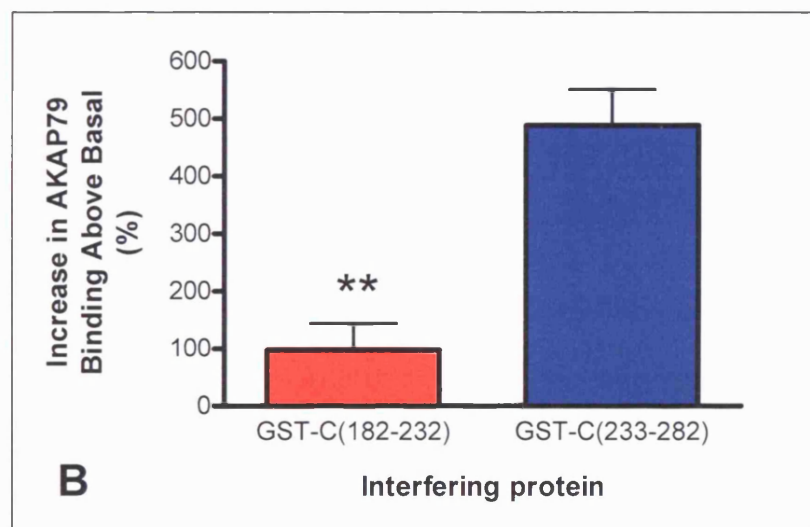
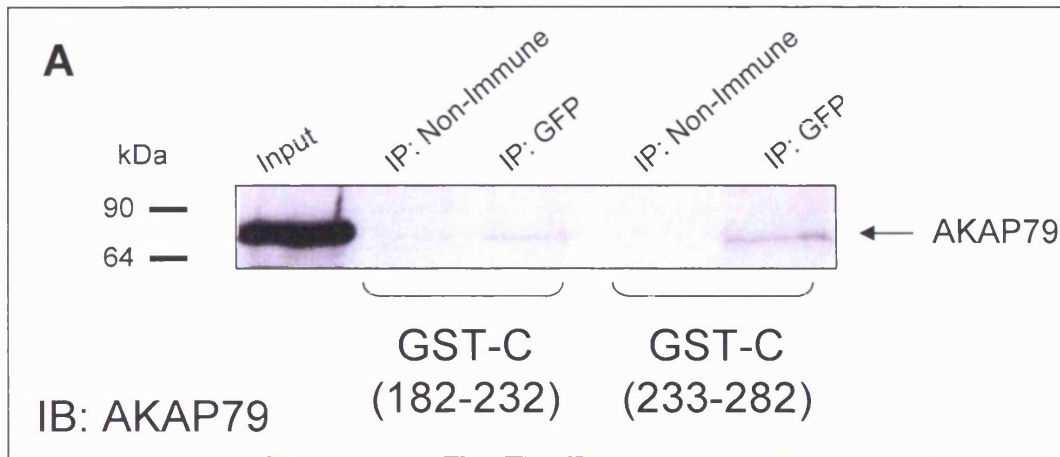


Figure 34. GST-C (182-232) appears to interfere with AKAP79-Kir2.1 complex. **A.** GST-C (182-232) & GST-C (233-282) were expressed and subsequently mixed with glutathione beads overnight prior to mixing the beads with lysates of HEK293-AKAP79 cells transiently transfected with cDNA encoding Kir2.1-EGFP. Immunoprecipitation was performed using an antibody directed against the EGFP epitope tag or rabbit non-immune serum as described in Methods & Materials. Precipitated proteins were separated by SDS-PAGE, transferred onto nitrocellulose membrane and immunoblotted with anti-AKAP79. 10% of cell lysate was run in the lysate lane. **B.** Histogram showing GST-C (182-232) significantly knocks down the level of AKAP79 co-immunoprecipitated with Kir2.1-EGFP compared to GST-C (233-282) (GST-C (182-232) = $98.4 \pm 45.9\%$; GST-C (233-282) = $488.5 \pm 62.2\%$). Unpaired, two-tailed Student's t-test.

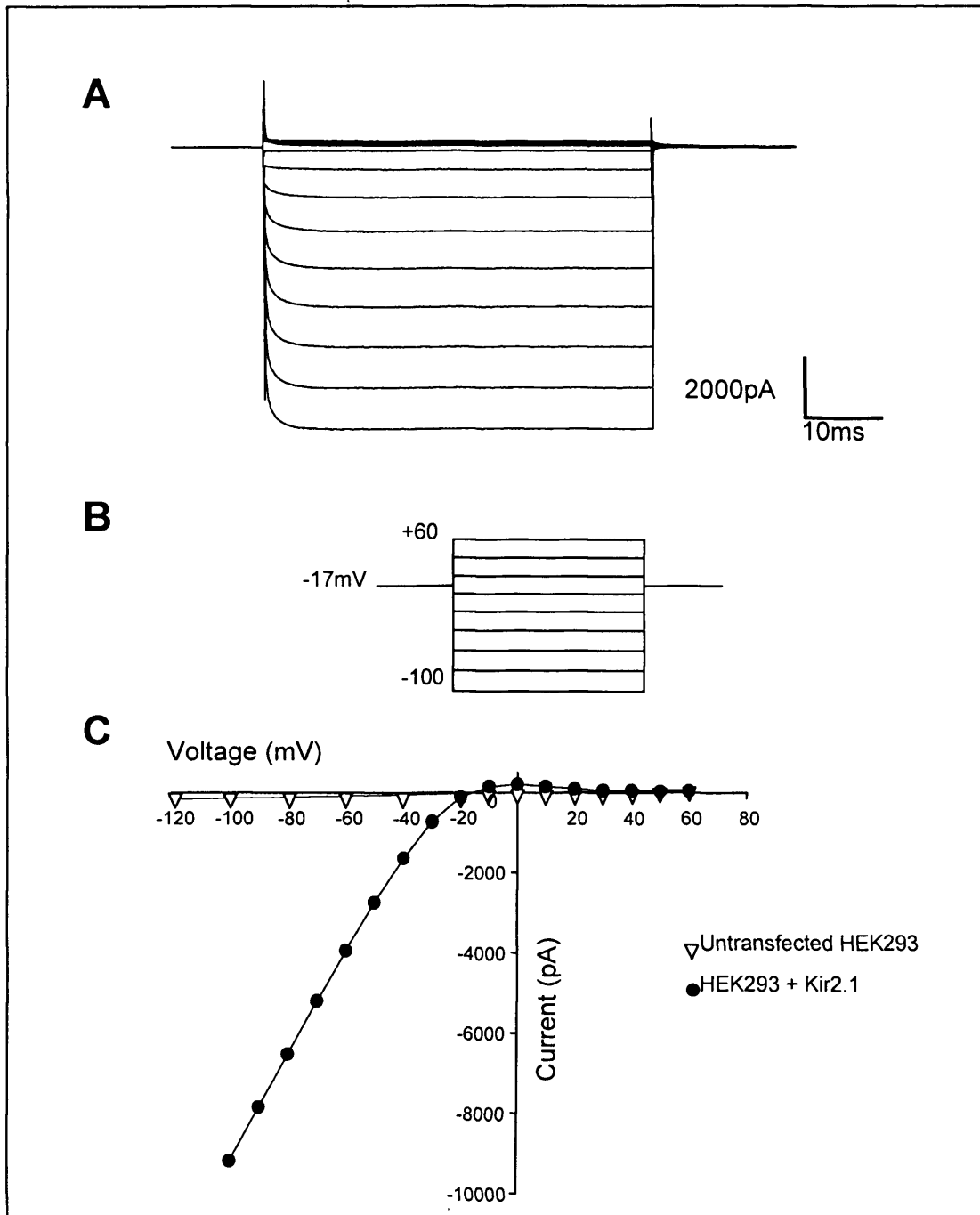


Figure 35. Characterisation of Kir2.1 currents in HEK293 cells. **A.** Membrane currents recorded from a single HEK293 cell, **B**, in response to voltage steps from a holding potential of -17mV to test potentials ranging from +60mV to -100mV in 10mV increments. Extracellular [K⁺] was 70mM; intracellular [K⁺] was 140mM. Outward currents are defined as being positive and are shown as upward deflections; inward currents are defined as being negative. **C.** Mean current-voltage relation for a single HEK293 cell expressing Kir2.1 (●) or untransfected cell (▲).

being positive and so are shown as upward deflections, whilst inward currents are defined as being negative and hence downward deflections.

In HEK293 cells, voltage steps positive to E_K elicited only small outward currents, while steps negative to E_K produced substantial inward currents, no significant whole-cell currents were detected in non-transfected cells, figure 35C. Co-expression of AKAP79 with Kir2.1 did not significantly affect whole-cell Kir2.1 current amplitudes, figure 36. This suggests that basal Kir2.1 channel activity is unaffected by co-expression with AKAP79.

AKAP79 not only anchors PKA, but also binds protein phosphatase 2B (Coghlan *et al*, 1995). This therefore means that while AKAP79-associated proteins may experience rapid phosphorylation they may also be subject to equally efficient dephosphorylation (Gao, 1997). Indeed previous reports have shown that it is only after pre-treatment with phosphatase inhibitors such as okadaic acid and cypermethrin that whole cell currents could be seen to increase in the presence of agents capable of increasing intracellular PKA (Gao *et al*, 1997; Dart & Leyland, 2001). Consequently, in all subsequent experiments cells were pre-treated for 30-40 minutes with 200nM okadaic acid and 200nM cypermethrin to ensure that any potential PKA-dependent regulation of channel activity was not masked by rapid dephosphorylation.

In wildtype HEK293 cells, elevation of intracellular cAMP, through inclusion of cAMP in the patch pipette, had little effect on whole-cell Kir2.1 currents, $8.4 \pm 4.7\%$ ($n=7$) increase in whole cell current over 10 minutes, figure 37C filled circles. Time point zero in these recordings represents the point at which the whole-cell recording configuration was established and hence dialysis of the cell with cAMP begins. Upon co-expression of AKAP79 with Kir2.1, however, the effect of elevated intracellular cAMP on whole-cell current increased to $21.6 \pm 4.5\%$ ($n=6$) compared to basal whole-cell currents, figure 37C open circles.

4 Endogenous Expression of an Interfering Peptide

We have seen previously the GST-Kir2.1 C (182-232) peptide may be used to specifically disrupt the association between Kir2.1 and AKAP79. Unfortunately, use

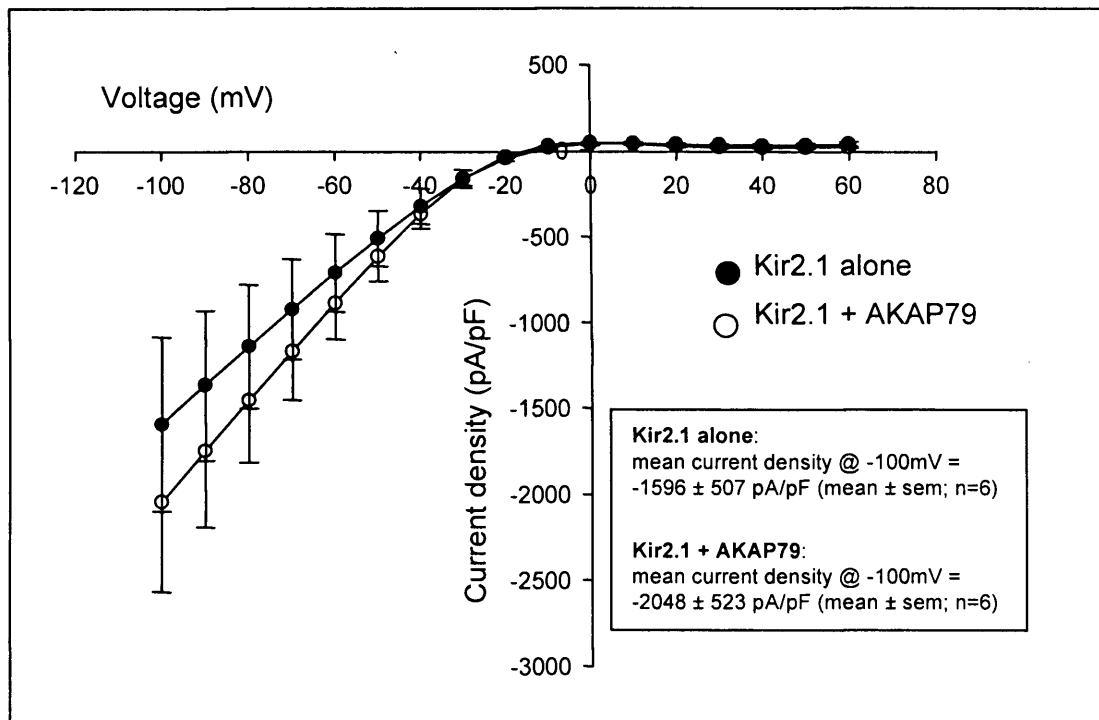


Figure 36. AKAP79 does not affect whole cell Kir2.1 currents. Mean current-voltage relation for HEK293 cells expressing Kir2.1 alone (●) or AKAP79 and Kir2.1 (○) (n=6 each).

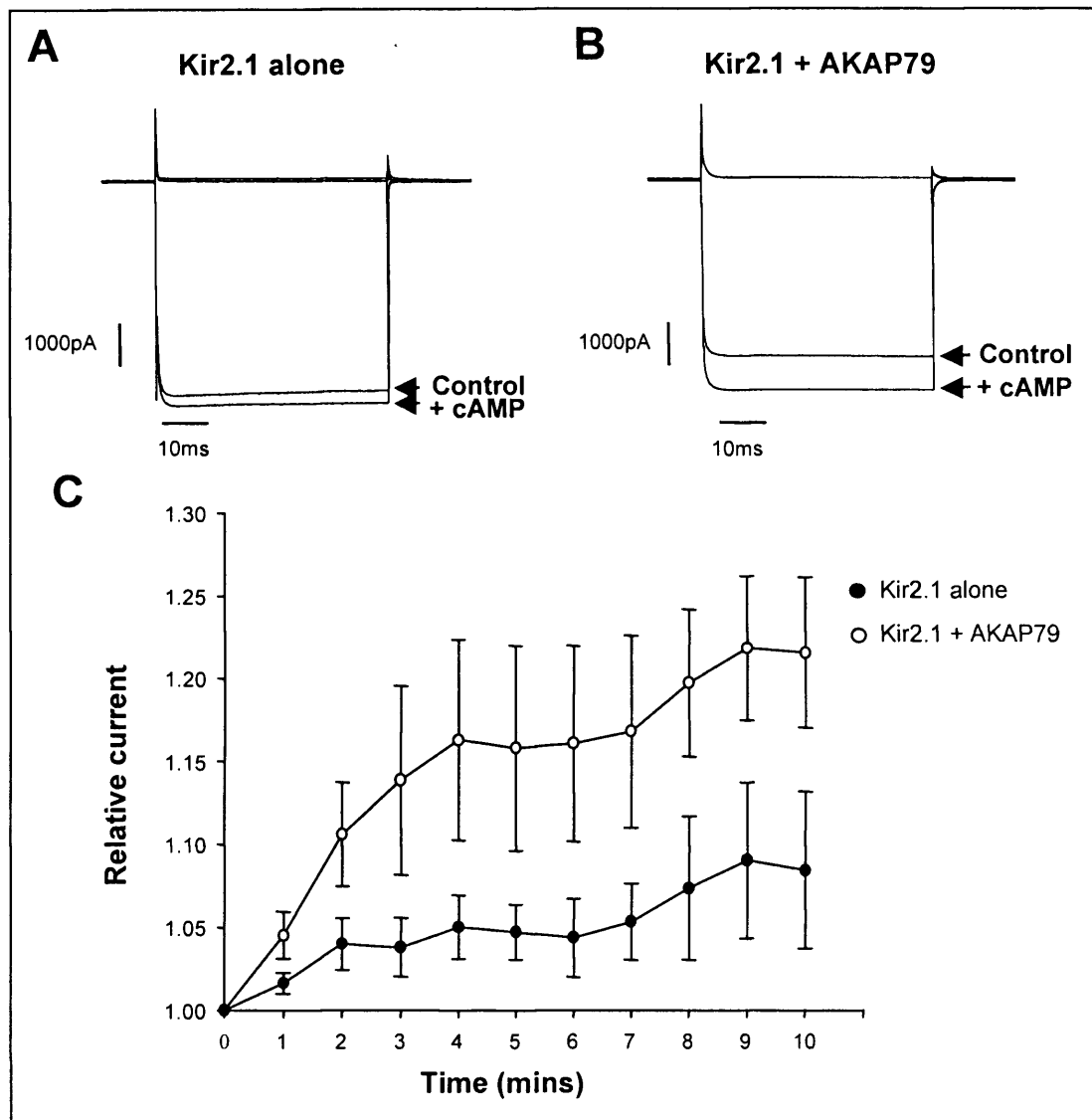


Figure 37. Whole cell Kir2.1 currents affected by increase in intracellular cAMP. Whole cell currents recorded in response to a voltage step from the holding potential of -17mV to test potentials of +60 and -100mV under control conditions (immediately after patch break-in) and after 10mins exposure to 100 μ M intracellular cAMP, 200nM okadaic acid and 200nM cypermethrin, ($[K^+]_o = 70$ mM; $[K^+]_i = 140$ mM) from **A**, a single HEK293 cell transfected with Kir2.1 only or **B**, a single HEK293 cell stably expressing AKAP79 and transiently transfected with cDNA encoding Kir2.1. **C**. Relative increase in whole cell current recorded at -100mV over time for cells expressing Kir2.1 alone (●) or Kir2.1 + AKAP79 (○). Cells expressing both AKAP79 and Kir2.1 show a $21.6 \pm 4.5\%$ increase in whole-cell current over a 10 minute period ($n = 6$) significantly greater ($p < 0.05$) than the $8.4 \pm 4.7\%$ increase seen in cells expressing Kir2.1 alone ($n = 7$). All cells were pre-treated for 30-40mins with 200nM okadaic acid and 200nM cypermethrin before recording.

of this GST fusion protein in electrophysiological experiments is not appropriate due to the sheer size of the protein. GST-Kir2.1 C (182-232) is a 31.2kDa protein which simply would not diffuse easily into the cell during whole-cell recording. Instead, a common way in which peptides are expressed in whole cells is with the use of the bicistronic expression vector pIRES2-EGFP. This is a vector under control of the CMV promoter where the internal ribosomal entry site (IRES) from the encephalomyocarditis virus is situated between the multi-cloning site and region coding EGFP. Consequently, the protein of interest, in this case the AKAP79 binding region on Kir2.1 (residues 182-232), could be translated concurrently but separately from EGFP. Expression of EGFP in the cells acts as a positive marker for expression of the protein of interest.

4.1 Characterisation of pIRES2-(182-232)-EGFP

The coding region for the AKAP79 binding site was PCR amplified from wild type Kir2.1 and ligated into pIRES2-EGFP (data not shown). Using uniquely designed primers, see Appendix 2.3, pIRES2-(182-232)-EGFP was sequence verified and subsequently transiently transfected in HEK293 cells to confirm expression.

Having confirmed pIRES2-(182-232)-EGFP expression through positive visualisation of green cells (data not shown), we then wanted to confirm that expression of the 182-232 peptide within cells could disrupt the AKAP79-Kir2.1 complex in a co-immunoprecipitation system. HEK293-AKAP79 cells were transiently transfected with cDNA encoding EGFP-Kir2.1 and either 'empty' pIRES2-EGFP or pIRES2-(182-232)-EGFP. Cells were lysed and proteins immunoprecipitated with either anti-GFP and rabbit non-immune serum or anti-AKAP79 and mouse non-immune serum, prior to separation by SDS-polyacrylamide gel electrophoresis, transferred onto nitrocellulose membrane and immunoblotted with anti-AKAP79 or anti-GFP (data not shown).

With this protocol Western blot analysis revealed that the levels of Kir2.1 expressed were markedly reduced compared with previous experiments and thus no conclusions could be drawn. To overcome these co-transfection problems, Kir2.1 was transiently transfected into one batch of HEK293-AKAP79 cells, while a separate

batch of HEK293-AKAP79 cells was transiently transfected with either 'empty' pIRES2-EGFP or pIRES2-(182-232)-EGFP.

Each set of cells were lysed and the supernatants pooled and mixed. Immunoprecipitation was then performed as before with proteins separated by SDS-PAGE, transferred onto nitrocellulose membrane and immunoblotted with anti-AKAP79.

The results of this set of experiments yielded inconclusive results, figure 38. It was possible to see a knockdown effect of the level of AKAP79 precipitated in only one blot carried out, as shown in figure 38B. However, the results of the duplicate experiments were so varied that statistical analysis shows no significant difference between cells transfected with 'empty' vector and those expressing the interfering peptide, pIRES2-(182-232)-EGFP, figure 38A. Thus results of the IRES experiment remain inconclusive and consequently, pIRES2-(182-232)-EGFP was not used in subsequent electrophysiological studies.

5 Synthetic Peptides

As an elegant alternative to expressing disrupter peptides within cells, we designed synthetic peptides specific to the AKAP79 binding regions on Kir2.1.

Three potential sections of the tertiary structure of Kir2.1 were previously shown to be exposed to the cytoplasm within the region 182-232 shown to bind AKAP79, thus providing ideal regions against which synthetic peptides could be designed, figure 39A. To test the effectiveness of these synthetic proteins to disrupt AKAP79-Kir2.1 complexes co-immunoprecipitation experiments were performed in the presence of each peptide. Figure 39 shows that the ability of antibodies directed against the EGFP tag on Kir2.1 to isolate AKAP79 from HEK293 cell lysates was largely unaffected by the addition of peptide 1, 2 or 3 to the cell lysate. In fact there was so much variability between repeat experiments (as evidenced by the large error bars Fig 37C), that no definite conclusion could be drawn.

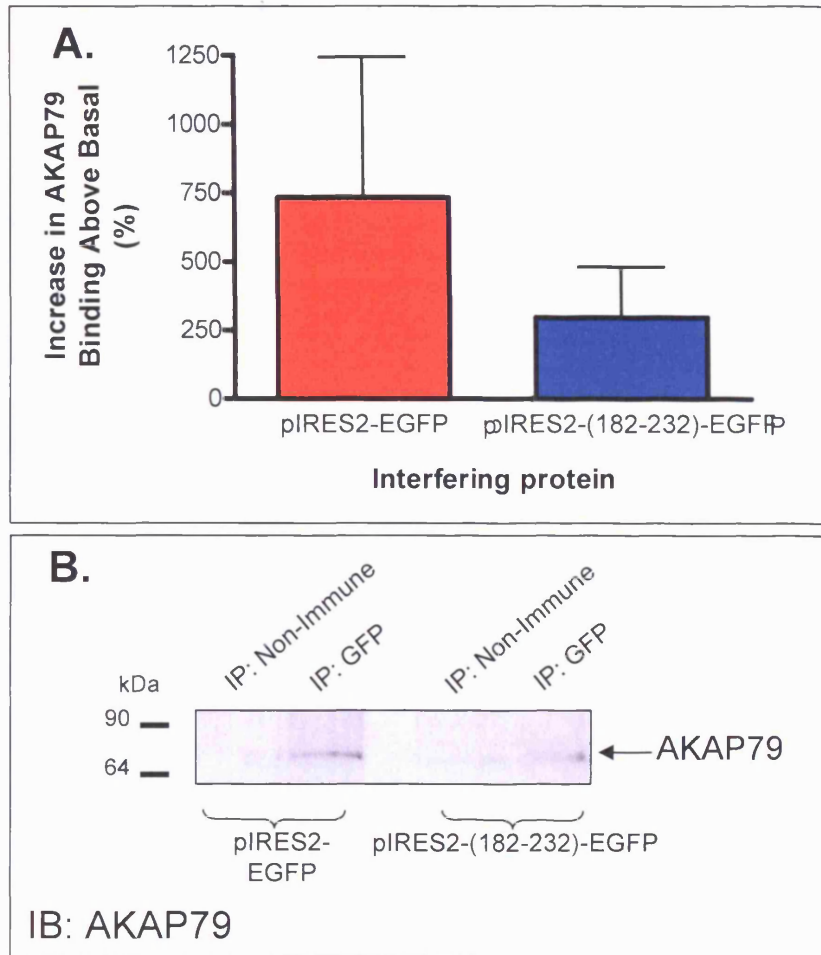


Figure 38. pIRES2-(182-232)-EGFP was unable to consistently reduce AKAP79 co-immunoprecipitation. **A.** HEK293-AKAP79 cells were transiently transfected with cDNA encoding either EGFP-Kir2.1 or pIRES2-EGFP/ pIRES2-(182-232)-EGFP. After lysis, EGFP-Kir2.1 containing cells were mixed with either pIRES2-EGFP or pIRES2-EGFP-Kir2.1(182-232) containing cell lysates for 6 hours prior to immunoprecipitation with antibodies directed against EGFP or non-immune serum as described in Methods and Materials. Precipitated proteins were separated by SDS-polyacrylamide gel electrophoresis, transferred onto nitrocellulose membrane and immunoblotted with anti-AKAP79. Densitometric analysis shows no significant difference in knockdown effect on increase in AKAP79 binding above basal between cells transfected with the 'empty' vector pIRES2-EGFP and those expressing the interfering peptide, pIRES2-(182-232)-EGFP (pIRES2-EGFP = $734 \pm 510\%$ increase in AKAP79 binding above basal; pIRES2-(182-232)-EGFP = $297 \pm 184\%$ increase in AKAP79 binding above basal; $n=3$). No significant difference; unpaired, two-tailed Student's t-test. **B** Western blot of individual experiment.

In parallel with these co-immunoprecipitation studies, we investigated the functional effects of these peptides on whole-cell Kir2.1 currents recorded in the presence of AKAP79 and elevated intracellular cAMP.

Whole-cell Kir2.1 currents were recorded at -100mV from HEK293-AKAP79 cells expressing Kir2.1 pre-treated for 30-40 minutes with 200nM okadaic acid and 200nM cypermethrin. Figure 40A shows the relative changes in whole cell current over time when cAMP is included in the pipette-filling solution under control conditions and when each synthetic peptide is also included in the pipette-filling solution. Time point zero represents the point at which the whole-cell recording configuration was established and hence dialysis of the cell with cAMP (and the synthetic peptides) begins. Whole cell currents recorded from cells exposed to 10mM peptide 1 decreased by 11.9 ± 7.0 % (mean \pm S.E.; n=4) compared to control cells over a period of no more than 14 minutes. Cells exposed to 10mM of peptide 2 or peptide 3, figure 40B and C respectively, did not show a significant difference in whole cell current above or below the whole cell currents from control cells.

6 Conclusions

The findings presented in this chapter expand the work presented previously in this thesis. By exploiting the previously constructed GST fusion proteins of the Kir2.1 AKAP79 binding site (GST-Kir2.1 C (182-232)) and using them as inhibitor peptides, we show the *in vitro* association between AKAP79 and Kir2.1 can be disrupted. In addition, through electrophysiological recordings in HEK293 cells, we confirm previous findings that in the presence of AKAP79, Kir2.1 currents are markedly increased by elevated levels of intracellular cAMP (Dart & Leyland, 2001). We also tested the ability of synthetic peptides mimicking the AKAP79 binding region on Kir2.1 to affect cAMP/PKA –dependent modulation of whole-cell Kir2.1 currents.

6.1 Interfering with the Kir2.1-AKAP79 Complex: Use of GST-fusion constructs

The ability of either GST-Kir2.1 C (182-232) or GST-Kir2.1 C (232-282) to compete with full-length Kir2.1 for AKAP79 binding in co-immunoprecipitation assays was tested. Only GST-Kir2.1 C (182-232) succeeded in abolishing the interaction between Kir2.1 and AKAP79, further supporting the notion that residues 182-232 of Kir2.1 are required for association with AKAP79.

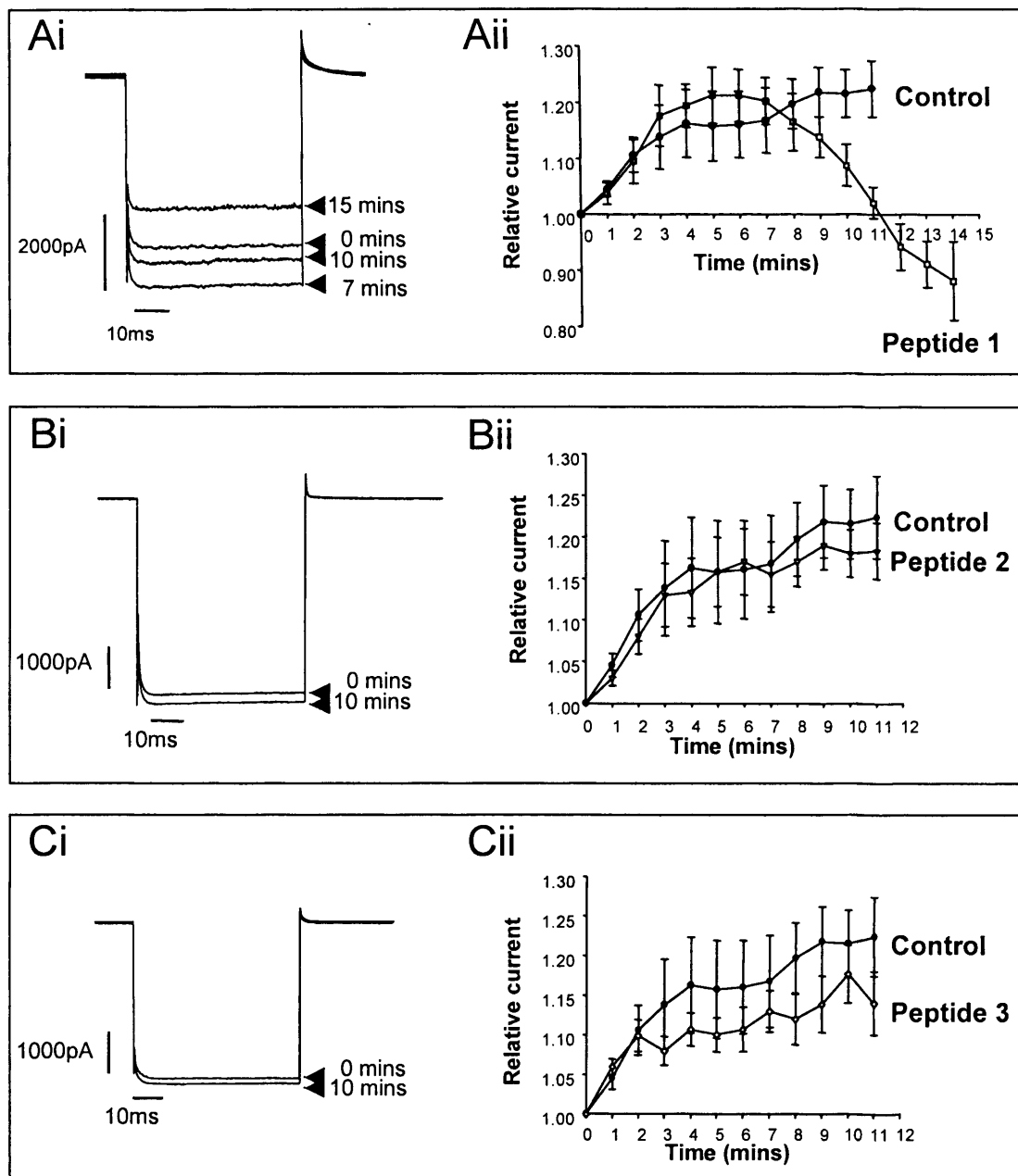


Figure 40. Kir2.1 whole cell currents affected by addition of peptide 1. cAMP-induced whole-cell currents recorded in response to a voltage step from the holding potential of -17mV to a test potentials of -100mV under control conditions ($100\mu\text{M}$ cAMP included in the pipette-filling solution) or with additional inclusion of 10mM synthetic peptide in the pipette-filling solution : **Ai.** peptide 1; **Bi.** peptide 2; **Ci.** peptide 3. Time point zero indicates point at which whole-cell configuration established. Relative increases in whole cell current recorded at -100mV over time for cells exposed to **Aii.** peptide 1; **Bii.** peptide 2; **Cii.** peptide 3. Cells exposed to peptide 1 show a $11.9 \pm 7.0\%$ decrease in whole cell current over a 14 minute period ($n = 4$) significantly greater ($p < 0.05$) than the $22.4 \pm 5.1\%$ increase seen in control cells. Peptides 2 and 3 did not elicit a significant difference in whole cell current above or below control ($n = 4$ and 4 respectively).

As an alternative means of specifically disrupting AKAP-channel complexes and one that could potentially be used in functional electrophysiological experiments, we attempted to express interfering peptides within intact HEK293 cells. A commonly used means in which to monitor expression of an untagged peptide within a whole cell is to use the bicistronic expression vector pIRES2-EGFP where the peptide of interest is translated concurrently but separately from EGFP. It appeared that expression of the pIRES vector alongside the EGFP-Kir2.1 vector inhibited the expression of Kir2.1, as levels of this protein (as determined by Western blot analysis) were markedly lower than previously observed. To overcome this, Kir2.1 and the pIRES vectors were expressed in separate batches of cells, which were subsequently lysed and mixed. Unfortunately, results of co-immunoprecipitation assays using this protocol remained inconclusive. There are many possible reasons for this, the most likely being that the small interfering peptide 182-232 was either not expressed, or if expressed was rapidly degraded. In addition, it remains to be tested whether the absolute concentration of the peptide 182-232 was at a suitable level for interference to occur. However, it has been reported that the proteins obtained using an IRES sequence are frequently not of equal proportion; the first protein being translated in large excess of the second (de Felipe, 2004). This seems unlikely in our case as attempts to establish levels of expressed 182-232 peptide, through immunoblotting, EZ™ staining and silver staining remained inconclusive (data not shown) suggesting the peptide may not have been expressed successfully.

Although widely used, the IRES strategy is not ideal as discussed above and as such alternative methods of co-expression are being developed. One such approach now being used, and of potential future application to the work here, utilises the small peptide from the foot-and-mouth disease virus. Here, the peptide is used as a linker between the proteins of interest thereby allowing autonomous intra-ribosomal self-processing of polyproteins; this process is termed CHYSEL (cis-acting hydrolase element; de Felipe, 2004).

6.2 Effect of AKAP79 on Kir2.1 Currents

Co-expression of AKAP79 with Kir2.1 in HEK293 cells had no significant effect upon whole-cell current amplitudes, suggesting basal activity of Kir2.1 channel function is

unaffected by the presence of AKAP79. Interestingly, a noticeable increase in whole cell Kir2.1 current was seen when recordings were taken in the presence of elevated intracellular cAMP, yet this was only observed in cells that had been previously treated with phosphatase inhibitors. This is in agreement with previous findings (Dart & Leyland, 2001) and suggests that phosphatase activity maybe relatively high in the vicinity of the membrane and that phosphorylation and dephosphorylation of the channel is a fast, dynamic process (Gao *et al*, 1997; Dart & Leyland, 2001).

6.3 Peptide 1 Inhibits cAMP Induced Kir2.1 Current

Disrupting the interactions between AKAPs and their target proteins may prove insightful in understanding the importance of kinase anchoring to cellular physiology. Having been unable to conclusively verify the expression of small interfering peptides within HEK293 cells, synthetic peptides that could be included in pipette-filling solutions during whole-cell electrophysiological experiments were designed. These peptides corresponded to the exposed regions of Kir2.1 between residues 182-232 that are predicted to bind AKAP79 (also see Chapter 5). Notably, the inclusion of peptide 1 (residues 190-202) to the pipette-filling solution had a profound effect upon the cAMP-induced Kir2.1 current. This manifested itself as a steady decline in whole-cell current, starting 6-7 minutes after the whole-cell recording configuration (and hence whole-cell dialysis) had been established. While this could indicate that residues 190-202 play a crucial role in AKAP79, and thus PKA, targeting to Kir2.1, the pronounced decline of the cAMP-induced current could also be indicative of the disruption of a more fundamental interaction. Kir channels are known to be regulated through association with the membrane phospholipid PtdIns(4,5)P₂ (Huang *et al*, 1998; Liou *et al*, 1999; Zhang *et al* 1999; Soom *et al*, 2001). Regulation of these ion channels may be through direct interactions, although of varying specificity depending on channel subtype, between the anionic head groups of phosphoinositides, such as phosphatidylinositol 4,5-bisphosphate (PtdIns(4,5)P₂), and the many positively charged residues in both the N- and C-terminal intracellular domains of the ion channel (Huang *et al*, 1998; Lopes *et al*, 2002; Schulze *et al*, 2003; Cukras, *et al*, 2002; Enketchakul *et al*, 2005). Studies have shown Kir2.1 has several C-terminal PtdIns(4,5)P₂ binding regions: residues 175-206, 207-246 and 324-365 (Soom *et al*, 2001); residues K185, K187, K188, R189, R218, K219, R228, R312 (Lopes *et al*, 2002), where mutation of any one of these residues resulted in

reduced or even abolished channel activity. It is noteworthy that peptide 1 (190-202) maps to part of the 175-206 PtdIns(4,5)P₂ binding regions and has the potential to disrupt Kir2.1's association with this regulatory phospholipid.

In conclusion, AKAP79 enhances the effects of cAMP on whole-cell Kir2.1 currents, probably by anchoring a pool of PKA close to channel phosphorylation sites. Attempts to disrupt the Kir2.1-AKAP79 complex *in vivo* by expressing interfering peptides (pIRES) gave inconsistent results, as did whole-cell patch clamping experiments using specifically designed interfering peptides. Peptide 1 produced a dramatic inhibition of cAMP induced current but may be due to interference with the PtdIns(4,5)P₂ binding site rather than via disruption of Kir2.1-AKAP79 association. Further studies are required to reveal the functional significance of AKAPs on Kir2.1 channel function.

CHAPTER SEVEN

FINAL DISCUSSION & CONCLUDING REMARKS

To elicit appropriate physiological responses, the specificity of signal transduction needs to be tightly controlled. Compartmentalisation of signalling molecules by scaffolding proteins appears to ensure optimal and specific signal transduction by forming multi-protein complexes that can be rapidly activated by incoming signals while limiting crosstalk between different yet related signalling pathways (Whitmarsh & Davis, 1998; Garrington & Johnson, 1999).

The results from this thesis make several advances in understanding the mechanisms used by a particular class of scaffolding protein, the prototypic AKAP, AKAP79, in targeting its associated signalling proteins to appropriate intracellular locations. The work presented here investigates the potential regulation of AKAP79 membrane association by PKA and PKC phosphorylation and receptor-driven depletion of its membrane anchor PtdIns(4,5)P₂, and also studies in detail the mode of interaction between AKAP79 and a membrane associated substrate, Kir2.1.

The key findings of this study are:

- Stimulation of protein kinase A (PKA) and protein kinase C (PKC) had no significant effect on the association of AKAP79 with the plasma membrane.
- G_q-coupled receptor-driven depletion of the lipid anchor PtdIns(4,5)P₂ causes release of AKAP79 from the membrane into cytosolic cell fractions.
- Immunocytochemical studies and real-time confocal imaging fail to show significant redistribution of AKAP79 following G_q-coupled receptor activation, possibly reflecting only limited short-range movement.
- AKAP79 is capable of interacting with three members of the inwardly rectifying potassium channel Kir2 family, Kir2.1, 2.2 and 2.3.
- The AKAP79 binding site on Kir2.1 is located in a region of 50 amino acid (residues 182-232), situated just after the point at which the channel protein leaves the plasma membrane and enters the cytoplasm.

- In contrast to other channel-AKAP interactions the association between Kir2.1 and AKAP79 does not involve a leucine zipper (-like) motif.
- The AKAP binding region on Kir2.1 is able to isolate a number of PKA binding proteins from homogenates of rat heart and brain. This suggests that it has the potential to interact with several different AKAPs and may thus form complexes with different sets of signalling proteins depending on tissue or cell type.
- cAMP-dependent modulation of Kir2.1 channel activity is significantly enhanced in the presence of AKAP79, thus confirming an important role for AKAP79 in targeting PKA to key channel phosphorylation sites.

In addition, this study has also resulted in the generation of a number of useful constructs, cell lines and inhibitor peptides for the future study of AKAP targeting interactions.

1 Control of intracellular localisation of AKAP-PKA complexes

Our findings show that the prototypic AKAP, AKAP79 targets PKA to the plasma membrane, as previously shown (Glantz *et al*, 1993; Ndubuka *et al*, 1993; Klauck *et al*, 1996). This subcellular localisation is mediated via interactions between basic regions on AKAP79 and acidic phospholipids in the plasma membrane (Dell'Acqua *et al*, 1998), however what regulates this targeting is currently unclear. Scott and colleagues suggested that AKAP79 may function not only as an anchor, but also as a substrate for the kinase PKC, with PKC-dependent phosphorylation of the membrane targeting regions of AKAP79 regulating their binding to PtdIns(4,5)P₂ (Dell'Acqua *et al*, 1998). Despite using a range of techniques, including cell fractionation, immunocytochemistry and real time confocal imaging, we find no evidence to support the idea that localisation of AKAP79 to the plasma membrane is regulated via phosphorylation. Instead we propose that AKAP79 targeting may be controlled through action of G_q-coupled GPCRs. Agonist stimulation of these receptors results in PtdIns(4,5)P₂ hydrolysis and depletion from the plasma membrane, and thus loss of AKAP79's primary lipid anchor. Although our results show that G_q-coupled receptor-driven depletion of PtdIns(4,5)P₂ causes a release of AKAP79 from the membrane into cytosolic fractions, our imaging studies show no significant redistribution of AKAP79 within the cell. We suggest this may reflect short-range

movement of AKAP79, which would allow for rapid re-association with the membrane upon repletion of PtdIns(4,5)P₂. This idea of a highly dynamic and regulated targeting will require the use of more sophisticated techniques, such as a FRET or TIRF, to confirm its validity.

Additionally, whilst we artificially stimulated PKA and/or PKC through the application of forskolin and/or PMA to intact cells, we did not measure AKAP79 phosphorylation levels. Future work to definitively eliminate that phosphorylation of AKAP79 does not regulate the association of the AKAP with the plasma membrane could include such work, potentially alongside mutagenesis of the putative AKAP79 PKA and PKC phosphorylation sites.

2 Interactions between AKAP79 and Kir channels

Although originally defined by their ability to isolate pools of PKA, many AKAPs bind other signalling enzymes thus allowing these multivalent anchoring proteins to target entire signalling complexes to specific substrates, such as the Kir2 family of inwardly rectifying potassium channels.

We show an increase in Kir2.1 whole-cell currents in response to elevated levels of cAMP, but only in the presence of AKAP79. This strongly suggests a requirement for a pool of PKA in close proximity to channel phosphorylation sites. In line with this, we present evidence for the direct association of AKAP79 with Kir2.1 via a polytopic binding site residing on the C-terminus of the ion channel. Previously, interactions between AKAPs and ion channels had been thought to occur predominantly via leucine zipper(-like) motifs (Hulme *et al*, 2002; Marx *et al*, 2002). Currently the only confirmed polytopic AKAP binding site has been identified on a G-protein coupled receptor, the β_2 -adrenergic receptor (Fan *et al*, 2001).

A lack of suitable antibodies against the members of the Kir2 family prevented us confirming the association between Kir2 and AKAP79 *in vivo*. However, the ability of the AKAP79 binding region on Kir2.1 to pulldown a number of potential AKAPs from brain and heart tissue raises the intriguing possibility that the various members of this family may interact with several different AKAPs, and thus different sets of signalling proteins, in a cell and/or tissue-dependent manner.

3 Concluding Remarks

The majority of biological effects of cAMP have been associated with PKA. Alongside PKA, scaffolding proteins work to organise these cAMP-mediated signalling events; serving to place PKA close to particular substrates to increase speed and specificity in signal transduction.

Through a multidisciplinary approach, this thesis has extended the current knowledge of an important class of scaffolding proteins, the A-kinase-anchoring proteins (AKAPs), and the intracellular targeting of cAMP-dependant protein kinase. It has also highlighted important areas for additional investigation, in particular the potentially complex interplay/regulation of membrane and substrate targeting. Future research should allow a more complete appreciation of not only the role of AKAPs as static anchors in the spatial organisation of PKA pathways, but also the extent to which these complexes are dynamically regulated and their ultimate importance to cellular physiology.

CHAPTER EIGHT

REFERENCES

- Aldape, R. A., O. Futer, et al. (1992). Charged surface residues of FKBP12 participate in formation of the FKBP12-FK506-calcineurin complex. Journal of Biological Chemistry **267**: 16029-16032
- Aderem, A. (1992). The MARCKS brothers: a family of protein kinase C substrates. Cell. **71**(5): 713-716.
- Alexander, S. P. H., A. Mathie, et al. (2006). Guide to Receptors and Channels, 2nd Edition. British Journal of Pharmacology **147**: S114-S116.
- Ali, S., X. Chen, et al. (1998). The A Kinase Anchoring Protein is Required for Mediating the Effect of Protein Kinase A on ROMK1 Channels. Proceedings of the National Academy of Sciences of the United States of America **95**(17): 10274-8.
- Alto, N. M., S. Soderling, et al. (2003). Bioinformatic Design of A-kinase Anchoring Protein-*in silico*: A Potent and Selective Peptide Antagonist of Type II Protein Kinase A Anchoring. Proceedings of the National Academy of Sciences of the United States of America **100**(8): 4445-4450.
- Angelo, R. and C. S. Rubin (1998). Molecular Characterization of an Anchor Protein (AKAPCE) That Binds the RI Subunit (RCE) of Type I Protein Kinase A from *Caenorhabditis elegans*. Journal of Biological Chemistry **273**(23): 14633-14643.
- Angelo, R. G. and C. S. Rubin (2000). Characterisation of Structural Features That Mediate the Tethering of *Caenorhabditis elegans* Protein Kinase A to a Novel A Kinase Anchor Protein. Journal of Biological Chemistry **275**(6): 4351-4362.
- Ashcroft, F. M. and F. M. Gribble (1998). Correlating Structure and Function in ATP-sensitive K⁺ Channels. Trends in Neurosciences **21**: 288-294.
- Baillie, G. S. and M. D. Houslay (2005). Arrestin times for compartmentalised cAMP signalling and phosphodiesterase-4 enzymes. Current Opinion in Cell Biology **17**(2): 129-134.
- Baillie, G. S., J. D. Scott, et al. (2005). Compartmentalisation of Phosphodiesterases and Protein Kinase A: Opposites Attract. FEBS Letters **579**(15):3264-70.

- Banky, P., M. G. Newlon, et al (2000). Isoform-Specific Differences Between the Type I α and II α Cyclic AMP-Dependent Protein Kinase Anchoring domains revealed by solution NMR. Journal Biological Chemistry **275**(45):35146-52.
- Banky, P., M. Roy, et al. (2003). Related Protein-Protein Interaction Modules Present Drastically Different Surface Topographies Despite A conserved Helical Platform. Journal of Molecular Biology **330**: 1117-1129.
- Batty, I. H., C. P. Downes (1996). Thrombin Receptors Modulate Insulin-Stimulated Phosphatidylinositol 3,4,5-Trisphosphate Accumulation in 1321N1 Astrocytoma Cells. Biochemical Journal. **317**(Pt 2):347-51.
- Bauer, C. K. and J. R. Schwarz (2001). Physiology of EAG K⁺ Channels. Journal of Membrane Biology **182**: 1-15.
- Beavo, J. A., P. J. Bechtel, et al. (1975). Mechanisms of control for cAMP-dependent protein kinase from skeletal muscle. Advances in Cyclic Nucleotide Research **5**: 241-51.
- Beavo, J. A. (1988). Multiple isozymes of cyclic nucleotide phosphodiesterase. Advances in Second Messenger Phosphoprotein Research **22**: 1-38.
- Beavo, J. A. (1995). Cyclic nucleotide phosphodiesterases: functional implications of multiple isoforms. Physiological Reviews **75**(4): 725-748.
- Beene, D. L. and J. D. Scott (2007). A-kinase anchoring proteins take shape. Current Opinion in Cell Biology **19**(2): 192-198.
- Blackshear, P. (1993). The MARCKS family of cellular protein kinase C substrates. Journal of Biological Chemistry **268**(3): 1501-1504.
- Bolger, G. B., S. Erdogan, et al. (1997). Characterization of five different proteins produced by alternatively spliced mRNAs from the human cAMP-specific phosphodiesterase PDE4D gene. Biochemical Journal **328**(2): 539-548.
- Bregman, D., N. Bhattacharyya, et al. (1989). High affinity binding protein for the regulatory subunit of cAMP- dependent protein kinase II-B. Cloning, characterization, and expression of cDNAs for rat brain P150. Journal of Biological Chemistry **264**(8): 4648-4656.
- Brown, A. M., A. Yatani, et al. (1988). Direct coupling of G proteins to ionic channels. Cold Spring Harbour Symposium for Quantitative Biology **53** (Pt 1): 365-373.
- Brown, P.R., K. Miki, et al. (2003). A-kinase anchoring protein 4 binding proteins in the fibrous sheath of the sperm flagellum. Biology of Reproduction. **68**(6):2241-8.

- Burns-Hamuro, L. L., D. M. Barraclough, et al. (2004). Identification and functional analysis of dual-specific A kinase-anchoring protein-2. Methods in Enzymology **390**: 354-374.
- Burton, K. A., B. D. Johnson, et al. (1997). Type II Regulatory Subunits are not Required for the Anchoring-Dependent Modulation of Ca²⁺ Channel Activity by cAMP-Dependent Protein Kinase. Proceedings of the National Academy of Sciences of the United States of America **94**: 11067-11072.
- Buxton, I. L. and L. L. Brunton (1983). Compartments of cyclic AMP and protein kinase in mammalian cardiomyocytes. Journal of Biological Chemistry **258**(17): 10233-10239.
- Cali, J. J., R. S. Parekh, et al. (1996). Splice Variants of Type VIII Adenylyl Cyclase. Journal of Biological Chemistry **271**(2): 1089-1095.
- Carl, A., J. L. Kenyon, et al. (1991). Regulation of Ca(2+)-activated K⁺ channels by protein kinase A and phosphatase inhibitors. American Journal of Physiology & Cell Physiology **261**(2): C387-392.
- Carlisle Michel, J. J. and J. Scott, D. (2002). AKAP Mediated Signal Transduction. Annual Review of Pharmacology & Toxicology **42**: 235-257.
- Carlisle Michel, J. J., K. L. Dodge, et al. (2004). PKA-phosphorylation of PDE4D3 facilitates recruitment of the mAKAP signalling complex. Biochemical Journal **381**: 587-592.
- Carlson, C. R., O. Witczak, et al. (2001). CDK1-Mediated Phosphorylation of the RIIalpha Regulatory Subunit of PKA Works as a Molecular Switch that Promotes Dissociation of RIIalpha from Centrosomes at Mitosis. Journal of Cell Science. **114**(Pt 18):3243-54.
- Carnegie, G. K. and J. Scott, D. (2003). A-Kinase Anchoring Proteins and Neuronal Signaling Mechanisms. Genes & Development **17**: 1557-1568.
- Carnegie, G. K., F. D. Smith, et al. (2004). AKAP-Lbc nucleates a protein kinase D activation scaffold. Molecular Cell **15**(6): 889-899.
- Carr, D. W., R. E. Stofko-Hahn, et al. (1991). Interaction of the Regulatory Subunit (RII) of cAMP-dependent Protein Kinase with RII-anchoring Proteins Occurs through an Amphipathic Helix Binding Motif. Journal of Biological Chemistry **266**(22): 14188-14192.

- Carr, D. W., Z. E. Hausken, et al. (1992a). Association of the Type II cAMP-Dependent Protein Kinase with a Human Thyroid RII-Anchoring Protein. Journal of Biological Science **267**(5): 13376-13382.
- Carr, D. W., R. E. Stofko-Hahn, et al. (1992b). Localization of the cAMP-dependent Protein Kinase to the Postsynaptic Densities by A-Kinase Anchoring Proteins. Characterization of AKAP79. Journal of Biological Chemistry **267**(24): 16816-16823.
- Carr, D., D. DeManno, et al. (1993). Follicle-stimulating hormone regulation of A-kinase anchoring proteins in granulosa cells. Journal of Biological Chemistry **268**(28): 20729-20732.
- Chen, Q., R.-Y. Lin, et al. (1997). Organelle-specific Targeting of Protein Kinase All (PKAll). Molecular and in situ Characterisation of Murine A-Kinase Anchor Proteins That Recruit Regulatory Subunits of PKAll to the Cytoplasmic Surface of Mitochondria. Journal of Biological Chemistry **272**(24): 15247-15257.
- Chen, L., J. Kurokawa, et al. (2005). Phosphorylation of the A-kinase-anchoring Protein Yotiao Contributes to Protein Kinase A Regulation of a Heart Potassium Channel. Journal of Biological Chemistry **280**(36): 31347-31352.
- Chen, L. and R. S. Kass (2006). Dual roles of the A kinase-anchoring protein Yotiao in the modulation of a cardiac potassium channel: a passive adaptor versus an active regulator. European Journal of Cell Biology **85**(7): 623-626.
- Cho, W. (2006). Building Signalling Complexes at the Membrane. Science's STKE **pe7**.
- Clapham, D. E. (1994). Direct G Protein Activation of Ion channels? Annual Review of Neuroscience **17**: 441-464.
- Coetzee, W. A., Y. Amarillo, et al. (1999). Molecular Diversity of K⁺ Channels.
- Coghlan, V., L. Langeberg, et al. (1994). Cloning and characterization of AKAP 95, a nuclear protein that associates with the regulatory subunit of type II cAMP-dependent protein kinase. Journal of Biological Chemistry **269**(10): 7658-7665.
- Coghlan, V. M., B. A. Perrino, et al. (1995). Association of Protein Kinase A and Protein Phosphatase 2B with a Common Anchoring Protein. Science **267**: 108-111.

- Collas, P., K. Le Guellec, et al. (1999). The A-kinase-anchoring protein AKAP95 is a multivalent protein with a key role in chromatin condensation at mitosis. Journal of Cell Biology **147**(6):1167-80.
- Colledge, M. and J. D. Scott (1999). AKAPs: from Structure to Function. Trends in Cell Biology **9**: 216-221.
- Colledge, M., R. A. Dean, et al. (2000). Targeting of PKA to Glutamate Receptors through a MAGUK-AKAP Complex. Neuron **27**: 107-119.
- Cong, M., S. J. Perry, et al. (2001). Regulation of Membrane Targeting of the G Protein-Coupled Receptor Kinase 2 by Protein Kinase A and Its Anchoring Protein AKAP79. Journal of Biological Chemistry **276**(18): 15192-15199.
- Conti, M., S. Iona, et al. (1995). Characterization of a hormone-inducible, high affinity adenosine 3'-5'-cyclic monophosphate phosphodiesterase from the rat Sertoli cell. Biochemistry **34**(25): 7979-7987.
- Cooper, D. M. F., N. Mons, et al. (1995). Adenylyl cyclases and the interaction between calcium and cAMP signalling. Nature **374**(6521): 421-424.
- Corbin, J. D., P. H. Sugden, et al. (1978). Studies on the properties and mode of action of the purified regulatory subunit of bovine heart adenosine 3':5'-monophosphate-dependent protein kinase. Journal of Biological Chemistry **253**(11): 3997-4003.
- Cukras, C. A., I. Jeliaskova, et al. (2002). The role of NH₂-terminal positive charges in the activity of inward rectifier KATP channels. Journal of General Physiology **120**(3):437-46.
- Dart, C. and M. L. Leyland (2001). Targeting of an A Kinase-anchoring Protein, AKAP79, to an Inwardly Rectifying Potassium Channel. Journal of Biological Chemistry **276**(23): 20499-20505.
- Dascal, N. (1997). Signalling via the G Protein-Activated K⁺ Channels. Cell Signalling **9**: 551-573.
- Davare, M. A., F. Dong, et al. (1999). The A-kinase anchor protein MAP2B and cAMP-dependent protein kinase are associated with class C L-type calcium channels in neurons. Journal of Biological Chemistry **274**(42):30280-30287.
- De Camilli, P., M. Moretti, et al. (1986). Heterogeneous distribution of the cAMP receptor protein RII in the nervous system: evidence for its intracellular accumulation on microtubules, microtubule-organizing centers, and in the area of the Golgi complex. Journal of Cell Biology **103**(1): 189-203.

- de Felipe. (2004). Skipping the Co-Expression Problem: The New 2A "CHYSEL" Technology. Genetic Vaccines And Therapy **2**:13.
- de Ruyter, P.G., O.P. Kuipers, et al. (1996). Controlled gene expression systems for *Lactococcus lactis* with the food- grade inducer nisin. Applied and Environmental Microbiology **62**: 3662-3667.
- Dell'Acqua, M. L. and J. Scott, D. (1997). Protein Kinase A Anchoring. Journal of Biological Chemistry **272**(20): 12881-12884.
- Dell'Acqua, M. L., M. C. Faux, et al. (1998). Membrane-Targeting Sequences on AKAP79 Bind Phosphatidylinositol-4,5-bisphosphate. EMBO Journal **17**(8): 2246-2260.
- Diviani, D., L. K. Langeberg, et al. (2000). Pericentrin Anchors Protein Kinase A at the Centrosome Through a Newly Identified RII-Binding Domain. Current Biology. **10**: 417-420.
- Diviani, D. and J. D. Scott (2001). AKAP Signaling Complexes at the Cytoskeleton. Journal of Cell Science **114**(Part 8): 1431-1437.
- Dodge, K. L., S. Khouangsathiene, et al. (2001). mAKAP assembles a protein kinase A/PDE4 phosphodiesterase cAMP signaling module. EMBO Journal **20**(8): 1921-1930.
- Dodge-Kafka, K. L., J. Soughayer, et al. (2005). The protein kinase A anchoring protein mAKAP coordinates two integrated cAMP effector pathways. Nature **437**(7058): 574-578.
- Dong, F., M. Feldmesser, et al. (1998). Molecular Characterization of a cDNA That Encodes Six Isoforms of a Novel Murine A Kinase Anchor Protein. Journal of Biological Chemistry. **273**(11): 6533-6541.
- Doupnik, D. A., N. Davidson, et al. (1995). The Inward Rectifier Potassium Channel Family. Current Opinions in Neurobiology **5**: 268-277.
- Downes, C. P. and M. M. Wusteman. (1983). Breakdown of polyphosphoinositides and not phosphatidylinositol accounts for muscarinic agonist-stimulated inositol phospholipid metabolism in rat parotid glands. Biochemical Journal. **216**(3):633-40.
- Dransfield, D.T., A. J. Bradford, et al. (1997a). Ezrin is a cyclic AMP-dependent protein kinase anchoring protein. EMBO Journal. **16**(1):35-43.

- Dransfield, D.T., J. L. Yeh, et al. (1997b). Identification and characterization of a novel A-kinase-anchoring protein (AKAP120) from rabbit gastric parietal cells. Biochemical Journal. **322** (Pt 3):801-8.
- Drummond, G. I. and S. Perrott-Yee (1961). Enzymatic Hydrolysis of Adenosine 3',5'-Phosphoric Acid. Journal of Biological Chemistry. **236**(4): 1126-1129.
- Eide, T., V. Coghlan, et al. (1998). Molecular cloning, chromosomal localization, and cell cycle-dependent subcellular distribution of the A-kinase anchoring protein, AKAP95. Experimental Cell Research. **238**(2): 305-316.
- Eide, T., C. Carlson, et al. (2002). Distinct but overlapping domains of AKAP95 are implicated in chromosome condensation and condensin targeting. EMBO Reports. **3**(5):426-32.
- Elcock, A. H. and J. A. McCammon (1996). Evidence for electrostatic channeling in a fusion protein of malate dehydrogenase and citrate synthase. Biochemistry **35**(39):12652-12658.
- Enkvetchakul, D., I. Jeliaskova, et al. (2005). Direct modulation of Kir channel gating by membrane phosphatidylinositol 4,5-bisphosphate. Journal of Biological Chemistry. **280**(43):35785-8.
- Esteban, J. A., S.-H. Shi, et al. (2003). PKA phosphorylation of AMPA receptor subunits controls synaptic trafficking underlying plasticity. Nature Neuroscience **6**(2): 136-143.
- Fakler, B., E. Brandle, et al. (1994). $K_{ir}2.1$ Inward Rectifier K^+ Channels Are Regulated Independently by Protein Kinases and ATP Hydrolysis. Neuron **13**: 1413-1420.
- Fakler, B., U. Brandle, et al. (1995). Strong voltage-dependent inward rectification of inward rectifier K^+ channels is caused by intracellular spermine. Cell **80**(1): 149-154
- Fan, G., E. Shumay, et al. (2001). The Scaffold Protein Gravin (cAMP-dependent Protein Kinase-anchoring Protein 250) Binds the β_2 -Adrenergic Receptor via the Receptor Cytoplasmic Arg-329 to Leu413 Domain and Provides a Mobile Scaffold during Desensitisation. Journal of Biological Chemistry **276**(26): 24005-24014.
- Feliciello, A., L. Cardone, et al. (1999). Yotiao protein, a ligand for the NMDA receptor, binds and targets cAMP-dependent protein kinase II(1). FEBS Letters. **464**(3):174-8.

- Ferguson, K. M., M. A. Lemmon, et al. (1995). Structure of the high affinity complex of inositol trisphosphate with a phospholipase C pleckstrin homology domain. Cell **83**(6):1037-46.
- Ficker, E., M. Tagliatela, et al. (1994). Spermine and spermidine as gating molecules for inward rectifier K⁺ channels. Science **266**(5187): 1068-1072.
- Frangioni, J. V. and B. G. Neel (1993). Solubilization and Purification of Enzymatically Active Glutathione S-Transferase (pGEX) Fusion Proteins. Analytical Biochemistry **210**: 179-187.
- Fraser, I. D., S. J. Tavalin, et al. (1998). A Novel Lipid-Anchored A-Kinase Anchoring Protein Facilitates cAMP-Responsive Membrane Events. EMBO Journal **17**(8): 2261-2272.
- Fraser, I. D., M. Cong, et al. (2000). Assembly of an A-Kinase -Anchoring Protein- β_2 -Adrenergic Receptor Complex Facilitates Receptor Phosphorylation and Signalling. Current Biology. **10**: 409-412.
- Gao, T., A. Yatani, et al. (1997). cAMP-Dependent Regulation of Cardiac L-Type Ca²⁺ Channels Requires Membrane Targeting of PKA and Phosphorylation of Channel Subunits. Neuron **19**: 185-196.
- Garcia, P., R. Gupta, et al. (1995). The pleckstrin homology domain of phospholipase C-delta 1 binds with high affinity to phosphatidylinositol 4,5-bisphosphate in bilayer membranes. Biochemistry. **34**(49):16228-34.
- Gibbs, C. S., D. R. Knighton, et al. (1992). Systematic Mutational Analysis of cAMP-Dependent Protein Kinase Identifies Unregulated Catalytic Subunits and Defines Regions Important for the Recognition of the Regulatory Subunit. Journal of Biological Chemistry **267**(7): 4806-4814.
- Gillingham, A. K. and S. Munro (2000). The PACT domain, a conserved centrosomal targeting motif in the coiled-coil proteins AKAP450 and pericentrin. EMBO Reports **1**(6): 524-529.
- Glantz, S. B., J. A. Amat, et al. (1992). cAMP signaling in neurons: patterns of neuronal expression and intracellular localization for a novel protein, AKAP 150, that anchors the regulatory subunit of cAMP-dependent protein kinase II beta. Mol. Biol. Cell **3**(11): 1215-1228.
- Glantz, S. B., Y. Li, et al. (1993). Characterisation of Distinct Tethering and Intracellular Targeting Domains in AKAP75, a Protein That Links cAMP-

- dependent Protein Kinase II β to the Cytoskeleton. Journal of Biological Chemistry **268**(17): 12796-12804.
- Gold, M. G., B. Lygren, et al. (2006). Molecular Basis of AKAP Specificity for PKA Regulatory Subunits Molecular Cell **24**: 383-395.
- Gomez, L. L., S. Alam, et al. (2002). Regulation of A-Kinase Anchoring Protein 79/150-cAMP-Dependent Protein Kinase Postsynaptic targeting by NMDA Receptor Activation of Calcineurin and remodeling of Dendritic Actin. Journal of Neuroscience **22**(16): 7027-7044.
- Gordon, T., B. Grove, et al (1992). Molecular cloning and preliminary characterization of a novel cytoplasmic antigen recognized by myasthenia gravis sera. Journal of Clinical Investigations. **90**(3):992-9.
- Gray, P. C., V. C. Tibbs, et al. (1997). Identification of a 15-kDa cAMP-Dependent Protein Kinase-anchoring Protein Associated with Skeletal Muscle L-Type Calcium Channels. Journal of Biological Chemistry **272**(10): 6297-6302.
- Gray, P. C., J. Scott, D., et al. (1998a). Regulation of Ion Channels by cAMP-dependent Protein Kinase and A-kinase Anchoring Proteins. Current Opinions in Neurobiology **8**: 330-334.
- Gray, P. C., B. D. Johnson, et al. (1998b). Primary Structure and Function of an A Kinase Anchoring Protein Associated with Calcium Channels. Neuron **20**: 1017-1026.
- Grove, B. D. and A. K. Bruchey (2001). Intracellular distribution of gravin, a PKA and PKC binding protein, in vascular endothelial cells. Journal Vascular Research **38**(2): 163-75.
- Hahne, K., V. Haucke, et al. (1994). Incomplete arrest in the outer membrane sorts NADH-cytochrome b5 reductase to two different submitochondrial compartments. Cell **79** (5): 829-839.
- Hall, D. D. and J. W. Hell (2001). The Fourth Dimension In Cellular Signalling - Response. Science **293**(5538): 2204-2205.
- Hanoune, J. and N. Defer (2001). Regulation and Role of Adenylyl Cyclase Isoforms. Annual Review of Pharmacology and Toxicology **41**(1): 145-174.
- Harlan, J. E., P. J. Hajduk, et al. (1994). Pleckstrin homology domains bind to phosphatidylinositol-4,5-bisphosphate. Nature. **371**(6493):168-70.
- Hausken, Z. E., V. M. Coghlan, et al. (1994). Type II Regulatory Subunit (RII) of the cAMP-dependent Protein Kinase Interaction with A-kinase Anchor Proteins

- Requires Isoleucines 3 and 5. Journal of Biological Chemistry **269**(39): 24245-24251.
- Hausken, Z. E., M. L. Dell'Acqua, et al. (1996a). Mutational Analysis of the A-Kinase Anchoring Protein (AKAP)-Binding Site on RII. Journal of Biological Chemistry **271**(46): 29016-29022.
- Hausken, Z. E. and J. D. Scott (1996b). Properties of A-kinase Anchoring Proteins. Biochemical Society Transactions **24**: 986-991.
- Hayes, J. S., L. L. Brunton et al. (1979). Hormonally Specific Expression of Cardiac Protein Kinase Activity. Proceedings of the National Academy of Sciences of the United States of America **76**: 1570-1574.
- Hayes, J. S. and L. L. Brunton (1982). Functional compartments in cyclic nucleotide action. Journal of Cyclic Nucleotide Research **8**(1): 1-16.
- Herberg, F. W., A. Maleszka, et al. (2000). Analysis of A-Kinase Anchoring Protein (AKAP) Interaction with Protein Kinase A (PKA) Regulatory Subunits: PKA Isoform Specificity in AKAP Binding. Journal of Molecular Biology **298**(2): 329-339.
- Herzog, W. and K. Weber. (1978). Fractionation of brain microtubule-associated proteins. Isolation of two different proteins which stimulate tubulin polymerization in vitro. European Journal of Biochemistry. **92**(1):1-8.
- Hilgemann, D.W., S. Feng, et al. (2001). The complex and intriguing lives of PIP2 with ion channels and transporters. Science STKE. **2001**(111):RE19.
- Hille, B. (2001). Ion Channels of Excitable Membranes. USA, Sinauer Associates, Inc.
- Hirsch, A. H., S. B. Glantz, et al. (1992). Cloning and Expression of an Intron-less Gene for AKAP 75, an Anchor Protein for the Regulatory Subunit of cAMP-dependent Protein Kinase II β . Journal of Biological Chemistry **267**(4): 2131-2134.
- Ho, K., C. G. Nichols, et al. (1993). Cloning and expression of an inwardly rectifying ATP-regulated potassium channel. Nature **362**(6415): 31-38.
- Hoshi, N., J. S. Zhang, et al. (2003). AKAP150 Signaling Complex Promotes Suppression of the M-Current by Muscarinic Agonists. Nature Neuroscience **6**(6): 564-571.

- Hoshi, N., L. K. Langeberg, et al. (2005). Distinct enzyme combinations in AKAP signalling complexes permit functional diversity. Nature Cell Biology **7**(11): 1066-1073.
- Houbre, D., G. Duportail, et al. (1991). The interactions of the brain-specific calmodulin-binding protein kinase C substrate, neuromodulin (GAP 43), with membrane phospholipids. Journal of Biological Chemistry. **266**(11): 7121-7131.
- Houslay, M. D. and G. Milligan (1997). Tailoring cAMP-Signalling Responses Through Isoform Multiplicity. Trends in Biochemical Sciences **22**: 217-224.
- Houslay, M. D. and D. R. Adams (2003). PDE4 cAMP phosphodiesterases: modular enzymes that orchestrate signalling cross-talk, desensitization and compartmentalization. Biochemical Journal **370**: 1-18.
- Huang, C.L., S. Feng, et al. (1998). Direct activation of inward rectifier potassium channels by PIP2 and its stabilization by Gbetagamma. Nature. **391**(6669):803-6.
- Huang, L. J.-s., K. Durick, et al. (1997a). Identification of a Novel Protein Kinase A Anchoring Protein That Binds Both Type I and Type II Regulatory Subunits. Journal of Biological Chemistry. **272**(12): 8057-8064.
- Huang, L. J., K. Durick, et al. (1997b). D-AKAP2, a Novel Protein Kinase A Anchoring Protein with a Putative RGS Domain. Proceedings of the National Academy of Sciences of the United States of America **94**: 11184-11189.
- Huang, L. J., L. Wang, et al. (1999). NH₂-Terminal Targeting Motifs Direct Dual Specificity A-Kinase-Anchoring Protein 1 (D-AKAP1) to Either Mitochondria or Endoplasmic Reticulum. Journal of Cell Biology **145**: 951-959.
- Hulme, J. T., M. Ahn, et al. (2002). A Novel Leucine Zipper Targets AKAP15 and Cyclic AMP-dependent Protein Kinase to the C Terminus of the Skeletal Muscle Ca²⁺ Channel and Modulates Its Function. Journal of Biological Chemistry **277**(6): 4079-4087.
- Hulme, J. T., T. W.-C. Lin, et al. (2003). β -Adrenergic Regulation Requires Direct Anchoring of PKA to Cardiac Ca_v1.2 Channels Via a Leucine Zipper Interaction with A Kinase-Anchoring Protein 15. Proceedings of the National Academy of Sciences of the United States of America **100**(22): 13093-13098.

- Hyde, C. C., S. A. Ahmed, et al. (1988). Three-dimensional structure of the tryptophan synthase alpha 2 beta 2 multienzyme complex from *Salmonella typhimurium*. Journal of Biological Chemistry. **263**(33): 17857-17871.
- Iyengar, R. (1993). Molecular and functional diversity of mammalian Gs-stimulated adenylyl cyclases. FASEB Journal **7**(9): 768-775.
- Jackson, T. R., L. R. Stephens, et al. (1992). Receptor specificity of growth factor-stimulated synthesis of 3-phosphorylated inositol lipids in Swiss 3T3 cells. Journal of Biological Chemistry. **267**(23):16627-36.
- James, P., T. Vorherr, et al. (1995). Calmodulin-binding domains: just two faced or multi-faceted? Trends in Biochemical Sciences **20**: 38-42.
- Jan, L. Y. and Y. N. Jan (1994). Potassium channels and their evolving gates. Nature **371**(6493): 119-122.
- Jan, L. Y. and Y. N. Jan (1997a). Annual Review Prize Lecture - Voltage-gated and Inwardly Rectifying Potassium Channels. Journal of Physiology - London **505**: 267-282.
- Jan, L. Y. and Y. N. Jan (1997b). Cloned Potassium Channels from Eukaryotes & Prokaryotes. Annual Review of Neuroscience **20**: 91-123.
- Jeffreys, A. J., V. Wilson, et al. (1988). Amplification of Human Minisatellites by the Polymerase Chain Reaction: Towards DNA Fingerprinting of Single Cells. Nucleic Acids Research **16**(23): 10953-10971.
- Jenkinson, S., S. R. Nahorski, et al. (1994). Disruption by Lithium of Phosphatidylinositol-4,5-bisphosphate Supply and Inositol-1,4,5-trisphosphate Generation in Chinese Hamster Ovary Cells Expressing Human Recombinant M1 Muscarinic receptors. Molecular Pharmacology. **46**(6):1138-48.
- Jenkinson, D. H. (2006). Potassium channels - multiplicity and challenges. British Journal of Pharmacology **147**(S1): S63-S71.
- Johnson, B. D., T. Scheuer, et al. (1994). Voltage-Dependent Potentiation of L-Type Ca²⁺ Channels in Skeletal Muscle Cells Requires Anchored cAMP-Dependent Protein Kinase. Proceedings of the National Academy of Sciences of the United States of America **91**(24): 11492-11496.
- Johnson, L. R., J. A. Foster, et al. (1997). Assembly of AKAP82, a Protein Kinase A Anchor Protein, into the Fibrous Sheath of Mouse Sperm. Developmental Biology **192**(2): 340-350(11).

- Jones, S. V. (1996). Modulation of the inwardly rectifying potassium channel IRK1 by the m1 muscarinic receptor. Molecular Pharmacology **49**(4): 662-667.
- Kamouchi, M., K. Van Den Bremt, et al. (1997). Modulation of Inwardly Rectifying Potassium Channels in Cultured Bovine Pulmonary Artery Endothelial Cells. Journal of Physiology **504**(3): 545-556.
- Kapiloff, M. S., R. V. Schillace, et al. (1999). mAKAP: an A-kinase anchoring protein targeted to the nuclear membrane of differentiated myocytes. Journal of Cell Science **112**(16): 2725-2736.
- Kapiloff, M. S. (2002). Contributions of Protein Kinase A Anchoring Proteins to Compartmentation of cAMP Signaling in the Heart. Molecular Pharmacology **62**: 193-199.
- Karschin, C., E. Dibmann, et al. (1996). IRK (1-3) and GIRK (1-4) Inwardly Rectifying K⁺ Channels mRNAs Are Differentially Expressed in the Adult Rat Brain. Journal of Neuroscience **16**(11): 3559-3569.
- Kawano, S., F. Nakamura, et al. (1992). Cardiac sarcoplasmic reticulum chloride channels regulated by protein kinase A. Circulation Research. **71**(3):585-9.
- Keller, G. A., S. Krisans, et al. (1991). Evolutionary conservation of a microbody targeting signal that targets proteins to peroxisomes, glyoxysomes, and glycosomes. Journal of Cell Biology **114**(5): 893-904.
- Kinderman, F. S., C. Kim, et al. (2006). A Dynamic Mechanism for AKAP Binding to RII Isoforms of cAMP-Dependent Protein Kinase. Molecular Cell **24**(3): 397-408.
- Klauck, T. M., M. C. Faux, et al. (1996). Coordination of Three Signaling Enzymes by AKAP79, a Mammalian Scaffold Protein. Science **271**: 1589-1592.
- Klussmann, E., B. Edemir, et al. (2001). Ht31: the First Protein Kinase A Anchoring Protein to Integrate Protein Kinase A and Rho Signalling. FEBS Letters **507**: 264-268.
- Koumi, S., C. L. Backer, et al. (1995a). Molecular and Cellular Cardiology: Characterization of Inwardly Rectifying K⁺ Channel in Human Cardiac Myocytes: Alterations in Channel Behavior in Myocytes Isolated From Patients With Idiopathic Dilated Cardiomyopathy. Circulation **92**: 164-174.
- Koumi, S., C. L. Backer, et al. (1995b). beta-Adrenergic modulation of the inwardly rectifying potassium channel in isolated human ventricular myocytes.

- Alteration in channel response to beta-adrenergic stimulation in failing human hearts. Journal of Clinical Investigation **96**(6): 2870-2881.
- Koyama, H., K. Morishige, et al. (1994). Molecular cloning, functional expression and localization of a novel inward rectifier potassium channel in the rat brain. FEBS Letters **341**(2-3): 303-307.
- Kubo, Y., T. J. Baldwin, et al. (1993). Primary structure and functional Expression of a Mouse Inward Rectifier Potassium Channel. Nature **362**: 127-133.
- Kume, H., A. Takai, et al. (1989). Regulation of Ca²⁺ -dependent K⁺ -channel activity in tracheal myocytes by phosphorylation. Nature **341**(6238): 152-154.
- Kunji, E.R.S and M. Harding. (2003). Projection Structure of the Atractyloside-inhibited Mitochondrial ADP/ATP Carrier of *Saccharomyces cerevisiae* Journal of Biological Chemistry. **278**: 36985-36988.
- Kuo, A., J. M. Gulbis, et al. (2003). Crystal Structure of the Potassium Channel KirBac1.1 in the Closed State. Science **300**: 1922-1926.
- Landschulz, W. H., P. F. Johnson, et al. (1988). The Leucine Zipper - A Hypothetical Structure Common to a New Class of DNA-Binding Proteins. Science **240**(4860): 1759-1764.
- Lavine, N., N. Ethier, et al. (2002). G Protein-coupled Receptors Form Stable Complexes with Inwardly Rectifying Potassium Channels and Adenylyl Cyclase. Journal of Biological Chemistry. **277**(48): 46010-46019.
- Lemmon, M.A., K. M. Ferguson, et al. (1995). Specific and high-affinity binding of inositol phosphates to an isolated pleckstrin homology domain. Proceedings of the National Academy of Sciences of the United States of America. **92**(23):10472-6.
- Lesage, F. and M. Lazdunski (2000). Molecular and Functional Properties of Two-Pore-Domain Potassium Channels. American Journal of Physiology - Renal Physiology **279**: F793-F801.
- Lester, L. B., V. M. Coghlan, et al. (1996). Cloning and Characterisation of a Novel A-Kinase Anchoring Protein. Journal of Biological Chemistry **271**(16): 9460-9465.
- Leyland, M. L., C. Dart, et al. (1999). The Possible Role of a Disulphide Bond in Forming Functional Kir2.1 Potassium Channels. Pflügers Archiv - European Journal of Physiology **438**: 778-781.

- Li, Y., C. Ndubuka, et al. (1996). A Kinase Anchor Protein 75 Targets Regulatory (RII) Subunits of cAMP-dependent Protein Kinase II to the Cortical Actin Cytoskeleton in Non-neuronal Cells. Journal of Biological Chemistry **271**(28): 16862-16869.
- Lieberman, S. J., W. Wasco, et al. (1988). Immunogold localization of the regulatory subunit of a type II cAMP- dependent protein kinase tightly associated with mammalian sperm flagella. Journal of Cell Biology **107**(5): 1809-1816.
- Lilly, S. M., F. J. Alvarez, et al. (2005). Synaptic and Subcellular Localisation of A-Kinase Anchoring Protein 150 in Rat Hippocampal CA1 Pyramidal Cells: Co-localisation with Excitatory Synaptic Markers. Neuroscience **134**(1): 155-163.
- Lin, R.-Y., S. B. Moss, et al. (1995). Characterisation of S-AKAP84, a Novel Developmentally Regulated A Kinase Anchor Protein of Male Germ Cells. Journal of Biological Chemistry **270**(46): 27804-27811.
- Lin, J. W., M. Wyszynski, et al. (1998). Yotiao, a Novel Protein of Neuromuscular Junction and Brain That Interacts with Specific Splice Variants of NMDA Receptor Subunit NR1. Journal of Neuroscience **18**(6): 2017-2027.
- Lohmann, S. M., P. DeCamilli, et al. (1984). High-Affinity Binding of the Regulatory Subunit (RII) of cAMP-Dependent Protein Kinase to Microtubule-Associated and Other Cellular Proteins. Proceedings of the National Academy of Sciences of the United States of America **81**(21): 6723-6727.
- Lopatin, A. N., E. N. Makhina, et al. (1994). Potassium Channel Block by Cytoplasmic Polyamines as the Mechanism of Intrinsic Rectification. Nature **372**: 366-369.
- Lopatin, A., E. Makhina, et al. (1995). The mechanism of inward rectification of potassium channels: "long-pore plugging" by cytoplasmic polyamines. Journal of General Physiology **106**(5): 923-955.
- Lopes, C. M. B., H. Zhang, et al. (2002). Alterations in Conserved Kir Channel-PIP₂ Interactions Underlie Channelopathies. Neuron **34**: 933-944.
- Lu, P.-J. and C.-S. Chen (1997). Selective Recognition of Phosphatidylinositol 3,4,5-Trisphosphate by a Synthetic Peptide. Journal of Biological Chemistry **272**(1): 466-472.
- Lu, Z. and R. MacKinnon (1994). Electrostatic tuning of Mg²⁺ affinity in an inward-rectifier K⁺ channel. Nature **371**(6494): 243-246.

- Luo, Z., B. Shafit, et al. (1990). Identification of the MAP2- and P75-binding Domain in the Regulatory Subunit (RII β) of Type II cAMP-dependent Protein Kinase. Journal of Biological Chemistry **265**(35): 21804-21810.
- Lynch, M. J., G. S. Baillie, et al. (2005). RNA Silencing Identifies PDE4D5 as the Functionally Relevant cAMP Phosphodiesterase Interacting with β -Arrestin to Control the Protein Kinase A/AKAP79-mediated Switching of the β 2-Adrenergic Receptor to Activation of ERK in HEK293B2 Cells. Journal of Biological Chemistry. **280**(39): 33178-33189.
- Makhina, E. N., A. J. Kelly, et al. (1994). Cloning and expression of a novel human brain inward rectifier potassium channel. Journal of Biological Chemistry. **269**(32): 20468-20474.
- Malbon, C. C., J. Tao, et al. (2004). AKAPs (A-Kinase Anchoring Proteins) and Molecules That Compose Their G-Protein-Coupled Receptor Signalling Complexes. Biochemical Journal **379**: 1-9.
- Mandal, A., S. Naaby-Hansen, et al. (1999). FSP95, a testis-specific 95-kilodalton fibrous sheath antigen that undergoes tyrosine phosphorylation in capacitated human spermatozoa. Biology of Reproduction. **61**(5):1184-97.
- Marrion, N. V. (1997). Control of M-Current. Annual Review of Physiology **59**(1): 483-504.
- Marx, S. O., S. Reiken, et al. (2000). PKA phosphorylation dissociates FKBP12.6 from the calcium release channel (ryanodine receptor): defective regulation in failing hearts. Cell **101**(4): 365-376.
- Marx, S. O., J. Kurokawa, et al. (2002). Requirement of a Macromolecular Signalling Complex for β Adrenergic Receptor Modulation of the KCNQ1-KCNE1 Potassium Channel. Science **295**(5554): 496-499.
- Matsuda, H., A. Saigusa, et al. (1987). Ohmic conductance through the inwardly rectifying K channel and blocking by internal Mg²⁺. Nature **325**(6100): 156-159.
- McCartney, S., B. M. Little, et al. (1995). Cloning and Characterization of A-kinase Anchor Protein 100 (AKAP100). Journal of Biological Chemistry. **270**(16): 9327-9333.
- McLaughlin, S. and A. Aderem (1995). The myristoyl-electrostatic switch: a modulator of reversible protein-membrane interactions. Trends in Biochemical Sciences **20**(7): 272-276.

- Mehats, C., C. B. Andersen, et al. (2002). Cyclic nucleotide phosphodiesterases and their role in endocrine cell signaling. Trends in Endocrinology and Metabolism **13**(1): 29-35.
- Mei, X., I. S. Singh, et al. (1997). Cloning and characterization of a testis-specific, developmentally regulated A-kinase-anchoring protein (TAKAP-80) present on the fibrous sheath of rat sperm. European Journal of Biochemistry **246**(2): 425-432.
- Miki, K. and E. M. Eddy (1998). Identification of tethering domains for protein kinase A type Ialpha regulatory subunits on sperm fibrous sheath protein FSC1. Journal of Biological Chemistry. **273**(51):34384-90.
- Miki, K. and E. M. Eddy (1999). Single Amino Acids Determine Specificity of Binding of Protein Kinase A Regulatory Subunits by Protein Kinase A Anchoring Proteins. Journal of Biological Chemistry **274**(41): 29057-29062.
- Minor, J. D. L., S. J. Masseling, et al. (1999). Transmembrane Structure of an Inwardly Rectifying Potassium Channel. Cell **96**: 879-891.
- Monaghan, A. S., D. L. Baines, et al. (1999). Inwardly Rectifying K⁺ Currents in Fetal Alveolar Type II Cells: Regulation by Protein Kinase A and Protein Phosphatases. Pflügers Archiv - European Journal of Physiology **438**: 371-377.
- Monne, M., K.W. Chan, et al. (2005). Functional Expression of Eukaryotic Membrane Proteins in *Lactococcus lactis*. Biochimica et Biophysica Acta **14**: 3048-3065.
- Morikis, D., M. Roy, et al. (2002). Electrostatic Properties of the Structure of the Docking and Dimerisation Domain of Protein Kinase A II α . European Journal of Biochemistry **269**: 2040-2051.
- Nauert, J.B., T. M. Klauck, et al. (1997). Gravin, an autoantigen recognized by serum from myasthenia gravis patients, is a kinase scaffold protein. Current Biology. **7**(1):52-62.
- Ndubuka, C., Y. Li, et al. (1993). Expression of A Kinase Anchor Protein 75 Depletes Type II cAMP-dependent Protein Kinases from the Cytoplasm and Sequesters the Kinases in a Particulate Pool. Journal of Biological Chemistry **268**(11): 7621-7624.
- Newlon, M. G., M. Roy, et al. (1997). The A-kinase Anchoring Domain of Type II α cAMP-dependent Protein Kinase Is Highly Helical. Journal of Biological Chemistry. **272**(38): 23637-23644.

- Newlon, M. G., M. Roy, et al. (1999). The Molecular Basis for Protein Kinase A Anchoring Revealed by Solution NMR. Nature Structural Biology **6**(3): 222-227.
- Newlon, M. G., M. Roy, et al. (2001). A Novel Mechanism of PKA Anchoring Revealed by Solution Structures of Anchoring Complexes. EMBO Journal **20**(7): 1651-1662.
- Nichols, C. G. and A. N. Lopatin (1997). Inward Rectifier Potassium Channels. Annual Review of Physiology **59**: 171-191.
- Nigg, E. A., G. Schäfer, et al. (1985). Cyclic-AMP-dependent protein kinase type II is associated with the Golgi complex and with centrosomes. Cell **41**(3):1039-51.
- Nishida, M. and R. MacKinnon (2002). Structural Basis of Inward Rectification: Cytoplasmic Pore of the G Protein-Gated Inward Rectifier GIRK1 at 1.8Å Resolution. Cell **111**: 957-965.
- Notredame, C., D. G. Higgins, et al. (2000). T-Coffee: A novel method for fast and accurate multiple sequence alignment. Journal of Molecular Biology. **302**(1):205-17.
- Oki, N., S.-I. Takahashi, et al. (2000). Short Term Feedback Regulation of cAMP in FRTL-5 Thyroid Cells. Role of PDE4D3 Phosphodiesterase Activation. Journal of Biological Chemistry. **275**(15): 10831-10837.
- Oliveria, S. F., L. L. Gomez, et al. (2003). Imaging Kinase-AKAP79-phosphatase Scaffold Complexes at the Plasma Membrane in Living Cells Using FRET Microscopy. Journal of Cell Biology **160**(1): 101-112.
- Ostroveanu, A., E. A. Van der Zee, et al. (2007). A-Kinase Anchoring Protein 150 in the Mouse Brain is Concentrated in Areas Involved in Learning and Memory. Brain Research **1145**: 97-107.
- Panama, B. K. and A. N. Lopatin (2006). Differential polyamine sensitivity in inwardly rectifying Kir2 potassium channels. Journal of Physiology **571**(2): 287-302.
- Patel, A. J. and E. Honore (2001). Properties and Modulation of Mammalian 2P Domain K⁺ Channels. Trends in Neurosciences **24**: 339-346.
- Pegan, S., C. Arrabit, et al. (2005). Cytoplasmic Domain Structures of Kir2.1 and Kir3.1 Show Sites for Modulating Gating and Rectification. Nature Neuroscience **8**(3): 279-287.

- Perez, G. and L. Toro (1994). Differential modulation of large-conductance KCa channels by PKA in pregnant and nonpregnant myometrium. American Journal of Physiology & Cell Physiology **266**(5): C1459-1463.
- Perier, F., C. Radeke, et al. (1994). Primary Structure and Characterization of a Small-Conductance Inwardly Rectifying Potassium Channel from Human Hippocampus. Proceedings of the National Academy of Sciences of the United States of America **91**(13): 6240-6244.
- Perkins, G. A., L. Wang, et al. (2001). PKA, PKC and AKAP Localisation in and around the Neuromuscular Junction. BMC Neuroscience **2**(17).
- Perry, S. J., G. S. Baillie, et al. (2002). Targeting of Cyclic AMP Degradation to β_2 -Adrenergic Receptors by β -Arrestins. Science **298**: 834836.
- Pitcher, J. A., J. J. G. Tesmer, et al. (1999). Feedback Inhibition of G Protein-coupled Receptor Kinase 2 (GRK2) Activity by Extracellular Signal-regulated Kinases. Journal of Biological Chemistry. **274**(49): 34531-34534.
- Prüss, H., C. Derst, et al. (2005). Differential distribution of individual subunits of strongly inwardly rectifying potassium channels (Kir2 family) in rat brain. Molecular Brain Research **139**(1): 63-79.
- Rall, T. W. and E. W. Sutherland. (1958). Formation of Cyclic Adenine Ribonucleotide by Tissue Particles. Journal of Biological Chemistry. **232**(2): 1065-1076.
- Rall, T.W. (1975). Introduction. Advances in Cyclic Nucleotide Research. **5**:1-2.
- Rana, R.S., L. E. Hokin. (1990). Role of phosphoinositides in transmembrane signaling. Physiological Reviews. **70**(1):115-64.
- Rebecchi, M. J. and S. N. Pentylala (2000). Structure, Function, and Control of Phosphoinositide-Specific Phospholipase C. Physiol. Rev. **80**(4): 1291-1335.
- Reimann, F. and F. M. Ashcroft (1999). Inwardly Rectifying Potassium Channels. Current Opinions in Cell Biology. **11**: 503-508.
- Reinton, N., P. Collas, et al. (2000). Localization of a novel human A-kinase-anchoring protein, hAKAP220, during spermatogenesis. Developmental Biology **223**(1): 194-204.
- Rich, T. C., K. A. Fagan, et al. (2000). Cyclic Nucleotide-gated Channels Colocalize with Adenylyl Cyclase in Regions of Restricted cAMP Diffusion. Journal of General Physiology **116**(2): 147-162.

- Rich, T. C., T. E. Tse, et al. (2001a). In Vivo Assessment of Local Phosphodiesterase Activity Using Tailored Cyclic Nucleotide-gated Channels as cAMP Sensors. Journal of General Physiology **118**(1): 63-78.
- Rich, T. C., K. A. Fagan, et al. (2001b). A uniform extracellular stimulus triggers distinct cAMP signals in different compartments of a simple cell. Proceedings of the National Academy of Sciences of the United States of America **98**(23): 13049-13054.
- Robbins, J. (2001). KCNQ Potassium Channels: Physiology, Pathophysiology and Pharmacology. Pharmacology & Therapeutics **90**: 1-19.
- Robertson, B. E., R. Schubert, et al. (1993). cGMP-dependent protein kinase activates Ca-activated K channels in cerebral artery smooth muscle cells. American Journal of Physiology & Cell Physiology **265**(1): C299-303.
- Rosenmund, C., D. W. Carr, et al. (1994). Anchoring of Protein Kinase A is Required for Modulation of AMPA/Kainate Receptors on Hippocampal Neurones. Nature **268**: 853-856.
- Rubin, C. S. (1994). A Kinase Anchor Proteins and the Intracellular Targeting of Signals Carried by Cyclic AMP. Biochimica et Biophysica Acta **1224**: 467-479.
- Ruppersberg, J. P. and B. Fakler (1996). Complexity of the regulation of Kir2.1 K⁺ channels. Neuropharmacology **35**(7): 887-893.
- Salim, K., M. J. Bottomley, et al. (1996). Distinct specificity in the recognition of phosphoinositides by the pleckstrin homology domains of dynamin and Bruton's tyrosine kinase. EMBO Journal. **15**(22):6241-50.
- Sampson, L. J., M. Leyland et al. (2003). Direct Interaction between the Actin-binding Protein Filamin-A and the Inwardly Rectifying Potassium Channel, Kir2.1. Journal of Biological Chemistry **278**(43):41988-41997.
- Sánchez, C., J. Díaz-Nido, et al. (2001). Phosphorylation of microtubule-associated protein 2 (MAP2) and its relevance for the regulation of the neuronal cytoskeleton function. Progress in Neurobiology. **61**(2):133-68.
- Sarkar, D., J. Erlichman, et al. (1984). Identification of a Calmodulin-binding Protein that Co-purifies with the Regulatory Subunit of Brain Protein Kinase II. Journal of Biological Chemistry **259**(15): 9840-9846.
- Schillace, R. V. and J. Scott, D. (1999). Organisation of Kinases, Phosphatases and Receptor Signaling Complexes. Journal of Clinical Investigation **103**(6): 761-765.

- Schillace, R. V., J. W., et al. (2001). Multiple interactions within the AKAP220 signaling complex contribute to protein phosphatase 1 regulation. Journal of Biological Chemistry. **276**(15):12128-34.
- Schmidt, P. H., D. T. Dransfield, et al. (1999). AKAP350, a Multiply Spliced Protein Kinase A-anchoring Protein Associated with Centrosomes. Journal of Biological Chemistry. **274**(5): 3055-3066.
- Schröder, W., G. Seifert, et al. (2002). AMPA Receptor-Mediated Modulation of Inward Rectifier K⁺ Channels in Astrocytes of Mouse Hippocampus. Molecular and Cellular Neuroscience **19**: 447-458.
- Schulze, D., T. Krauter, et al. (2003). Phosphatidylinositol 4,5-Bisphosphate (PIP₂) Modulation of ATP and pH Sensitivity in Kir Channels. A Tale of an Active and a Silent PIP₂ Site in the N Terminus. Journal of Biological Chemistry. **278**(12): 10500-10505.
- Scott, J. D., R. E. Stofko, et al. (1990). Type II Regulatory Subunit Dimerization Determines the Subcellular Localization of the cAMP-dependent Protein Kinase. Journal of Biological Chemistry **265**(35): 21561-21566.
- Scott, J., D. (1991). Cyclic Nucleotide-Dependent Protein Kinases. Pharmacology & Therapeutics **50**(1): 123-145.
- Sette, C. and M. Conti (1996). Phosphorylation and Activation of a cAMP-specific Phosphodiesterase by the cAMP-dependent Protein Kinase. Involvement of Serine 54 in the Enzyme Activation. Journal of Biological Chemistry. **271**(28): 16526-16534.
- Seykora, J. T., M. M. Myat, et al. (1996). Molecular Determinants of the Myristoyl-electrostatic Switch of MARCKS. Journal of Biological Chemistry. **271**(31): 18797-18802.
- Shih, M., F. Lin, et al. (1999). Dynamic Complexes of β_2 -Adrenergic Receptors with Protein Kinases and Phosphatases and the Role of Gravin. Journal of Biological Chemistry **274**(3): 1588-1595.
- Skålhegg, B. S. and K. Tasken (2000). Specificity in the cAMP/PKA Signalling Pathway. Differential Expression, Regulation, and Subcellular Localization of Subunits of PKA. Frontiers in Bioscience **5**: 678-693.
- Smith, F. D. and J. D. Scott (2002). Signaling Complexes: Junctions on the Intracellular Information Super Highway. Current Biology **12**(1): R32-R40.

- Smith, F. D., L. K. Langeberg, et al. (2006). The where's and when's of kinase anchoring. Trends in Biochemical Sciences **31**(6): 316-323.
- Soderling, S. H. and J. A. Beavo (2000). Regulation of cAMP and cGMP signaling: new phosphodiesterases and new functions. Current Opinion in Cell Biology **12**(2): 174-179.
- Soom, M., R. Schonherr, et al. (2001). Multiple PIP₂ Binding Sites in Kir2.1 Inwardly Rectifying Potassium Channels. FEBS Letters **490**: 49-53.
- Srere, P. A. (2000). Macromolecular interactions: tracing the roots. Trends in Biochemical Sciences **25**(3): 150-153.
- Stanfield, P. R., S. Nakajima, et al. (2002). Constitutively Active and G-Protein Coupled Inward Rectifier K⁺ Channels: Kir2.0 and Kir3.0. Reviews of Physiology, Biochemistry and Pharmacology. **145**: 47-179.
- Stauffer, T. P., S. Ahn, et al. (1998). Receptor-induced transient reduction in plasma membrane PtdIns(4,5)P₂ concentration monitored in living cells. Current Biology. **8**(6):343-6.
- Steen, R. L., F. Cubizolles, et al. (2000). A kinase-anchoring protein (AKAP)95 recruits human chromosome-associated protein (hCAP)-D2/Eg7 for chromosome condensation in mitotic extract. Journal of Cell Biology. **149**(3):531-6.
- Steinberg, S. F. and L. L. Brunton (2001). Compartmentation of G Protein-Coupled Signalling Pathways in Cardiac Myocytes. Annual Review of Pharmacology and Toxicology **41**(1): 751-773.
- Stocker, M. (2004). Ca²⁺-activated K⁺ Channels: Molecular Determinants and Function of the SK Family. Nature Reviews Neuroscience **5**: 758-770.
- Streb, J. W. and J. M. Miano (2005). AKAP12 α , an Atypical Serum Response Factor-dependent Target Gene. Journal of Biological Chemistry. **280**(6): 4125-4134.
- Sun, F., M. J. Hug, et al. (2000a). Protein kinase A associates with cystic fibrosis transmembrane conductance regulator via an interaction with ezrin. Journal of Biological Chemistry. **275**(19):14360-6.
- Sun, F., M. J. Hug, et al. (2000b). E3KARP mediates the association of ezrin and protein kinase A with the cystic fibrosis transmembrane conductance regulator in airway cells. Journal of Biological Chemistry. **275**(38):29539-46.
- Swierczynski, S. L. and P. J. Blackshear (1996). Myristoylation-dependent and Electrostatic Interactions Exert Independent Effects on the Membrane

- Association of the Myristoylated Alanine-rich Protein Kinase C Substrate Protein in Intact Cells. Journal of Biological Chemistry. **271**(38): 23424-23430.
- Takahashi, M., H. Shibata, et al. (1999). Characterization of a Novel Giant Scaffolding Protein, CG-NAP, That Anchors Multiple Signaling Enzymes to Centrosome and the Golgi Apparatus. Journal of Biological Chemistry. **274**(24): 17267-17274.
- Tang, W. J., J. Krupinski, et al. (1991). Expression and characterization of calmodulin-activated (type I) adenylylcyclase. Journal of Biological Chemistry. **266**(13): 8595-8603.
- Tao, J., H.-Y. Wang, et al. (2003). Protein Kinase A Regulates AKAP250 (Gravin) Scaffold Binding to the β_2 -Adrenergic Receptor. EMBO Journal **22**(24): 6419-6429.
- Tasken, K. A., P. Collas, et al. (2001). Phosphodiesterase 4D and Protein Kinase A Type II Constitute a Signaling Unit in the Centrosomal Area. Journal of Biological Chemistry. **276**(25): 21999-22002.
- Tasken, K. and E. M. Aandahl (2004). Localized Effects of cAMP Mediated by Distinct Routes of Protein Kinase A. Physiological Reviews. **84**: 137-167.
- Taussig, R. and A. G. Gilman (1995). Mammalian Membrane-bound Adenylyl Cyclases. Journal of Biological Chemistry. **270**(1): 1-4.
- Tavalin, S. J., M. Colledge, et al. (2002). Regulation of GluR1 by the A-Kinase Anchoring Protein 79 (AKAP79) Signaling Complex Shares Properties with Long-Term Depression. Journal of Neuroscience **22**(8): 3044-3051.
- Theurkauf, W. and R. Vallee (1982). Molecular characterization of the cAMP-dependent protein kinase bound to microtubule-associated protein 2. Journal of Biological Chemistry. **257**(6): 3284-3290.
- Topert, C., F. Doring, et al. (1998). Kir2.4: A Novel K⁺ Inward Rectifier Channel Associated with Motoneurons of Cranial Nerve Nuclei. Journal of Neuroscience **18**(11): 4096-4105.
- Tovey, S. C. and G. B. Willars (2004). Single-Cell Imaging of Intracellular Ca²⁺ and Phospholipase C Activity Reveals That RGS 2, 3, and 4 Differentially Regulate Signaling via the G α_q /11-Linked Muscarinic M3 Receptor. Molecular Pharmacology **66**(6): 1453-1464.

- Trendelenburg G., M. Hummel, et al. (1996). Molecular characterization of AKAP149, a novel A kinase anchor protein with a KH domain. Biochem Biophys Res Commun. **225**(1):313-9.
- Vandenberg, C. A. (1987). Inward Rectification of a Potassium Channel in Cardiac Ventricular Cells Depends on Internal Magnesium Ions. Proceedings of the National Academy of Sciences of the United States of America **84**(8): 2560-2564.
- Varnai, P. and T. Balla (1998). Visualization of Phosphoinositides That Bind Pleckstrin Homology Domains: Calcium- and Agonist-induced Dynamic Changes and Relationship to Myo-[3H]inositol-labeled Phosphoinositide Pools. Journal of Cell Biology **143**(2): 501-510.
- Venter, J. C., M. D. Adams, et al. (2001). The Sequence of the Human Genome. Science **291**(5507): 1304-1351.
- Vijayaraghavan, S., S. A. Goueli, et al. (1997). Protein Kinase A-Anchoring Inhibitor Peptides Arrest Mammalian Sperm Motility. Journal of Biological Chemistry **272**(8): 4747-4752.
- Vijayaraghavan, S., G. A. Liberty, et al. (1999). Isolation and Molecular Characterization of AKAP110, a Novel, Sperm-Specific Protein Kinase A-Anchoring Protein. Molecular Endocrinology **13**(5): 705-717.
- Wang, Y., J. Scott, et al. (1991). A Constitutively Active Holoenzyme Form of the cAMP-Dependent Protein Kinase. Proceedings of the National Academy of Sciences of the United States of America **88**(6): 2446-2450.
- Wang, Z. W. and M. I. Kotlikoff (1996). Activation of KCa Channels in Airway Smooth Muscle Cells by Endogenous Protein Kinase A. American journal of Physiology **271**: L100-L105.
- Wang, L., R. K. Sunahara, et al. (2001). Cloning and mitochondrial localization of full-length D-AKAP2, a protein kinase A anchoring protein. Proceedings of the National Academy of Sciences of the United States of America **98**(6):3220-5
- Wang, H.-Y., J. Tao, et al. (2006). G-protein-coupled receptor-associated A-kinase anchoring proteins: AKAP79 and AKAP250 (gravin) European Journal of Cell Biology **85**(7): 643-650.
- Weldon, S. L. and S. S. Taylor (1985). Monoclonal antibodies as probes for functional domains in cAMP- dependent protein kinase II. Journal of Biological Chemistry. **260**(7): 4203-4209.

- Westphal, R., S. J. Tavalin, et al. (1999). Regulation of NMDA Receptors by an Associated Phosphatase-Kinase Signalling Complex. Science **285**: 93-96.
- Wible, B. A., M. Tagliatela, et al. (1994). Gating of inwardly rectifying K⁺ channels localized to a single negatively charged residue. Nature **371**(6494): 246-249.
- Willars, G. B., S. R. Nahorski, et al. (1998). Differential Regulation of Muscarinic Acetylcholine Receptor-sensitive Polyphosphoinositide Pools and Consequences for Signalling in Human Neuroblastoma Cells. Journal of Biological Chemistry **273**(9): 5037-5046.
- Wischmeyer, E. and A. Karschin (1996). Receptor Stimulation Causes Slow Inhibition of IRK1 Inwardly Rectifying K⁺ Channels by Direct Protein Kinase A-Mediated Phosphorylation. Proceedings of the National Academy of Sciences of the United States of America **93**: 5819-5823.
- Witczak, O., B. S. Skalhegg, et al. (1999). Cloning and characterization of a cDNA encoding an A-kinase anchoring protein located in the centrosome, AKAP450. EMBO Journal **18**(7): 1858-1868.
- Wong, W. and J. D. Scott (2004). AKAP Signalling Complexes: Focal Points in Space and Time. Nature Reviews Molecular Cell Biology **5**(12): 959-970.
- Xia, Z., E. J. Choi, et al. (1993). Type I calmodulin-sensitive adenylyl cyclase is neural specific. Journal of Neurochemistry **60**(1): 305-11.
- Xu, Z.-C., Y. Yang, et al. (1996). Phosphorylation of the ATP-sensitive, Inwardly Rectifying K⁺ Channel, by Cyclic AMP-dependent Protein Kinase. Journal of Biological Chemistry **271**: 9313-9319.
- Yang, J., Y. N. Jan, et al. (1995). Control of rectification and permeation by residues in two distinct domains in an inward rectifier K⁺ channel. Neuron **14**: 1047-1054.
- Yang, J., J. A. Drazba, et al. (1998). A-kinase Anchoring Protein 100 (AKAP100) is Localised in Multiple Subcellular Compartments in the Adult Rat Heart. Journal of Cell Biology **142**(2): 511-522.
- Yellen, G. (2002). The Voltage-gated Potassium Channels and their Relatives. Nature **419**: 35-42.
- Zaccolo, M., P. Magalhaes, et al. (2002). Compartmentalisation of cAMP and Ca²⁺ signals. Current Opinion in Cell Biology **14**(2): 160-166.

- Zaccolo, M. and T. Pozzan (2002). Discrete Microdomains with High Concentration of cAMP in Stimulated Rat Neonatal Cardiac Myocytes. Science **295**: 1711-1715.
- Zhang, H., C. He, et al. (1999). Activation of inwardly rectifying K⁺ channels by distinct PtdIns(4,5)P₂ interactions. Nature Cell Biology **1**: 183-188.

APPENDIX ONE

A1.1 Composition of 4% Stacking Gel

1.3ml Acrylamide
2.5ml 0.5M Tris-HCl (pH 6.8)
100 μ l 10% sodium dodecyl sulphate (S.D.S.)
6.0ml distilled water
100 μ l 10% ammonium persulphate (A.P.S.)*
5 μ l Tetramethylethylenediamine (TEMED)*

A1.2 Composition of 10% Resolving Gel

3.33ml Acrylamide
2.5ml 1.5M Tris-HCl (pH 8.8)
100 μ l 10% S.D.S.
3.97ml distilled water
100 μ l 10% A.P.S.*
10 μ l TEMED*

* These constituents are to be added last for acrylamide polymerisation.

APPENDIX TWO

All synthetic oligonucleotides were purchased from Invitrogen and came at desalted purity unless otherwise stated.

A2.1 Synthetic Oligonucleotides Used to Construct RII α -EGFP

Forward: CTC GAG GCC ACC ATG AGC CAC ATC CAG

Reverse: CCG CGG CTG CCC GAG GTT GCC CAG ATC CAC

A2.2 Synthetic Oligonucleotides Used to Construct Kir2.1 Truncations

pGEX 6P-1 Kir2.1 (182-282):

Forward: GGA TCC AAG ATG GCA AAG CCA AAG AAG AGA AAT GAG

Reverse: CTC GAG CTA CAA GTC ATA TAA AGG GC

pGEX 6P-1 Kir2.1 (283-428):

Forward: GGA TCC AGT AAG CAG GAC ATT GAC AAT GCA GAC

Reverse: CTC GAG TCA TAT CTC CGA TTC TCG CC

pGEX 6P-1 Kir2.1 (182-232):

Forward: GGA TCC AAG ATG GCA AAG CCA AAG AAG AGA AAT GAG

Reverse: CTC GAG TCA GAG AAG CTG TGC CCG GAC ATG

pGEX 6P-1 Kir2.1 (233-282):

Forward: GGA TCC AAA TCT AGG ATC ACT TCA GAA GGG G

Reverse: CTC GAG CTA CAA GTC ATA TAA AGG GC

pGEX 6P-1 Kir2.1 (182-232 V194A):

Forward: AGA AAT GAG ACT CTT GCC TTC AGT CAC AAT GCT

Reverse: AGC ATT GTG ACT GAA GGC AAG AGT CTC ATT TCT

pGEX 6P-1 Kir2.1 (182-232 I201A):

Forward: TTC AGT CAC AAT GCT GTG GCC GCC ATG AGG GAT GGC AAA

Reverse: TTT GCC ATC CCT CAT GGC GGC CAC AGC ATT GTG ACT GAA

pGEX 6P-1 Kir2.1 (182-232 L208A):

Forward: GCC ATG AGG GAT GGC AAG GCC TGC TTG ATG TGG AGA GTG
GGT AAC

Reverse: GTT ACC CAC TCT CCA CAT CAA GCA GGC CTT GCC ATC CCT
CAT GGC

pGEX 6P-1 Kir2.1 (182-206):

Forward: GGA TCC AAG ATG GCA AAG CCA AAG

Reverse: CTC GAG TCA GCC ATC CCT CAT GGC

pGEX 6P-1 Kir2.1 (207-232):

Forward: GGA TCC AAA CTC TGC TTG ATG TGG

Reverse: CTC GAG TCA GAG AAG CTG TGC CCG

A2.3 Sequencing Primers Used Sequence pIRES2-(182-232)-EGFP

Forward sequencing primer 1:

GGA GGT CTA TAT AAG CAG AGC T

Forward sequencing primer 2:

ATT GAC GCA AAT GGG CGG TAG GCG T

Forward sequencing primer 3:

GTA GGG GTG TAC GGT GGG AGG TCT ATA TAA

Reverse sequencing primer 1:

AAA AGA CGG CAA TAT GGT GGA AAA

Reverse sequencing primer 2:

ACA AAC GCA CAC CGG CCT TAT TCC AA

Reverse sequencing primer 3:

AAA ATA ACA TAT AGA CAA A

APPENDIX THREE

A3.1 EGFP-tagging RII α

The region of the RII regulatory subunit responsible for AKAP-binding is situated at the N-terminus (Hausken *et al*, 1994; Hausken & Scott, 1996). This region, within the first 45 residues of each regulatory subunit, appears to serve at least two functions: dimerisation and docking, and hence has been termed the D/D domain (Newlon *et al*, 2001). In order to cause minimal disruption to its interaction with AKAPs, the EGFP tag was added to the C-terminus of RII α . RII α was PCR amplified out of the expression vector pET-28b and the resulting fragment analysed on an agarose gel, figure 41A. This shows a band running at a molecular weight of approximately 1,215 bp; nothing is present in the negative control lane therefore suggesting successful amplification of RII α . After purification of this PCR product, RII α was subsequently ligated into the subcloning vector pCR[®]-Blunt, transformed into One-Shot TOP10 bacterial cells, plated out, and resultant colonies picked and the DNA isolated. It was confirmed that RII α had been successfully incorporated into the pCR[®]-Blunt vector in only one of the colonies picked, as shown when a restriction digest was carried out using *Xho* and *SacII*, figure 41B. Two bands were seen that corresponded to the approximate weights of the 'empty' pCR[®]-Blunt vector and RII α , 3.5kb and 1,215bp respectively. The positive clone was sequenced and confirmed to be pCR-Blunt-RII α . This construct was then restriction digested, using *Xho* and *SacII*, and RII α subsequently ligated into the pEGFP-N1 vector, also cut at the restriction digest points *Xho* and *SacII*.

Again successful ligation of RII α into the pEGFP-N1 vector was confirmed by purifying the DNA from six bacterial colonies, restriction digested and analysed by agarose gel electrophoresis, figure 41C. It can be seen that colonies 1-5 show the successful incorporation of RII α in the pEGFP-N1 vector.

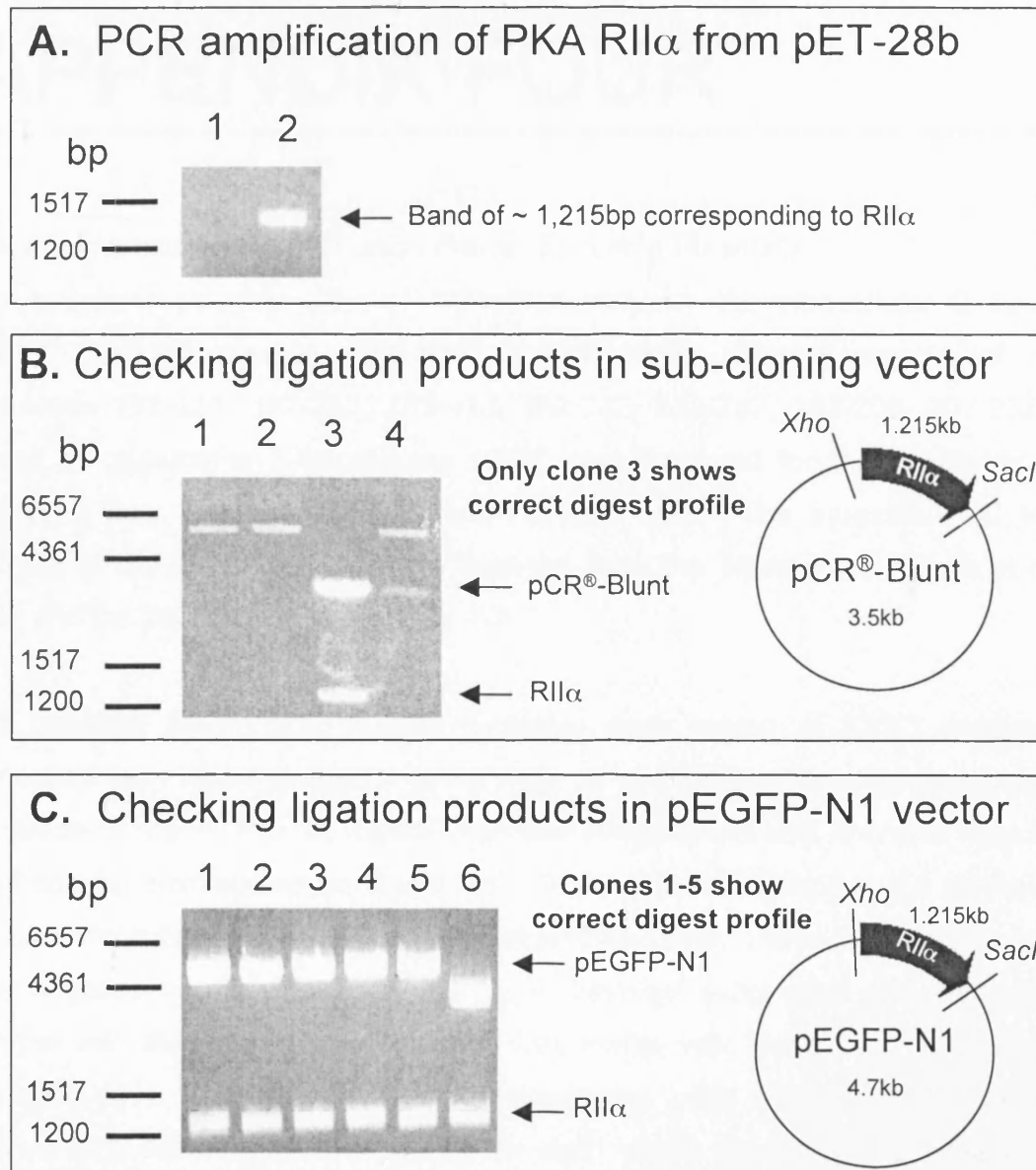


Figure 41. Construction of RII α -EGFP. **A.** PCR amplification of RII α from pET-28b using primers to introduce *Xho* and *SacII* restriction sites. Lane 1: control (i.e. no DNA template added to the PCR reaction, lane 2: the PCR product, PKA RII α). **B.** Analytical digest of products formed by ligation of RII α into the subcloning pCR[®]-Blunt vector. TAE gel showing restriction digest, using *Xho* and *SacII*, on 4 potential RII α -pCR[®]-Blunt clones. Lane 3 shows only clone with correct digest profile as show by the vector map. **C.** Analytical digest of products formed by ligation of RII α into the pEGFP-N1 vector. TAE gel showing restriction digest, using *Xho* and *SacII*, on 6 potential clones, however only 1-5 show successful ligation and hence incorporation of RII α (1.215kb) into the pEGFP-N1 vector (4.7kb).

APPENDIX FOUR

A4.1 Construction of GST-Fusion Protein Encoding Plasmids

To determine possible sites of interaction between the intracellular C domain of Kir2.1 (Kir2.1C; residues 182-428) and AKAP79, different regions of Kir2.1C (residues 182-428, 182-282, 283-428, 182-232, 233-282, 182-206, 207-232) were fused to glutathione S-transferase (GST) and screened for their ability to isolate AKAP79 from lysates of transfected HEK293 cells. The intracellular C terminal portion of the ion channel protein emerges from the plasma membrane at residue 182 and the last residue of Kir2.1 is 428.

To generate these GST fusion proteins, each region of Kir2.1 required was amplified from wild-type Kir2.1 using PCR as described in Methods and Materials. Products of the PCR were digested analysed using *Bam*HI and *Xho* and visualised by agarose gel electrophoresis, figure 42A. A band corresponding to the correct weight of each fragment was visualised in the experiment lane. When no DNA was visible in the negative control lane, the PCR was deemed successful and each fragment ligated into the vector pCR[®]-Blunt. This vector was used in a subcloning step because M13 forward and reverse sequencing sites are present, there are no sequencing sites in pGEX-6P-1 and as such allows each fragment inserted to be sequence verified before insertion into the final GST gene fusion vector. After each fragment had been positively sequenced they were then digested out of pCR[®]-Blunt with *Bam*H1 and *Xho*, figure 42B, and finally cloned in to the pGEX-6P-1 bacterial expression vector, figure 42C. Each pGEX-6P-1-GST fusion protein was then transformed into *E. coli*, the bacteria grown and the expression of GST fusion proteins induced by addition of IPTG as previously described Methods & Materials. The bacteria were then pelleted, lysed and relative levels of expression of each GST fusion protein assessed.

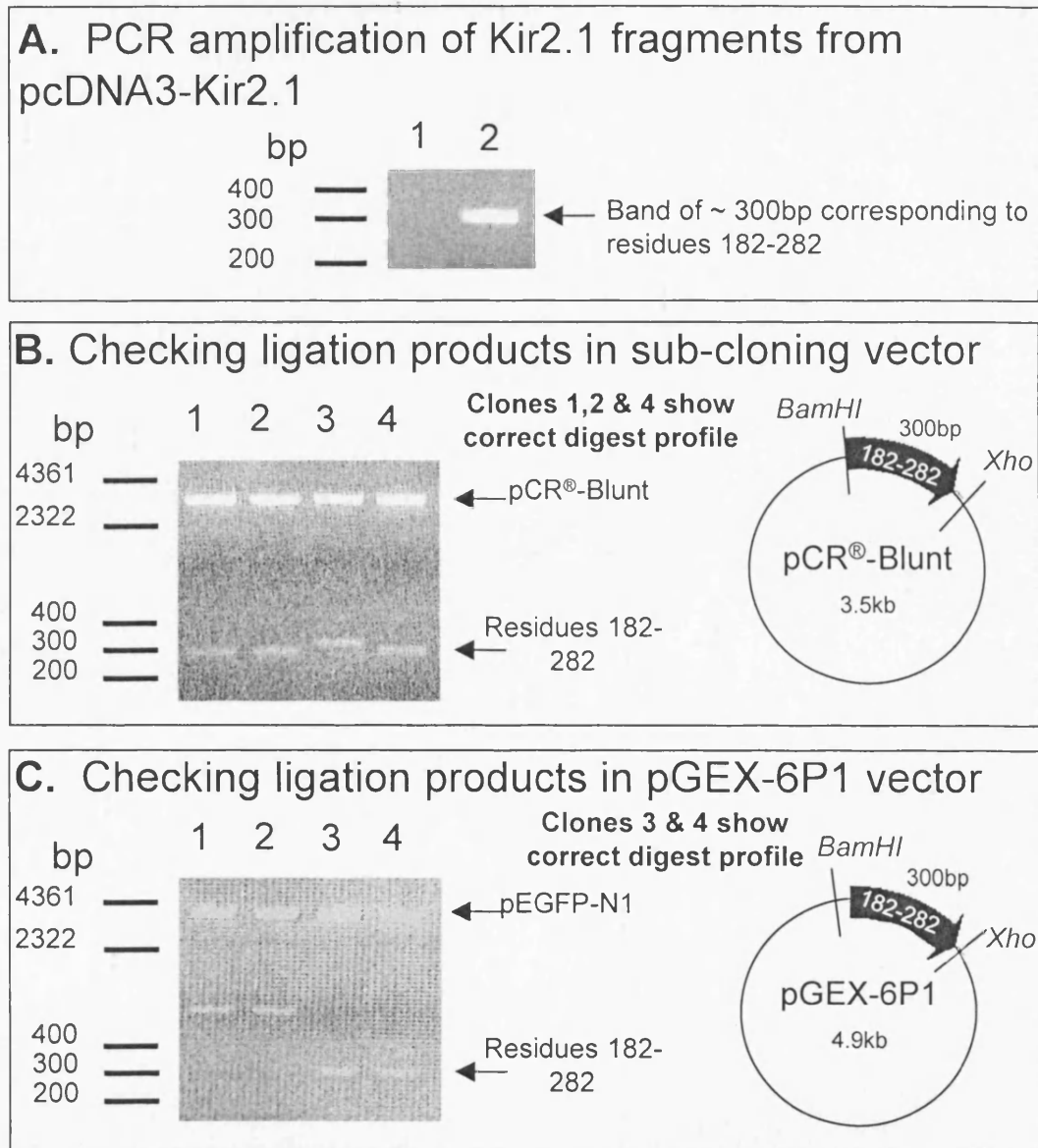


Figure 42. Construction of GST-fusion protein plasmids. **A.** PCR amplification of Kir2.1 fragments from pcDNA3-Kir2.1 using primers to introduce *Bam*HI and *Xho* restriction sites. Lane 1: control (i.e. no DNA template added to the PCR reaction), lane 2: the PCR product, in this case residues 182-282. **B.** Analytical digest of products formed by ligation of residues 182-282 into the subcloning pCR®-Blunt vector. TAE gel showing restriction digest, using *Bam*HI and *Xho*, on 4 potential (182-282)-pCR®-Blunt clones. Lanes 1, 2 & 4 show clones with correct digest profile as show by the vector map. **C.** Analytical digest of products formed by ligation of residues 182-282 into the pGEX-6P1 vector. TAE gel showing restriction digest, using *Bam*HI and *Xho*, on 4 potential clones, however only 3 & 4 show successful ligation and hence incorporation of residues 182-282 (300bp) into the pGEX-6P1 vector (4.9kb).